

Copyright © by  
Mark Stephen Wrighton  
1972

PHOTOPROCESSES IN METAL  
CONTAINING MOLECULES

Thesis by  
Mark Stephen Wrighton

In Partial Fulfillment of the Requirements  
for the Degree of  
Doctor of Philosophy

California Institute of Technology  
Pasadena, California

1972

(Submitted May 15, 1972)

## ACKNOWLEDGMENT

I wish to express my gratitude to my advisors Professors George S. Hammond and Harry B. Gray for their interest in and support of this work. Their help and encouragement during my stay at Caltech are deeply appreciated. It has been a privilege to have been associated with them scientifically, and working with them has been a personally rewarding experience.

My colleagues in the Gray and Hammond groups are acknowledged for their assistance with certain aspects of this work. I wish to thank Frank Quina and Vince Miskowski for the synthesis of a number of compounds. Dale Bredesen is acknowledged for his contributions to the work in the energy transfer experiments. I thank my wife, Debbie, for typing this thesis.

## ABSTRACT

Recent results obtained in the area of transition metal photochemistry are presented. Previous developments in this field are included. The two introductory chapters deal with structure, bonding, and electronic absorption spectroscopy of transition metal complexes. The remaining six chapters deal with pathways for decay of electronically excited states: radiative decay, nonradiative decay, electronic energy transfer, redox photochemistry, photosubstitution, and photoreactions of the coordinated ligands.

Highlights of this work include new convincing evidence for assigning the low lying transitions in  $d^6$  metal carbonyls as ligand field excitations; the first definitive study of luminescence phenomena of metal carbonyls; a study of the non-radiative decay of metal carbonyl excited states with the conclusion that specific ligands can dominate the process of nonradiative decay; the first correlation of the quenching activity of a transition metal complex and its electronic properties; intramolecular energy transfer studies where one chromophore is a transition metal complex; data showing that the direct formation of  $\text{Co(II)}$  occurs via photolysis of some disubstituted cyanocobaltate(III) complexes; presentation of an associative type mechanism for the photoaquation of  $\text{Co(CN)}_6^{3-}$ ; a description of a set of considerations (Wrighton-Gray rules)



to predict and interpret photosubstitution reactions; and  
a discussion of the photoreactivity of alkenes, dienes, and  
stilbenes when coordinated to Cr(0), Mo(0) or W(0).

## TABLE OF CONTENTS

	page
Acknowledgment. . . . .	ii
Abstract. . . . .	iii
Introduction. . . . .	1
Chapter I   Bonding and Structure of Coordination Compounds . . . . .	4
Chapter II   Electronic Absorption Spectroscopy of Transition Metal Complexes. . . . .	20
Chapter III   Luminescence Studies in Transition Metal Complexes . . . . .	66
Chapter IV   Nonradiative Decay Processes in Metal Containing Molecules . . . . .	140
Chapter V   Energy Transfer Studies in Metal Containing Systems . . . . .	161
Chapter VI   Photoredox Reactions in Metal Containing Molecules . . . . .	190
Chapter VII   Photosubstitution Processes in Coordination Compounds. . . . .	208
Chapter VIII   Photoreactions of Coordinated Ligands. .	264
Appendix   Experimental Methods . . . . .	303

## INTRODUCTION

The absorption of ultraviolet and visible light by molecules produces electronically excited states in the absorbing species. The study of the decay of the excited state molecules constitutes the field of photochemistry. Excited state chemistry differs markedly from ground state chemistry and, thus, for the synthetically minded chemist an impetus is provided for investigations at all levels. A fleetingly short lifetime for excited states coupled with its other dynamic aspects makes the excited state structure determination an impressive challenge for structural chemists. Unique physical properties of the excited state molecules exist and a clear understanding of them will provide fundamental knowledge related to the nature of matter. In this work we focus on the photoprocesses in transition metal containing molecules, and we apply all that is known about these dynamic systems toward an understanding of chemical reactivity.

The electronically excited molecule can undergo several modes of decay. In solution relaxation of an electronic excited state to the zero vibrational level is fast relative to other processes. The vibrationally deactivated excited state can undergo decay to give lower lying states by (a) undergoing a chemical reaction to give ground state products, (b) emitting a photon (radiative decay), (c) internally converting to a high vibrational level of the lower state without undergoing chemical change or emitting a photon

(nonradiative decay), or (d) transferring its electronic excitation to a quencher (energy transfer). The reaction quantum yield,  $\Phi$ , is defined in equation (i). The quantum yields for the

$$\Phi = \frac{\# \text{ molecules reacted}}{\# \text{ photons absorbed}} \quad (i)$$

other processes are defined similarly. In discussing the photoprocesses of metal containing molecules we will be concerned with modes (a) through (d) and will present a critical analysis of important results in each area.

The photochemistry of metal containing molecules is intimately related to the nature of the interaction between the metal and its ligands. In Chapter I we review the common modes of binding between ligand and metal and discuss important structures for coordination compounds.

The absorption of light by transition metal compounds produces the reactive species. In Chapter II we introduce electronic absorption spectroscopy for transition metal complexes with emphasis on model systems and important electronic and geometrical structures.

The remaining chapters deal with the modes of decay of the excited states formed by absorption of light. The topics covered can be crudely divided into photophysical processes and photochemical processes. Radiative decay (luminescence) is covered in Chapter III; nonradiative decay processes are presented in Chapter IV; and Chapter V deals with energy transfer phenomena.

Photochemistry includes redox reactions (Chapter VI), substitution reactions (Chapter VII), and ligand reactions (Chapter VIII).

This work is not intended to be a literature summary of all of the above topics, rather we are attempting a critical review of our results against the background of previous developments.

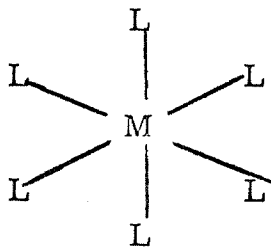
Neither is this a defense for work in this area. Interest in possible synthetic applications, physical properties of excited states, instrumentation for dynamical studies, and the bringing together of disciplines provides incentive. The possibility of mimicking nature's energy transfer and storage systems (photosynthesis) and photoimaging systems (vision) provides a real challenge. Finally, these prospects do not always surpass the personal pleasure derived from scientific inquiry.

## CHAPTER I

Bonding and Structure of Coordination  
Compounds

To gain an understanding of photoprocesses in transition metal compounds we establish at the outset the important features of bonding and geometrical structure. The number of ligands directly attached to the central metal is called the coordination number. This number can range from one to nine, but some coordination numbers have not received attention from photochemists. We will deal with coordination number and geometry in degree of importance. An introduction to molecular orbital theory to describe bonding in transition metal complexes follows the section on coordination and geometry.

Six Coordination. The  $ML_6$  system is by far the most important and most studied structure in coordination chemistry. The six ligands are generally in an octahedral arrangement about the central metal as in 1-I. Most of the important photochemical work

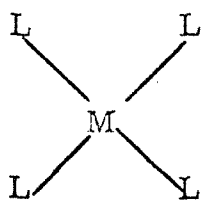


1-I

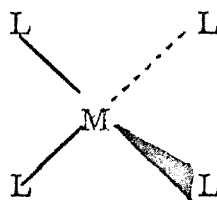
has been done with six-coordinate compounds of octahedral, or distorted octahedral structure. A second possible arrangement

of the six ligands is a trigonal prismatic structure which has been of no interest to photochemists to date. Interest has been shown in the excited state processes of six-coordinate complexes of vanadium, chromium, manganese, iron, cobalt, nickel, molybdenum, technetium, ruthenium, rhodium, tungsten, rhenium, osmium, iridium, and platinum.

Four Coordination. Four-coordinate complexes of manganese, nickel, palladium, platinum, copper, silver, gold, and cobalt are important. The four ligands can assume either a square planar arrangement, I-II, or a tetrahedral arrangement, I-III, about



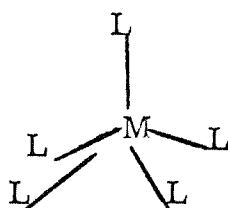
I-II



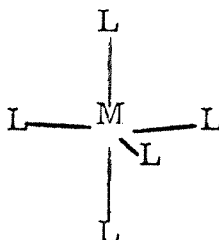
I-III

the central metal.

Five Coordination. Five coordination is important in photochemistry in that intermediates of photosubstitution reactions of six-coordinate species are thought to be five-coordinate. The structure of  $ML_5$  can be one of two idealized forms: a square pyramid I-IV or the trigonal bipyramid, I-V. One stable



1-IV



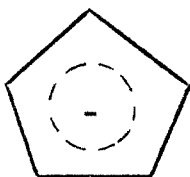
1-V

compound of structure 1-V,  $\text{Fe}(\text{CO})_5$ , has been photolysed.

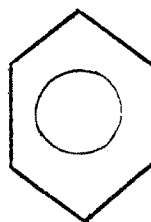
Organic  $\pi$  -Metal Systems. Some coordination compounds of considerable interest are organic  $\pi$  -metal complexes. These compounds include metal systems containing the organic ligands 1-VI through 1-X where the coordination number is not always



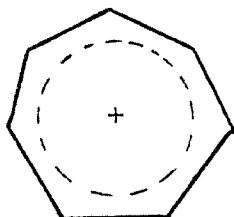
1-VI



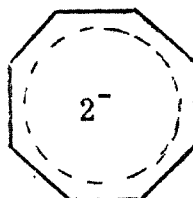
1-VII



1-VIII



1-IX

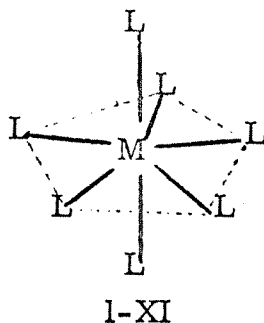


1-X

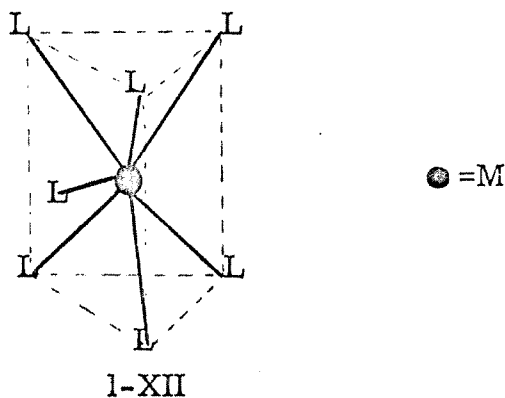


clear. It is usually true that a two-electron donor occupies one coordination site.

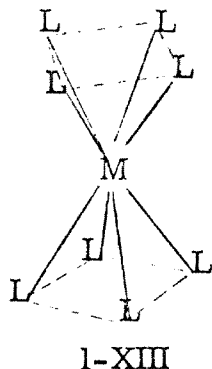
Seven and Eight Coordination. The coordination numbers of seven and eight are of increasing importance and interest. The  $ML_7$  structure can be one of three types. One seven-coordinate structure involves putting a ligand in the face of an octahedron, another is the pentagonal bipyramid 1-XI, and the third structure



involves placing a ligand in one of the faces of a trigonal prism, 1-XII. A few seven-coordinate complexes of molybdenum and



tungsten are important here. Eight coordination again involves Mo and W, and the two probable structures are the square antiprism 1-XIII or a dodecahedron.



Oxidation States. The oxidation state of the central metal in coordination compounds helps to characterize its electronic structure and the coordination sphere. Generally, the transition metals to the left on the periodic chart have higher oxidation states than the ones to the right since ionization is easier for the early metals. We associate high coordination numbers with high oxidation states, with the larger number of ligands supplying more electron density to the highly positive central metal. The large physical size for the ions to the left in the periodic chart also serves to support higher coordination numbers. The small size and low oxidation states for elements to the right in the periodic chart prevent high coordination numbers.

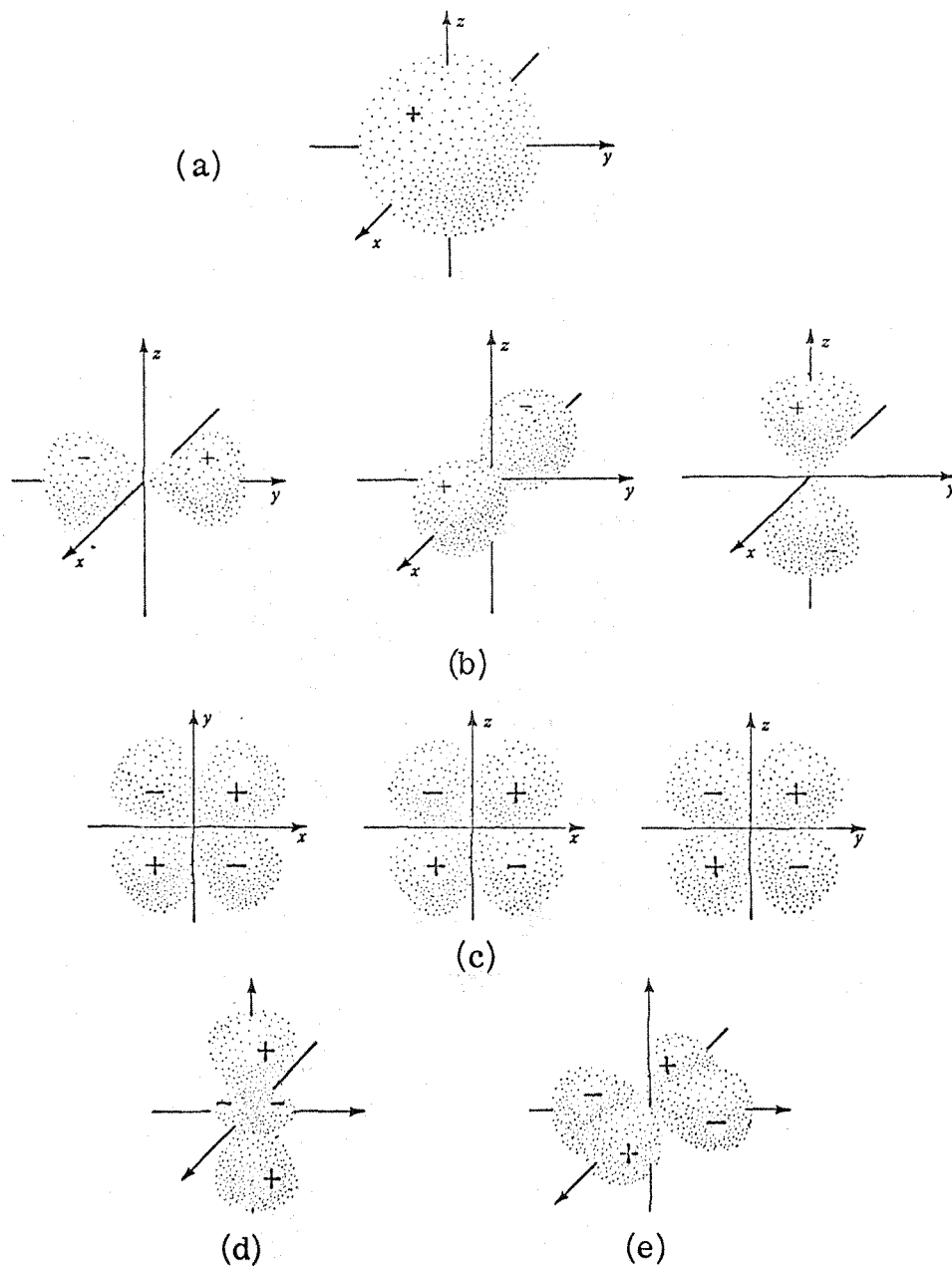
The oxidation state can be as high as seven with many examples below seven. There are few examples of anionic central metals with the ligands in these cases serving to delocalize electron density away from the metal and into the ligand. The oxidation

state of two is common, corresponding to the removal of two s electrons from the atom. The oxidation state of three is found in many thermally stable coordination compounds.

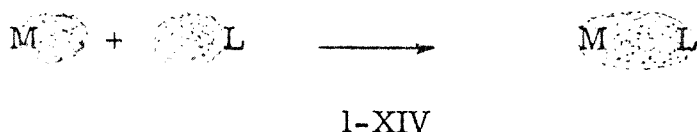
Since photochemists are interested in thermally stable systems they have focused on the systems which have stable  $d^n$  configurations. There is special stability associated with filled and half-filled configurations. The configurations  $d^3$  and  $d^6$  for six-coordinate complexes represent half-filled or filled low-lying d orbitals, and it is not surprising that most photochemistry is found here. The  $d^3$  system of most fame is Cr(III) while  $d^6$  systems include Cr(0), Mo(0), W(0), Mn(I), Re(I), Fe(II), Ru(II), Os(II), Co(III), Rh(III), Ir(III), and Pt(IV). All of the above metals have been explored by photochemists, and the oxidation states zero through four are well represented. The eight-coordinate cyanide complexes of Mo(V) and W(V) provide two examples of oxidation state (V). Other oxidation states have received little or no attention from photochemists.

Bonding. The ligands, L of  $ML_n$  molecules can be classified on the basis in which they are bonded to the metal. The transition metals have d, s, and p orbitals available for bonding interactions. The ligand orbitals of the same symmetry as the metal orbitals can have non-zero overlap with the metal orbitals and give rise to a binding interaction. The shapes of the electron density cloud of metal orbitals are shown in Figure I-1.

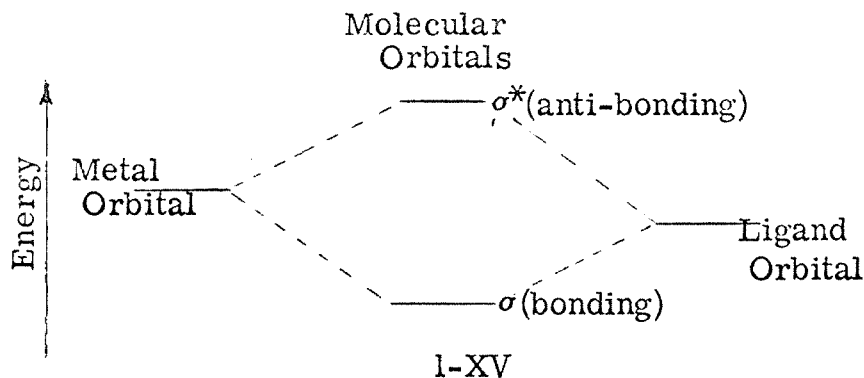
Figure I-1. Shapes of metal orbitals available for bonding:  
 (a) s orbital, (b)  $p_y$ ,  $p_x$ , and  $p_z$  orbitals, (c)  $d_{xy}$ ,  
 $d_{xz}$  and  $d_{yz}$  orbitals, (d)  $d_{z^2}$  orbital and (e)  
 $d_{x^2-y^2}$  orbital.



The simplest ligand is one which has an orbital able to give rise to sigma ( $\sigma$ ) bonds as in 1-XIV. Positive orbital overlap

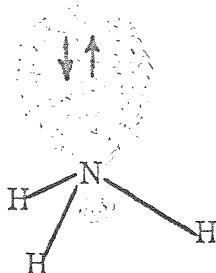


results in a bonding situation while an anti-bonding orbital is formed by negative overlap. The combination of the metal orbital of  $\sigma$  symmetry and a ligand orbital of  $\sigma$  symmetry gives the  $\sigma$  molecular orbital. For a simple case this is shown in 1-XV. Virtually all ligands interact in a  $\sigma$  fashion to some



degree. Ligands which are almost exclusively interacting in a  $\sigma$  fashion include those that have a pair of nonbonding electrons. These so called  $\sigma$ -donor ligands include amines, ethers, alcohols, water, ketones, etc. The orbital containing the lone pair of electrons, say for  $\text{NH}_3$ , has a spatial distribution of electron density represented by the cloud above the nitrogen as

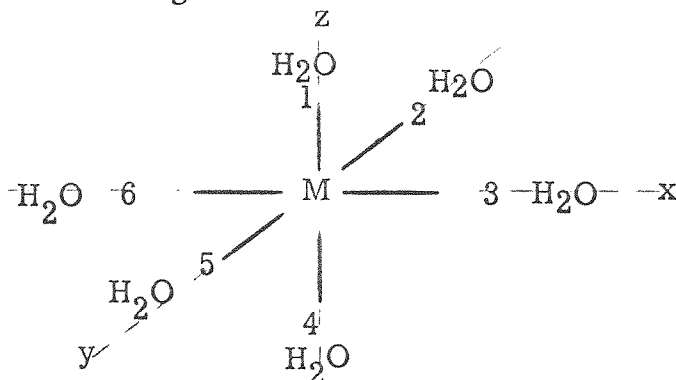
shown in 1-XVI. This orbital can have positive overlap with the



1-XVI

metal s, p, and d orbitals. We should point out that we can see from symmetry which orbitals will have positive overlap, but evaluating the contribution of a particular interaction is often a guess. However, we are describing the sharing of electrons between two atomic nuclei which constitutes a bonding interaction. A pictorial representation of the overlap of the metal orbitals with a  $\sigma$ -donor is shown in Figure I-2.

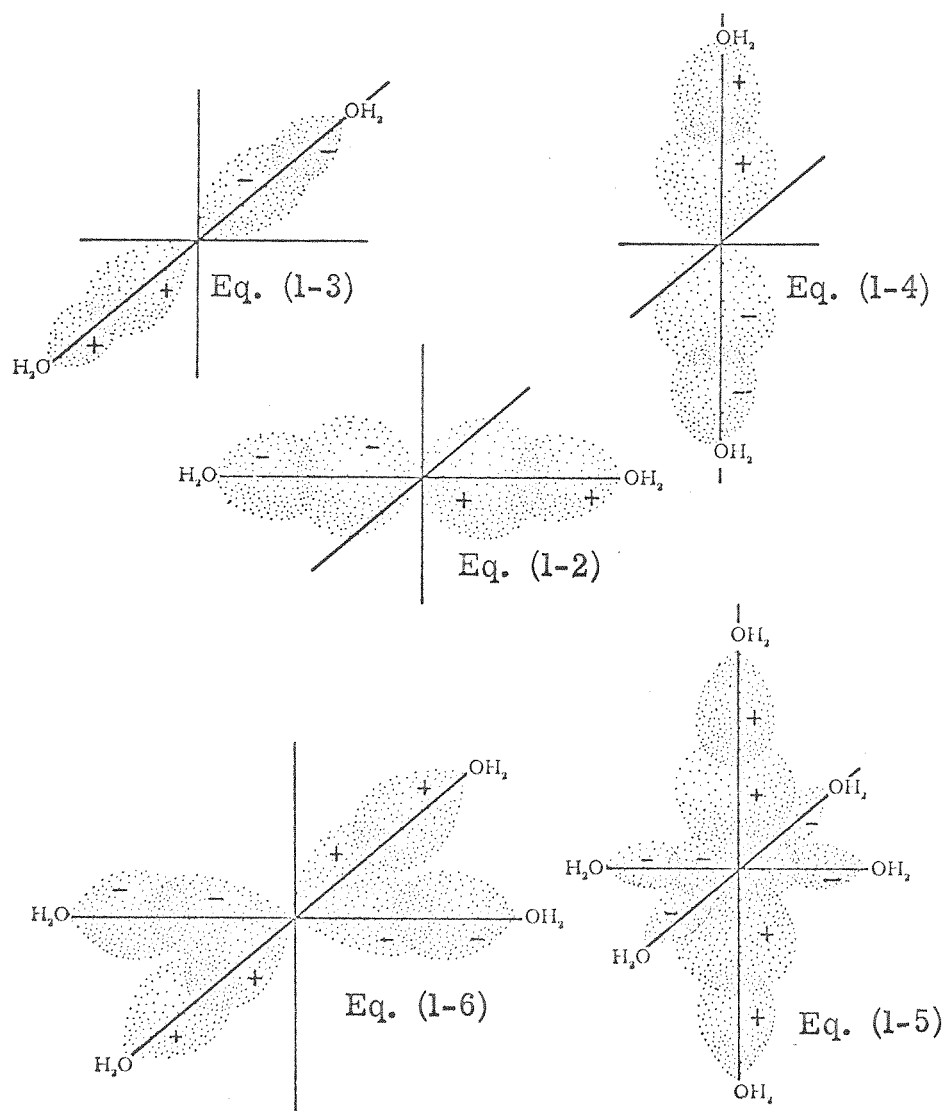
As pointed out above six coordination is the most important structure so we will discuss bonding of a metal with six  $\sigma$ -donor ligands. The labeling scheme will be that of 1-XVII. The ligands



1-XVII

present six  $\sigma$  orbitals,  $\sigma_1$ ,  $\sigma_2$ ,  $\sigma_3$ ,  $\sigma_4$ ,  $\sigma_5$ ,  $\sigma_6$ , and

Figure I-2. Overlap of metal orbitals and ligand sigma orbitals to form the molecular orbitals defined by equations (1-2) through (1-6) in the text.



the metal has the  $s$ ,  $p_x$ ,  $p_y$ ,  $p_z$ ,  $d_{x^2-y^2}$ , and  $d_{z^2}$  available to form positive overlap. The  $s$  orbital has no nodes and combines with the positive  $\sigma_n$  orbitals, equation (1-1). The other metal

$$\sigma_s = c_1 s + c_2 (\sigma_1 + \sigma_2 + \sigma_3 + \sigma_4 + \sigma_5 + \sigma_6) \quad (1-1)$$

orbitals will interact with ligands of appropriate sign and magnitude to form the other molecular bonding orbitals, equations (1-2) through (1-6). The negative overlap forms the  $\sigma^*$  orbitals.

$$\sigma_x = c_3(p_x) + c_4(\sigma_3 - \sigma_6) \quad (1-2)$$

$$\sigma_y = c_5(p_y) + c_6(\sigma_5 - \sigma_2) \quad (1-3)$$

$$\sigma_z = c_7(p_z) + c_8(\sigma_1 - \sigma_4) \quad (1-4)$$

$$\sigma_{z^2} = c_9(d_{z^2}) + c_{10}(\sigma_1 + \sigma_4 - \sigma_2 - \sigma_3 - \sigma_5 - \sigma_6) \quad (1-5)$$

$$\sigma_{x^2-y^2} = c_{10}(d_{x^2-y^2}) + c_{11}(\sigma_3 - \sigma_2 + \sigma_6 - \sigma_5) \quad (1-6)$$

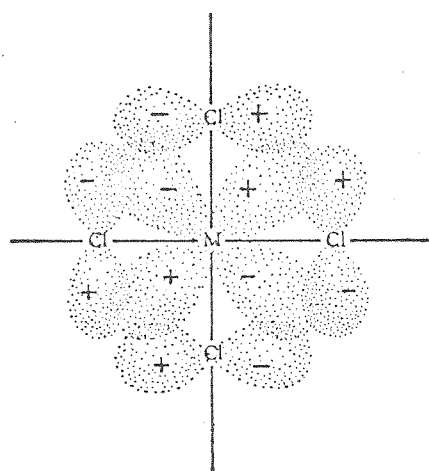
Only the metal  $d_{xy}$ ,  $d_{xz}$ , and  $d_{yz}$  orbitals have no possibilities for overlap in  $O_h$  symmetry with  $\sigma$ -donor ligands. These orbitals are thus nonbonding and maintain their metal localized character in such complexes. The remaining metal orbitals, however, do contribute to the bonding and in  $ML_6$  cannot be thought of as strictly metal-localized. The magnitude of the coefficients  $c_1$  through  $c_{11}$  and their contribution to the bonding occupies the minds of theorists and experimentalists alike.

The second type of bonding that can occur concomitant with  $\sigma$ -bonding is referred to as  $\pi$  bonding. Good  $\pi$  bonding



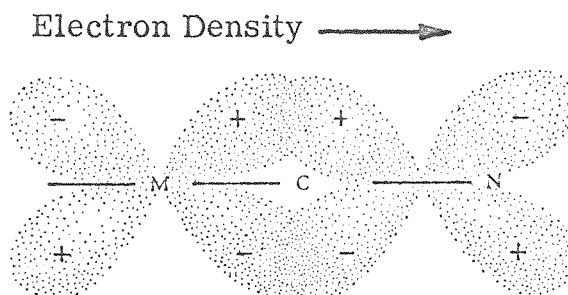
ligands can be of two types:  $\pi$ -donor or  $\pi$ -acceptor. The

$\pi$ -donor ligands are characterized by having electrons in orbitals of  $\pi$  symmetry which can be delocalized into metal orbitals of appropriate symmetry. Typical examples of  $\pi$ -donor ligands include  $F^-$ ,  $Cl^-$ ,  $Br^-$ ,  $I^-$ ,  $OH^-$ , and  $SCN^-$ . The overlap of a  $Cl^-$  and a metal  $d_{xz}$  orbital is shown in 1-XVIII. It is clear



pi-donor bonding

1-XVIII



pi-acceptor bonding

1-XIX

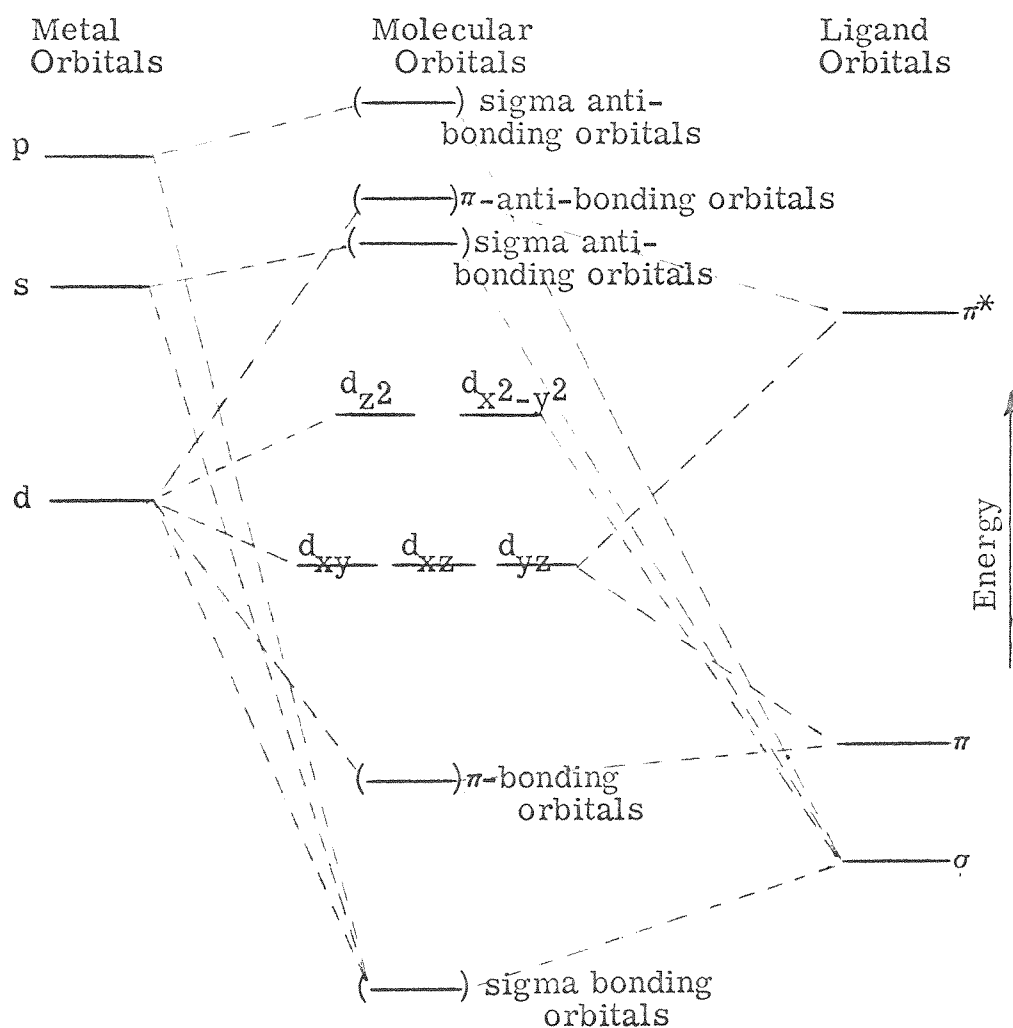
that for  $\pi$ -donor interaction to be significant there must be some metal orbital of appropriate symmetry which is unfilled, that is, a metal orbital with two electrons cannot serve as an acceptor of electron density from the ligand. The  $\pi$ -acceptor ligands play an important role in delocalizing electrons in filled metal orbitals of  $\pi$  symmetry. Good  $\pi$ -acceptor ligands have an unfilled orbital of  $\pi$  symmetry at low energies. Typical

examples are ligands which have  $\pi^*$  orbitals at low energies including  $\text{CN}^-$ , CO, ethylene, NO, etc. This  $\pi$  back bonding is illustrated in I-XIX.

The  $\pi$ -bonding ligands combine their orbitals with the  $d_{xy}$ ,  $d_{xz}$ , and  $d_{yz}$  orbitals of the metal in  $O_h$  symmetry to form  $\pi$ -molecular orbitals. To understand the effect of ligands on the metal orbitals even qualitatively we must know something about the energies of the orbitals involved. The metal orbitals generally have the order  $nd < (n+1)s < (n+1)p$  and  $\sigma$  and  $\pi$  orbitals of the ligand are more stable than the metal d orbitals. The  $\pi^*$  levels of a ligand are usually higher than the metal d orbitals. Thus we arrive at the ordering scheme in Figure I-3. In formulating the MO scheme we treat the metal orbitals in four sets: s; p;  $d_{z^2}$ ,  $d_{x^2-y^2}$  (all interacting with  $\sigma$  ligand orbitals); and  $d_{xy}$ ,  $d_{xz}$ ,  $d_{yz}$  (interacting with  $\pi$  and  $\pi^*$  ligand orbitals). The absolute placement of the energy levels is unspecified here but can be determined experimentally in some cases. The interaction of metal and ligand orbitals was developed here for the six-coordinate  $O_h$  system, but other coordination numbers and geometries are similar, and the reader is referred to the texts listed at the end of the chapter.

The MO scheme of energy levels tells us what contributes to the bonding of a metal and ligand, but it does not yield a satisfying description of bonding like the two electron localized

Figure I-3. Molecular orbital formulation for an octahedral  $ML_6$  system. Diagram indicates typical ordering of orbitals and shows which metal and ligand orbitals overlap to form the molecular orbitals.



bonding picture presented for carbon-carbon bonds. However, we can gain some feel for the important binding interaction by experiments associated with ligand exchange. Photochemical ligand exchange may clarify the bonding picture since we can change the electronic structure discretely and compare reactivity of the excited states with the ground states.

Bibliography

1. H. B. Gray, "Electrons and Chemical Bonding", W. A. Benjamin, Inc., New York, 1965.
2. F. A. Cotton and G. Wilkinson, "Advanced Inorganic Chemistry", Interscience, New York, 1966.
3. C. S. G. Phillips and R. J. P. Williams, "Inorganic Chemistry", vols. I and II, Oxford University Press, New York, 1965.

## CHAPTER II

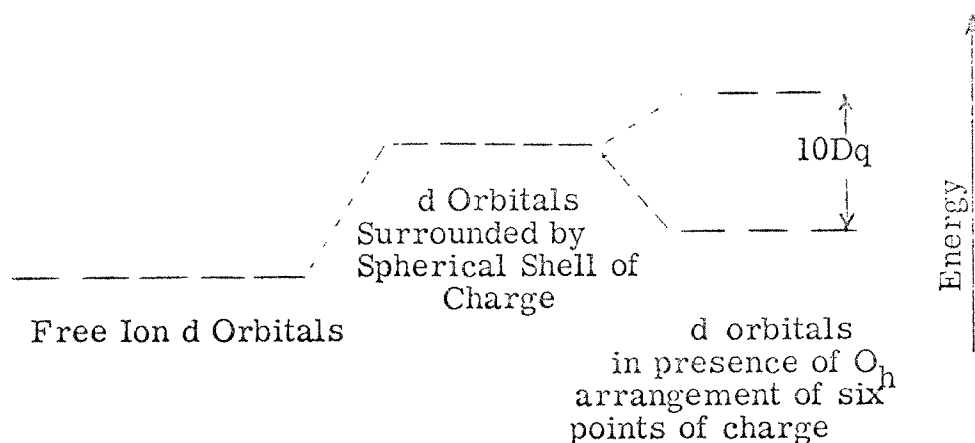
Electronic Absorption Spectroscopy of  
Transition Metal Complexes

The electronic absorption spectroscopy of transition metal-containing molecules has proved to be a powerful tool in the elucidation of electronic structure. Interest has been focused on the transitions which give rise to the wide array of colors associated with coordination compounds. The d-d (metal-localized) transitions give rise to the colors, but the charge transfer and ligand localized transitions are also important for an understanding of the excited state properties of these molecules.

Since transition metals may be defined as systems whose highest occupied orbitals are d orbitals, we will consider first the characteristic d-d transitions. A free metal ion of  $d^n$  configuration where  $9 > n > 1$  can be perturbed by large inter-electronic repulsion effects which give rise to a number of atomic terms. The ion can then be subjected, say, to an electrostatic type of perturbation brought about by surrounding the ion with ligands. The ligand field causes splitting of the atomic terms and gives rise to electronic states of the complex. The case where the ligand field is a small perturbation on the ion relative to the perturbation of interelectronic repulsion is called the weak field case, and the ligands are referred to as weak field ligands. Alternately, the ligand field can be a very large perturbation on the ion relative to the interelectronic repulsion,

and this is called the strong field case. In the strong field case the d orbitals provide a set of wavefunctions for the system (when the interelectronic repulsions are neglected). Application of the perturbation of interelectronic repulsion gives rise to electronic states for the system.

Let us apply the perturbation of a ligand field on the free ion d orbitals. A spherical shell of charge surrounding an ion will cause a rise in the energy of all of the d orbitals. Distributing the spherical charge as six points of charge in an octahedral arrangement will affect the free ion d orbitals differently (2-I).

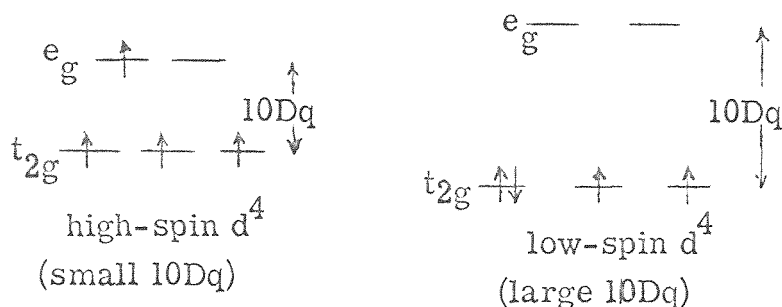


2-I

Orbitals with lobes pointing directly at the point charges will be increased in energy ( $d_{z^2}$ ,  $d_{x^2-y^2}$ ), and those with lobes between the point charges are stabilized. The orbitals  $d_{z^2}$  and  $d_{x^2-y^2}$  have

the symmetry representation  $e_g$  in  $O_h$  symmetry and  $d_{xy}$ ,  $d_{xz}$ ,  $d_{yz}$  are  $t_{2g}$ . The orbitals are filled with electrons, filling lowest energy orbitals first but obeying Hund's rule of maximum multiplicity and the Pauli exclusion principle. The energy separation of the  $e_g$  and  $t_{2g}$  orbitals is  $10Dq$ . The value of  $10Dq$  ranges from  $\sim 5000 \text{ cm}^{-1}$  to  $\sim 40,000 \text{ cm}^{-1}$  for typical coordination compounds. The strong field configurations are  $t_{2g}^n e_g^m$  where  $n$  and  $m$  refer to the number of electrons occupying either  $t_{2g}$  or  $e_g$ . In filling the orbitals no problems arise with the  $d^1(t_{2g}^1)$  doublet state,  $d^2(t_{2g}^2)$  triplet state, or the  $d^3(t_{2g}^3)$  quartet state. However, at  $d^4$ ,  $d^5$ ,  $d^6$ , and  $d^7$  two possibilities exist: for example, at  $d^4$  we can have a  $t_{2g}^3 e_g^1$  (quintet) or a  $t_{2g}^4$  (triplet) configuration. In the quintet we obey Hund's rule of maximum multiplicity at the expense of the  $10Dq$ , but in the triplet we get instability from the spin pairing energy. The configuration, then, will depend on  $10Dq$  (ultimately, therefore, the nature of the ligands). The population of the  $e_g$  orbitals before spin pairing in the  $t_{2g}$  orbitals gives rise to high spin complexes, and population of  $t_{2g}$  and spin pairing gives low spin complexes. Strong field ligands (large  $10Dq$ ) give low spin complexes, and weak field ligands (small  $10Dq$ ) give high spin complexes. The high spin and low spin configurations for  $d^4$  are diagrammed in 2-II.





## 2-II

The different configurations have different energies and interconversion of the configurations requires absorption of energy in some form. Ultraviolet, visible, and sometimes infrared light are energetic enough to change the electronic configuration. The theory of the interaction of electromagnetic energy and matter is beyond the scope of this discussion, but suffice it to say that the absorption of light can convert the ground state configuration to a more energetic, excited state, configuration. The ground and excited states have different physical properties and thus, photochemistry is possible.

In coordination compounds we are not dealing with ligands which are point charges, rather the ligands do interact with the metal with a degree of covalent bonding between the metal and the ligand. In Chapter I we pointed out the possible overlap between metal d orbitals and the ligand orbitals and found that the d orbitals are split due to different modes of interaction.

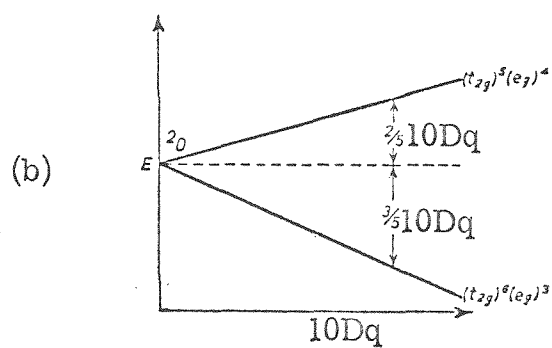
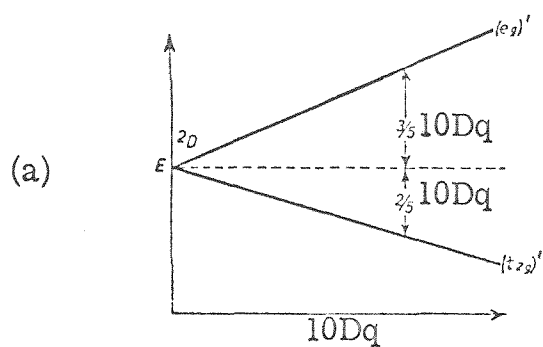
It is now generally accepted that the MO scheme is a reasonable approach to consideration of the splitting of the d orbitals.

Further, the interconverting of electronic configurations with light resulting in different bonding interactions is more compatible with the notion that irradiation at energies of so-called d-d transitions results in new chemistry.

Even in the MO framework the highest occupied orbitals are those mainly associated with the metal. Thus, the lowest energy transitions are typically the  $\pi\text{-d}(t_{2g}) \rightarrow \sigma^*\text{d}(e_g)$  in  $O_h$  symmetry.

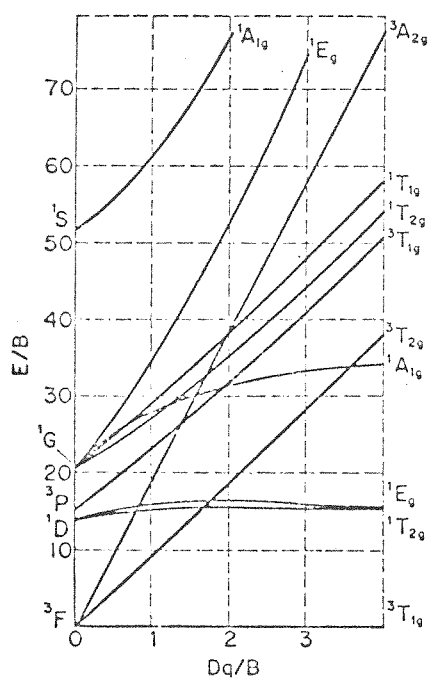
The  $d^1$  case represents the simplest configuration since there will be no interelectronic repulsion. The free ion term  $^2D$  (where the superscript is the multiplicity and D represents the total angular momentum) is affected by the ligand field and gives a smooth dependence on the ligand field strength, Figure II-1. Since no interelectronic repulsion perturbation is present the one electron configurations in the strong field case represent the true electronic states for all values of the ligand field. The only two configurations are the  $t_{2g}^1$  and the  $e_g^1$  giving the  $^2T_{2g}$  and  $^2E_g$  states separated by the energy  $10Dq$ . Since only one electron is present only one multiplicity is possible. In the  $d^1 \text{ Ti(H}_2\text{O)}_6^{3+}$  ion the d-d transition occurs at  $\sim 20 \text{ km}^{-1}$ . The value of  $10Dq$  is thus the transition energy in this simple case. It can be shown that a  $d^n$  configuration and a  $d^{10-n}$

Figure II-1. Splitting of ground and excited states as a function of  $10Dq$  in  $O_h$  field for (a) the  $d^1$  case and (b) the  $d^9$  case.

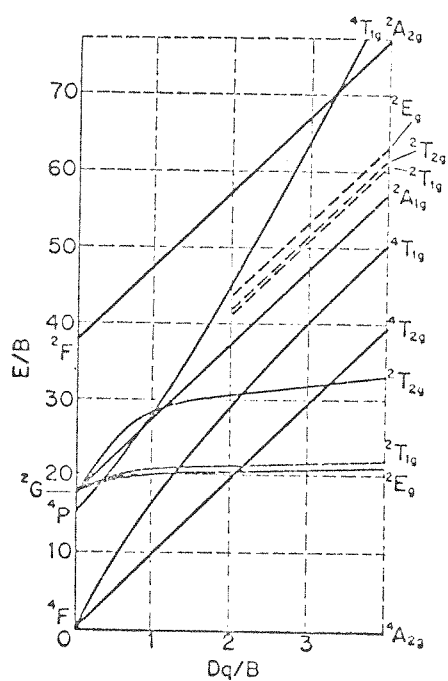


configuration are closely related: they contain the same states. However, the states are ordered differently energetically. The "hole formalism" allows us to determine the relative ordering. Consider  $d^9$  compared to  $d^1$ . The configurations for  $d^9$  are  $t_{2g}^6 e_g^3$  (ground state) and  $t_{2g}^5 e_g^4$  (excited state). The ground state has one hole in  $e_g$  and thus is the  ${}^2E_g$  state corresponding to the one electron in  $e_g$  for  $d^1$ . The excited state  $d^9$  configuration has a hole in  $t_{2g}$  and is analogously the  ${}^2T_{2g}$  state. The notion is that "holes" of  $d^{10-n}$  can be treated as the electrons of  $d^n$ .

As pointed out above, for  $d^n$ ,  $9 > n > 1$ , the interelectronic repulsion perturbation will not be negligible. In these cases the dependence of the energy ordering of the states is not a simple or even monotonic function of the ligand field strength. Fortunately the problem can be worked out, and the relative energy of the states and the dependence on  $10Dq$  is generally found in Tanabe-Sugano diagrams for octahedral or tetrahedral complexes, Figures II-2 through II-5. The Tanabe-Sugano diagrams presented here must be used with some caution. The contribution of interelectronic repulsions to the energy splittings of the electronic states is a function of two parameters  $B$  and  $C$  (Racah parameters). These two parameters are the only ones required if attention is restricted to  $d$  electrons. The Tanabe-Sugano diagrams have been calculated for only one value of



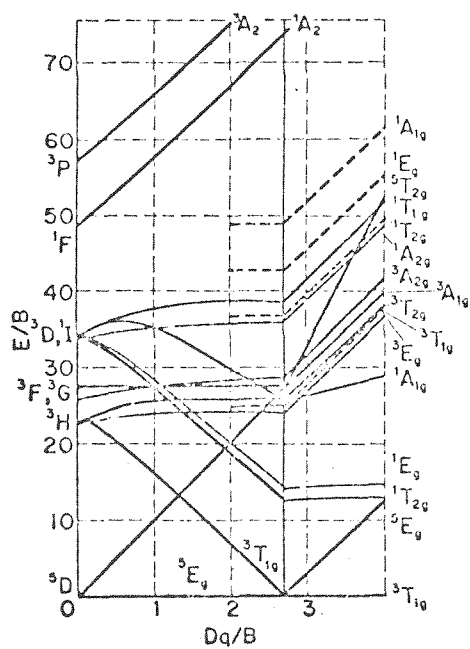
(a)



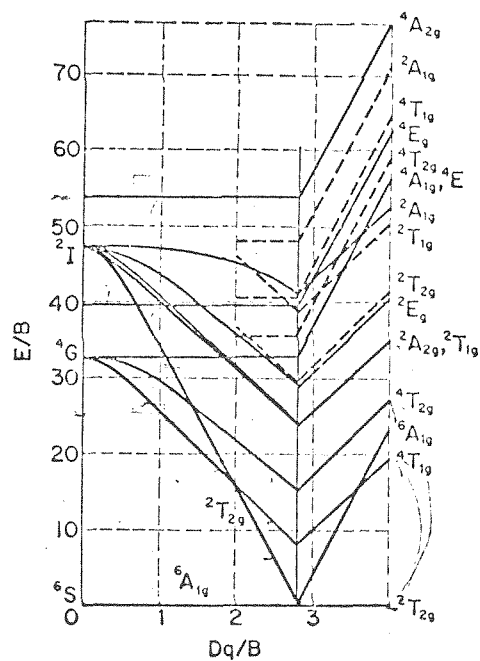
(b)

Figure II-2. Tanabe-Sugano diagrams for  $d^2$ ,  $C/B=4.42$  (a) and  $d^3$ ,  $C/B=4.50$  (b). (From reference 7.)

Figure II-3. Tanabe-Sugano diagrams for  $d^4$ ,  $C/B=4.6$  (a) and  $d^5$ ,  $C/B=4.48$  (b). (From reference 7.)



(a)



(b)

Figure II-4. Tanabe-Sugano diagram for  $d^6$ . (From ref. 7.)

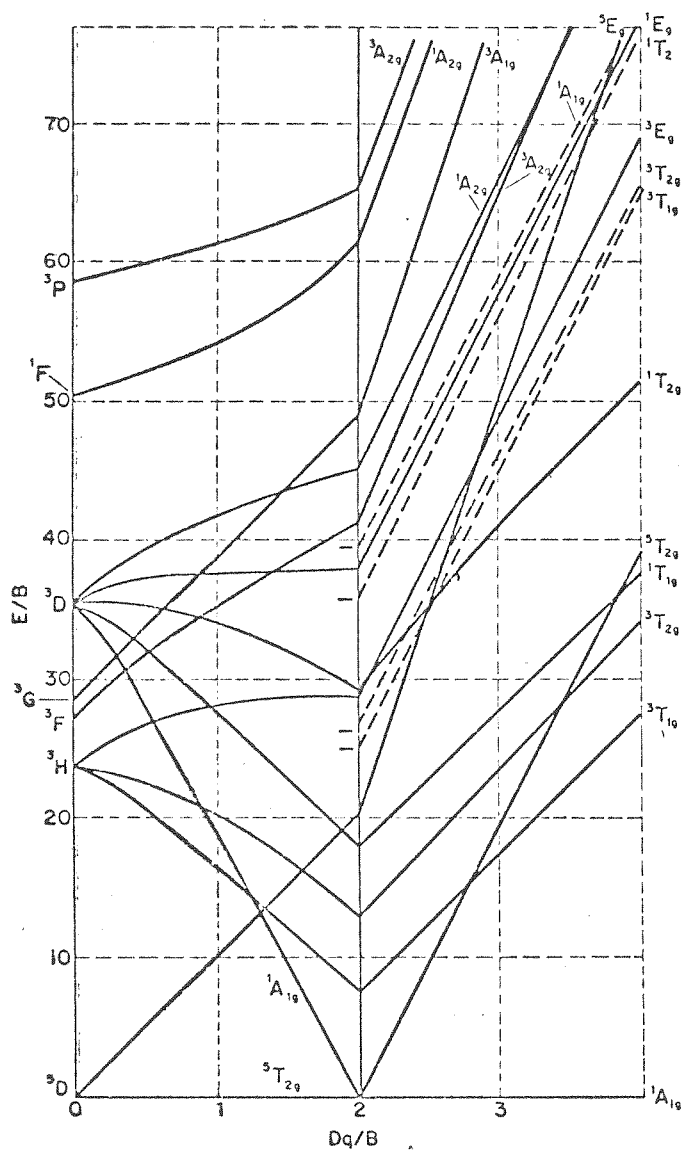
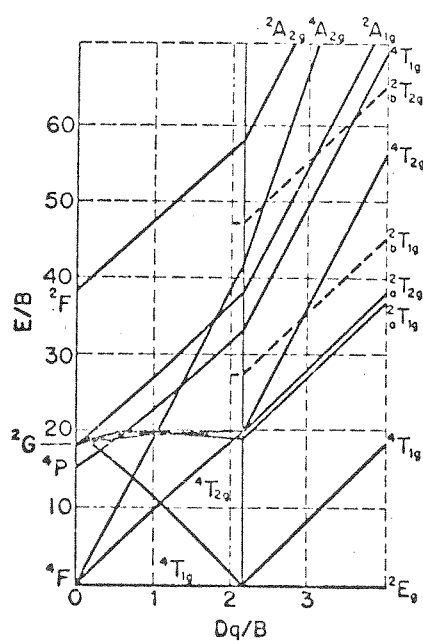
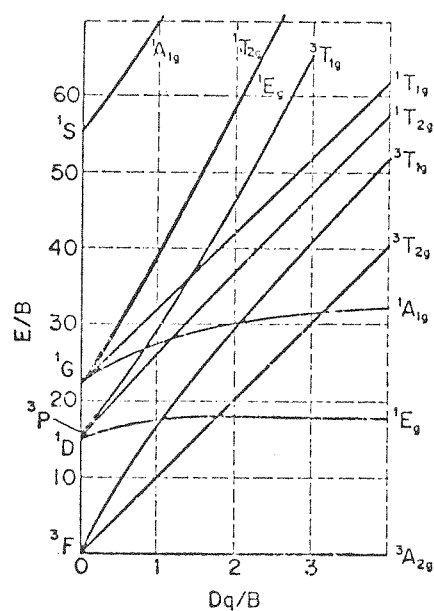


Figure II-5. Tanabe-Sugano diagrams for  $d^7$ ,  $C/B=4.63$  (a) and  $d^8$ ,  $C/B=4.71$  (b). (From ref. 7.)



(a)



(b)



$C/B$ , and it is not possible to predict how the diagrams will change for other values of  $C/B$ . The value of  $C/B$  in the diagrams are for representative first row transition metal ions. In Table II-1 we show some  $B$  values and the  $C/B$  ratio for the free ions. It is helpful that splittings of states of the same multiplicity are only functions of  $B$ , but photochemists often deal with spin-forbidden electronic transitions. Further, the Tanabe-Sugano diagrams do not include the perturbation of spin-orbital coupling. This perturbation, the coupling between the spin and orbital angular momenta of the electrons, serves to remove the degeneracy of some states. For the first row transition metals the perturbation is small relative to the interelectronic repulsions, but for the heavy second and third row metals this is not a valid statement. The energy splitting of states is related to the spin-orbital coupling parameter,  $\zeta$ , and some free ion spin-orbital coupling parameters are shown in Table II-2. The spin-orbital coupling usually results in splitting of the states by only a small amount compared to absorption bandwidths. However, the first row metals may have splittings of several hundred wavenumbers, and the heavy metals may have a much larger value. The Tanabe-Sugano diagrams do provide a good qualitative feel for the energies of states as a function of  $10Dq$ . Further, since it can be shown that  $O_h$   $d^n$  configurations are equivalent to  $T_d$   $d^{10-n}$  configurations we can gain an qualitative feel for the position of states in the four-coordinate  $T_d$  complexes.

Table II-1. The Parameters of Electron Repulsion for Transition Element Free Ions. The Entries are B in cm<sup>-1</sup>. The Ratio C/B is in Parentheses. For the Second and Third Transition Series the Values Quoted are not Always Very Reliable<sup>a</sup>

Charge	0	1+	2+	3+	4+
Element					
Ti	560, (3.3)	680, (3.7)	720, (3.7)		
Zr	250, (7.9)	450, (3.9)	540, (3.0)		
Hf	280	440, (3.4)			
V	580, (3.9)	660, (4.2)	765, (3.9)	860, (4.8)	
Nb	300, (8.0)	260, (7.7)	530, (3.8)	600, (2.3)	
Ta	350, (3.7)	480, (3.8)			
Cr	790, (3.2)	710, (3.9)	830, (4.1)	1030, (3.7)	1040, (4.1)
Mo	460, (3.9)	440, (4.5)			680
W	370, (5.1)				
Mn	720, (4.3)	870, (3.8)	960, (3.5)	1140, (3.2)	
Te					
Re	850, (1.4)	470, (4.0)			
Fe	805, (4.4)	870, (4.2)	1060, (4.1)		
Ru	600, (5.4)	670, (3.5)	620, (6.5)		
Os					
Co	780, (5.3)	880, (4.4)	1120, (3.9)		
Rh					
Ir					
Ni	1025, (4.1)	1040, (4.2)	1080, (4.5)		
Pd			830, (3.2)		
Pt					
Cu		1220, (4.0)	1240, (3.8)		
Ag					
Au					

<sup>a</sup>Reference 7.

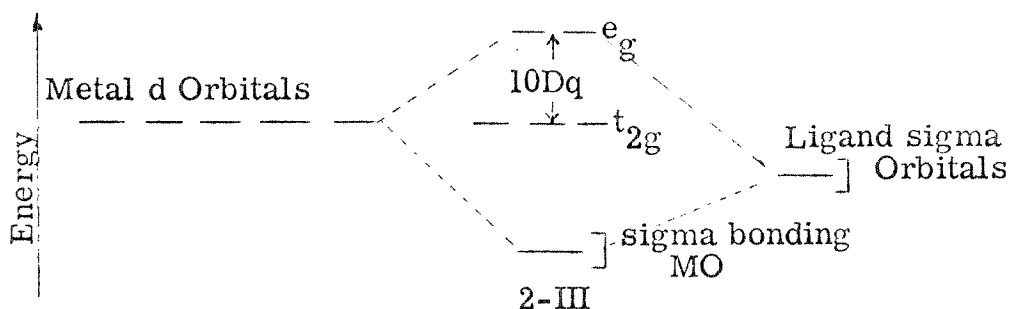
Table II-2. Free Ion Single Electron Spin-Orbit Coupling Parameters  
( $\zeta_{nd}$ ) for Transition Elements (cm<sup>-1</sup>). Values in  
Parenthesis are Only Estimates<sup>a</sup>

Metal	Charge	0	1+	2+	3+	4+	5+	6+
Ti		70	90	123	155			
Zr			(300)	(400)	(500)			
Hf								
V		95	135	170	210	250		
Nb			(420)	(610)	(800)			
Ta					(1400)			
Cr		135	185	230	275	355	380	
Mo				(670)	800	(850)	(900)	
W				(1500)	(1800)	(2300)	(2700)	
Mn		190	255	300	355	415	475	540
Te				(950)	(1200)	(1300)	(1500)	(1700)
Re				(2100)	(2500)	(3300)	(3700)	(4200)
Fe		275	335	400	460	520	590	665
Pu					(1250)	(1400)	(1500)	(1700)
Os					(3000)	(4000)	(4500)	(5000)
Co		390	455	515	580	650	715	790
Rh						(1700)	(1850)	(2100)
Ir						(5000)	(5500)	(6000)
Ni			565	630	705	790	865	950
Pd			(1300)	(1600)				
Pt			(3400)					
Cu				830	890	960	1030	1130
Ag				(1800)				
Au				(5000)				

<sup>a</sup>Reference 7.

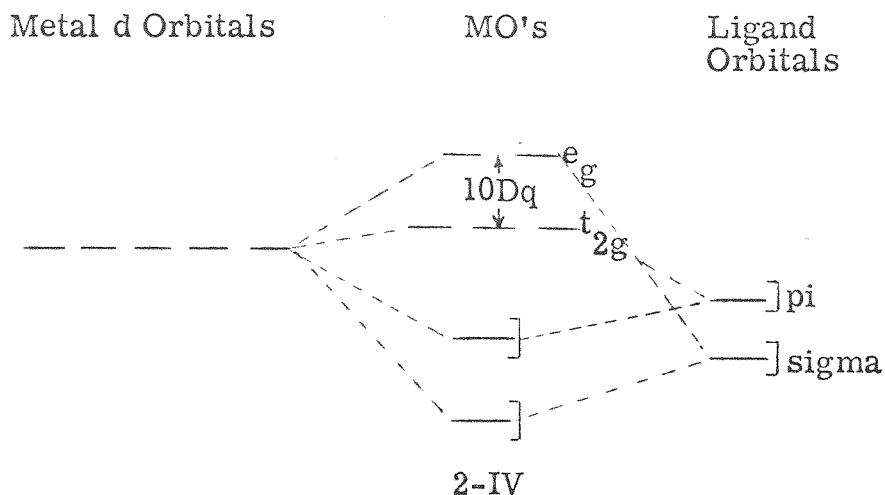
It is both useful and interesting to consider which configuration is associated with the states. For example, consider the  $d^2$  case. The first excited state merely involves the transformation  $t_{2g}^2$  (triplet)  $\rightarrow$   $t_{2g}^2$  (singlet); i. e., spin pairing, not the  $t_{2g}^2 \rightarrow t_{2g}^1 e_g^1$  conversion. This is a somewhat confusing point, but it is to be emphasized that the molecular orbital schemes themselves do not provide a complete picture of the possible excited states; on the other hand, a clearer picture of the distribution of electron density can be obtained by examining the possible one-electron excitations.

Let us now consider in more detail the origin and magnitude of the splitting of the d orbitals in  $O_h$  symmetry. Basically, there are three types of interactions with d orbitals and ligand orbitals:  $\sigma$ ,  $\pi$ -donor, and  $\pi$ -acceptor. The  $\sigma$ -donor ligands interact only with the  $d_{z^2}$  and  $d_{x^2-y^2}$  ( $e_g$ ) orbitals, 2-III. The

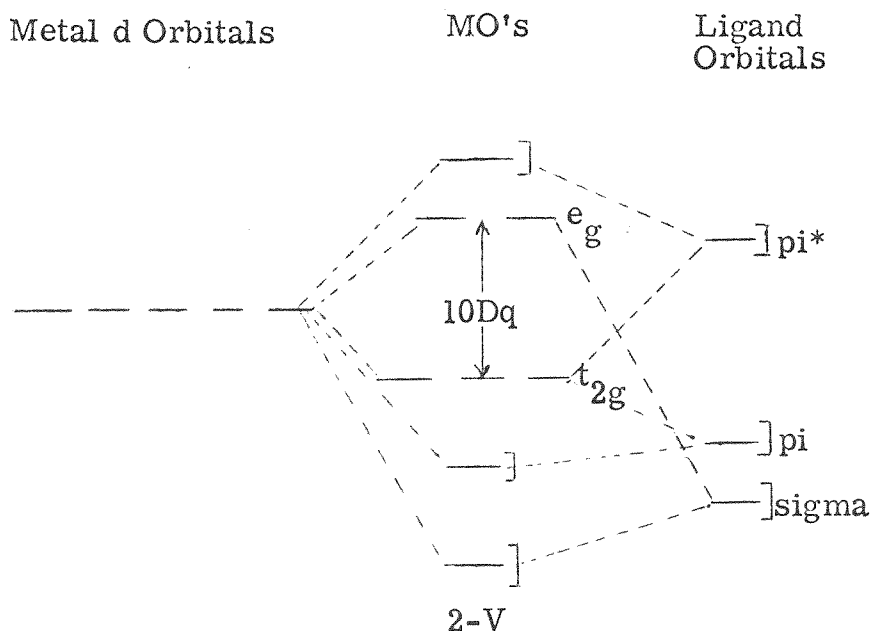


$\pi$ -donor ligands also interact with  $d_{xy}$ ,  $d_{xz}$ ,  $d_{yz}$  giving rise

to a scheme as in 2-IV. Good  $\pi$ -acceptor ligands have a large



stabilizing effect on the  $t_{2g}$  ( $\pi$ -d) orbitals and give rise to a scheme as in 2-V. The MO scheme predicts that good



$\pi$ -acceptor ligands will give the largest  $10Dq$ ,  $\sigma$ -donors intermediate values, and strong  $\pi$ -donors will give the smallest

10Dq. From investigation of the electronic transitions in coordination compounds this trend has been verified (cf. below Table II-5).

Before we turn to a consideration of the absorption spectroscopy of some model systems we will discuss selection rules for metal localized transitions. In general, transitions involving changes in multiplicity are forbidden. However, a mechanism for obtaining observable transition intensities is available. The spin selection rule is relaxed by the coupling between spin and orbital angular momenta. The spin-orbital coupling increases as one moves to the right in the transition series and as one moves from first to third row transition metals. The observation of spin-forbidden bands is common even on the first row. Consider the high spin  $d^5$  configuration  $t_{2g}^3 e_g^2$ . In this case all transitions are spin-forbidden, but we do see transitions in high spin  $Mn^{2+}$  complexes. In the lighter metals spin-forbidden bands have intensities an order of magnitude less than the spin-allowed bands, while third row metals can have spin-forbidden bands approaching the intensity of the allowed transitions. A second selection rule of great importance here is the Laporte selection rule. The origin of this rule is from the orbital properties of the wave functions. The rule states that transitions between states with symmetry designations having subscripts that are the same are Laporte forbidden. Thus,  ${}^3T_{1g} \rightarrow {}^3T_{2g}$  is forbidden, but a  ${}^3T_{1g} \rightarrow {}^3T_{1u}$  is

allowed; both  $u \rightarrow u$  and  $g \rightarrow g$  transitions are Laporte forbidden. The states of  $O_h$  symmetry have g subscripts and are all Laporte forbidden. Other symmetries, which do not have a center of symmetry, do not have the subscripts, and this orbital selection rule is relaxed.

Laporte forbidden bands can gain intensity in two ways: by (1) vibronic coupling and (2) intensity stealing. The combination of electronic and vibrational wave functions gives vibronic wave functions which often relax the Laporte selection rule. Physically we can consider a molecule to be vibrating, and one can imagine distortions during vibration removing the center of symmetry and thus removing the g and u designations for the distorted geometry. Since, by the Franck-Condon principle, electronic transitions occur faster than any internuclear motion, we have a mechanism for absorption when the transition is formally Laporte forbidden. Intensity stealing merely refers to the fact that d-d transitions which are close in energy to fully allowed transitions can themselves have enhanced intensity. The effect is often observed when the d-d transition occurs in the vicinity of charge-transfer transitions. A summary of expected molar extinction coefficients for the various types of transitions is shown in Table II-3.

We will now consider the spectra of the  $d^n$  configurations in  $O_h$  symmetry for some model systems whose photochemistry is of interest.

Table II-3. Representative Values for Intensities of Electronic Transitions in Transition Metal Complexes

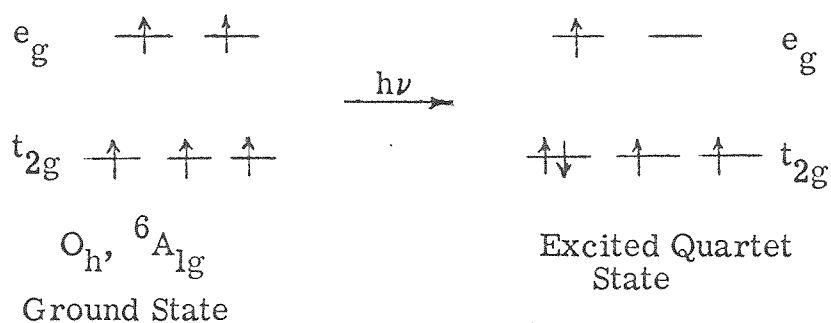
Type of Transition	Approximate $\epsilon$
Spin-forbidden, Laporte Forbidden	0.1
Spin-allowed, Laporte Forbidden	10
Spin-allowed, Laporte Forbidden but with d-p mixing ( $T_d$ complexes)	100
Spin-allowed, Laporte Forbidden but with "intensity stealing"	1,000
Spin-allowed, Laporte Allowed (charge transfer)	10,000



Six-Coordinate Complexes,  $d^3$  Systems. The Cr(III) complexes have been extensively studied. The ground state configuration is the  $t_{2g}^3$  and gives rise to the  $^4A_{2g}$  state. The Tanabe-Sugano diagram shown in Figure II-2 depicts two excited states at low energy which are not sensitive to  $10Dq$ , the  $^2E_g$  and the  $^2T_{1g}$ . These two states also arise from the  $t_{2g}^3$  configuration, and since there is no change in configuration from the ground state, the separation from the ground state is essentially independent of the splitting of the  $t_{2g}$  and  $e_g$  orbitals. The  $^4T_{2g}$  and  $^4T_{1g}$  excited states have the  $t_{2g}^2e_g^1$  configuration, and their energy relative to the ground state is strongly dependent on the value of  $10Dq$ . The absorption spectra of  $O_h$  Cr(III) fit the Tanabe-Sugano predictions giving low energy spin-forbidden transitions independent of the ligand field strength and two spin-allowed quartet to quartet transitions.<sup>1-4</sup> Other high energy electronic transitions are not always observable being masked by fully allowed charge-transfer bands. The photochemistry of Cr(III) complexes will be related to the nature of the excited state in Chapter VII.

$d^5$  Systems. While only a few systems of the  $d^5$  configuration have been of interest to photochemists several interesting points can be made concerning the electronic structure. First, since  $d^5 = d^{10-5}$ , the same Tanabe-Sugano diagram can be used for both  $O_h$  and  $T_d$  complexes. Secondly, the high spin complexes of  $d^5$  are unique in that only spin-forbidden ligand field transitions

are possible. Further, the  $10Dq$  dependence on the energy of the low lying excited state is unusual in that at high values of  $10Dq$  the state is at lower energy. This situation arises since the lowest transitions involve configurational changes like that shown in 2-VI. The energy of the transition is dominated



2-VI

by the energy necessary to pair the electrons in the  $t_{2g}$  orbitals, but an important contribution is the energy obtained ( $10Dq$ ) from demoting an electron from  $e_g$  to  $t_{2g}$ . When  $10Dq$  is large, less external energy is needed to overcome the spin-pairing energy, thus the excited state is at lower energy for strong field complexes. Manganese(II) is the most well studied high-spin  $d^5$  system, and the d-d transitions have extinction coefficients of 0.01 for  $Mn(H_2O)_6^{2+}$ .

$d^6$  Systems. Besides  $d^3$  the only other important six-coordinate  $d^n$  system is  $d^6$ . The  $d^6$  low-spin systems have good thermal stability having the  $t_{2g}^6$  configuration which only gives rise to the  ${}^1A_{1g}$  ground state. The  $t_{2g}^5 e_g^1$  configuration can give singlet and

triplet excited states:  ${}^1T_{1g}$ ,  ${}^1T_{2g}$ ,  ${}^3T_{1g}$ ,  ${}^3T_{2g}$ . The Tanabe-Sugano diagram as shown in Figure II-4 reveals a quintet state at low values of  $10Dq$  for low-spin  $d^6$ . The quintet arises from the  $t_{2g}^4 e_g^2$  configuration. Direct absorption from the singlet ground state to the quintet is strongly forbidden. The singlet to triplet transitions are expected to have some intensity especially with the second and third row transition metals.

Consider the three Co(III) complexes  $\text{CoF}_6^{3-}$ ,  $\text{Co}(\text{NH}_3)_6^{3+}$ , and  $\text{Co}(\text{CN})_6^{3-}$ . The  $\text{CoF}_6^{3-}$  has four unpaired electrons and is thus high spin. The  $\text{Co}(\text{NH}_3)_6^{3+}$  and the  $\text{Co}(\text{CN})_6^{3-}$  are both diamagnetic low-spin complexes. This magnetic information leads to the conclusion that the value of  $10Dq$  for the hexafluoro complex is less than  $10Dq$  for the hexacyano or the hexaammine complex. The absorption maximum for the  ${}^1A_{1g} \rightarrow {}^1T_{1g}$  transition for the  $\text{Co}(\text{CN})_6^{3-}$  and the  $\text{Co}(\text{NH}_3)_6^{3+}$  is shown in Table II-4.<sup>6</sup> We see that the cyanide complex has higher energy transitions than the ammine complex giving the  $\text{CN}^-$  ligand a higher field strength than  $\text{NH}_3$ . The splitting of the  $e_g$  and  $t_{2g}$  orbitals for the three Co(III) complexes is shown schematically in 2-VII.

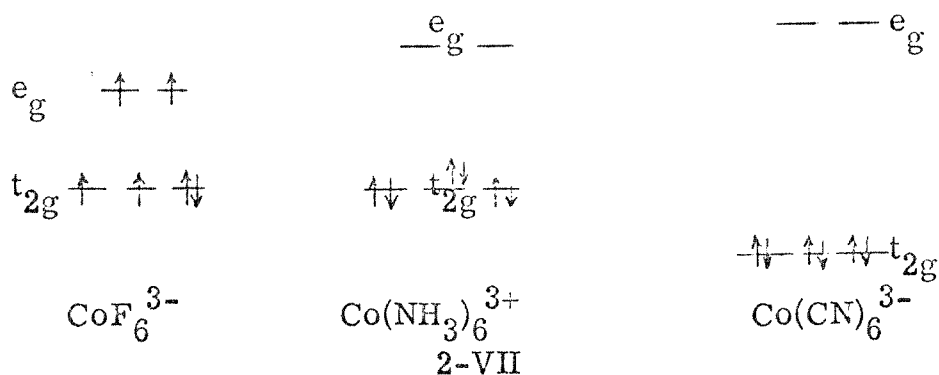
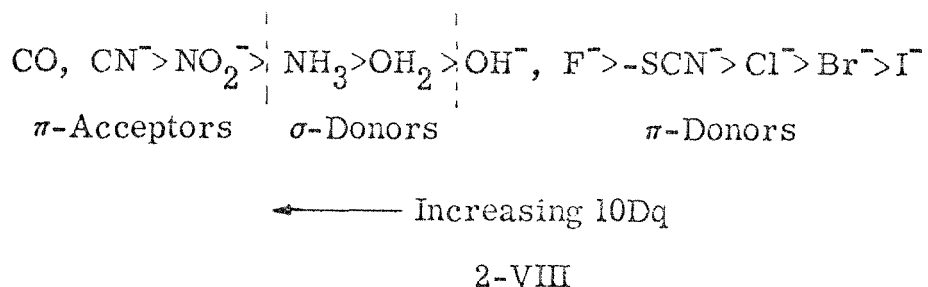


Table II-4. Band Maxima for  $O_h$  Co(III) Complexes<sup>a</sup>

Complex	${}^1A_{1g} \rightarrow {}^1T_{1g}(\text{cm}^{-1})$	${}^1A_{1g} \rightarrow {}^1T_{2g}(\text{cm}^{-1})$
$\text{Co}(\text{CN})_6^{3-}$	32,100	38,600
$\text{Co}(\text{NH}_3)_6^{3+}$	21,400	30,000

<sup>a</sup>Reference 6.

These three complexes demonstrate the effect of different types of bonding on the electronic structure of the molecule:  $F^-$  is a  $\sigma$ -donor, weak  $\pi$ -donor,  $NH_3$  is a  $\sigma$ -donor, and  $CN^-$  is a  $\sigma$ -donor,  $\pi$ -acceptor ligand. The splitting of the  $t_{2g}$  and  $e_g$  orbitals correlates well with the ligand binding modes as in 2-VIII. Compare also the diagrams 2-III through



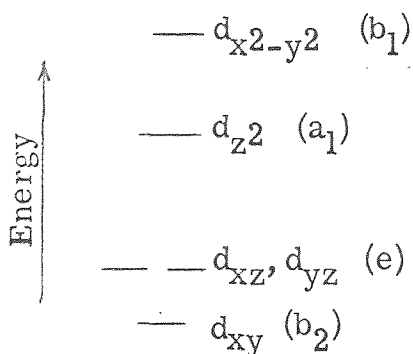
2-V. This ordering of ligands with 10Dq is called the spectrochemical series and is qualitatively maintained for all coordination compounds. The value of 10Dq can be obtained by fitting the absorption bands to the Tanabe-Sugano diagrams. In Table II-5 we present values for 10Dq for several ligands and metals.<sup>7</sup>

Lower symmetry six-coordinate systems are of interest, and an understanding of their electronic structure is essential to interpreting photochemical experiments. The spectroscopy of some  $ML_5X$  complexes has been investigated. Since the symmetry is  $C_{4v}$ , the d orbitals are ordered differently. Some  $d^6$  systems have been studied and an ordering like that in 2-IX has been found. The magnitude

Table II-5. Representative Values of 10Dq for Various Metal Ions and Ligand Groups

Deduced from Spectral Data. The Units are $\text{cm}^{-1} \times 10^{-3}$ . <sup>a</sup>									
No. of d electrons	Ion	6F	6Cl	6Br	6H <sub>2</sub> O	3ox	6NH <sub>3</sub>	3en	6CN
1	Ti <sup>3+</sup>		13		20		17?		
2	V <sup>3+</sup>	16	13		19	18	18?		
3	Cr <sup>3+</sup>		13		17	17	22	22	26
	Re <sup>4+</sup>	32	33						
4	Cr <sup>2+</sup>		13?		14			18?	
	Mn <sup>3+</sup>	22	20		21				30
5	Mn <sup>2+</sup>	8	8		8			10	
	Fe <sup>3+</sup>	14			14	14			35
6	Fe <sup>2+</sup>				10				33
	Co <sup>3+</sup>	13			19	18	24	24	34
	Rh <sup>3+</sup>		20	19	27	26	34	35	
	Ir <sup>3+</sup>		25	23				41	
	Pt <sup>4+</sup>	33	29	25					
7	Co <sup>2+</sup>				10	11	11	11	
8	Ni <sup>2+</sup>		7	6	9		11	12	
9	Cu <sup>2+</sup>				13		15	16	

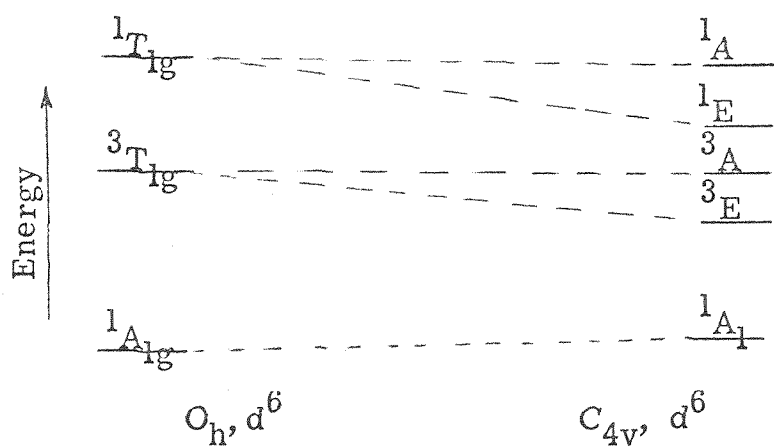
<sup>a</sup>Reference 7.



Ordering of d Orbitals  
for  $C_{4v}$  Symmetry

2-IX

of the splittings and the ordering of the orbitals will depend on the ligand field strength of X compared to the other five ligands. When the symmetry of a complex is  $C_{4v}$  the T states of  $O_h$  symmetry are split removing some degeneracy, and since there is no center of symmetry the g subscripts are not on the state designations. In 2-X we show the cor-



2-X

relation of electronic energy levels of an  $ML_6$  and an

$ML_5X$  complex when the  $C_{4v}$  has the ordering of d orbitals as shown in 2-IX. In this case the  $C_{4v}$  complex should exhibit more absorption bands, and the first absorption should be at a lower energy than the  $O_h$  complex. In cases where X is significantly weaker field than L, the E excited state can be associated with occupation of the  $d_{z^2}$  orbital in the one-electron energy level scheme.

In Table II-6 we list the position of the first transition in the  $C_{4v}$   $Co(CN)_5(X)^{n-} d^6$  complexes. This band has been assigned as the  ${}^1A_1(b_2^2 e^4) \rightarrow {}^1E(b_2^2 e^3 a_1^1)$ .<sup>8</sup> The position of this band correlates nicely with the position of X in the spectrochemical series. The higher energy transitions in these complexes are not easily assigned but are associated with the population of the  $d_{x^2-y^2}$  orbital.

Spectroscopic investigations of trans- and cis- $ML_4X_2$  complexes have been undertaken for complexes of the first row metals  $Co(III)$ <sup>9</sup>,  $Cr(III)$ ,<sup>10</sup>  $Fe(II)$ <sup>11</sup>, and  $Ni(II)$ <sup>12</sup>. While a detailed discussion of their electronic structure is not possible, we will point out a few key results. The trans- $ML_4X_2$  complexes have  $D_{4h}$  symmetry and thus have a center of inversion making the d-d transitions Laporte forbidden. The cis complexes have no center of symmetry and like the  $ML_5X$  complexes have transitions which are not affected by the Laporte selection rule. If X is a weaker field ligand than L the trans disubstituted complexes



Table II-6. Absorption Data for  $\text{Co}(\text{CN})_5(\text{X}^-)^{3-}$  Complexes

Complex	Absorption Maximum for First d-d Spin-Allowed Transition, $\text{kcm}^{-1}$ ( $\epsilon$ )
$\text{Co}(\text{CN})_6^{3-}$	32.1 (243)
$\text{Co}(\text{CN})_5(\text{SO}_3)^{4-}$	30.0 (440)
$\text{Co}(\text{CN})_5(\text{pyridine})^{2-}$	28.0 (250)
$\text{Co}(\text{CN})_5(\text{NCS})^{3-}$	27.6 (500)
$\text{Co}(\text{CN})_5(\text{SCN})^{3-}$	26.5 (191)
$\text{Co}(\text{CN})_5(\text{OH}_2)^{2-}$	26.3 (280)
$\text{Co}(\text{CN})_5(\text{N}_3)^{3-}$	26.1 (743)
$\text{Co}(\text{CN})_5(\text{I})^{3-}$	20.0 (87)

have a lower energy first transition than the  $C_{4v}$   $ML_5X$  complexes. Further, cis- $ML_4X_2$  should have a band at an energy lower than the  $C_{4v}$  complex but higher than the trans complex. The ordering of the first band should be as shown in 2-XI. The ordering



←— Energy of First Transition

L > X in the Spectrochemical Series

2-XI

of 2-XI has been verified experimentally for a number of  $d^6$  Co(III) complexes.<sup>9</sup> While the d orbital and state energy orderings vary, the qualitative energy scale may be helpful in identifying complexes.

$d^6$  Metal Carbonyls. The photosensitivity of  $d^6$  metal carbonyls makes a discussion of the electronic structure of importance. The  $M(CO)_6$  ( $M=Cr(0)$ ,  $Mo(0)$ ,  $W(0)$ ,  $Mn(I)$ , or  $Re(I)$ ) complexes have been studied.<sup>13</sup> While the complexes exhibit relatively intense transitions at low energies they are best interpreted as ligand field transitions. For the light metals the two spin-allowed bands,  $^1A_{1g} \rightarrow ^1T_{1g}$  and the  $^1A_{1g} \rightarrow ^1T_{2g}$ , were observed, and with the  $W(0)$  and  $Re(I)$  complexes the spin-forbidden  $^1A_{1g} \rightarrow ^3T_{1g}$  transition was easily discernible. In Figure II-6 we show a comparison of the  $Mo(CO)_6$  and  $W(CO)_6$  absorption spectra. We have now extended the studies to include the  $M(CO)_5X$  complexes. In

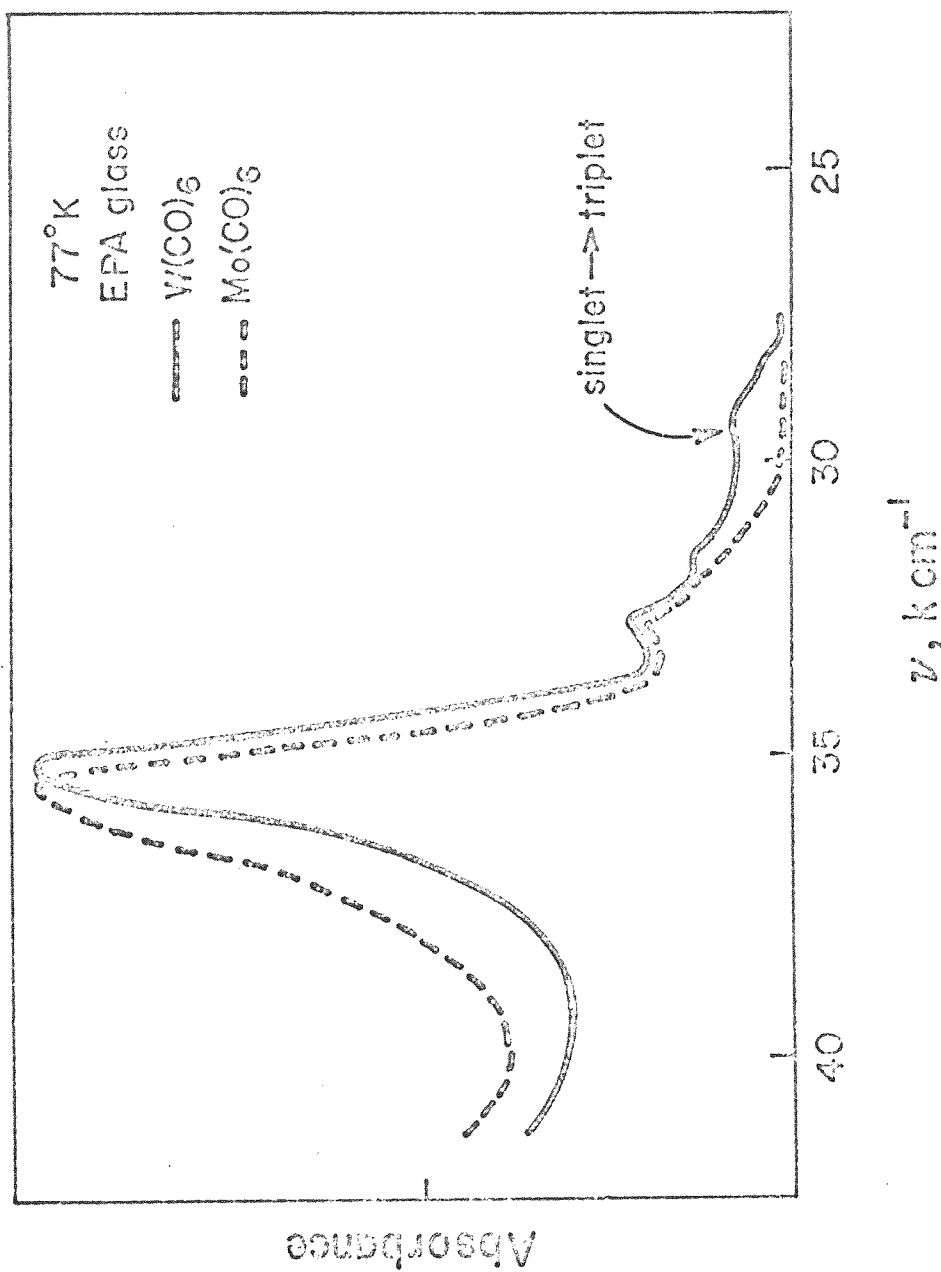


Figure II-6. Comparison of the  $W(CO)_6$  and  $Mo(CO)_6$  absorption spectra showing the position of the  $S \rightarrow T$  transition.

Table II-7 we summarize some absorption data for the  $d^6$  metal carbonyls. In analogy with the  $d^6$  cyanocobaltate(III) complexes the low energy band in the  $M(CO)_5X$  complexes is assigned as the  $^1A_1 \rightarrow ^1E$ . The low energy shoulder in the  $Re(I)$  and  $W(0)$  complexes is assigned as the  $^1A_1 \rightarrow ^3E$  absorption, Figure II-7. The following facts support the notion that the low energy absorptions in the metal carbonyls are primarily d-d transitions: (1) the position of the first band for the  $M(CO)_5X$  complexes is dependent on the ligand field strength of X, (2) the reduction in symmetry from  $O_h$  to  $C_{4v}$  gives results similar to those obtained with the cyanocobaltate(III) complexes, Figure II-8, (3) the heavy metal effect is that expected for ligand field transitions, and (4) the luminescence and photochemistry for the  $W(0)$  complexes are best rationalized assuming metal-localized excited states (Chapters III and VII). The energy of the first band of cis- $W(CO)_4(pyridine)_2$  complex is lower than that for the  $W(CO)_5(pyridine)$  consistent with the scheme 2-XI. The higher energy transitions in the  $W(CO)_5(NH_3)$  complex are seen in Figure II-9 but have not been assigned. We associate these transitions with population of the  $d_{x^2-y^2}$  orbital while the E state at low energy can be identified with population of the  $d_{z^2}$  orbital.

Four-Coordinate Systems, Tetrahedral Geometry. Four-coordinate systems of tetrahedral geometry have not been of particular interest to photochemists, but their unique relationship

Table II-7. Absorption Data for  $d^6$  Metal Carbonyls<sup>a</sup>

Compound	Abs. Max. ( $\epsilon$ ) $\text{kcm}^{-1}$	Assignment
$\text{Cr}(\text{CO})_6$	31.55 (2670)	${}^1A_{1g} \rightarrow {}^1T_{1g}$
	35.70 (13,700)	CT
	38.85 (3500)	${}^1A_{1g} \rightarrow {}^1T_{2g}$
$\text{Mo}(\text{CO})_6$	28.85 (350)	${}^1A_{1g} \rightarrow {}^3T_{1g}$
	31.95 (2820)	${}^1A_{1g} \rightarrow {}^1T_{1g}$
	34.60 (16,800)	CT
	37.20 (7900)	${}^1A_{1g} \rightarrow {}^1T_{2g}$
$\text{W}(\text{CO})_6$	28.30 (1000)	${}^1A_{1g} \rightarrow {}^3T_{1g}$
	31.85 (3250)	${}^1A_{1g} \rightarrow {}^1T_{1g}$
	34.65 (17,600)	CT
	37.10 (7400)	${}^1A_{1g} \rightarrow {}^1T_{2g}$
$(n\text{-Bu}_4)(\text{V}(\text{CO})_6)$	23.2 (300)	$\left\{ {}^1A_{1g} \rightarrow {}^1T_{1g} \right.$
	25.1 (1640)	
	28.4 (6240)	CT
	31.1 (3300)	${}^1A_{1g} \rightarrow {}^1T_{2g}$
$(\text{BF}_4)\text{Mn}(\text{CO})_6$	33.25 (600)	${}^1A_{1g} \rightarrow {}^3T_{1g}$
	39.60 (2200)	$\left\{ {}^1A_{1g} \rightarrow {}^1T_{1g} \right.$
	37.30 (1100)	
$(\text{AlCl}_4)\text{Re}(\text{CO})_6$	36.85 (708)	${}^1A_{1g} \rightarrow {}^3T_{1g}$
	38.50 (1500)	$\left\{ {}^1A_{1g} \rightarrow {}^1T_{1g} \right.$
	40.70 (2900)	

Table II-7. (continued):

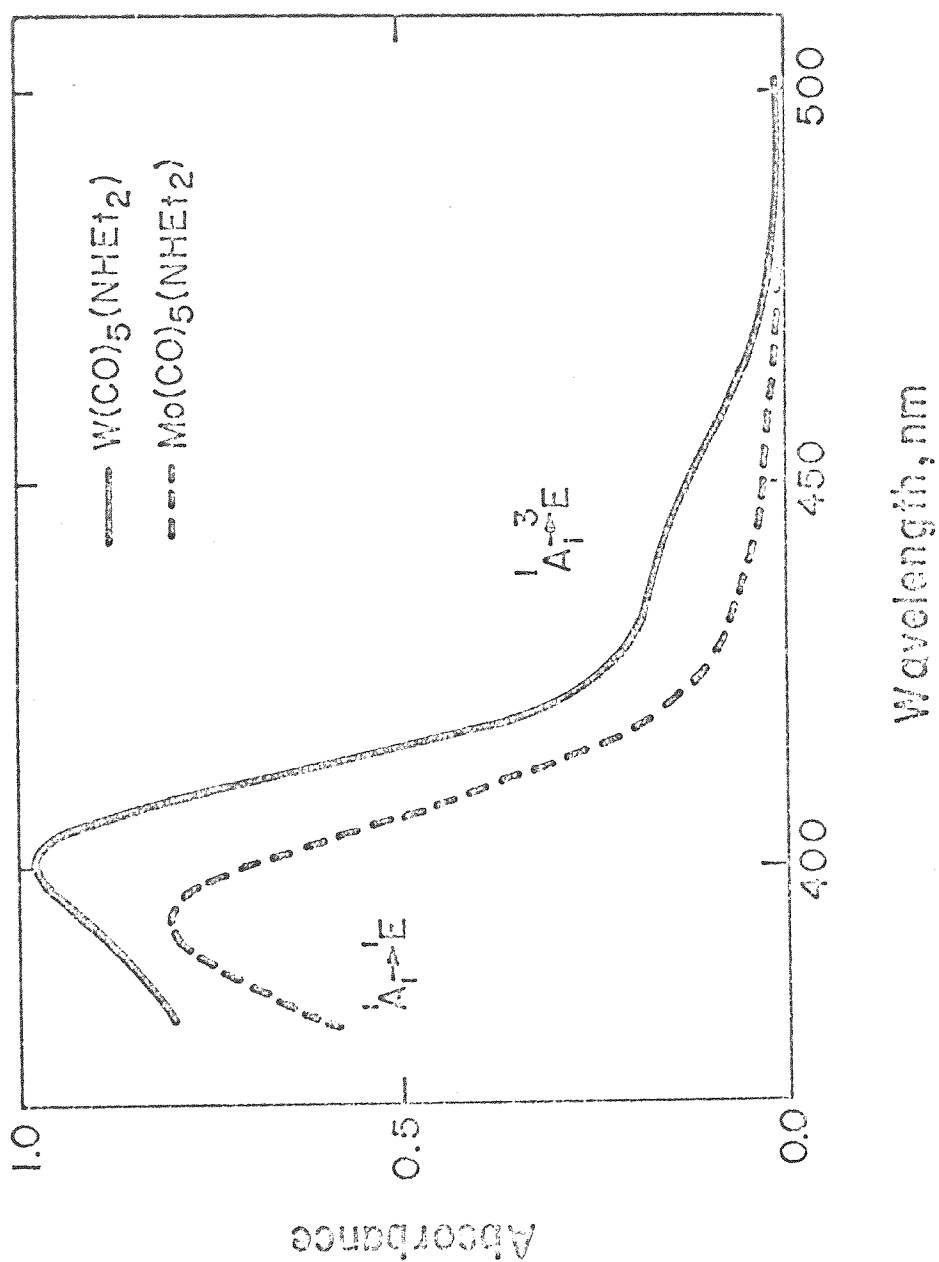
Compound	Abs. Max. ( $\epsilon$ ) $\text{kcm}^{-1}$	Assignment
$(\text{NEt}_4)\text{Cr}(\text{CO})_5\text{Br}$	22.90	${}^1\text{A}_1 \rightarrow {}^1\text{E}$
$\text{Cr}(\text{CO})_5(\text{piperidine})$	23.81 (3500)	${}^1\text{A}_1 \rightarrow {}^1\text{E}$
$\text{Cr}(\text{CO})_5(\text{py})$	25.64 (5600)	${}^1\text{A}_1 \rightarrow {}^1\text{E}$
$\text{Cr}(\text{CO})_5(\text{PPh}_3)$	27.86 (1400)	${}^1\text{A}_1 \rightarrow {}^1\text{E}$
$\text{Mo}(\text{CO})_5(\text{PPh}_3)$	29.0 (2000)	${}^1\text{A}_1 \rightarrow {}^1\text{E}$
$\text{Mo}(\text{CO})_5(\text{py})$	25.97 (6600)	${}^1\text{A}_1 \rightarrow {}^1\text{E}$
$\text{Mo}(\text{CO})_5(\text{piperidine})$	25.13 (5000)	${}^1\text{A}_1 \rightarrow {}^1\text{E}$
$\text{W}(\text{CO})_5(\text{PPh}_3)$	27.5 ( 400)	${}^1\text{A}_1 \rightarrow {}^3\text{E}$
	28.8 (2200)	${}^1\text{A}_1 \rightarrow {}^1\text{E}$
$\text{W}(\text{CO})_5(\text{py})$	22.80 (630)	${}^1\text{A}_1 \rightarrow {}^3\text{E}$
	26.32 (6900)	${}^1\text{A}_1 \rightarrow {}^1\text{E}$
$\text{W}(\text{CO})_5(\text{NHEt}_2)$	22.80 (727)	${}^1\text{A}_1 \rightarrow {}^3\text{E}$
	24.88 (2790)	${}^1\text{A}_1 \rightarrow {}^1\text{E}$
$\text{W}(\text{CO})_5(\text{acetone})$	22.20 (910)	${}^1\text{A}_1 \rightarrow {}^3\text{E}$
	24.63 (5100)	${}^1\text{A}_1 \rightarrow {}^1\text{E}$
$\text{Mn}(\text{CO})_5\text{Br}$	22.00 (20)	${}^1\text{A}_1 \rightarrow {}^3\text{E}$
	25.60 (410)	${}^1\text{A}_1 \rightarrow {}^1\text{E}$
$\text{Re}(\text{CO})_5\text{Cl}$	28.90	${}^1\text{A}_1 \rightarrow {}^3\text{E}$
	31.35	${}^1\text{A}_1 \rightarrow {}^1\text{E}$

Table II-7. (continued):

Compound	Abs. Max. ( $\epsilon$ ) $\text{kcm}^{-1}$	Assignment
$\text{Re}(\text{CO})_5\text{Br}$	28.49 (300)	${}^1\text{A}_1 \rightarrow {}^3\text{E}$
	31.06 (2260)	${}^1\text{A}_1 \rightarrow {}^1\text{E}$
$\text{Re}(\text{CO})_5\text{I}$	26.46 (200)	${}^1\text{A}_1 \rightarrow {}^3\text{E}$
	29.67 (1990)	${}^1\text{A}_1 \rightarrow {}^1\text{E}$

<sup>a</sup>Reference 13.

Figure II-7. Comparison of  $\text{Mo}(\text{CO})_5(\text{X})$  and  $\text{W}(\text{CO})_5(\text{X})$  absorption spectra showing the pronounced S→T in the heavier metal complex.





Correlation of  
Electronic Energy Levels

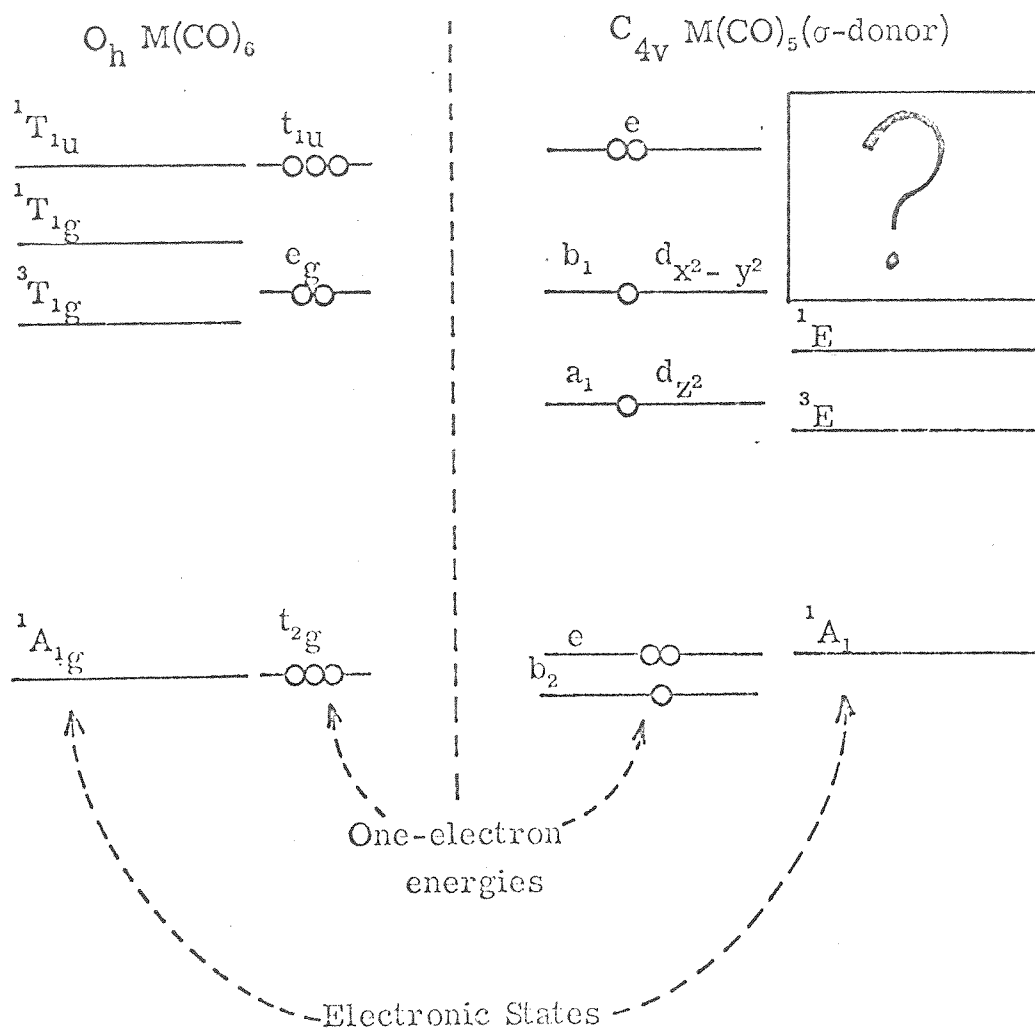


Figure II-8. Correlation of electronic energy levels for an  $O_h$  and  $C_{4v}$  molecule.

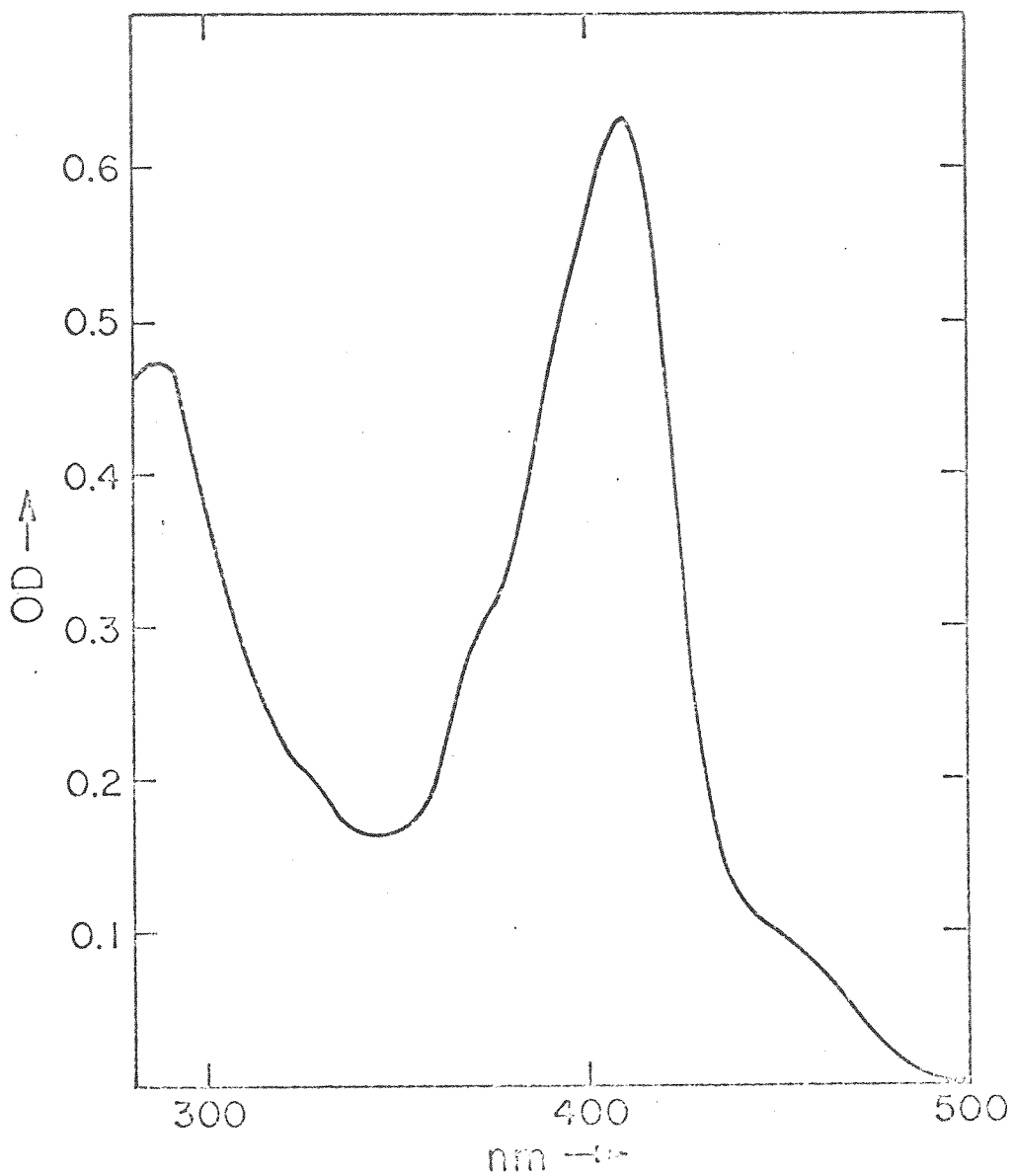
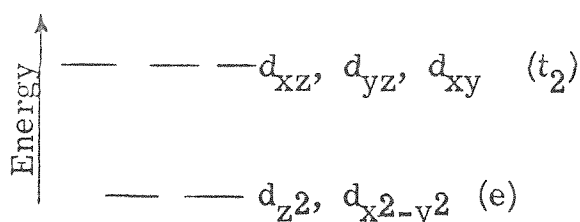


Figure II-9. Electronic absorption spectrum of  $\text{W(CO)}_5\text{NH}_3$  showing high energy transitions associated with population of  $d_{x^2-y^2}$ .

to the electronic structure of  $O_h$  complexes makes them of interest here. The ordering of d orbitals is that shown in 2-XII, and since there is no center of symmetry

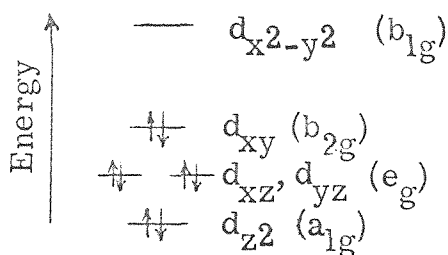


2-XII

for the  $T_d$  geometry the symmetry designations do not have the g subscripts. The value of  $10Dq$  for a  $T_d ML_4$  complex is  $4/9$  that of  $10Dq$  for the  $O_h ML_6$  complex. Tetrahedral complexes typically have higher extinction coefficients than the octahedral systems. The excited states of  $T_d$  complexes may distort toward square planar geometries which may help in interpreting the photosubstitution chemistry. A square planar geometry may favor an associative mechanism for substitution like that commonly found in the thermal substitution of square planar  $Pt(II)$  complexes. Spectra of the  $T_d$  systems can be interpreted using the Tanabe-Sugano diagrams in Figures II-2 through II-5 with  $d_{oct.}^n = d_{tet.}^{10-n}$ .

Square Planar Geometry. The four-coordinate, square planar geometry is found for the complexes of the  $d^8$  metals  $Ni(II)$ ,  $Pd(II)$ , and  $Pt(II)$ . Since no ligands lie on the z-axis of these molecules, the  $d_{z^2}$  is typically lowest in energy. The four ligands

lie on the x- and y-axis, and thus the  $d_{x^2-y^2}$  orbital is highest in energy being significantly  $\sigma$ -antibonding. The ordering of the  $d_{z^2}$ ,  $d_{xy}$ , and the degenerate  $d_{xz}$ ,  $d_{yz}$  pair depends on the nature of the ligands. When strong  $\pi$ -back bonding is possible the  $d_{xz}$ ,  $d_{yz}$  may be stabilized considerably, while  $\pi$ -donor ligands may affect  $d_{xy}$  significantly. A reasonable ordering of the d levels is shown in 2-XIII. The one-electron scheme predicts three spin-allowed

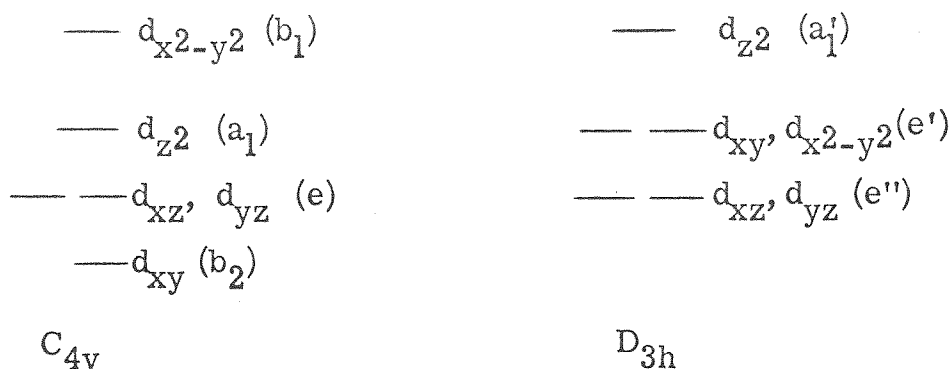


2-XIII

d-d transitions which are Laporte forbidden. The Pt(II) systems have been actively investigated<sup>14</sup> and are complicated by the fact that spin-orbital coupling effects are large enough to provide observable spin-forbidden transitions. The  $d^8$  systems may be complicated, also, by their tendency to form strong  $\pi$ -back bonds and to undergo oxidative addition. The possibility that these systems have tetrahedral geometry in the excited state should be recognized to understand their photochemistry.

Five-Coordinate Systems. Five-coordinate systems have received a great deal of attention from spectroscopists, kineticists, and biochemists. Structurally, five-coordinate systems have been

particularly intriguing. Often the two idealized  $ML_5$  structures of  $C_{4v}$  and  $D_{3h}$  are readily interconvertible. A d orbital ordering for a  $C_{4v}$  complex and a  $D_{3h}$  are shown in 2-XIV. Model  $D_{3h}$

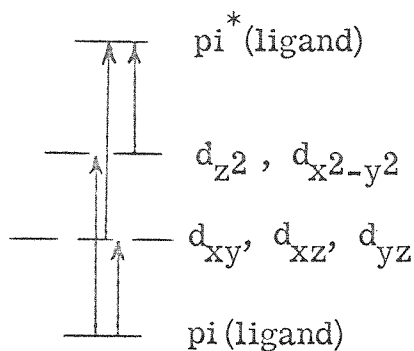


2-XIV

systems have been the  $d^8$  metals forced into a five-coordinate geometry by using tetradentate ligands. The fifth ligand is variable and lies on the z-axis giving transitions which are dependent on the nature of its bonding. The tetradentate tripod-like ligands have been used to make the  $ML_4X, D_{3h}$  complexes of Ni(II), Pd(II), Pt(II), Rh(I), and Co(I). The spectra are characterized by the presence of the predicted two spin-allowed d-d transitions.<sup>15</sup>

Charge Transfer Transitions. Charge transfer transitions are associated with large changes in the distribution of electron density in the vicinity of the metal and ligand. We think of such transitions as arising from removal of an electron from an orbital associated primarily with one atom and placing it in an orbital associated with another atom. Intramolecular

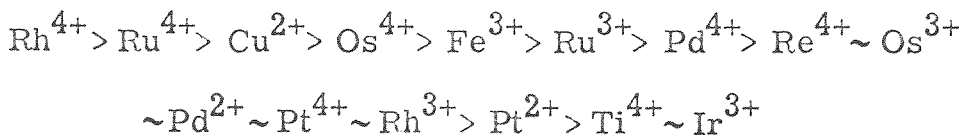
charge transfer can be of two types: (1) excitation of an electron from a metal localized orbital to a ligand localized orbital or (2) excitation of an electron in a ligand localized orbital into a metal localized orbital. These transitions are typically very intense, and are of great interest to photochemists since charge transfer excited states are logical precursors to redox reactions. The possible charge transfer transitions are shown schematically in 2-XV. The ligand to metal ( $L \rightarrow M$ ) transition



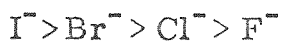
2-XV

will occur at lower energies if the  $\pi$ -d orbitals are unfilled. This effect is observed in comparing the spectra of  $\text{Fe}(\text{CN})_6^{4-}$  and  $\text{Fe}(\text{CN})_6^{3-}$ : the  $d^5$  system has an unfilled  $t_{2g}$  orbital, and the excited electron can occupy this hole in the  $L \rightarrow M$  transition; the  $d^6$  system, on the other hand, has a filled  $t_{2g}$  orbital, and the  $L \rightarrow M$  band is seen at a higher energy. A similar effect is observed in comparing the  $d^5$  ferricinium and  $d^6$  ferrocene spectra.<sup>16</sup> In general if the oxidizing power of the metal and the reducing power of the ligand is greater the energy of the  $L \rightarrow M$

charge transfer band will be lower. In 2-XVI we show an



Oxidizing Power



Reducing Power

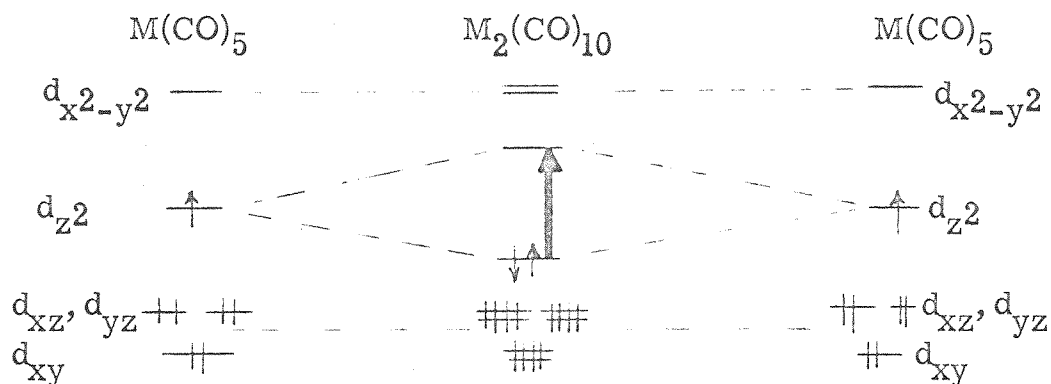
## 2-XVI

ordering of metals and halides derived from the spectra of hexahalo complexes.<sup>17</sup>

Intermolecular charge transfer transitions can occur, and these can be important to photochemists to understand photocatalyzed redox chemistry. Typical examples of the intermolecular charge transfer transitions include transitions due to ion pairing and charge transfer transitions in weak solvent complexes of the metal compound.

Transitions in Metal-Metal Bonded Species. In addition to the d-d and CT transitions in molecules containing direct metal-metal bonds there are unique transitions associated with the metal-metal bond. Key examples are the  $\text{M}_2(\text{CO})_{10}$  (M=Mn, Re) complexes containing a metal-metal single bond. The absorption spectrum is dominated by a very intense band which is assigned as an excitation of an electron from the bonding molecular orbital for the metal-metal bond into the corresponding anti-bonding

orbital.<sup>18</sup> The dimeric  $M_2(CO)_{10}$  can be thought of as arising from the  $d^7 C_{4v} M(CO)_5$  monomers. The single electrons in the  $d_{z^2}$  orbitals give the monomers a radical-like nature, and stabilization is gained by the formation of the dimer via the metal-metal bond. The situation is diagrammed in 2-XVII. The electronic



2-XVII

transition associated with the M-M bond is the  $\sigma \rightarrow \sigma^*$  indicated in the diagram by the heavy arrow.

Intraligand Transitions. Chromophores within a ligand which are not perturbed by coordination to the metal can exhibit electronic characteristics of the free ligand. Usually, changes in absorption intensity, energy, and vibrational structure can aid in determining the degree of perturbation by coordination. One must take care in differentiating between CT and ligand localized transitions, especially when interpreting excited state reactions.



# General References for Electronic Spectroscopy of Coordination Compounds:

C. J. Ballhausen, "Introduction to Ligand Fields", McGraw-Hill Book Company, New York, 1962.

B. N. Figgis, "Introduction to Ligand Fields", Interscience, New York, 1966.

L. E. Orgel, "An Introduction to Transition-Metal Chemistry: Ligand Field Theory", Methuen & Co., London, 1966.

## References

1. C. J. Ballhausen, "Introduction to Ligand Fields", McGraw-Hill Book Company, New York, 1962, pp. 235-239.
2. (a) C. K. Jørgensen, Acta Chem. Scand., 8, 1495 (1954);  
(b) F. H. Spedding and G. C. Nutting, J. Chem. Phys., 2, 421 (1934) and 3, 369 (1935).
3. (a) H. L. Schläfer, Z. Physik. Chem. (Frankfurt), 11, 65 (1957); (b) C. E. Schäffer, J. Inorg. Nucl. Chem., 8, 149 (1958).
4. A. Mead, Trans. Faraday Soc., 30, 1052 (1934).
5. (a) H. L. Schläfer, Z. Physik. Chem. (Frankfurt), 6, 201 (1956); (b) C. K. Jørgensen, Acta Chem. Scand., 11, 53 (1957); (c) L. J. Heidt, G. F. Koster, and A. M. Johnson, J. Am. Chem. Soc., 80, 6471 (1958).
6. (a) M. Linhard, Z. Elektrochem., 50, 224 (1944);  
(b) J. J. Alexander and H. B. Gray, J. Am. Chem. Soc., 90, 4260 (1968).
7. B. N. Figgis, "Introduction to Ligand Fields", Interscience, New York, 1966, p. 242.
8. D. F. Gutterman and H. B. Gray, J. Am. Chem. Soc., 93, 3364 (1971).

9. (a) R.A.D. Wentworth and T.S. Piper, Inorg. Chem., 4, 709 (1965) and 4, 1524 (1965); (b) F. Basolo, C.J. Ballhausen, and J. Bjerrum, Acta Chem. Scand., 9, 810 (1955); (c) H. Yamatera, Bull. Chem. Soc. Japan, 31, 95 (1958); (d) S. Yamada, A. Nakahara, Y. Shimura, and R. Tsuchida, ibid., 28, 222 (1955); (e) K. Nakamoto, J. Fujita, M. Kobayashi, and R. Tsuchida, J. Chem. Phys., 27, 439 (1957).
10. (a) D.A. Rowley, Inorg. Chem., 10, 397 (1971); (b) W.A. Baker, and M.S. Philips, ibid., 5, 1042 (1966); (c) H. Hartmann and H.H. Kruse, Z. Physik. Chem. (Frankfurt), 5, 9 (1955); (d) M. Linhard and M. Weigel, ibid., 5, 20 (1955) and 11, 308 (1957); (e) J.R. Perumareddi, J. Phys. Chem., 71, 3144 (1967) and 71, 3155 (1967); (f) R. Krishnamurthy, W.B. Schapp, and J.R. Perumareddi, Inorg. Chem., 6, 1338 (1967); (g) L. Dubicki and R.L. Martin, Aust. J. Chem., 22, 839 (1969); (h) L. Dubicki, M.A. Hitchman, and P. Day, Inorg. Chem. 9, 188 (1970).
11. D.M.L. Goodgame, M. Goodgame, M.A. Hitchman, and M.J. Waks, ibid., 5, 635 (1966).
12. D.A. Rowley and R.S. Drago, ibid., 7, 795 (1968) and 6, 1092 (1967).
13. (a) N.A. Beach and H.B. Gray, J. Am. Chem. Soc., 90, 5713 (1968); (b) D. Ottesen, M. Wrighton, H.B. Gray, and G.S. Hammond, manuscript in preparation.
14. Spectroscopy of square planar systems: (a) J. Chatt, G.A. Gamlen, and L.E. Orgel, J. Chem. Soc., 486 (1958); (b) H.B. Gray and C.J. Ballhausen, J. Am. Chem. Soc., 85, 260 (1963); (c) H.B. Gray, Progr. Transition Metal Chem., 1, 240 (1965); (d) D.S. Martin, Jr., M.A. Tucker, and A.J. Kassman, Inorg. Chem., 4, 1682 (1965) (amended 5, 1298 (1966)); (e) A.J. McCaffery, P.N. Schatz, and P.J. Stephens, J. Am. Chem. Soc., 90, 5730 (1968); (f) W.R. Mason and H.B. Gray, ibid., 90, 5721 (1968); (g) S.B. Piepho, P.N. Schatz, and A.J. McCaffery, ibid., 5994 (1969).
15. Spectroscopy of five coordination: (a) C. Furlani, Coord. Chem. Rev., 3, 141 (1968); (b) L. Sacconi, Pure Appl. Chem., 17, 95 (1968); (c) M. Ciampolini, Struct. Bonding (Berlin), 6, 52 (1969); (d) J.R. Preer and H.B. Gray, J. Am. Chem. Soc., 92, 7306 (1970).

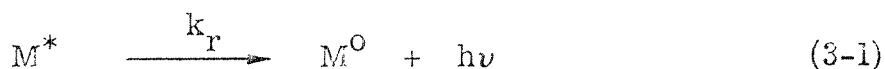
16. Y.S. Sohn, D.N. Hendrickson, and H.B. Gray, ibid., 93, 3603 (1971).
17. C.K. Jørgensen, "Absorption Spectra and Chemical Bonding in Complexes" Pergamon Press, 1962.
18. R.A. Levenson, Ph.D. Thesis, Columbia University, 1970.

## CHAPTER III

Luminescence Studies in Transition  
Metal Complexes

The process of radiative decay from excited states of metal containing molecules is one of the major modes of degrading excited states and has received a great deal of attention.<sup>1</sup> Luminescence from transition metal complexes can be one of three types: metal localized (d-d) luminescence, charge transfer emission, or ligand localized emission. The nature of the emission generally reflects the character of the lowest excited state in the system and allows predictions to be made concerning expected photochemical reactions.

Radiative Decay. Radiative decay is a process by which electronic excitation is converted into energy in the form of light, equation (3-1). Being a radiative process, emission is subject to



the same selection rules governing the radiative process of absorption of light. Indeed, the molecules with more fully allowed transitions in absorption have correspondingly high luminescence probabilities. Whether emission can be observed from a given excited state depends on the magnitude of  $k_r$  relative to the magnitude of the rate constant for decay of the excited state by all other means including chemical change and

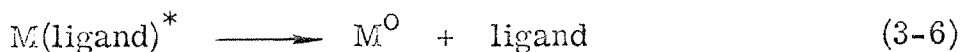
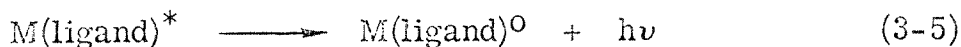
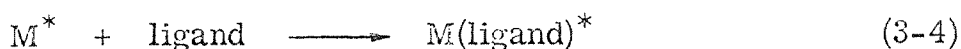
nonradiative decay. The quantum efficiency,  $\Phi_e$ , of emission is defined in equation (3-2) and is related to the decay rate constants

$$\Phi_e = \frac{\text{number quanta emitted}}{\text{number quanta absorbed}} \quad (3-2)$$

in equation (3-3). In most cases, if  $\Phi_e = 1.0$ , then no

$$\Phi_e = \frac{k_r}{\text{sum of all decay constants}} \quad (3-3)$$

chemical change occurs upon photolysis. However, it is conceivable that excited state geometries dictate loss in optical activity resulting in racemization and emission. A second phenomenon involving chemistry is outlined in the scheme below:



This situation is obtained, for instance, when the acid dissociation constant for the ground and excited states is very different so that excited states of new stoichiometry are produced. Acid-base reactions are an example of reactions occurring in the excited state without electronic deactivation. The  $pK_a$  values for ground and excited states of several molecules are shown in Table III-1.<sup>2,3</sup> Another example is the interaction of amines and aromatic singlet excited states<sup>4</sup> to produce an "exciplex" which undergoes radiative dissociative decay as outlined in equations (3-4) through (3-6).

Table III-1. Acid Strengths of Ground  
and Excited States<sup>a</sup>

Compound	pK <sub>a</sub> of Ground State	pK <sub>a</sub> of Singlet Excited State
2-Naphthol	9.5	3.1
2-Naphthoic Acid	4.2	10 to 12
Acridine	5.5	10.6

<sup>a</sup>References 2 and 3.

The correlation between  $k_r$  and the allowedness of the corresponding absorption band can become quantitative. The inherent radiative lifetime  $\tau^0 = (k_r)^{-1}$ , and is related to the absorption in equation (3-7).<sup>5</sup> The ratio  $\frac{G_2}{G_1}$  is the ratio of the

$$\tau^0 = \frac{1}{k_r} = \frac{3.5 \times 10^8 G_2}{G_1 \bar{\nu}^2 \int \epsilon d\bar{\nu}} \quad (3-7)$$

multiplicity of the excited state ( $G_2$ ) to the ground state ( $G_1$ );  $\bar{\nu}$  is the energy of the transition maximum; and  $\epsilon$  is the extinction coefficient. An order of magnitude value for  $\tau^0$  is given by equation (3-8) for uv-vis transitions.<sup>6</sup> Experimental tests of

$$\tau^0 = \frac{10^{-4}}{\epsilon_{\max}} \quad (3-8)$$

these predicted lifetimes give satisfactory results in a qualitative sense. Quantitative values for  $k_r$  can only be obtained by measuring the emission lifetime,  $\tau$ , equation (3-9) and  $\Phi_e$ . The quantum

$$\tau = \frac{1}{\text{sum of all decay constants}} \quad (3-9)$$

efficiency and  $\tau$  are simply related in equation (3-10).

$$\Phi_e = k_r \tau \quad (3-10)$$

The radiative transition of emission is a Franck-Condon (vertical) transition. In Figure III-1 straight vertical lines show transitions between the ground and excited states. Schematically in Figure III-1 we have shown that the equilibrium internuclear

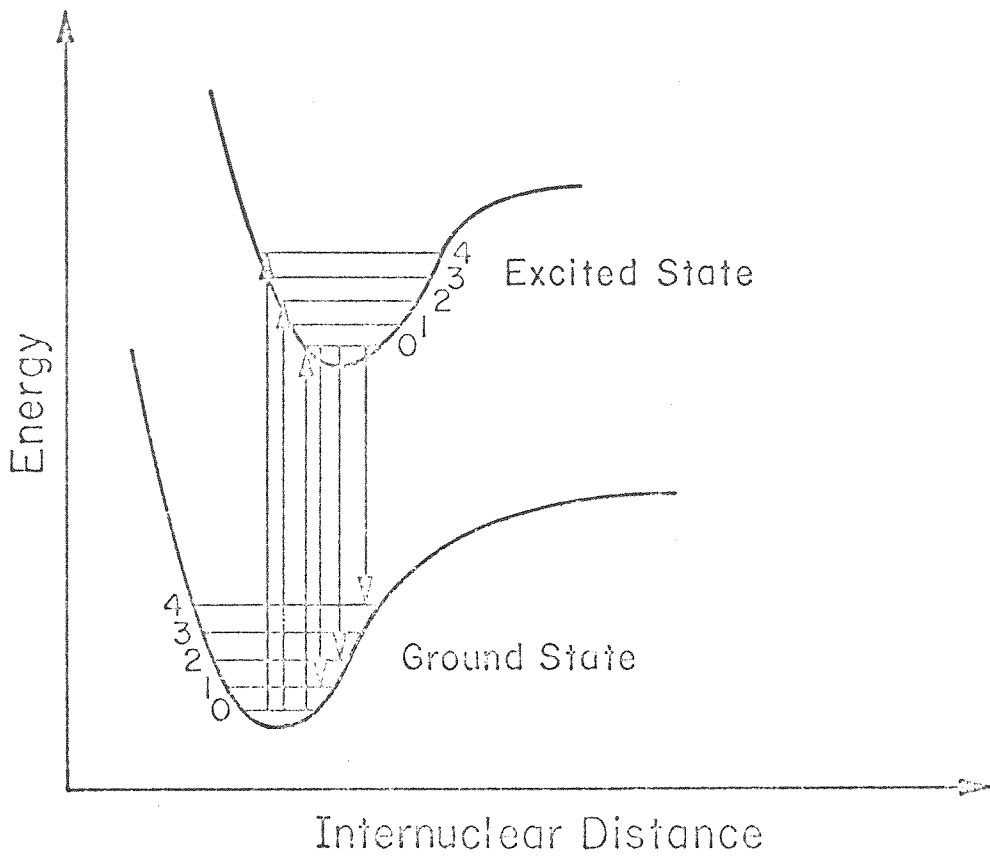


Figure III-1. Radiative transitions between ground and excited states illustrating effect on the relative energy of absorption and emission by increased internuclear distance in the excited state.

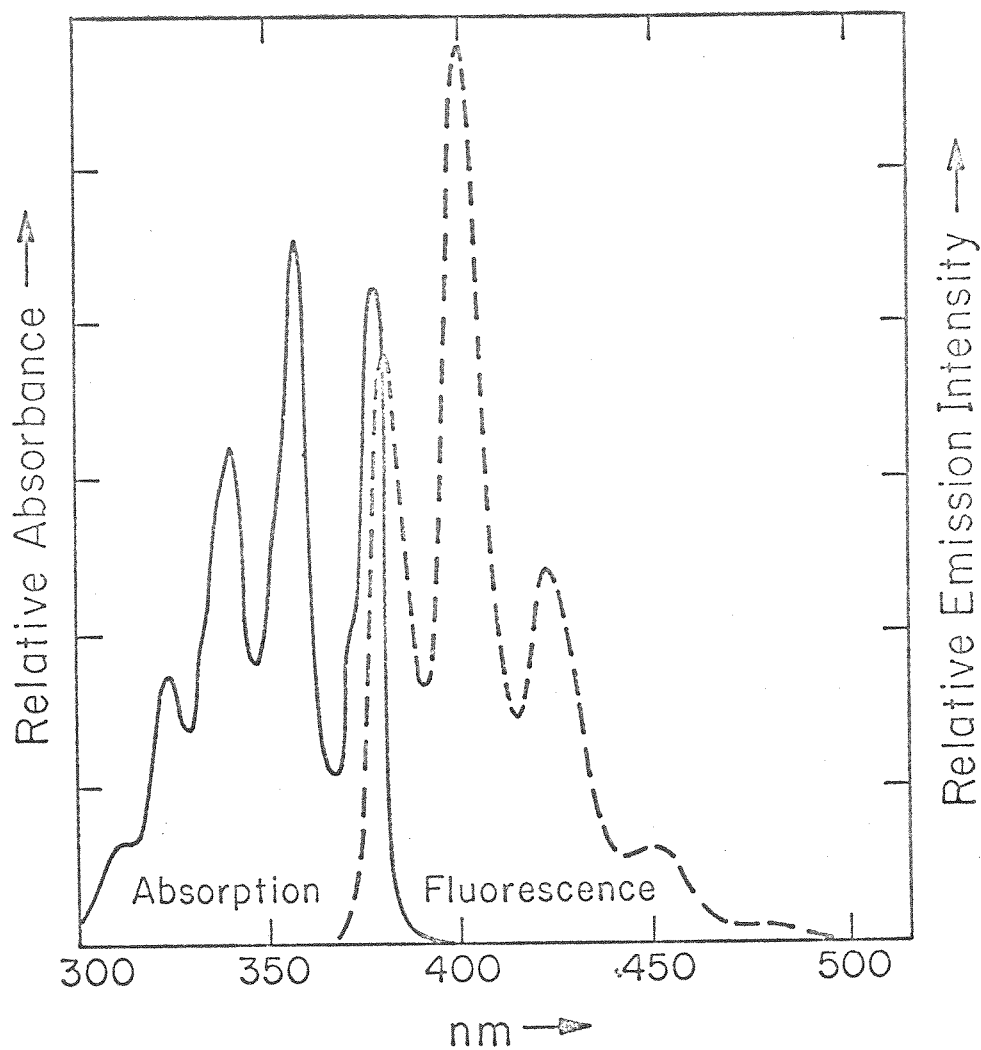


distance is larger in the excited state than in the ground state. Thus, if the excited state relaxes to the lowest vibrational level before emitting, transitions to the ground state will be of lower energy than the absorption bands. In Figure III-2 we show an absorption and an emission spectrum for anthracene which behave as predicted by Figure III-1. Overlap of the 0-0 transitions of absorption and emission is expected, and the mirror image relationship between the absorption and emission is common. Emission from states of different spin multiplicity than the ground state will not necessarily overlap spin-allowed absorption bands.

#### Ligand Localized Emission in Metal Containing Molecules.

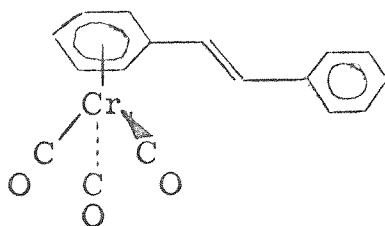
Emission from a transition characterized as ligand localized will be most probable when the internal ligand transition is the lowest energy transition in the system. This situation arises in a number of metal containing molecules. Emission may be characterized as ligand localized when the spectral characteristics reflect the electronic states of a slightly perturbed free ligand. A priori we expect red shifted emission reflecting stabilization by coordination to the metal and significant changes in lifetime due to internal heavy atom effect on both nonradiative and radiative decay rates. As in absorption we expect the emission spectrum to show vibrational structure similar to the free ligand.

Figure III-2. Anthracene fluorescence and absorption spectra illustrating overlap of 0-0 transitions and the mirror image relationship.



Some well studied systems are the metal o-phenanthroline complexes.<sup>1a</sup> With  $\text{Rh}(\text{o-phen})_3^{3+}$  the lowest energy absorption in the molecule is the  $\pi \rightarrow \pi^*$  ligand transition.<sup>7a</sup> The emission observed is very similar to free phenanthroline in the energy and in the vibrational spacing of the emission. Ligand localized luminescence is seen in  $d^{10}$  complexes of triphenylphosphine. The emission from the complexes is sometimes very long lived and is often structured.<sup>7b</sup> The emission occurs at different wavelengths depending on the metal involved. Numbers of metal complexes exhibit intense ligand localized emission, and the use of luminescence as an analysis for the metal has been explored.<sup>1e,f</sup> This area deserves some attention from photochemists. One question of great importance remains in many situations where the ligand localized transition is lowest in energy. Does  $\Phi_e$  change with excitation wavelength? That is, will population of high lying d-d or CT states convert to the lowest excited state in the molecule?

Another intriguing possibility is that ligand localized emission can occur even when it is not the lowest lying excited state. The trans-stilbene chromiumtricarbonyl 3-I is thought to exhibit



3-I

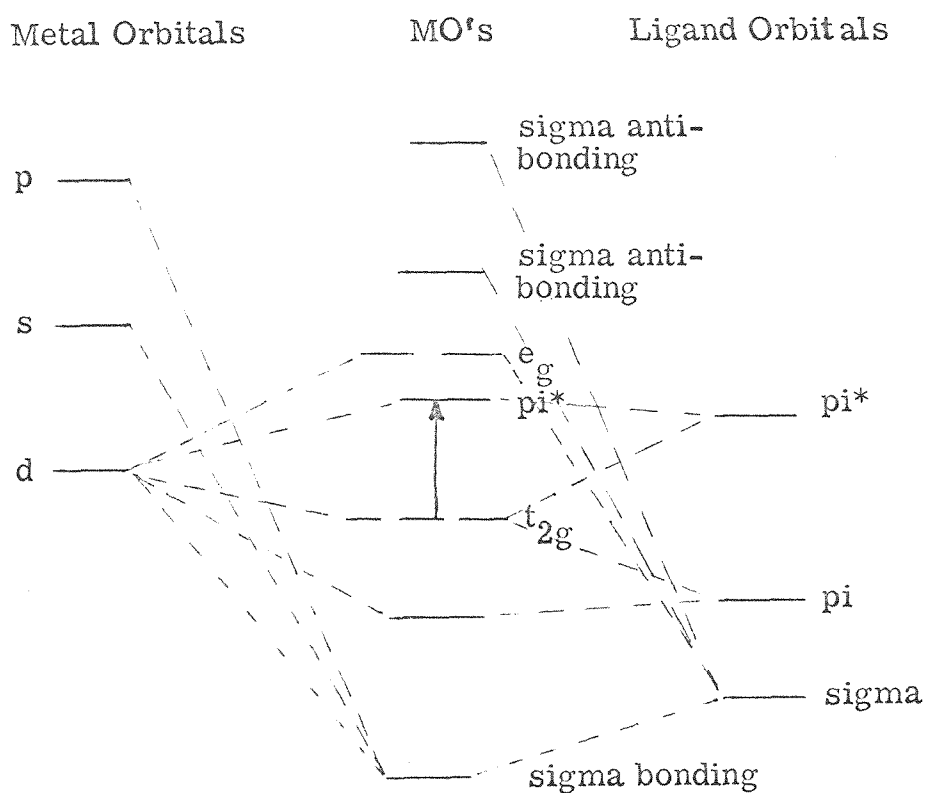
stilbene-like fluorescence even though there is a lower energy transition in the molecule.<sup>8</sup> Studies of this nature are important in understanding energy transfer and internal conversion rates.

### Charge Transfer Emission in Metal Containing Molecules.

There are several types of charge transfer transitions possible in metal containing molecules. Several features are common to the charge transfer transitions as pointed out earlier. The high extinction coefficients observed in absorption implicate high radiative probabilities, therefore, charge transfer emission should be both short-lived and intense. A large number of d<sup>6</sup> second and third row metal systems with o-phenanthroline or 2,2'-bipyridine ligands give charge transfer emission which is characterized as being ligand  $\pi^* \rightarrow$  metal  $\pi$  d emission.<sup>1a</sup> The energy level scheme is shown in Figure III-3. The Ru(II) systems of O<sub>h</sub> symmetry represent the most well studied charge transfer emission.<sup>9-15</sup> The emission lifetimes are of the order of 10<sup>-5</sup> sec. which would suggest spin-forbidden emission but with large spin-orbital coupling due to the heavy metal.

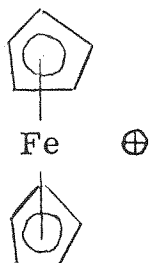
The observation of charge transfer photochemistry even when d-d transitions are at lower energies reveals that chemistry from charge transfer states can occur faster than internal conversion to the lowest excited state. Another interesting question is whether internal conversion can occur from the high lying charge transfer state to the ground state, bypassing the d-d levels. To date no one has demonstrated that charge transfer emission can

Figure III-3. Schematic representation of complex having a low lying metal to ligand charge transfer transition. The arrow indicates the  $t_{2g}$  to  $\pi^*$  one electron excitation.



occur from a high excited state. The probability for observing a high energy charge transfer emission should be greatest when the charge transfer band and the lowest d-d transition are well separated so that any mixing of the two excited states will be small by virtue of the large energy gap separating them. The observation of charge transfer luminescence in these situations will provide information regarding the importance of intermediate metal-localized transitions in deactivation of charge transfer excited states.

The ferricinium cation 3-II represents an extremely

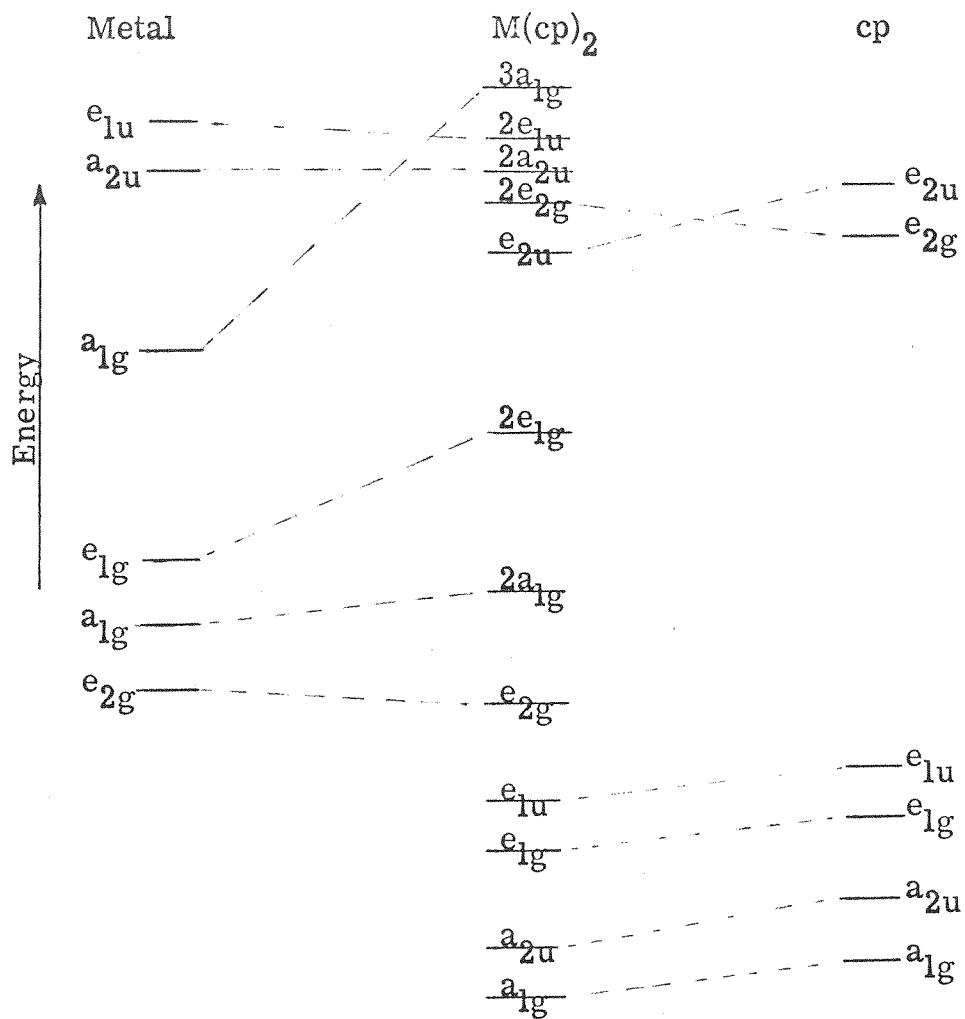


3-II

interesting molecule which has a charge transfer transition in the visible with a very low lying metal localized excited state.<sup>16,17</sup>

The low lying d-d and the charge transfer transitions arise because we have a  $d^5$  configuration. A schematic energy level diagram is shown in Figure III-4. Ring-to-metal charge transfer occurs at a low energy because the lower d orbitals are unfilled allowing a ligand electron to occupy the "hole" in the d orbitals.

Figure III-4. Level diagram for dicyclopentadienyl complexes from reference 17.



A d-d transition is expected to occur between the low lying closely spaced d orbitals.

The ferricinium cation and its alkyl derivatives were found to give emission from the room temperature solid  $\text{PF}_6$  salts when excited at 632.8 nm using a He-Ne laser. In Figure III-5 we show emission spectra for the  $\text{Fe}(\text{cp})_2^+$ ,  $\text{Fe}(\text{cp})(\text{cp-}\underline{\text{n}}\text{-butyl})^+$ , and the  $\text{Fe}(\text{cp-}\underline{\text{n}}\text{-butyl})_2^+$  complexes. Emissions are compared in Table III-2. The shift to lower energies with the more alkyl substituents is good evidence that the transition is the ring  $\rightarrow$  metal charge transfer transition in absorption.<sup>17</sup>

The ferricinium compounds represent the first sandwich complexes which give luminescence (cf. also pp.119-122). While the spectra taken are not corrected spectra there is a tendency for the emission intensity to be lowest with the more highly alkyl substituted ferricinium complexes. This decrease in the relative emission quantum yield can be due to a number of factors. Since we have not measured the emission lifetime it is not unequivocally clear whether the radiative decay rate is changing or whether changes in nonradiative decay rates are dominant. However, by equation (3-8) we see that relative radiative decay rates can be obtained from the relative maximum extinction coefficient for absorption. The ferricinium compounds have about the same extinction coefficients at the absorption maximum, thus, we expect that the large decrease in relative  $\Phi_e$  with the disubstituted ferricinium derivative is due to significant changes in the



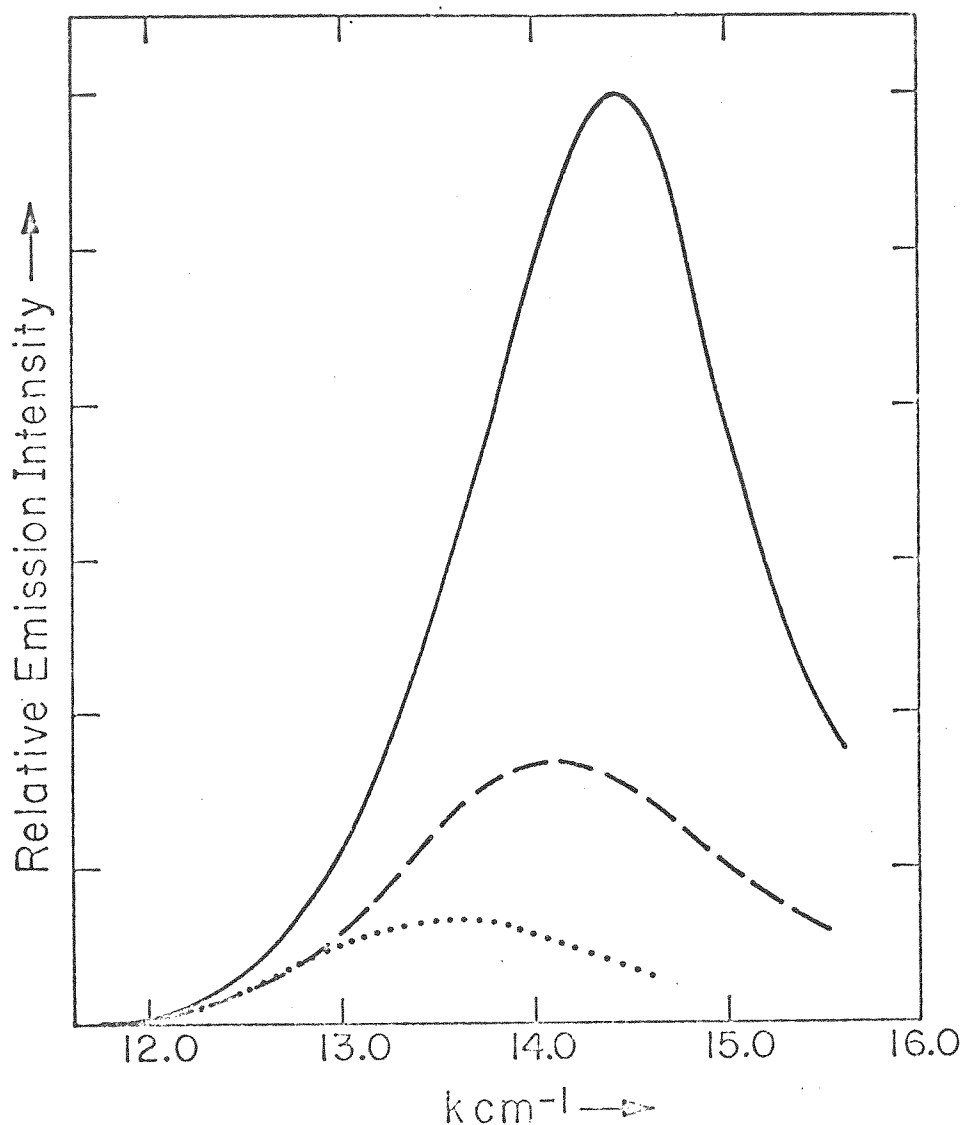


Figure III-5. He-Ne laser excited emission from  $\text{Fe}(\text{cp})_2^+$  (—),  $\text{Fe}(\text{cp})(\text{cp-n-butyl})^+$  (---) and  $\text{Fe}(\text{cp-n-butyl})_2^+$  (.....) as  $\text{PF}_6$  salts. The emission is observed from the room temperature solids.

Table III-2. Absorption and Emission Maxima  
for Ferricinium Derivatives

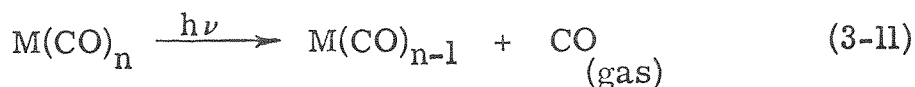
Compound	Absorption Max., <sup>a</sup> cm <sup>-1</sup> ( $\epsilon$ )	Emission Max., <sup>b</sup> cm <sup>-1</sup>
Fe(cp) <sub>2</sub> PF <sub>6</sub>	16,190 (450)	14,430
Fe(cp)(cp- <u>n</u> -butyl)PF <sub>6</sub>	16,000 (330)	14,130
Fe(cp- <u>n</u> -butyl) <sub>2</sub> PF <sub>6</sub>	15,390 (340)	13,600
Fe(cp) <sub>2</sub> BF <sub>4</sub>	16,190 (450)	14,450

<sup>a</sup>Reference 17.

<sup>b</sup>He-Ne laser excitation of room temperature solids.

nonradiative decay rates. The trend that we observe is reasonable in that we see highest rates of nonradiative decay from the compounds closest in energy to the ground state. With the data at hand this is a highly tentative statement. However, we have shown that sandwich compounds have sufficiently high radiative decay rates to exhibit charge transfer luminescence even when there is a d-d transition at lower energies. An interesting follow-up would be to consider derivatives of ferricinium with electron-withdrawing substituents to shift the charge transfer absorption to a higher energy than the high d-d transition at  $17,700\text{ cm}^{-1}$ .<sup>17</sup> The emission from the charge transfer state, then, is of fundamental importance in determining the role of the metal-localized states in the deactivation of the charge transfer state.

The observation of charge transfer emission from a metal containing molecule allows one to state unequivocally that chemical change (reaction) does not account for all of the exciting quanta. Metal carbonyl excited state processes are dominated by substitution reactions.<sup>18</sup> In many cases, reaction (3-11) is



thought to proceed with a quantum yield of 1.0.<sup>18</sup> We have observed emission from samples of  $\text{Mo(CO)}_4(\text{phen})$  and  $\text{W(CO)}_4(\text{phen})$ . A typical emission spectrum is shown in Figure III-6. The lowest energy transition in absorption for the complexes is a charge transfer transition with the lowest energy

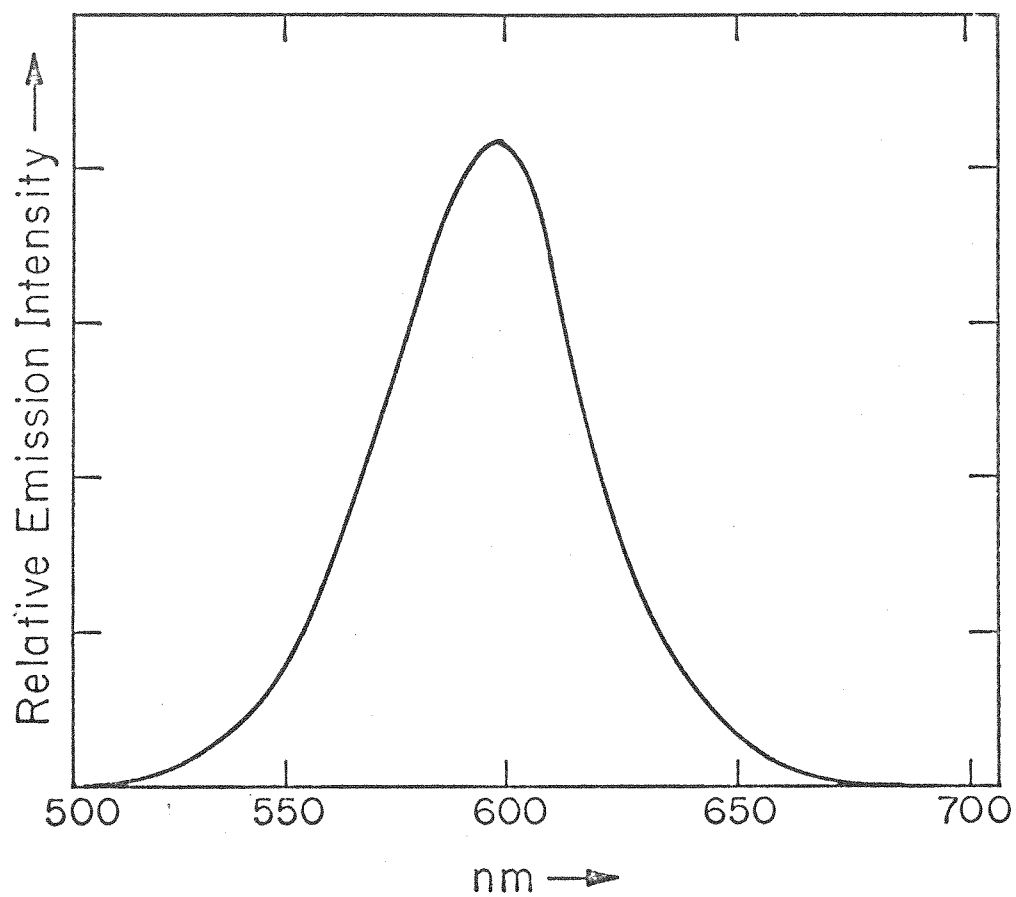


Figure III-6. Emission from  $\text{Mo}(\text{CO})_4(\text{phen})$  in methylcyclohexane at  $77^\circ \text{ K}$ .

bands showing tremendous solvent shifts (up to 85 nm!).<sup>19</sup> The excitation spectrum is similar in shape to the absorption spectrum for the molybdenum complex. Apart from measuring a decay process other than CO substitution for these metal carbonyl complexes one can gain insight into the effect of spin-orbital coupling. For example, we were able to measure the  $\text{Mo(CO)}_4(\text{phen})$  emission using a chopper and measured a lifetime of  $1 \times 10^{-3}$  sec. The  $\text{W(CO)}_4(\text{phen})$  emission, however, could not be seen with the chopper in place which means that the lifetime is shorter than the corresponding Mo complex. This effect is expected since the tungsten is a heavier atom and has enhanced spin-orbital coupling. Further evidence that the phenanthroline complexes are giving charge transfer emission is that we have been unable to observe emission from cis- $\text{Mo(CO)}_4(\text{pyridine})_2$  while cis- $\text{W(CO)}_4(\text{pyridine})_2$  gives emission. Neither of the pyridine complexes contains a low energy charge transfer absorption band, and the tungsten emission is associated with the singlet  $\rightarrow$  triplet metal localized absorption (cf. pp.110-115). We suggest that the  $\text{M(CO)}_4(\text{phen})$  emission is associated with the spin-forbidden charge transfer transition. The heaviest metal gives the shortest lifetime confirming our beliefs about spin-orbital coupling effects. We have also noted emission which is very similar to that of the phenanthroline complexes from  $\text{Mo(CO)}_4(\text{bipyridine})$  and  $\text{W(CO)}_4(\text{bipyridine})$ . Some pertinent data is collected in Table III-3. The fact that we observe room temperature

Table III-3. Luminescence Data for Molybdenum and Tungsten  
and Tungsten Complexes of  
2, 2'-Bipyridine and 1,10-o-Phenanthroline

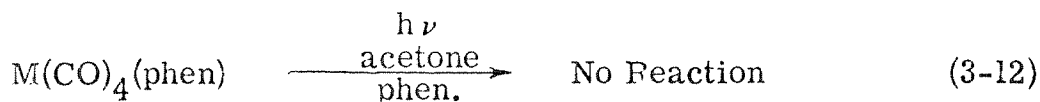
Compound	Emission Max., nm	Lifetime, sec
Mo(CO) <sub>4</sub> (phen)	584 <sup>a</sup> ± 5 nm 597 <sup>b</sup>	1.1 x 10 <sup>-3a</sup>
W(CO) <sub>4</sub> (phen)	580 <sup>a</sup>	< 1.1 x 10 <sup>-3a</sup>
Mo(CO) <sub>4</sub> (bipy)	582 <sup>a</sup>	1.0 x 10 <sup>-3a</sup>
W(CO) <sub>4</sub> (bipy)	580 <sup>a</sup>	< 1.0 x 10 <sup>-3a</sup>

<sup>a</sup>Methylcyclohexane solvent

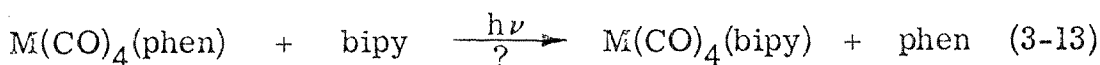
<sup>b</sup>EPA solvent

emission from the solids lends support to a charge transfer assignment since we have not been able to observe room temperature emission for either cis-W(CO)<sub>4</sub>(py)<sub>2</sub> or W(CO)<sub>5</sub>(py) which exhibit d-d luminescence only at low temperatures.

The lack of further facile photosubstitution of M(CO)<sub>4</sub>(phen), equation (3-12), is related to the fact that emission can be



observed. Nonradiative processes (reaction) become slower than, or, at best competitive with, radiative decay. The possibility that excitation is labilizing the phenanthroline or bipyridine has not been explored and merits investigation, equation (3-13).



A final point of interest here is the lack of observable emission from the M(CO)<sub>4</sub>(4, 7-diphenylphenanthroline) complexes. The 4, 7-diphenylphenanthroline binds in the same way that bipyridyl or phenanthroline binds and apparently gives a very similar electronic structure. The absorption maxima in isooctane are the same and the large changes in absorption due to changes in solvent polarity obtain as shown in Figure III-7. The large increase in the charge transfer intensity expected in these d<sup>6</sup> systems<sup>20-22</sup> should cause a faster radiative decay rate for the 4, 7-diphenylphenanthroline compared to phenanthroline.<sup>20</sup> This would result in a higher luminescence intensity, but apparently

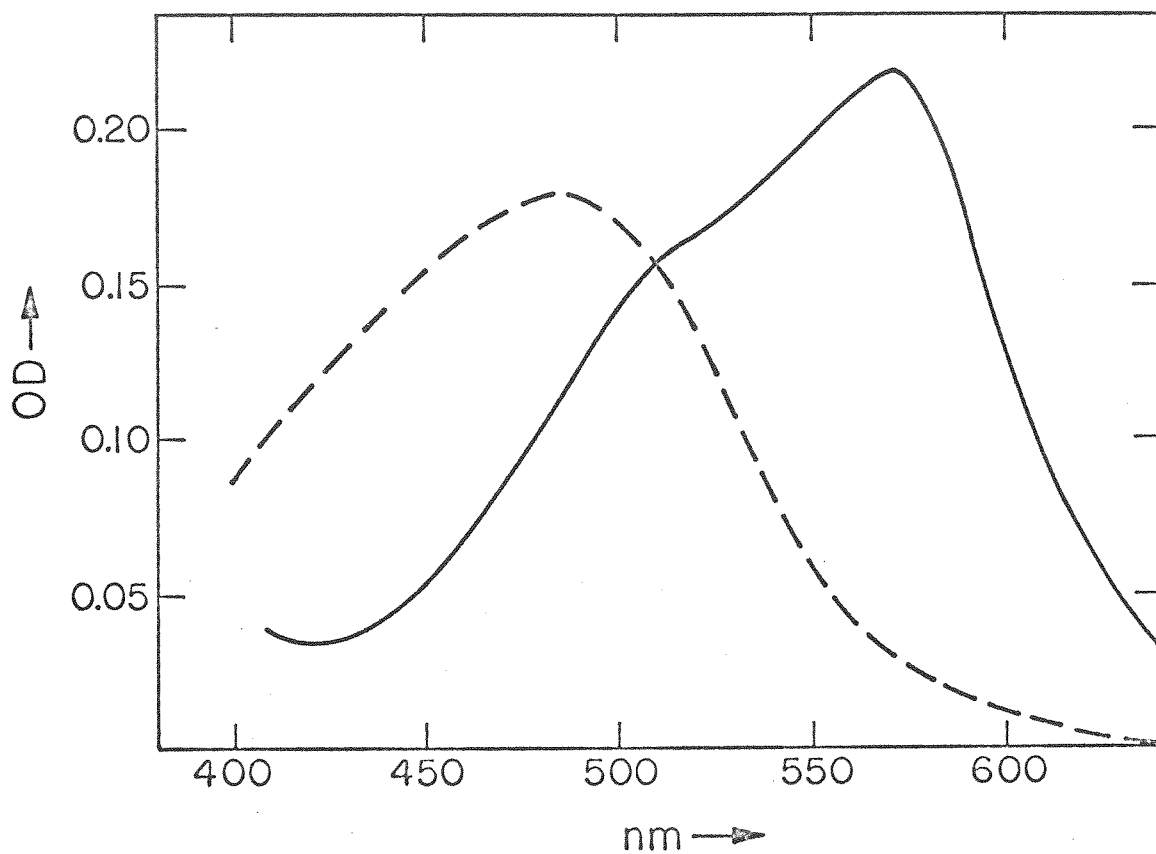


Figure III-7. Shift in room temperature absorption of  $W(CO)_4(4,7\text{-diphenylphenanthroline})$  with solvent: isooctane (—) and 4:1 isooctane:acetone (v/v) (— — —).



nonradiative decay is accelerated even more, resulting in no observable emission. A definitive assignment of the luminescence of  $M(CO)_4(phen)$  or  $M(CO)_4(bipy)$  cannot be made at this time in light of the 4, 7-diphenylphenanthroline results. A d-d assignment might be considered because the emission is weak and near in energy to the emission of cis- $W(CO)_4(pyridine)_2$ . The differences may arise from the fact that internal conversion must occur from the charge transfer state to the lowest d-d state while in the pyridine complex direct population of the metal localized state occurs. Finally, in contrast to Ru(II) and Ir(III) complexes of phenanthroline or 4, 7-diphenylphenanthroline,<sup>20</sup> the emission here is not structured. This system merits further investigation.

In marked contrast to the tungsten(0) and molybdenum(0) carbonyl complexes of phenanthroline or bipyridine the complexes  $ClRe(CO)_3(X)$  ( $X = 1, 10$ -phenanthroline, 2, 2'-bipyridine or 4, 7-diphenylphenanthroline) all luminesce at room temperature in fluid solution. The central metal has a  $d^6$  configuration like W(0) or Mo(0). A typical emission spectrum is shown in Figure III-8 and data are shown in Table III-4. The structure on the low energy side of the emission spectrum is reproducible and is present in the spectrum of each complex. Upon cooling to 77°K. a remarkable change occurs in the emission spectrum: the maximum shifts some 60 to 75 nm to the blue, and dramatic

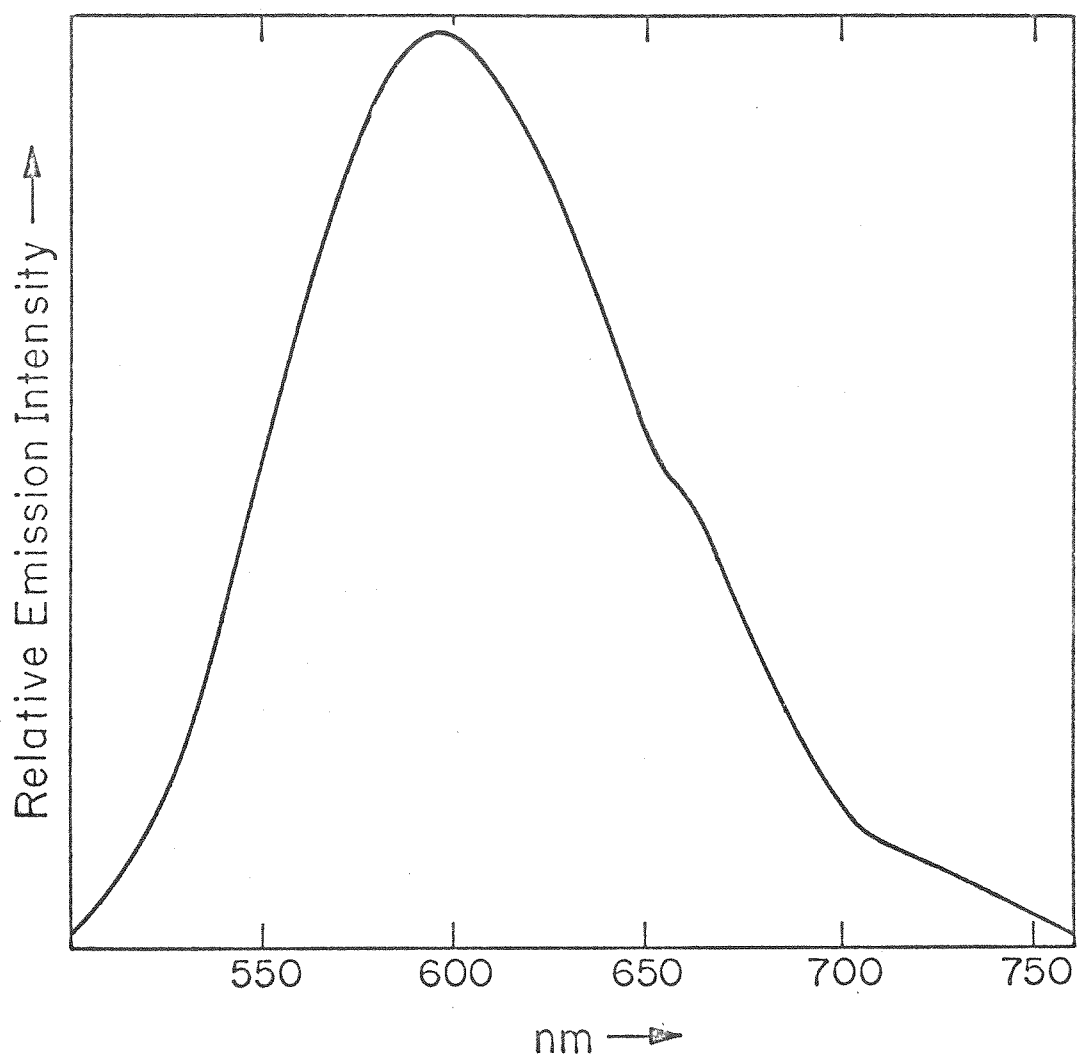


Figure III-8. Room temperature luminescence from  $\text{Re}(\text{CO})_3\text{Cl}(\text{phen})$  in aerated acetone solution.

Table III-4. Luminescence Data for  $\text{ClRe}(\text{CO})_3(\text{X})$  Complexes

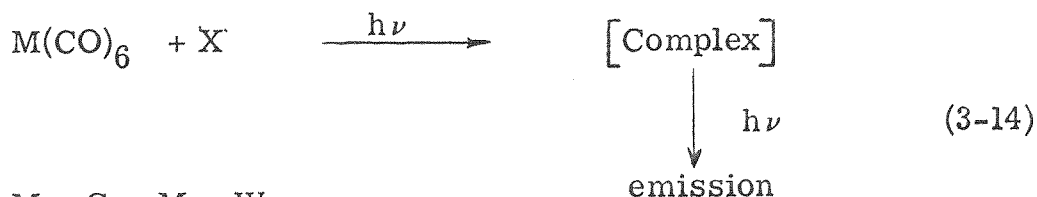
X	Solvent	Temperature, °K	Emission Max., nm	Lifetime, microsec.
1,10-phenanthroline	acetone	298	595	—
	EPA	298	—	0.30 <sup>a</sup> , 0.19 <sup>b</sup>
	EPA	77	525	11.4
	None	298	550	—
2,2'-bipyridine	acetone	298	601	—
	EPA	298	—	0.60 <sup>a</sup>
	EPA	77	528	3.8
4,7-diphenylphenanthroline	acetone	298	604	—
	isooctane	298	613	—
	EPA	298	—	0.42, 0.3 <sup>b</sup>
	4:1 EPA:benzene	298	605	0.73 <sup>a</sup> , 0.22 <sup>b</sup>
	EPA	77	548	9.9

<sup>a</sup>N<sub>2</sub> deoxygenated solutions.

<sup>b</sup>Aerated solution.

intensification of the luminescence is observed. Accompanying the blue shift and the intensification is a longer lived emission by a factor of  $\sim 50$ . The excitation maximum shifts less than 20 nm. The low temperature emission spectrum shows no structure. In analogy with  $\text{Ru}(\text{bipy})_3^{2+}$  we associate the emission here with a spin-forbidden  $\pi^* \longrightarrow \pi$ -d transition. The large shift in the spectrum upon cooling may be a solvent effect since the pure solid emits at higher energy than the acetone solution. Although measurements are not complete, this system allows quantitative evaluation of both nonradiative and radiative decay rates since emission occurs in fluid solution, removing experimental difficulties associated with 77°K. determinations. Oxygen appears to quench the luminescence at a rate near diffusion-controlled consistent with a triplet  $\longrightarrow$  singlet emission.

Another example of charge transfer emission involving metal carbonyls has been observed, equation (3-14). The emission from



M = Cr, Mo, W

X = 2, 4, 7-trinitrofluorenone

2, 7-dinitrofluorene

2, 4, 6-trinitrobenzoic acid

the complex of unknown structure occurs in aerated fluid solutions at room temperature. A typical emission and excitation

spectrum are shown in Figure III-9. The emission is fairly intense and is short lived. Extremely large solvent shifts are noted in some cases. When  $X = 2, 4, 7$ -trinitrofluorenone and  $M = W$  the emission is orange in acetone solutions and is green in isooctane solution. That this emission is charge transfer in nature is seemingly clear, but the identity of the complex giving the emission is thus far unknown.

At least it is certain that metal carbonyls do other things besides undergoing dissociative decay. More study is necessary to be able to predict precisely when luminescence will be dominant.

Metal Localized (d-d) Luminescence. The study of d-d luminescence has been most fruitful with six-coordinate Cr(III),  $d^3$ , systems. Of lesser importance has been study of six-coordinate  $d^6$  systems and four-coordinate Pt(II),  $d^8$ , systems.<sup>1</sup> While examples of other  $d^n$  configurations exist they are, to a large extent, isolated examples, and few structural correlations exist. In general, very little is known about factors controlling luminescence phenomena of metal localized excited states. The low radiative probability associated with d-d transitions led to the widespread belief that few examples of emission would be found in transition metal complexes. However, the advent of laser excitation makes certain the discovery of more luminescent coordination compounds. Few correlations between ligand and

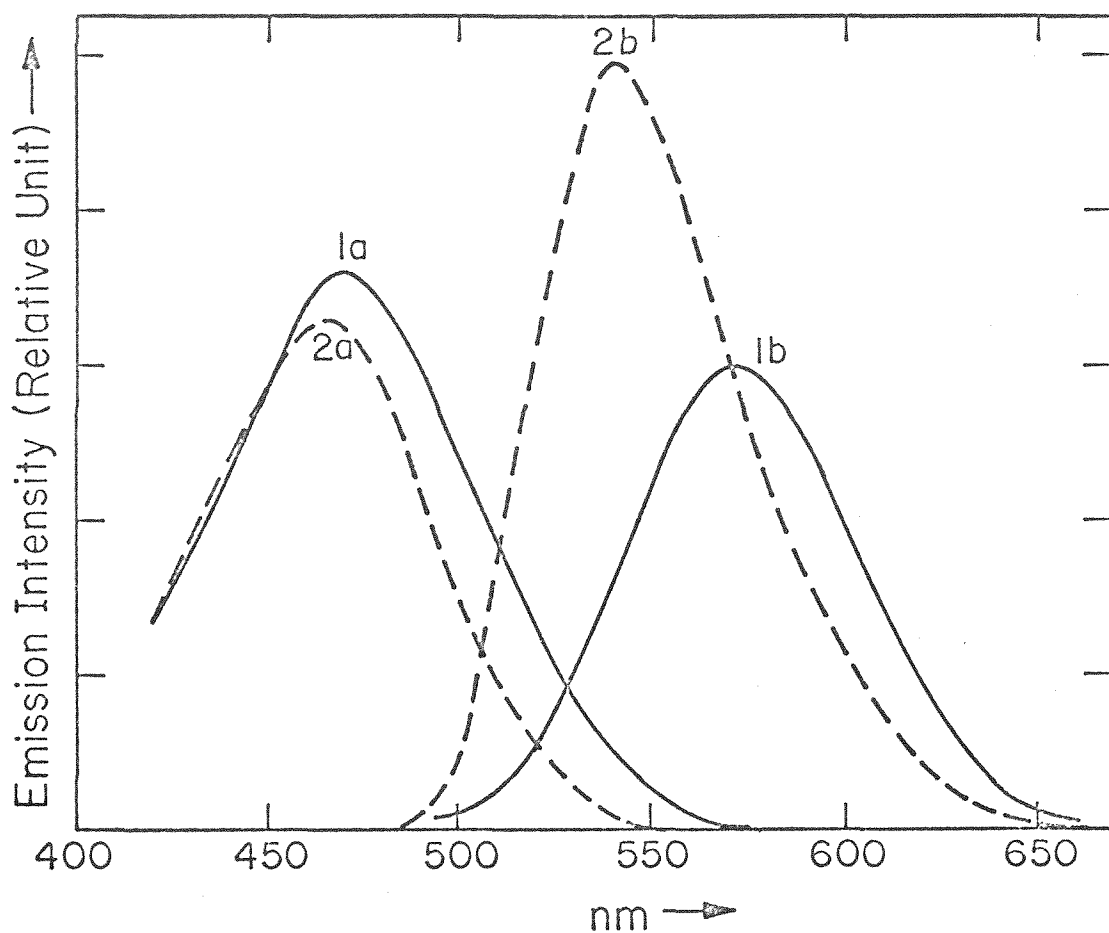


Figure III-9. Emission (curves b) and excitation (curves a) spectra of  $W(CO)_6(2,4,7\text{-trinitrofluorenone})$  in acetone (curves 2) and in isooctane-acetone (curves 1) (20:1 v/v) in aerated room temperature solutions.

luminescence exist, and as pointed out above only a few geometries and  $d^n$  configurations have been investigated in detail. Notably absent are five-coordinate complexes, metal-metal bonded species, and organometallic compounds.

$d^3$  Systems. The studies with the Cr(III) systems have yielded some interesting results which will be summarized here. The energy of the electronic states as a function of  $10Dq$  for  $d^3$  systems of  $O_h$  symmetry is shown in the Tanabe-Sugano diagram of Figure II-2. The lowest excited state can either be a  ${}^2E_g$  or a  ${}^4T_{2g}$  state depending on the value of  $10Dq$ . The energy of the  ${}^2E_g$  state is insensitive to changes in  $10Dq$  because the transition is only a spin pairing transition  $t_{2g}^3(\text{quartet}) \rightarrow t_{2g}^3(\text{doublet})$ . The  ${}^4T_{2g}$  energy, however, is very sensitive to  $10Dq$  because the transition is  $t_{2g}^3 \rightarrow t_{2g}^2 e_g^1$ . Thus, two types of emission are possible: phosphorescence,  ${}^2E_g \rightarrow {}^4A_{2g}$  or fluorescence,  ${}^4T_{2g} \rightarrow {}^4A_{2g}$ . The fluorescence is likely for weak field complexes, and phosphorescence is expected when strong field complexes are involved.

Table III-5 shows the type of emission occurring as a function of the  ${}^4T_2$ — ${}^2E$  energy separation.<sup>23, 24</sup> We see that the strong field ligands give emission from the  ${}^2E$  which is the lowest excited state while the weak field ligands give fluorescence from the low lying  ${}^4T_2$  state. A particularly interesting phenomenon occurs at values of  $10Dq$  where the  ${}^4T_2$

Table III-5. Dependence of Emission on Cr(III) Quartet-Doublet Separation<sup>a</sup>

Compound	${}^4T_2$ , $\text{kcm}^{-1}$	${}^2E$ , $\text{kcm}^{-1}$	$\Delta E$	Type of Emission <sup>b</sup>
$\text{CrCl}_6^{3-}$	13.06	14.48	1.42	F
$\text{CrF}_6^{3-}$	14.90	15.70	0.80	F
$\text{Cr(urea)}_6^{3+}$	16.15	14.35	1.80	B
$\text{Cr(OH}_2)_6^{3+}$	17.27	15.15	2.12	B
$\text{Cr(NCS)}_6^{3-}$	17.70	13.01	4.69	P
$\text{Cr(CN)}_6^{3-}$	26.70	12.47	14.23	P

<sup>a</sup>Ref. 23 and 24.

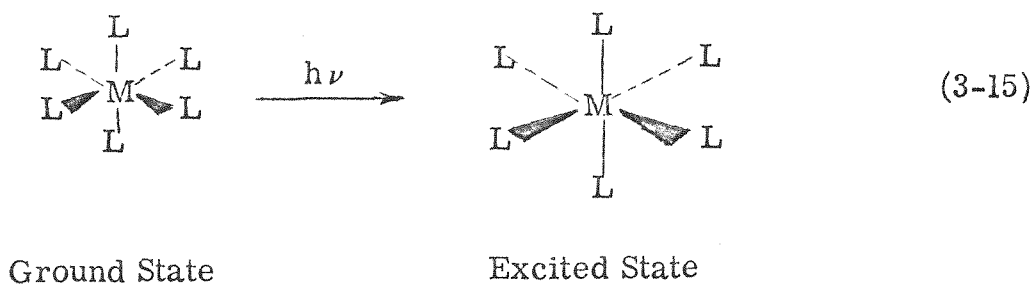
<sup>b</sup>F =  ${}^4T_2 \rightarrow {}^4A_2$  fluorescence

P =  ${}^2E \rightarrow {}^4A_2$  phosphorescence

B = both fluorescence and phosphorescence



and  $^2E$  states cross: both fluorescence and phosphorescence are observed. For this reason we see temperature dependent ratios of fluorescence to phosphorescence where both are observed. The cases of Cr(III) which exhibit the  $^4T_2 \rightarrow ^4A_2$  fluorescence gives us insight into the changes that occur in  $10Dq$  by populating the  $e_g$  orbitals with one electron. For example, the  $^4T_2$  state of  $[\text{Cr}(\text{OH}_2)_6]^{3+}$  lies above the  $^2E$  state in absorption while we see emission from the  $^4T_2$  state below the  $^2E$  emission.<sup>1a</sup> We have already pointed out that the average internuclear distance is larger in the excited than in the ground state. This is shown schematically by the transformation (3-15) where



the octahedral  $\text{ML}_6$  expands symmetrically in the excited state. The change in the bond distance gives a change in the value of  $10Dq$ . The Franck-Condon principle constrains the molecule to undergo the radiative transition without any internuclear motion, so the ground state is formed in a high vibrational state with the emission occurring at a significantly lower energy. The largest shift in the fluorescence maximum compared to the

absorption maximum for the  ${}^4A_2 \rightarrow {}^4T_2$  of Cr(III) complexes seems to be of the order of 3 to 4  $\text{km}^{-1}$ .<sup>1a</sup>

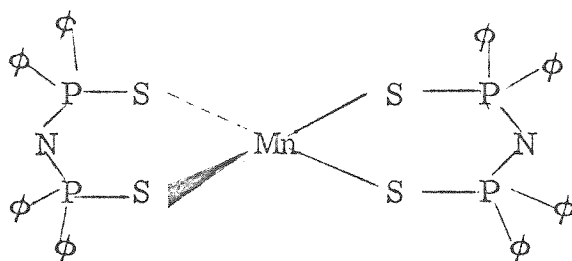
The temperature effects on the emission spectra of Cr(III) complexes suggest that a significant decay mode of the  ${}^2E$  state is thermal population of the  ${}^4T_2$  followed by fluorescence and nonradiative decay.

Other  $d^3$  systems especially of the second and third row transition metals have been sparsely studied. However, the Cr(III) system provides a rich source of information.

$d^5$  Luminescence. High spin octahedral or tetrahedral complexes of  $\text{Mn}^{2+}$  exhibit luminescence.<sup>1a</sup> This configuration represents an interesting situation in that electronic transitions involve configurational changes resulting in depopulation of upper d orbitals and population of the lower orbitals. The d-d transitions are, also, all spin-forbidden since the five d orbitals are singly occupied in the ground state giving the sextet with all one-electron excitations resulting in quartets. The lowest transition in  $O_h$  is the  ${}^6A_{1g}(t_{2g}^3 e_g^2) \rightarrow {}^4T_{1g}(t_{2g}^4 e_g^1)$  and in  $T_d$  the transition is  ${}^6A_1(t_2^3 e^2) \rightarrow {}^4T_1(t_2^2 e^3)$ . Since the transition involves a net gain of  $10Dq$  in energy, the energy required to convert the molecule to the lowest excited state is associated with a spin pairing energy. Thus, when  $10Dq$  is large the transition occurs at lower energies since spin pairing is more easily overcome by a large gain from  $10Dq$ . This fact has led

workers to generalize that  $T_d$  complexes will give higher energy emission than  $O_h$  complexes of  $Mn^{2+}$ .<sup>25</sup> Green or yellow emission is thought to be characteristic of  $T_d$   $Mn^{2+}$  while orange or red is taken to be  $O_h$   $Mn^{2+}$ .

We have measured the emission spectrum of  $Mn(TS)$ , 3-III.



$Mn(TS)$

3-III

Magnetic studies reveal a high spin  $Mn^{2+}$ , and the crystal structure confirms a slightly distorted  $T_d$  structure.<sup>26</sup> The 77°K. emission is shown in Figure III-10 with maxima at 695 nm and 718 nm. The emission is significantly red-shifted from the emission of  $Mn^{2+}$  doped into  $T_d$  sites in ZnS, CdS, etc.<sup>1a</sup> The complex 3-III represents the only  $Mn^{2+}$  molecular species of known crystal structure whose emission has been observed. At this point it appears to be premature to attempt a generalization concerning emission energy and the geometry of  $Mn^{2+}$  complexes.

The absorption  ${}^6A_1 \rightarrow {}^4T_1$  has a maximum at 545 nm and overlaps the emission only slightly. The  $T_d$  complex apparently

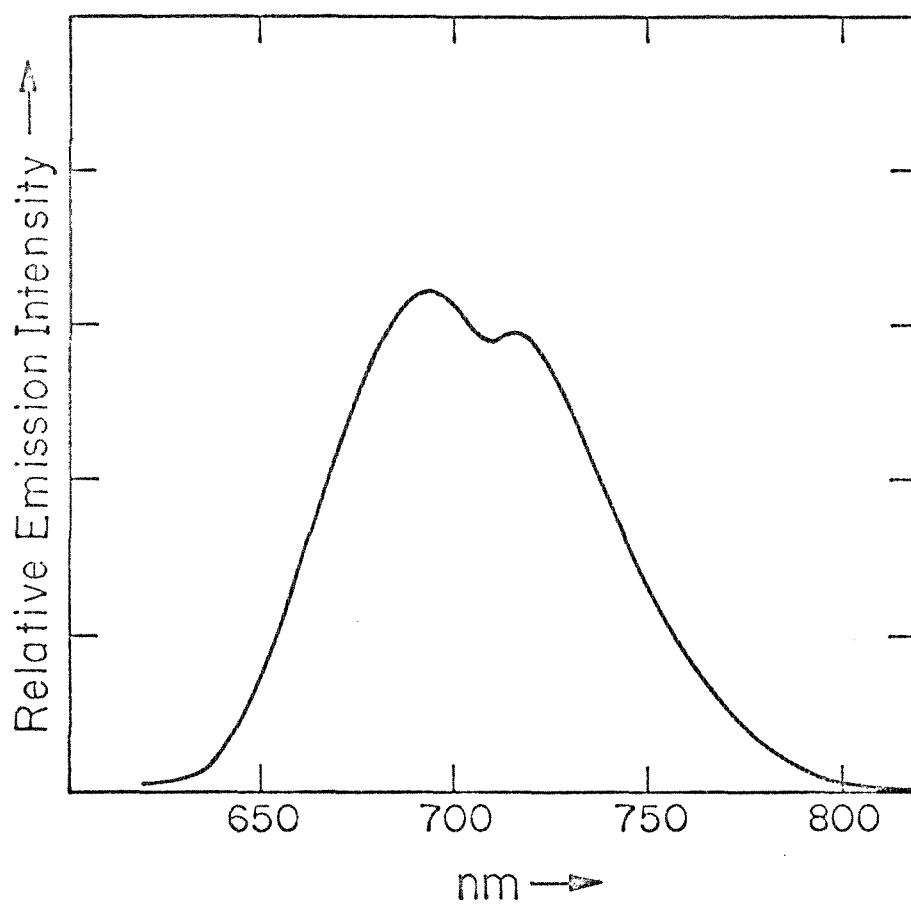


Figure III-10. Emission from Mn(TS) as the pure solid at 77° K.

undergoes a distortion in the excited state toward a square planar geometry since the  $\pi$ -d orbitals are depopulated. The distortion can be detected since the emission spectrum shows splitting. The emission, then, arises from  ${}^4E, {}^4A \rightarrow {}^6A_1$  transitions. This distortion suggests that nucleophilic attack could occur easily in the excited state to give a five-coordinate intermediate or even a stable product. Alternately, the splitting of the emission may be vibrational structure.

One other important fact can be demonstrated with the Mn(TS) complex. The excitation spectrum can be used to locate positions of the absorption maxima. In Figure III-11 we show the excitation spectrum for the Mn(TS) emission. Several bands are clearly defined and agree well with absorption data for the complex. When extinction coefficients are small the excitation spectrum allows easy determination of the band maxima and resolution of any splitting.

$d^6$  Luminescence. The  $d^6$  configuration has been studied to a limited extent, but is an important area because of the large number of stable compounds of this closed shell configuration. The stable complexes are invariably six-coordinate, octahedral systems. The energy diagram for the  $d^6 O_h$  system is shown in Figure II-4. At very low ligand field strengths the ground state is a quintet. As a ground state configuration this state is relatively unimportant here because most luminescence studies

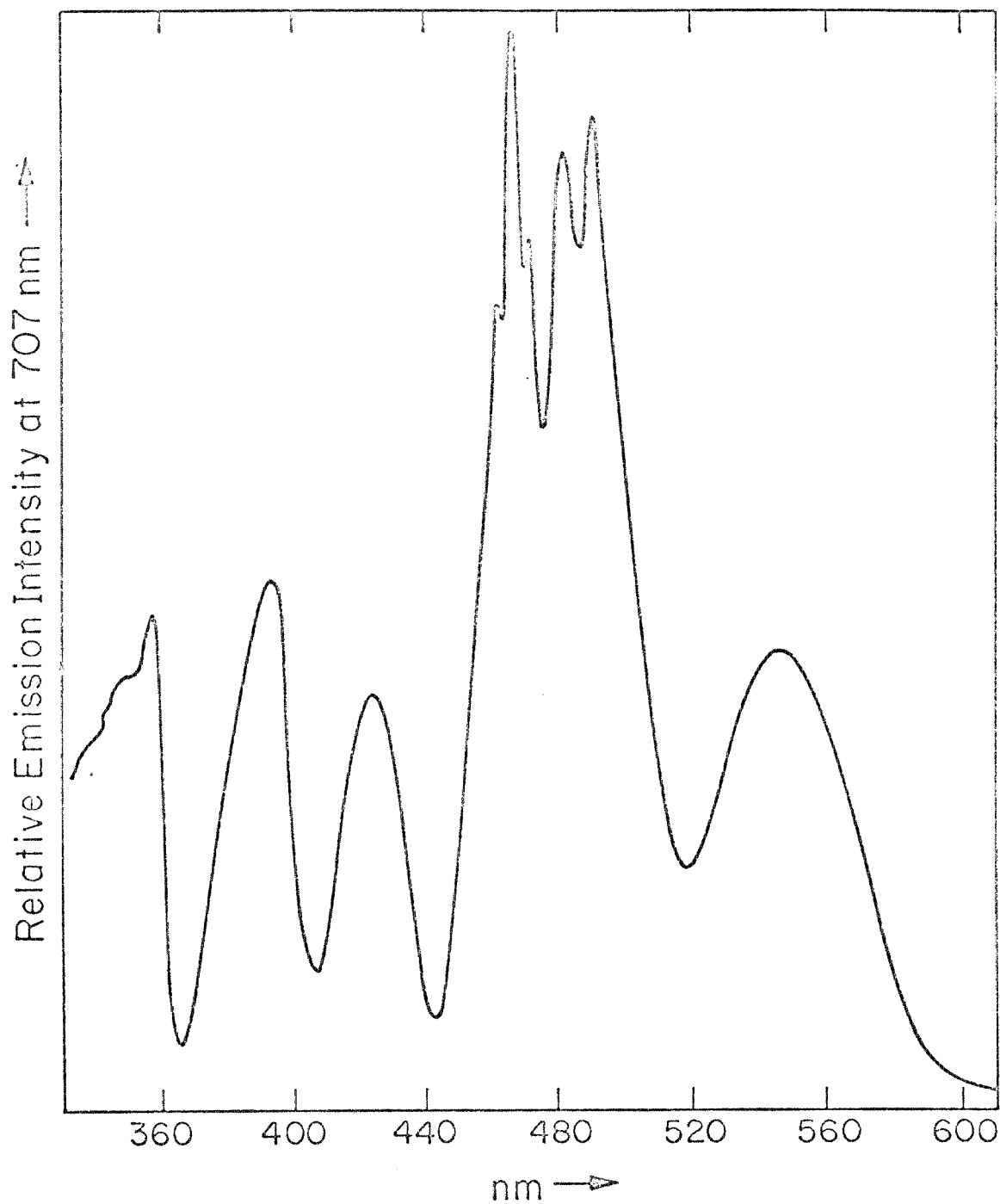


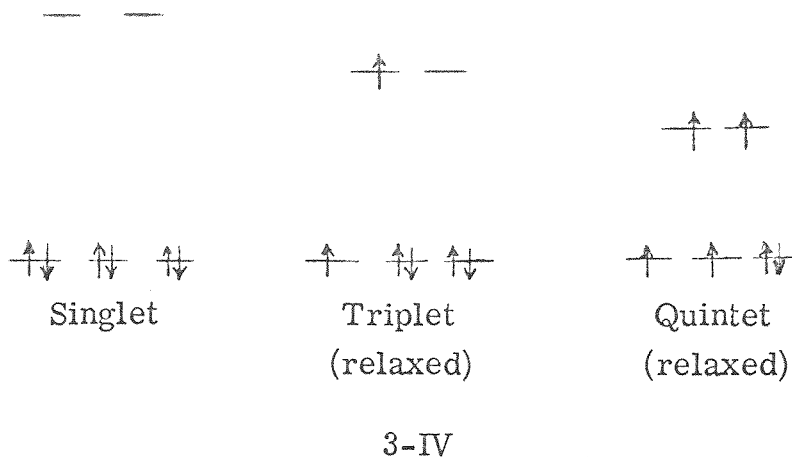
Figure III-11. Excitation spectrum for Mn(TS) monitoring the emission at 707 nm. Sample is the pure solid at 77° K. Excitation spectral bandwidth is 3 nm.

have dealt with the heavy metal complexes of Ru(II), Os(II), Pt(IV), Rh(III), and Ir(III). Only a few Co(III) complexes luminesce, and these contain strong field ligands.<sup>1a</sup> At high ligand field strengths the ground state is a  $^1A_{1g}$  and the excited states are singlets, triplets, and even quintets!

Quintet Emission. We suggest that in many true octahedral  $d^6$  complexes the  $^5T_{2g}$  is the state from which radiative decay occurs. All workers but Kasha<sup>27</sup> have neglected its importance in nonradiative decay. There are several reasons that compel one to assign  $d^6$  emission as  $^5T_{2g} \rightarrow ^1A_{1g}$ . First, from the Tanabe-Sugano diagram the  $^5T_{2g}$  is the lowest excited state at low values of  $10Dq$ . Secondly, experimental results give very long emission lifetimes for very heavy metal complexes. Third, emission quantum yields are weak which is consistent with a very poor radiative probability associated with  $\Delta S = 2$ . Finally, using  $d^6 O_h$  systems as quenchers of organic triplets reveals that the metal complexes are not always effective triplet quenchers even though the spin-forbidden emission occurs at low energies. We will develop these points below.

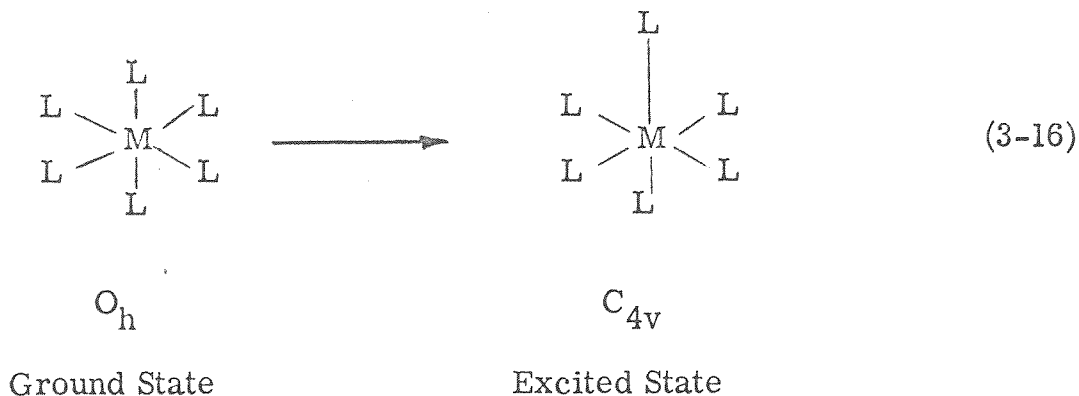
For  $^5T_{2g}$  to be the lowest excited state two criteria must be met: the system must remain octahedral, and the value of  $10Dq$  must be small. The value of  $10Dq$  is significantly decreased by placing one electron in the  $e_g$  orbitals as we discovered with the Cr(III) molecules. Placing two electrons in the  $e_g$  orbitals

as required for the quintet, 3-IV, would lower  $10Dq$  even more



and would certainly be the lowest lying excited state in  $O_h$  symmetry even with strong field ligands and second and third row metals. Population of the quintet directly would be forbidden by the spin selection rule, but direct population of the triplet in absorption followed by rapid intersystem crossing to the  ${}^5T_{2g}$  provides a mechanism for arriving at the lowest excited state. Direct absorption to the triplet state is facilitated by large spin-orbital coupling effects. The notion, then, is that with metal systems triplets are to quintets as singlets are to triplets in organic molecules. Whether the excited state of the  $d^6$  systems is octahedral is a key point. The likely alternative to the octahedral expansion in the excited state (cf. equation 3-15) is a large distortion as in equation (3-16) giving rise to an





excited state of  $C_{4v}$  symmetry. Both excited state geometries,  $C_{4v}$  or  $O_h$ , could undergo photosubstitution processes. Radiative decay from the  $C_{4v}$  excited state to the  $O_h$  ground state appears to be very unlikely since the  $C_{4v}$  represents partial dissociation of the ligand, and if emission did occur one would expect it to be very broad. The possibility exists with both geometries for a second minimum in the ground state as shown in Figure III-12. This would give rise to narrow band emission in either case. The octahedral  $d^6$  systems must have a second minimum as the internuclear distance increases corresponding to the crossover point to high spin on the Tanabe-Sugano diagram. The only truly definitive experiment would be to obtain structural data directly, say, by flash infrared spectroscopy. One point is clear though: whatever the geometry, the distortion from the ground state is significant. We can gain some feel for this by examining the data in Table III-6. For example, consider  $Co(CN)_6^{3-}$  <sup>28</sup> whose first spin-allowed d-d

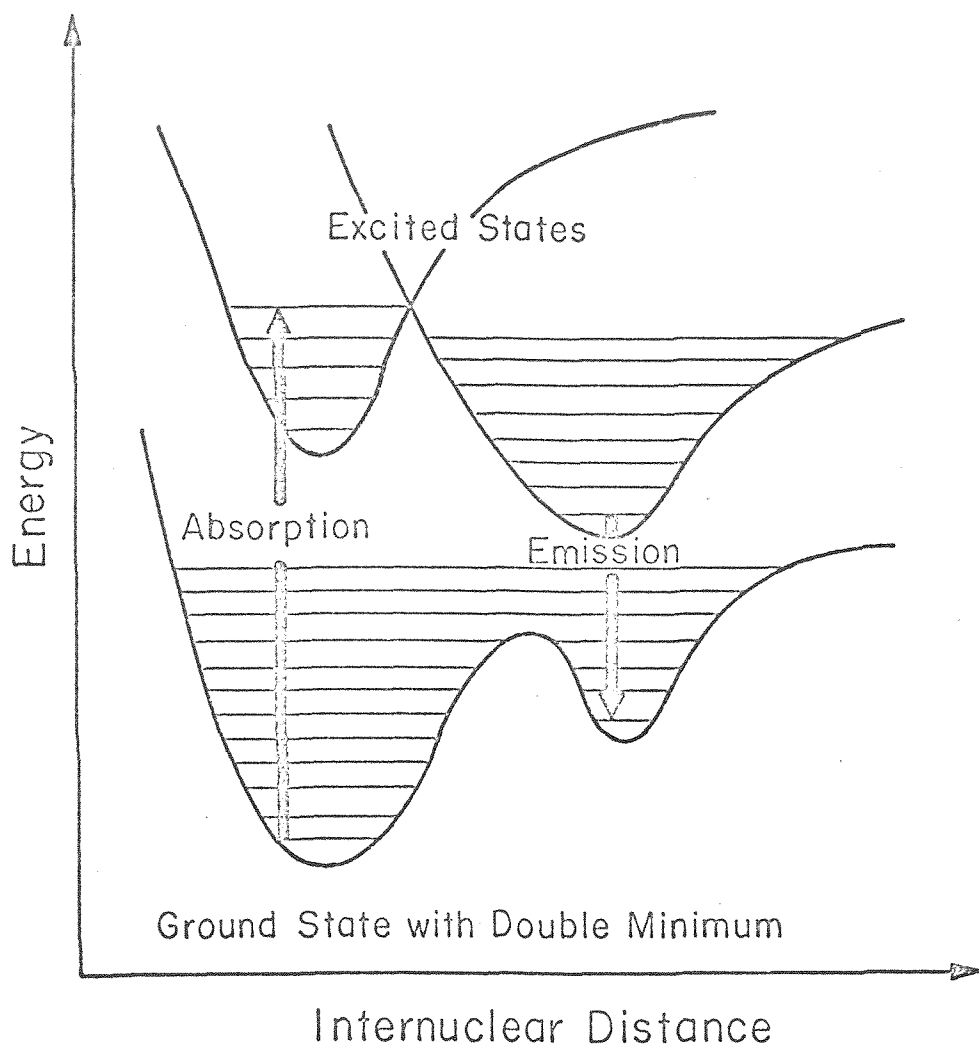


Figure III-12. Schematic diagram of molecule having a ground state with a double minimum.

Table III-6. Emission Data for  $O_h$   $d^6$  Complexes

	Ref.	Absorption Max., $\text{cm}^{-1}$	Emission Max., $\text{cm}^{-1}$	Lifetime, sec.
$\text{Co}(\text{CN})_6^{3-}$	28	32.3	13.4	$0.68 \times 10^{-3}$
$\text{Ru}(\text{CN})_6^{2-}$	31	31	22.65	$31 \times 10^{-3}$
$\text{Pt}(\text{F})_6^{2-}$	1a	—	15.0	—
$\text{Pt}(\text{Cl})_6^{2-}$	32	22.1	14.5	$0.3\text{--}0.8 \times 10^{-3}$
$\text{Pt}(\text{Br})_6^{2-}$	1a	19.0	13.51	
$\text{Rh}(\text{acac})_3$	29	31.25 <sup>a</sup>	11.8	—
$\text{Ir}(\text{acac})_3$	29	22.0 <sup>a</sup>	11.3	—
$\text{Rh}(\text{dtp})_3$	33	18.2	10.0	$1.6 \times 10^{-6}$
$\text{Rh}(\text{dmtc})_3$	33	20.0	11.6	$3.0 \times 10^{-6}$
$\text{Ir}(\text{dtp})_3$	33	21.5	10.2	—
$\text{Ir}(\text{dmtc})_3$	33	23.7	12.2	$2.5 \times 10^{-6}$
$\text{Rh}(\text{NH}_3)_6^{3+}$	34	33.3	16.33	$19 \times 10^{-6}$

<sup>a</sup>Ref. 30.

band occurs with a maximum at  $32.3 \text{ kcm}^{-1}$ . The emission from the  $\text{Co(CN)}_6^{3-}$  occurs, however, at  $13.4 \text{ kcm}^{-1} \text{ nm}$ . This represents a shift of  $\sim 20 \text{ kcm}^{-1}$ . Another dramatic example is that of  $\text{Ir(acac)}_3$ .<sup>29</sup> Being a third row transition metal one expects to observe direct  $S \rightarrow T$  absorption and the band should appear at energies greater than  $20 \text{ kcm}^{-1}$ .<sup>30</sup> The weak emission, however, from  $\text{Ir(acac)}_3$  is at  $11.3 \text{ kcm}^{-1}$ , red shifted almost  $10 \text{ kcm}^{-1}$  from the first spin-forbidden absorption band.

Significant red shifts away from the  ${}^1A_{1g} \rightarrow {}^3T_1$  are meaningful since one expects that  ${}^3T_{1g} \rightarrow {}^1A_{1g}$  emission would overlap the absorption because the same states are involved. If the  ${}^3T_{1g}$  state is accessible by direct absorption one generally expects some overlap with the emission from that state. Here though we are dealing with the  $O_h d^6$  configuration which has no stable triplet ground state possible. The excited state distorts either to the  $C_{4v}$  arrangement or to the  $O_h$  quintet. At least it is clear that it is unreasonable to correlate the luminescence with the spectroscopic triplet observed in absorption.

The lifetime observed for heavy metal  $d^6$  luminescence is too long to be consistent with a normal spectroscopic singlet-triplet transition in such systems. For example,  $\text{Ru(CN)}_6^{2-}$  is reported to luminesce with a lifetime of  $3.1 \times 10^{-2} \text{ sec}$ .<sup>31</sup> The  $\text{Pt(Cl)}_6^{2-}$  has a lifetime of  $1 \times 10^{-3} \text{ sec}$ .<sup>32</sup> The triplet state of these complexes can easily be seen in absorption, thus

the value for  $k_r$  is high. Triplet emission from heavy metal systems is more akin to fluorescence in organic systems rather than to organic phosphorescence. Direct singlet-triplet absorption in organic systems is only barely detectable so triplet  $\rightarrow$  singlet emission is expected to be long lived. The large spin-orbital coupling effect in the metals relaxes the selection rule so that  $S \rightarrow T$  absorption can be reasonably intense and give short lived emission. The quintet  $\rightarrow$  singlet transition represents a change in spin quantum number of two which should give long lifetimes even when spin-orbital coupling effects are large. The fact that the luminescence from  $d^6$  systems is not longer lived than observed means that the rates of nonradiative decay dominate the emission lifetime. That the nonradiative decay rate dominates may be especially true when the lifetime observed is very short as in Rh(III) and Ir(III) complexes with tris sulfur chelate ligands.<sup>33</sup> Large shifts in emission and absorption are observed here, but the lifetime is only of the order of  $10^{-6}$  sec.

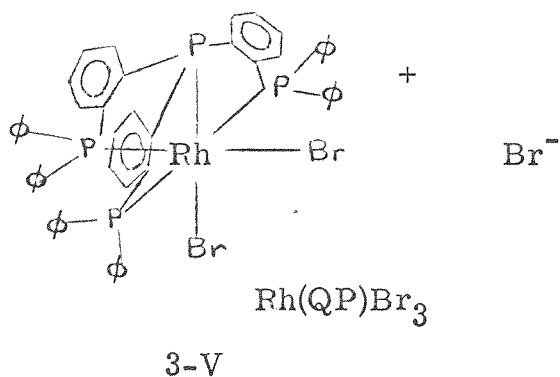
While very little emission quantum yield data is available for transition metal complexes one notes that d-d luminescence is very weak from most of the  $d^6$  metal systems. This is consistent both with a triplet or a quintet assignment for the emission.

A final point concerning the possibility of quintet emission is developed more fully in Chapter V. The major piece of

evidence is that  $\text{Co}(\text{CN})_6^{3-}$  with a very low lying excited state will not effectively quench organic triplets. This result again implies that the emission observed is not from a state which is accessible spectroscopically.

At this point quintet emission is only a strong possibility. Conclusive structural assignment of the excited state as either a  $\text{C}_{4v}$  or  $\text{O}_h$  geometry will provide the evidence for a final assessment of quintet  $\rightarrow$  singlet luminescence.

Few examples exist of  $d^6$  luminescence from systems of geometry besides  $\text{ML}_6$ . We have looked at  $\text{C}_{4v}$  tungsten carbonyl complexes in detail, and these are described below. It has also been noted that  $\text{Rh}(\text{III})$  complexes containing tetradentate phosphorous ligands exhibit luminescence at low temperature. As an example, 3-V gives luminescence as



shown in Figure III-13. Like most of the  $\text{O}_h$   $d^6$  systems no splitting of the emission is seen, but in contrast to  $\text{Rh}(\text{acac})_3$ ,

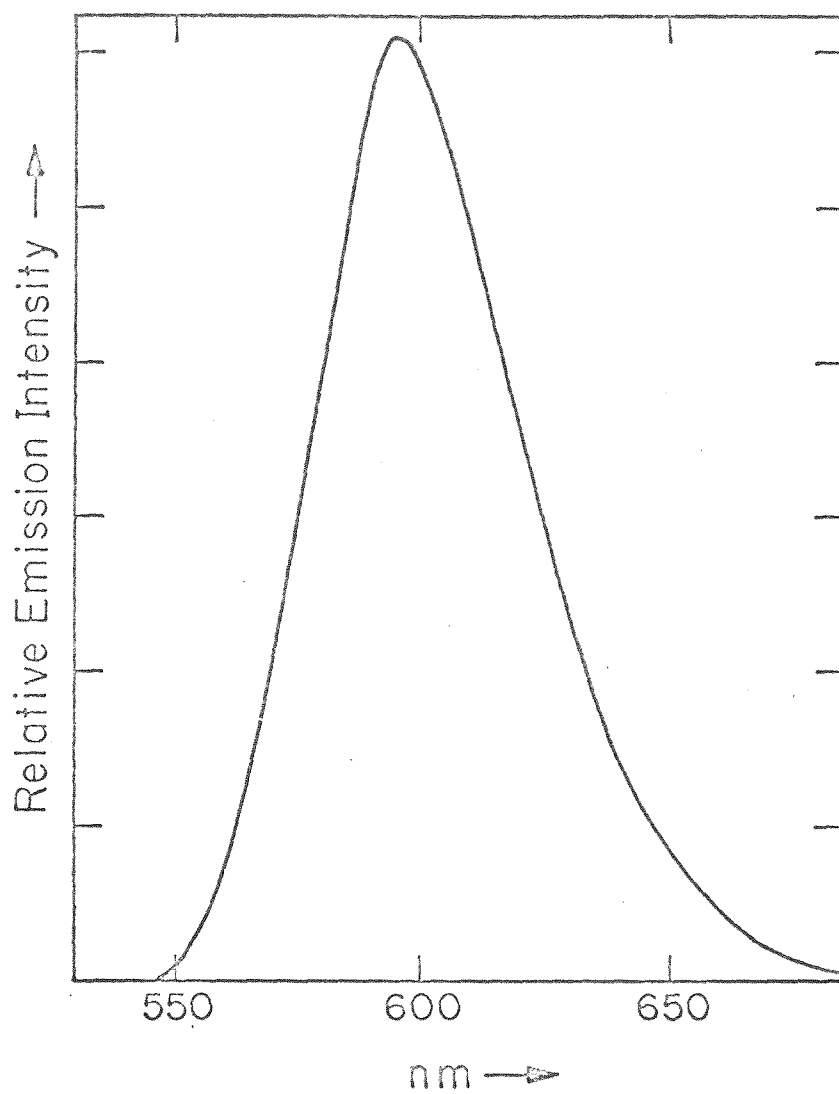
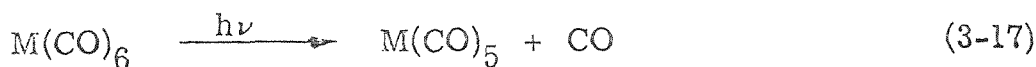


Figure III-13. Emission from Rh(QP)Br<sub>3</sub> as the pure solid at 77° K.

for example, the red shift from the first absorption band is rather small. On the other hand, emission from  $\text{trans-Co(CN)}_4(\text{SO}_3)_2^{5-}$  is at  $14.3 \text{ kcm}^{-1}$ ,<sup>27</sup> a  $12 \text{ kcm}^{-1}$  shift from the first spin-allowed d-d band at  $26.5 \text{ kcm}^{-1}$ . More systematic studies are needed to correlate geometrical structure with d-d luminescence phenomena in  $d^6$  systems.

$d^6$  Metal Carbonyl Luminescence. Toward a greater understanding of excited state chemistry and structure of metal carbonyls we have investigated luminescence phenomena from some  $d^6$  systems of symmetries other than  $O_h$  (cf. pp. 81-92). The luminescence from  $\text{M(CO)}_6$   $\text{M} = \text{Cr, Mo, or W}$  is not detectable due to the fact that reaction (3-17) occurs with unit



efficiency. However, as pointed out in Chapter II we have been able to observe d-d luminescence from some  $\text{M(CO)}_5(\text{X})$  complexes. The only other  $C_{4v}$  symmetry complexes of  $d^6$  configuration which have been investigated in detail are  $\text{Rh(NH}_3)_5(\text{X}^-)^{2+}$  species.<sup>34</sup>

We have observed luminescence at  $77^\circ\text{K.}$  from the complexes  $\text{W(CO)}_5(\text{X})$  where X is virtually any  $\pi$ -electron donor (ethers, ketones, nitrogen donors, etc.).<sup>35</sup> In Table III-7 we list some  $\text{W(CO)}_5(\text{X})$  complexes and their absorption and emission maxima. The complexes exhibit emission maxima between 510 nm and



Table III-7. Emission and Absorption Maxima for  $W(CO)_5(X)$  Complexes

	Abs. Max., <sup>a</sup> nm	Emission Max., <sup>b</sup> nm
$NEt_3$	428, 402	533
$HNEt_2$	438, 402	533
cyclohexylamine	438, 402	533
acetone	450, 406	538
ethylether	456, 418	533
pyridine	440, 385	510
$S-Et_2$	412, 386	545
$NH_3$	450, 408	535
2-methyl-pyridine	—	525
2, 4, 6-trimethyl-pyridine	—	530

<sup>a</sup>Room temperature hydrocarbon solutions.

<sup>b</sup>77°K. methylcyclohexane solutions.

545 nm in a 77°K. methylcyclohexane glassy solvent. The emission spectrum generally shows no structure and overlaps slightly with the first band in absorption. A representative emission spectrum is shown in Figure III-14. The luminescence lifetime of these complexes is of the order of  $10^{-6}$  sec. and quantum yields are estimated to be no greater than 0.1.

The characteristics of the  $W(CO)_5(X)$  emission strongly suggest that the transition is metal-localized and spin-forbidden. The key points are that the luminescence overlaps the absorption band that we assign as the  $^1A_1 \rightarrow ^3E$  in  $C_{4v}$  symmetry; no emission is seen from the Mo or Cr analogs which do not show the  $^1A_1 \rightarrow ^3E$  absorption; the emission energy is insensitive to ligands with the same donor atom; the luminescence yield is relatively small, and the lifetimes ( $10^{-6}$  sec) are characteristic of heavy metal spin-forbidden emission.<sup>1a</sup>

Some interesting aspects of the metal carbonyl system should be pointed out. First, the emission occurs whether the ligand X is firmly bound or not: compare  $W(CO)_5(\text{acetone})$  and  $W(CO)_5(\text{pyridine})$ . The acetone is very weakly coordinated as evidenced by our work with thermal exchange of the acetone<sup>36</sup> while the pyridine apparently does not exchange at all thermally at room temperature. However, there appear to be no qualitative differences in the luminescence properties of these two compounds. Further, we note that luminescence could be

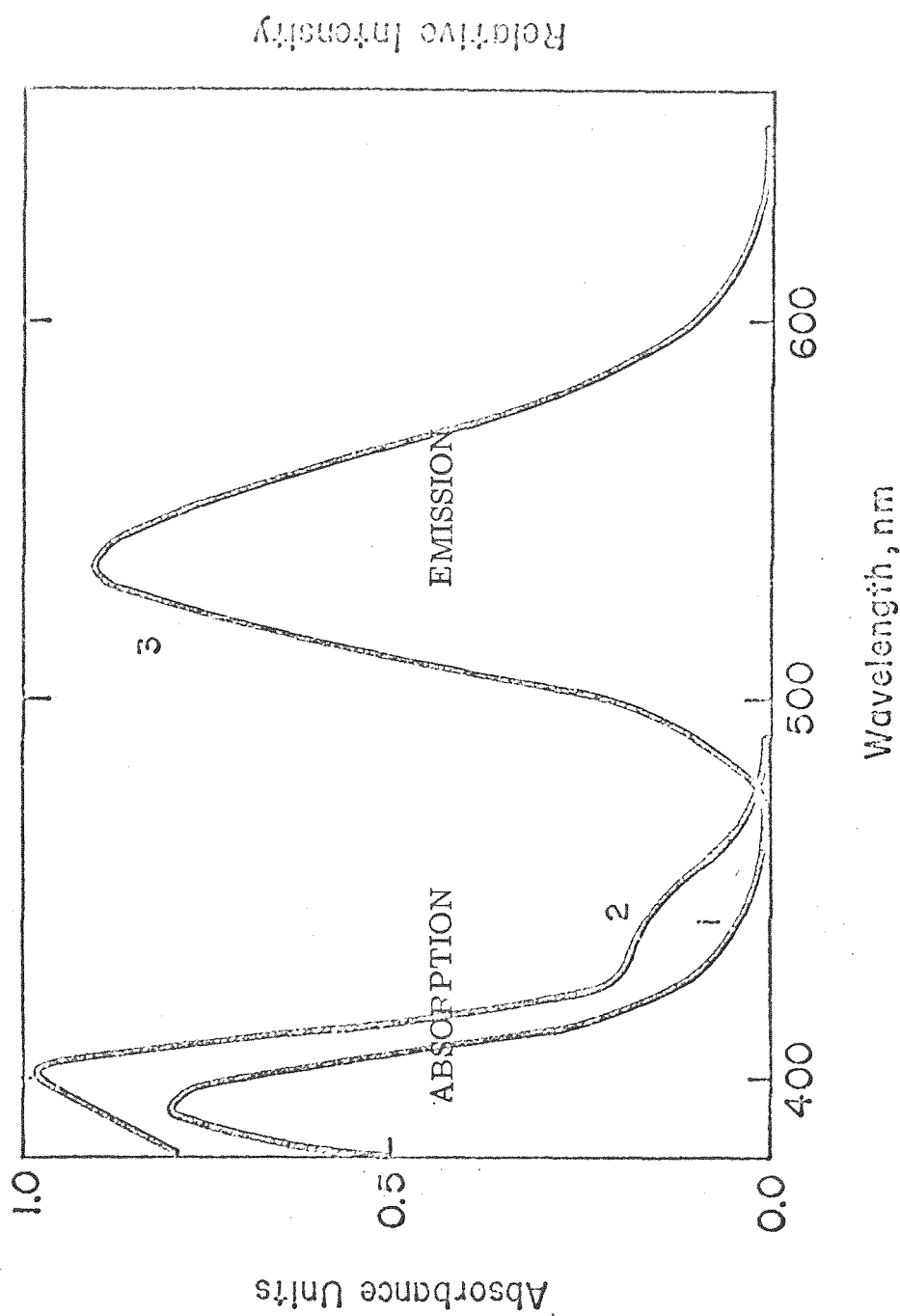


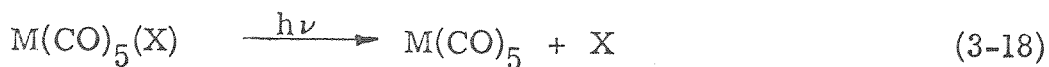
Figure III-14. Curve 1 is the absorption spectrum of  $\text{Mo(CO)}_5(\text{cyclohexylamine})$ , curve 2 the absorption spectrum of the corresponding tungsten complex, and curve 3 is the emission spectrum of the tungsten complex. Absorption is at room temperature and the emission at  $77^\circ\text{K}$ .

detected from  $\text{W}(\text{CO})_5$  itself (although there is some controversy concerning the nature of this complex), and importantly this emission is at the same energy as nitrogen donors. The conclusion is that the  $\text{W}(\text{CO})_5$  moiety dominates the electronic structure of the oxygen and nitrogen donor complexes. This may be occurring in the same way that the one NO ligand of  $\text{Cr}(\text{NO})(\text{H}_2\text{O})_5^{2+}$  dominates its electronic structure.<sup>37</sup>

Another interesting aspect of the  $\text{M}(\text{CO})_5(\text{X})$  emission is the fact that the emission spectrum of the pure solid  $\text{W}(\text{CO})_5(\text{py})$  is very temperature sensitive. At room temperature, for example, no luminescence is observed. The details of this effect will be discussed in Chapter IV, but it is difficult to understand an activation energy for nonradiative decay rates. Finally, the observation of luminescence from the  $d^6$  metal carbonyls is an unexpected phenomenon in light of the fact that chemistry occurs with such high efficiency.

The  $\text{C}_{4v}$  complexes studied give narrow band emission which overlaps the absorption. This suggests that further distortion from the  $\text{C}_{4v}$  ground state is not large. One should compare this effect with observations of no spectral overlap in cases where the quintet or a nonspectroscopic excited state is implicated for  $d^6$  complexes. The lack of a significant red shift in the emission is particularly interesting in that photochemical results (Chapter VII) reveal that the excited  $^1\text{E}$  and

$^3E$  states are involved in the dissociative reaction (3-18).



One can see this by noting that the E states involve population of the  $d_{z^2}$  ( $\sigma^*$ ) orbital which should cause weakening of M-L bonds on the z-axis thus giving large distortions in the excited state and bond breaking as an ultimate deactivation step.

The extension of these luminescence studies with ligands such as  $AsPh_3$  or  $PPh_3$  has not been completed. At this point we can only say that  $W(CO)_n(AsPh_3)_{6-n}$  and  $W(CO)_n(PPh_3)_{6-n}$  do give luminescence and more detailed studies are under way.

Luminescence studies with the lower symmetry cis- $W(CO)_4(L)_2$  ( $L = \text{pyridine}$ ) give results similar to those obtained with the  $C_{4v}$   $W(CO)_5(X)$  species. Emission from cis- $Mo(CO)_4(py)_2$  was not detectable nor does it have a low energy shoulder on the first absorption band which appears in the tungsten complex. The emission lifetime for the cis- $W(CO)_4(py)_2$  is  $6.7 \mu\text{sec}$  which is longer than the  $W(CO)_5(py)$  ( $1.5 \mu\text{sec}$ ). The significance of this difference awaits the study of other complexes. In Figures III-15 and III-16 we show the absorption and emission spectra of the cis- $M(CO)_4(X)_2$  complexes.

Luminescence from  $d^6 \pi$ -Complexes. The luminescence of metal carbonyls represents one area of organometallics.

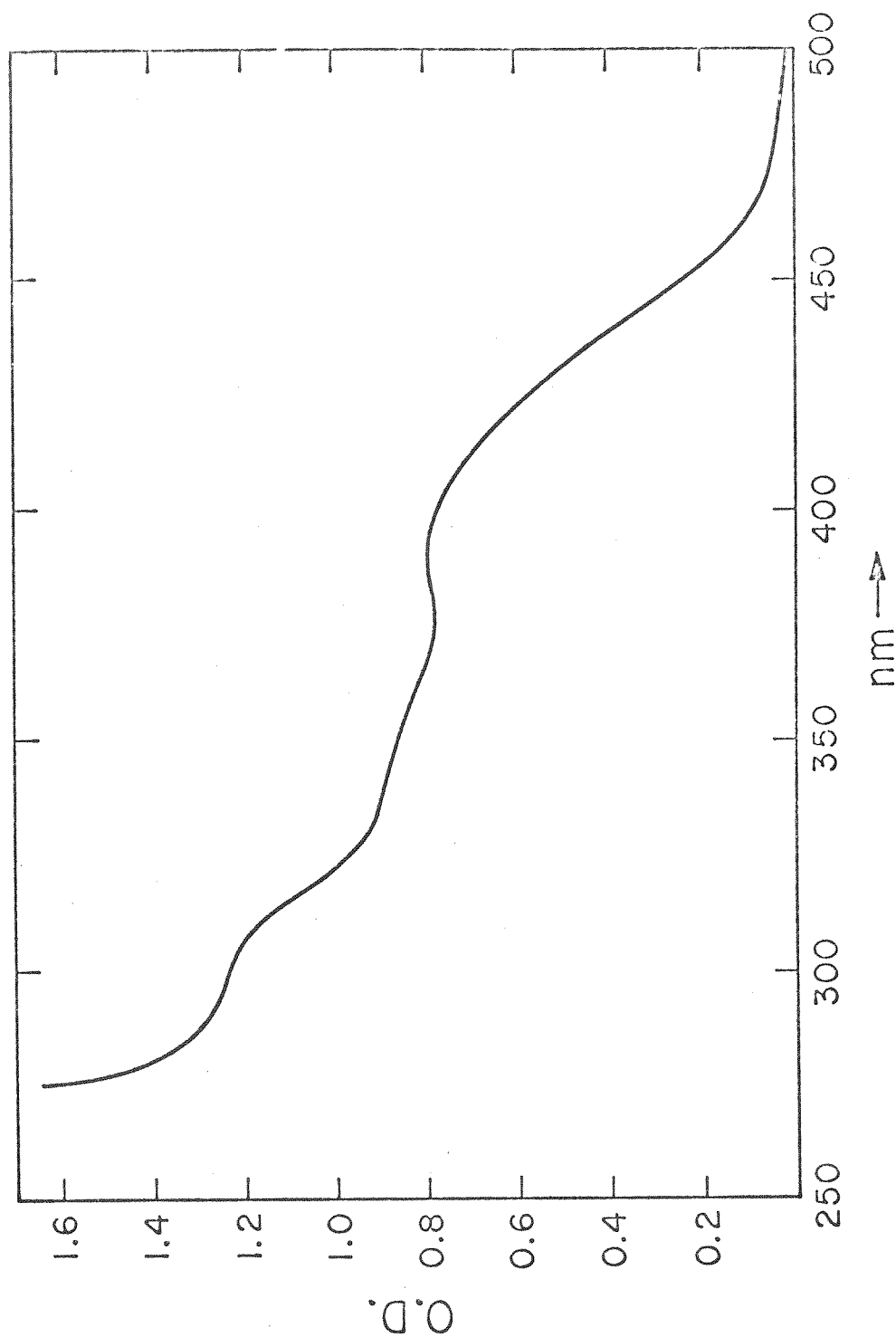


Figure III-15a. Electronic absorption spectrum of  $\text{cis-Mo(CO)}_4(\text{py})_2$  in  $\text{CHCl}_3$  at room temperature. Note the lack of a shoulder on the low energy side of the first absorption band.

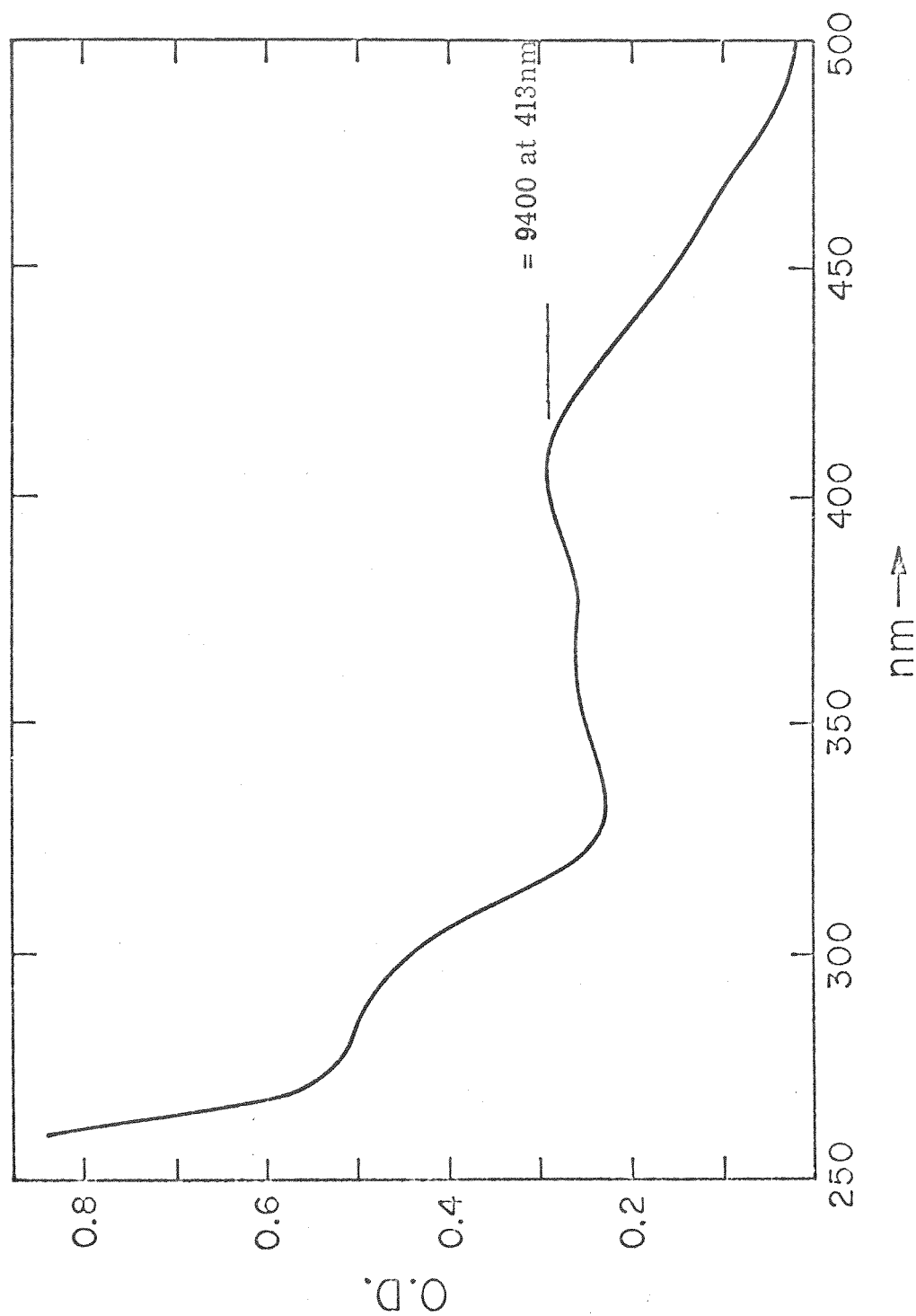


Figure III-15b. Electronic absorption spectrum of  $\text{cis-W(CO)}_4(\text{py})_2$  in  $\text{CHCl}_3$  at room temperature. Note the presence of the low energy shoulder on the low energy side of the first band.

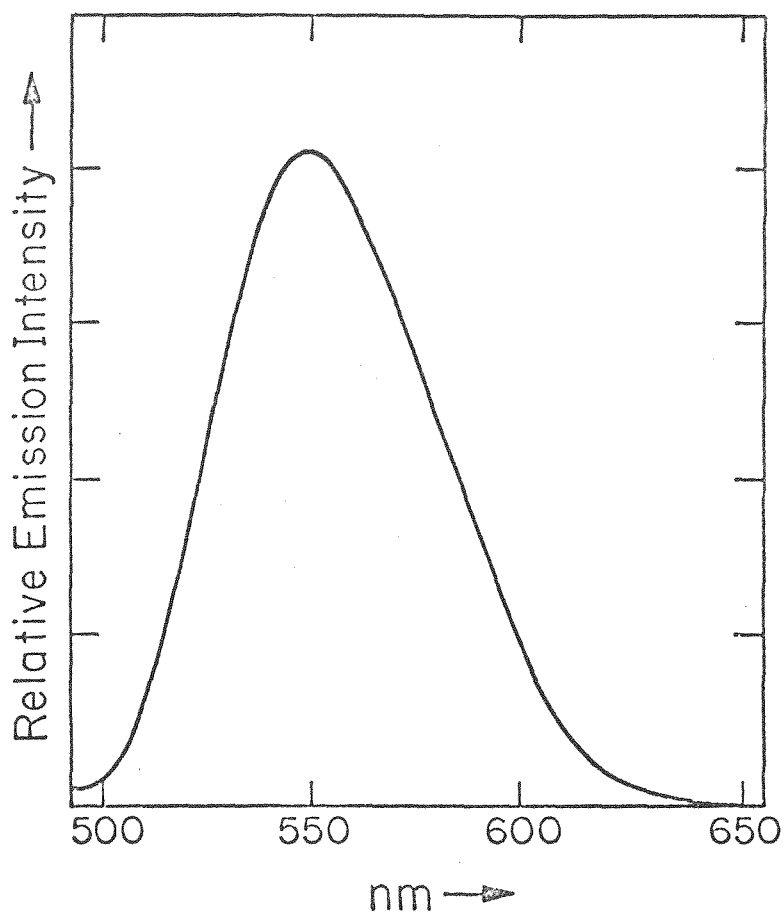


Figure III-16. Total emission spectrum of  $\text{cis-W(CO)}_4(\text{py})_2$  in EPA at 77°K.



Another important area is the  $\pi$  complexes formed with organic  $\pi$  systems and transition metals. The earliest of these, Zeise's salt,  $\text{PtCl}_3(\text{C}_2\text{H}_2)^-$ , has been shown to be luminescent<sup>38</sup> and is similar to the other  $\text{Pt(II)} d^8$  square-planar complexes. No other  $\pi$  complexes have been reported to give luminescence except for the model sandwich complex ferrocene.<sup>39</sup> (We have observed charge transfer luminescence in  $\text{Fe(cp)}_2^+$ , pp.78-81). However, the emission thought to be from ferrocene is now attributed to solvent impurity.<sup>40</sup>

We have observed luminescence from two  $d^6$  metallocenes. Ruthenocene, the second row analog of ferrocene, exhibits an emission maximum at 570 nm at 77°K. as the pure solid. The excitation spectrum resembles the absorption spectrum. Cobalticinium gives an emission maximum at  $14.9 \text{ kcm}^{-1}$  with either the perchlorate or the picrate anion. A He-Ne laser (632.8 nm) was used as the exciting source for  $\text{Co(cp)}_2^+$  at room temperature. The emission spectra are shown in Figures III-17 and III-18, and absorbance and emission maxima are detailed in Table III-8. The large red shift in the emission implicates a distorted triplet state or perhaps a quintet. Ruthenocene does not quench biacetyl triplets at a diffusion controlled rate providing evidence again for an inaccessible excited state. From the  $\text{Ru(cp)}_2$  and  $\text{Co(cp)}_2^+$  we predict that if luminescence is to be observed from  $\text{Fe(cp)}_2$  it should occur

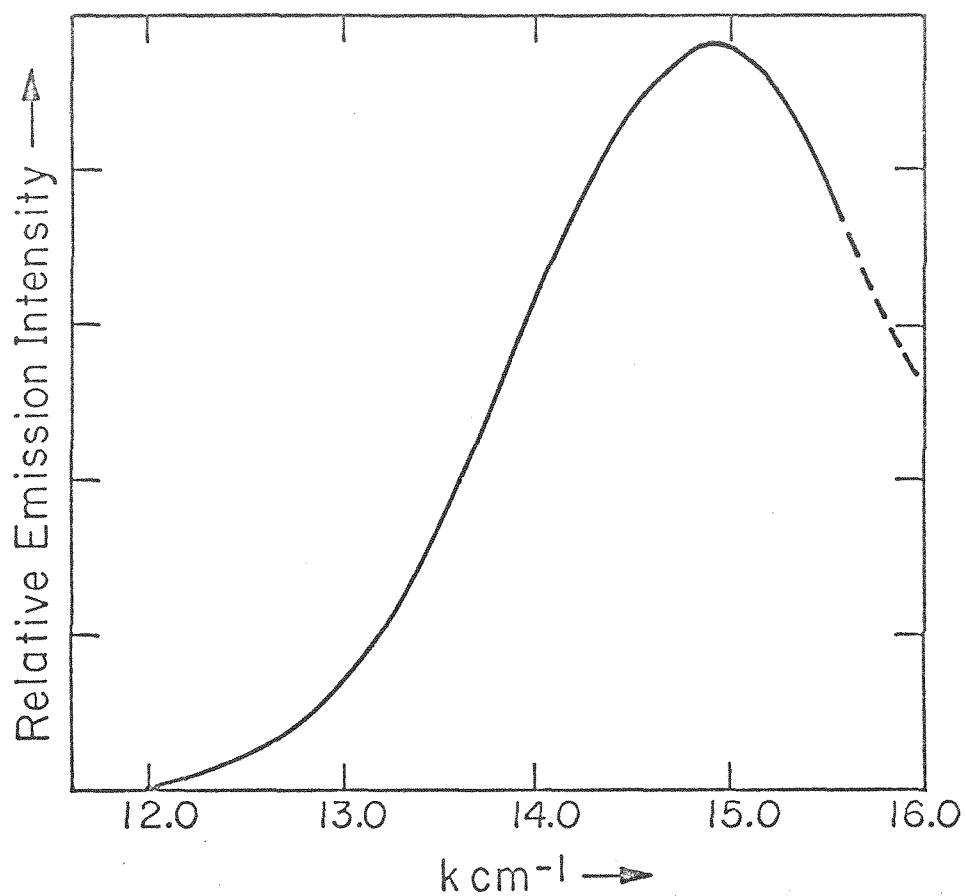


Figure III-17. He-Ne laser excited emission from  $[\text{Co}(\text{cp})_2]\text{ClO}_4$  as the pure solid at room temperature.

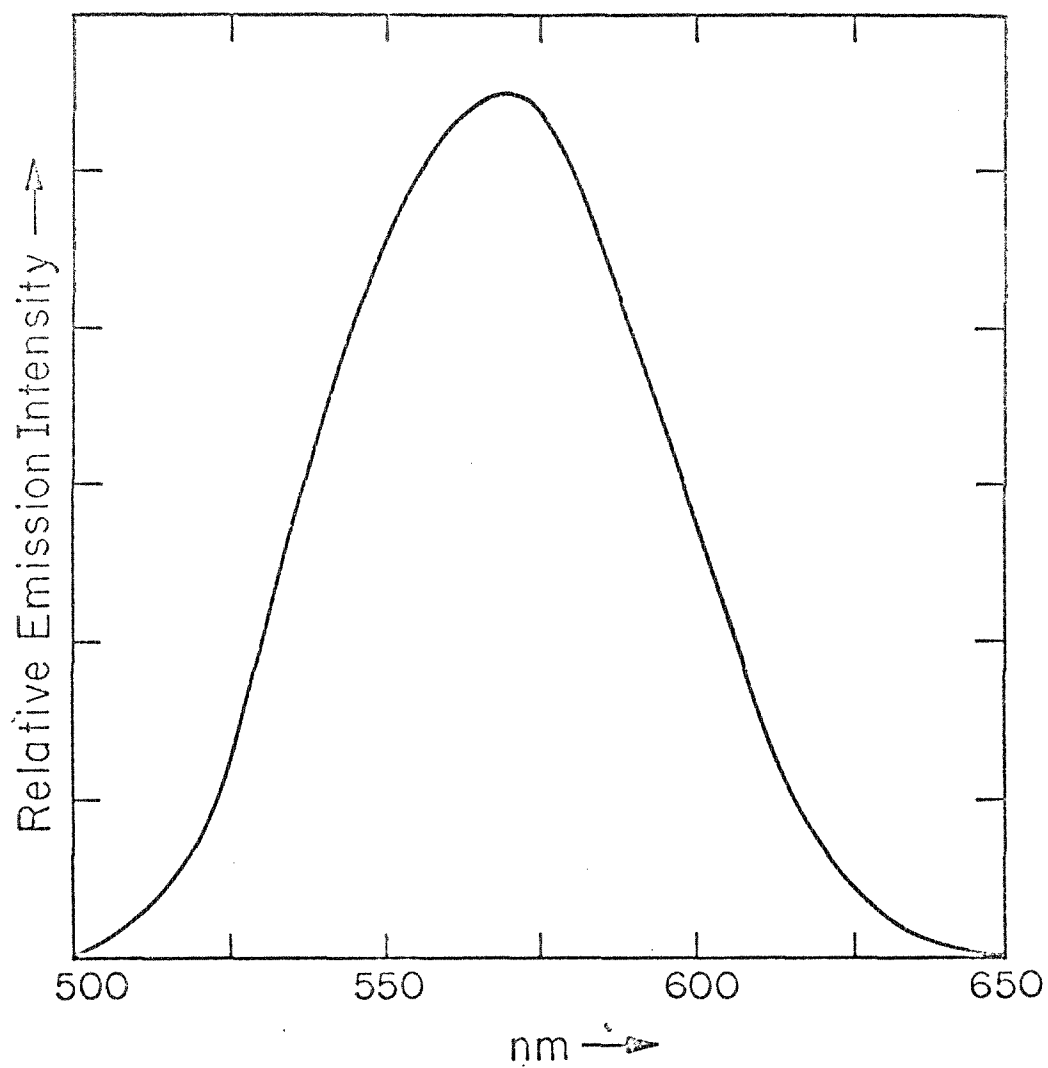


Figure III-18. Emission spectrum for Ru(cp)<sub>2</sub> as the pure solid at 77°K.

Table III-8. Emission and Absorption Data for d<sup>6</sup> Metallocene Complexes

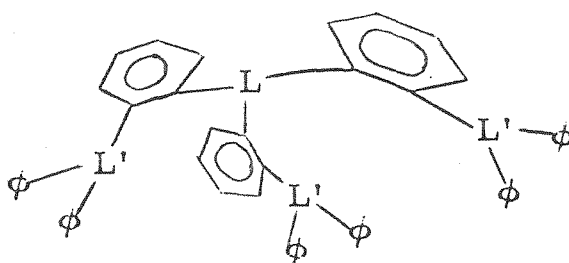
Complex	S → T ( ε ) <sup>a</sup>	Emission Max. <sup>b</sup>	Stoke Shift
Fe(cp) <sub>2</sub>	18.9 (7)	—	—
Ru(cp) <sub>2</sub>	26.0 (5)	17.5	8.5
[Co(cp) <sub>2</sub> <sup>+</sup> ] ClO <sub>4</sub>	21.8 (7)	14.9	6.9

<sup>a</sup>Ref. 17.

<sup>b</sup>Room temperature solids, 632.8 nm He-Ne laser excitation.

at an energy of  $\sim 11 \text{ kcm}^{-1}$ . The detailed data concerning lifetimes and quantum yields are not available but should provide insight into the nature of metallocene excited states.

Luminescence in  $d^8$  Five-Coordinate Systems. The luminescence studies of  $d^8$  systems have centered on the square planar Pt(II) complexes.<sup>1a</sup> Generally, emission associated with the spin-forbidden transitions is observed and emission is thought to occur as a metal-localized triplet  $\rightarrow$  singlet transition. Clear correlations of ligand structure and luminescence phenomena do not exist. No Pd(II) square planar complexes seem to have been reported as giving emission nor any five-coordinate complexes of defined structure of any  $d^n$  configuration. The Pd(II) and Pt(II) metals can be forced to assume a five-coordinate trigonal bipyramidal structure by using tetradentate ligands 3-VI. These systems have served as models for study



$L=L'=As$  : QAS

$L=L'=P$  : QP

$L=As, L'=P$  : AsTP

$L=P, L'=As$  : PTAs

$L=P, 2L'=As, 1L=P$  :  $PAs_2P$

of electronic structure of five-coordinate systems where the fifth ligand for Pt(II) or Pd(II) is variable being typically a halogen.<sup>41</sup> We have observed luminescence from both the Pt(II) and Pd(II) five-coordinate systems. We summarize some absorbance and emission data for these complexes in Table III-9. Typical emission spectra are shown in Figures III-19 and III-20. A lifetime determination was made for three Pt(II) complexes:  $[\text{Pt}(\text{PTAs})(\text{Cl})]^{+}[\text{Cl}]^{-}$ ,  $\tau = 21.5 \times 10^{-6}$  sec;  $[\text{Pt}(\text{QP})\text{Cl}]^{+}[\text{Cl}]^{-}$ ,  $\tau = 31.5 \times 10^{-6}$  sec; and  $[\text{Pt}(\text{QAs})\text{Cl}]^{+}[\text{Cl}]^{-}$ ,  $\tau = 23 \times 10^{-6}$  sec. These lifetimes were measured in EPA at 77°K. and suggest that the observed emission in these systems is spin-forbidden. Lifetime measurements for the other complexes were not possible with the apparatus available. Quantum yield measurements have not been made but would prove valuable in understanding changes in lifetime.

We see that, as in absorption, the nature of the ligand has only a small effect on the energy of the electronic transitions. However, the metal effect is significant: the Pt(II) complexes generally have higher energy transitions than the Pd(II) complexes reflecting the larger splitting of the d orbitals for the heavier metal. We assign the spin-forbidden emission as the  ${}^3\text{E}'_1 \rightarrow {}^1\text{A}'_1$  transition, corresponding to the lowest spin-allowed absorption band. Temperature effects have not been measured, but something may be said concerning the nature

Table III-9. Absorption and Emission Data for Five-Coordinate Pt(II) and Pd(II) Complexes

Complex	Absorption Max., $^1A_1 \rightarrow ^1aE$ $a \text{ cm}^{-1} (\epsilon)$	Emission Max., $b \text{ cm}^{-1}$
$[ClPt(PTAs)Cl]$	25,510(7430), 23,530 sh	17,540 <sup>c</sup>
$[ClPt(QAs)Cl]$	25,130(8600), 22,990 sh	17,060 <sup>c</sup>
$[BrPt(QAs)Br]$	24,210(10000), 22,320 sh	13,980
$[Pt(QAs)I^+][B\phi_4^-]$	22,470(3910), 20,830 sh	14,020
$[BrPt(QP)Br]$	25,250(6800), 22,900 sh	14,250
$[IPt(QP)I]$	23,400(5200) d	14,330
$[ClPt(PAs_2P)Cl]$	26,460(6000), 23,530 sh	14,230
$[ClPd(QP)Cl]$	22,300(8000) d	13,550
$[BrPd(QP)Br]$	21,500(7600) d	13,550
$[IPd(QP)I]$	19,800(6500) d	13,320
$[ClPd(PAs_2P)Cl]$	—	13,730
$[ClPd(PTAs)Cl]$	—	13,580
$[ClPd(AsTP)Cl]$	—	13,560
$[ClPd(QAs)Cl]$	20,830(7540), 18,690 sh	13,500

<sup>a</sup>Data from ref. 41.<sup>b</sup>Room temperature solid excited at 632.8 nm with He-Ne laser unless otherwise noted.<sup>c</sup>EPA solution at 77°K., Aminco-Bowman emission spectrometer.<sup>d</sup>Not reported.

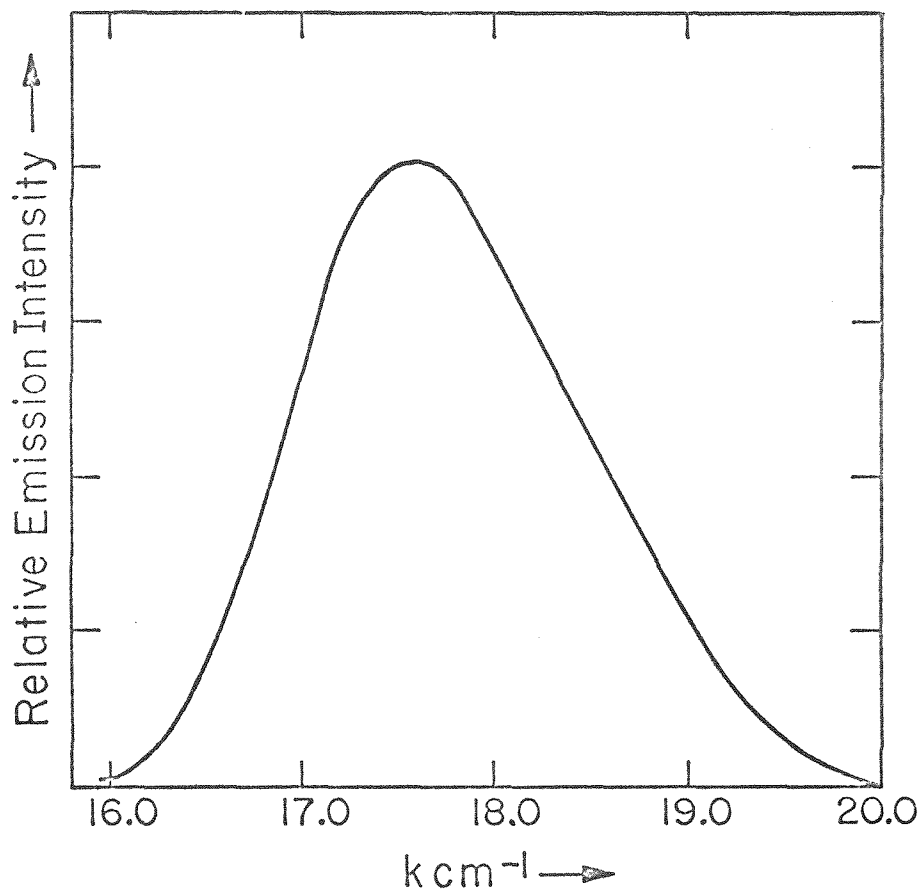


Figure III-19. Emission from  $\text{Pt(PTA's)Cl}_2$  in EPA at 77°K.



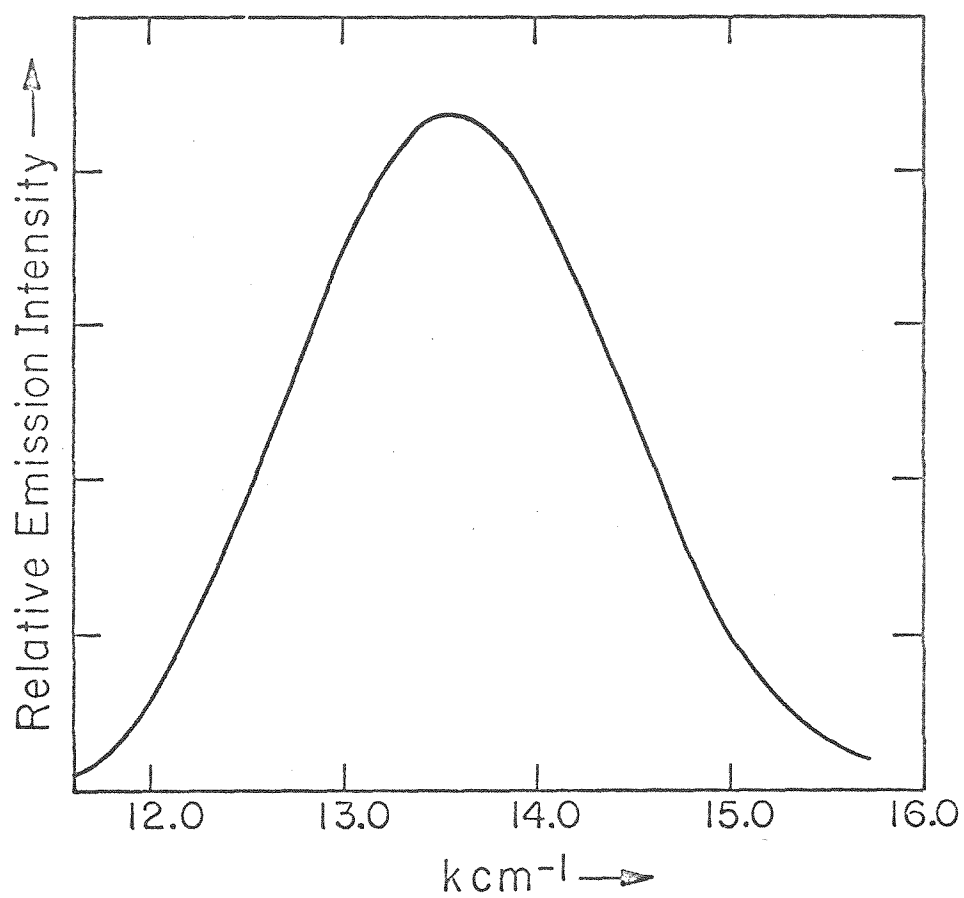


Figure III-20. He-Ne laser excited emission from  $\text{Pd}(\text{QP})\text{Cl}_2$  as the pure solid at room temperature.

of the observed distortion<sup>41</sup> in this system when these measurements are complete.

Luminescence of Tetrahedral  $d^7$  Co(II). Cobalt(II) when tetrahedrally coordinated is generally blue due to a spin-allowed transition at  $\sim 15 \text{ km}^{-1}$ . However, a lower energy d-d transition occurs in the infrared and is at  $\sim 5.8 \text{ km}^{-1}$  for  $\text{Co}(\text{Cl})_4^{2-}$ .<sup>42</sup> The large splitting between these first two spin-allowed transitions increases the possibility that decay occurs directly from the state at  $15 \text{ km}^{-1}$  to the ground state. Evidence could manifest itself in the form of emission from the upper excited state. We have examined some Co(II) complexes of  $T_d$  symmetry with the hope of observing emission from the second excited state to the ground state. In some cases, using He-Ne laser excitation, we were able to detect very weak luminescence from the room temperature solids, cf. Figure III-21. In Table III-10 we list the complexes for which emission was observed. That we are observing deactivation of an upper excited state directly to the ground state is unequivocal, but the efficiency is indeterminate. One must also look at the emission from the lowest excited state to gain some feel for the relative rates involved. Our observations make these experiments possible.

Emission in Metal-Metal Bonded Systems. The photophysical processes in systems containing direct metal-metal bonds

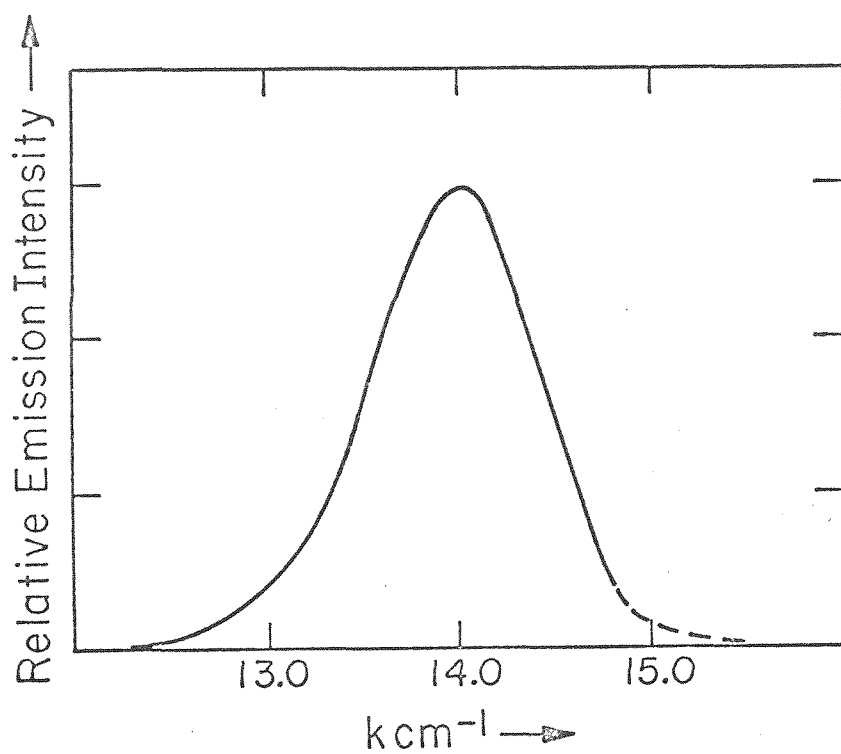


Figure III-21. He-Ne laser excited emission from  $\text{Co}(\text{Cl})_2(\text{X})_2$  as the pure solid at room temperature.

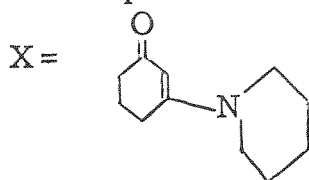
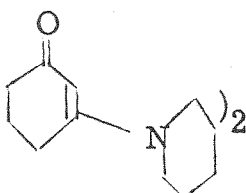
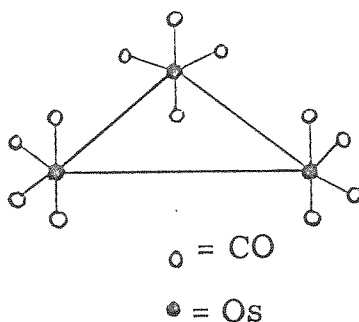


Table III-10. Emission Data for  $T_d$  Co(II) Complexes<sup>a</sup>

Complex	Emission Max., $\text{cm}^{-1}$
$\text{Co}(\text{Cl})_2$ 	14,200
$\text{HgCo}(\text{SCN})_4$	14,300
$\text{K}_2\text{Co}(\text{SCN})_4$	14,300
$\text{Na}_4 \text{Co}(\text{P}_2\text{O}_7)(\text{OH})_2$	14,200

<sup>a</sup>Room temperature solids using 632.8 nm exciting light from He-Ne laser.

have not been explored. Some electronic structural information is available,<sup>43</sup> however, and these systems may provide interesting photochemistry. We have noted luminescence from two compounds containing metal-metal bonds. The emission spectrum of  $\text{Os}_3(\text{CO})_{12}$  is shown in Figure III-22. Coupling the facts that we have three osmium atoms in the molecule and an emission lifetime of  $1.9 \times 10^{-6}$  sec we are almost certainly dealing with spin-forbidden emission. The corresponding  $\text{Ru}_3(\text{CO})_{12}$  showed no luminescence even upon He-Ne laser excitation. The emission may be associated with the excitation of the electrons of the metal-metal bonds. The structure of  $\text{Os}_3(\text{CO})_{12}$  is as shown in 3-VII. The Os atoms can be thought



3-VII

of as having six ligands accounting for 12 electrons and having

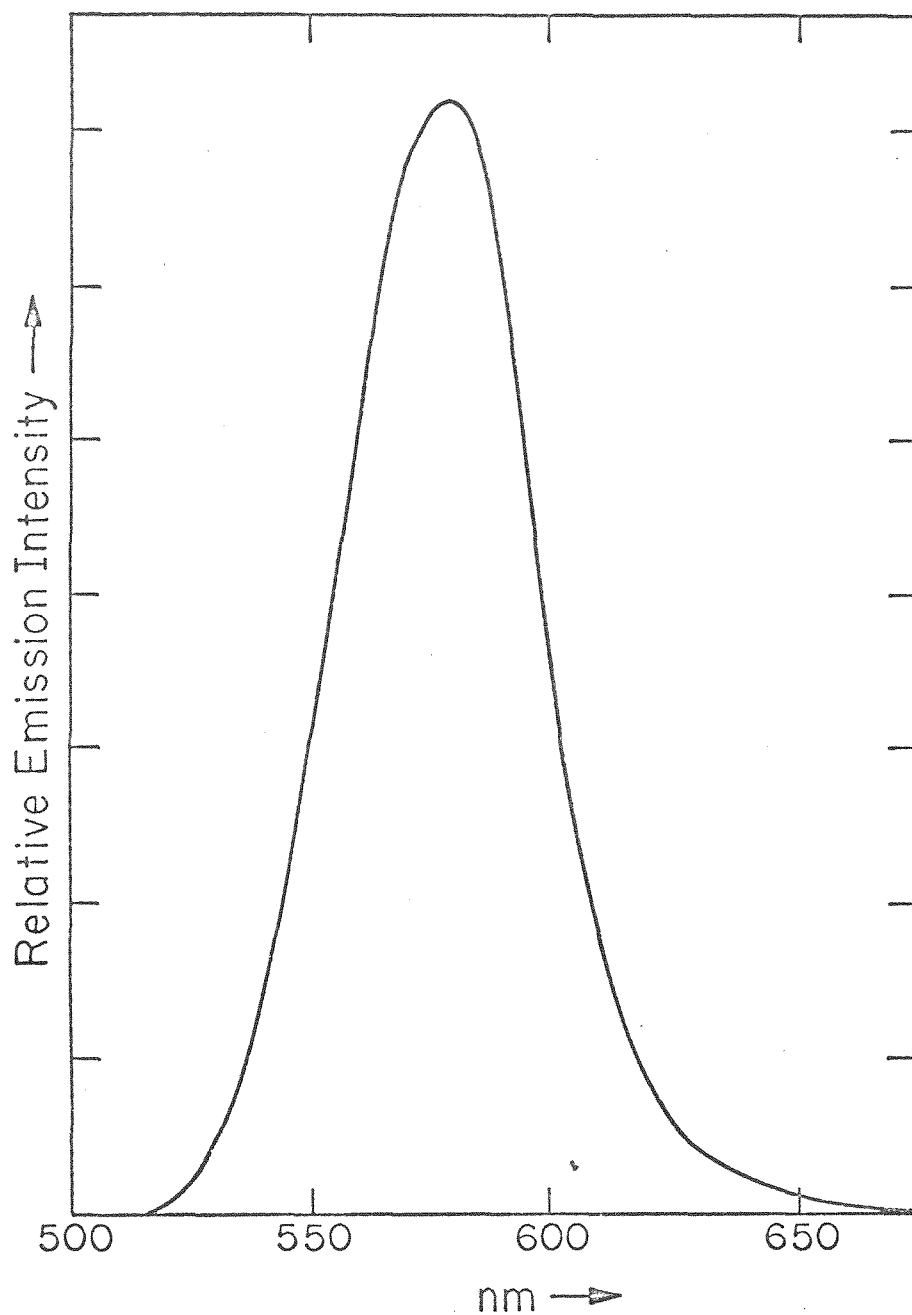
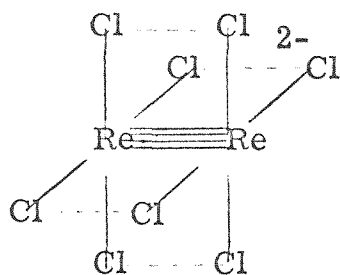


Figure III-22. Emission from  $\text{Os}_3(\text{CO})_{12}$  as the pure solid at 77°K.

a  $d^6$  configuration to give the eighteen electrons to satisfy the EAN rule. Thus, the  $\text{Os}_3(\text{CO})_{12}$  should show d-d transitions and low energy  $\sigma \rightarrow \sigma^*$  transitions associated with the metal-metal bonds. Correlation of the luminescence and absorption with photochemistry of this compound will be of interest.

A second compound which luminesces and contains a metal-metal bond is  $\text{Re}_2\text{Cl}_8^{2-}$  which has a M-M bond order of four. The chlorides are eclipsed, as shown in 3-VIII, enabling  $d_{xy}$



3-VIII

orbitals to overlap to form the fourth metal-metal bond,  $\delta$ . Intense emission is observed upon excitation of  $\text{Re}_2\text{Cl}_8^{2-}$  with a He-Ne laser at room temperature. The emission spectrum is shown in Figure III-23. The excitation by 632.8 nm produces a metal-metal transition:  $\delta \rightarrow \delta^*$  or a  $\delta \rightarrow$  metal p excitation.<sup>44</sup> Either of these transitions will reduce the strength of the metal-metal bond and thus give a red shifted emission band. Also, this excitation produces a coordinatively unsaturated excited state which should be reactive if the state is long-lived. The luminescence lifetime has not been measured.

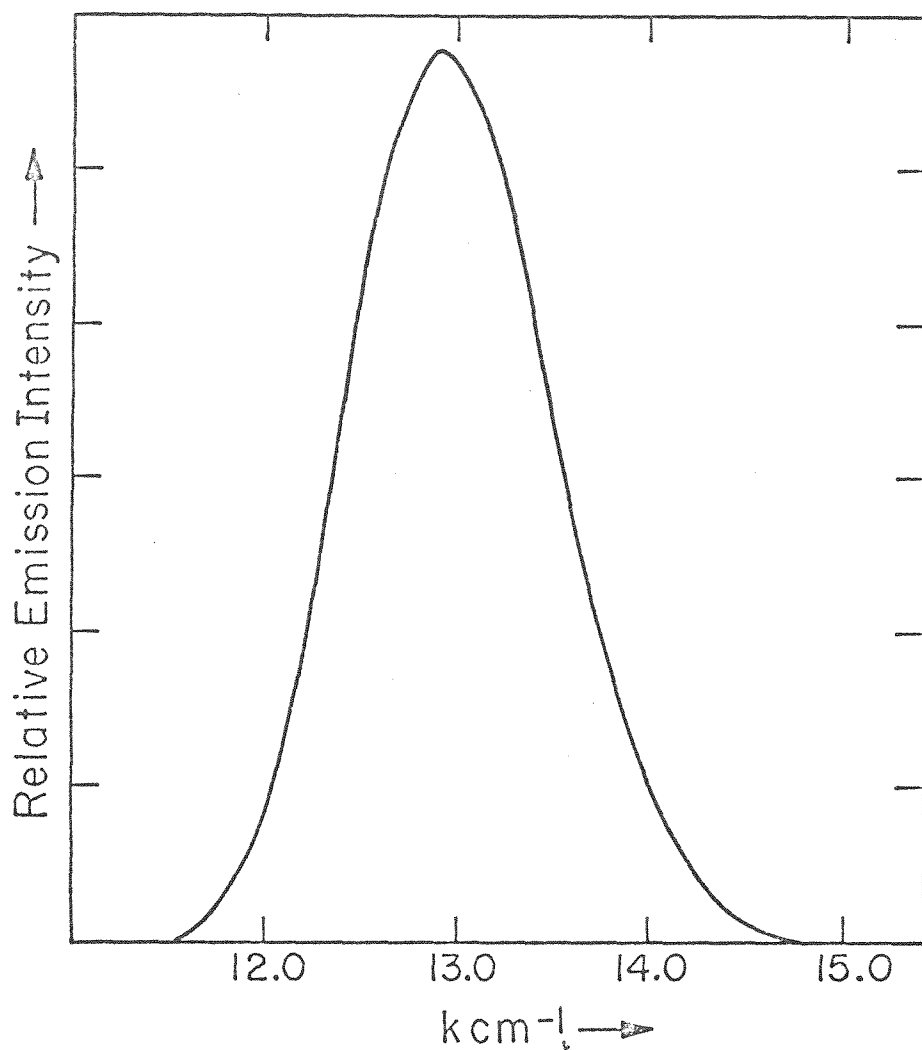


Figure III-23. He-Ne laser excited emission from  $\text{Re}_2\text{Cl}_8^{2-}$  as the  $\text{n-Bu}_4\text{N}^+$  salt at room temperature.



Conclusion. We have pointed out a number of new metal systems which have been found to luminesce via a ligand localized, charge transfer, or metal localized transition. The amount of quantitative work is grossly inadequate, but in defense of our work we point out that several years ago few systems were known to luminesce, and it was thought that few would be found. The potential for a clear understanding of the decay processes lies ahead.

## References

1. Recent discussions are included in: (a) P.D. Fleischauer and P. Fleischauer, Chem. Rev., 70, 199 (1970); (b) G.B. Porter and H.L. Schlaefer, Ber. Bunsenges. Physik. Chem., 68, 316 (1964); (c) G. Sartori, Proceeding of the XIth International Conference on Coordination Chemistry, Haifa, Israel, 1968; (d) L.S. Forster in "Transition Metal Chemistry", Vol. V, R.L. Carlin, Ed., Marcel Dekker, Inc., New York; (e) M. Margoshes and B.F. Scribner, Anal. Chem., 40, 223R (1968); (f) C.E. White and A. Weissler, ibid., 116R (1968).
2. A. Weller, J. Phys. Chem., 3, 238 (1955).
3. G. Jackson and G. Porter, Proc. Royal Soc., A260, 13 (1961).
4. S.P. Van, Ph.D. Thesis, California Institute of Technology, 1969.
5. N.J. Turro, "Molecular Photochemistry", Benjamin, New York, 1967, p. 24.
6. V. Balzani and V. Carassiti, "Photochemistry of Coordination Compounds", Academic Press, New York, 1970, p. 20.
7. (a) G.A. Crosby and D.H.W. Carstens, "Molecular Luminescence", E.C. Lim, Ed., Benjamin, New York, 1969; (b) R.F. Ziolo, S. Lipton, and Z. Dori, Chem. Comm., 1124, (1970).
8. D. Valentine, private communication. This complex merits further investigation since photolysis in oxygenated fluid solution results in decomposition to give trans-stilbene.
9. J.P. Paris and W.W. Brandt, J. Am. Chem. Soc., 81, 5001 (1959).
10. H. Veening and W.W. Brandt, Anal. Chem., 32, 1426 (1960).
11. G.A. Crosby, W.G. Perkins, and D.M. Klassen, J. Chem. Phys., 43, 1498 (1965).
12. D.M. Klassen and G.A. Crosby, Chem. Phys. Lett., 1, 127 (1967).
13. D.M. Klassen and G.A. Crosby, J. Chem. Phys., 48, 1853 (1968).

14. J.N. Demas and G.A. Crosby, J. Mol. Spectrosc., 26, 72 (1968).
15. F.E. Lytle and D.M. Hercules, J. Am. Chem. Soc., 91, 253 (1969).
16. Y.S. Sohn, D.N. Hendrickson, and H.B. Gray, ibid., 92, 3233 (1970).
17. Y.S. Sohn, D.N. Hendrickson, and H.B. Gray, ibid., 93, 3603 (1971).
18. (a) E.K. von Gustorf and F. Grevels, Fort. Chem. Forsch., 13, 366 (1969); (b) W. Strohmeier, Angew. Chem., 76, 873 (1964); (c) I.W. Stolz, G.R. Dobson, and R.K. Sheline, J. Am. Chem. Soc., 87, 716 (1965); (d) see also ref. 6, pp. 323-348 and references cited therein.
19. H. Saito, J. Fujita, and K. Saito, Bull. Chem. Soc. Japan, 41, 863 (1968) and 41, 359 (1968).
20. R.J. Watts and G.A. Crosby, J. Am. Chem. Soc., 93, 3184 (1971).
21. G.F. Smith, W.A. McCurdy, Jr., and H. Diehl, Analyst (London), 77, 418 (1952).
22. A.A. Schilt and G.F. Smith, Anal. Chim. Acta., 16, 404 (1957).
23. H. L. Schlaefter, H. Gausman, and H. U. Zander, Inorg. Chem., 6, 1528 (1967).
24. H. L. Schlaefter, H. Gausman, and H. Witzke, J. Chem. Phys., 46, 1423 (1967).
25. See ref. 1a and specifically: (a) I. Adams, T.R. Au Coin, and G.A. Wolff, J. Electrochem. Soc., 109, 1050 (1962), (b) S. Kumar and P. Nath, Trans. Indian Ceram. Soc., 25, 12 (1966); (c) G.A. Tsurikova, Opt. Spectrosc., 24, 151 (1968); (d) A.N. Tarashchan, Itogi Nauki: Geokhim., Mineral., Petrogr., 137 (1966).
26. O. Siimann, unpublished results.
27. (a) M. Kasha in "Fluorescence", G.G. Guilbault, Ed., Marcel Dekker, New York, N.Y., 1967, p. 220; (b) F. Zuloaga and M. Kasha, Photochem. Photobiol., 7, 549 (1968).

28. (a) G.A. Crosby, J. Chim. Phys., 64, 166 (1967); (b) M. Mingardi and G.B. Porter, J. Chem. Phys., 44, 4354 (1966).
29. G.A. Crosby, R.J. Watts, and S.J. Westlake, ibid., 55, 4663 (1971).
30. M.K. De Armond and J.E. Hillis, ibid., 49, 466 (1968).
31. M. Mingardi and G.B. Porter, Spectrosc. Lett., 1, 293 (1968).
32. I.N. Douglas, J.V. Nicholas, and B.G. Wybourne, J. Chem. Phys., 48, 1415 (1968).
33. J.E. Hillis and M.K. DeArmond, Chem. Phys. Lett., 10, 325 (1971).
34. T.R. Thomas and G.A. Crosby, J. Mol. Spectrosc., 38, 118 (1971).
35. M. Wrighton, H.B. Gray, and G.S. Hammond, J. Am. Chem. Soc., 93, 4336 (1971).
36. M. Wrighton, G.S. Hammond, and H.B. Gray, ibid., 93, 6048 (1971).
37. C.J. Ballhausen and H.B. Gray, Inorg. Chem., 2, 426 (1963).
38. P. Natarajan and A.W. Adamson, J. Am. Chem. Soc., 93, 5599 (1971).
39. (a) D.R. Scott and R.S. Becker, J. Chem. Phys., 35, 516, 2246 (1961); (b) J.J. Smith and B. Meyer, ibid., 48, 5436 (1968).
40. (a) A. Muller-Goldegg and J. Voitlander, Z. Naturforsch., 23a, 1236 (1968); (b) M. Wrighton, unpublished observations.
41. (a) J.A. Brewster, C.A. Savage, and L.M. Venanzi, J. Am. Chem. Soc., 3699 (1961); (b) C.A. Savage and L.M. Venanzi, ibid., 1548 (1962); (c) C. Furlani, Coodin. Chem. Rev., 3, 141 (1968); (d) J.W. Dawson, H.B. Gray, J.E. Hix, Jr., J.R. Preer, and L.M. Venanzi, J. Am. Chem. Soc., in press; (e) J.W. Dawson, L.M. Venanzi, J.R. Preer, J.E. Hix, Jr., and H.B. Gray, ibid., 93, 778 (1971); (f) G. Loughner, unpublished results.

42. For a discussion of the spectrum of  $\text{Co}(\text{Cl})_4^{2-}$  see:  
B.N. Figgis, "Introduction to Ligand Fields", Interscience  
Publishers, New York, 1966, pp. 239-240.
43. (a) R.A. Levenson, Ph.D. Thesis, Columbia University,  
1970 and references cited therein; (b) F.A. Cotton,  
Accs. Chem. Res., 2, 240 (1969); (c) M.C. Baird,  
"Progress in Inorganic Chemistry", Vol. 9, Interscience  
Publishers, New York, 1968, p. 1.
44. This point is under investigation by H.B. Gray and C.  
Cowman who interpret their observations as indicative of  
a  $\delta \rightarrow \delta^*$  transition.

## CHAPTER IV

Nonradiative Decay Processes in Metal  
Containing Molecules

We define a nonradiative decay process as being a deactivation pathway involving conversion of electronic excitation into vibrational excitation without the emission of light or chemical change occurring in the molecule. Historically, nonradiative decay became a reality when it was found that the sum of the quantum yields for emission and chemical reaction was not unity for some aromatic compounds.<sup>1</sup> For example, the fluorescence quantum yield for naphthalene is 0.29 and the phosphorescence yield is 0.03 accounting for only 32% of the incident light.<sup>1a</sup> The substantial portion of the energy remaining is converted into vibrational excitation in the naphthalene, the solvent, or a combination of these. A study of the factors affecting nonradiative decay rates in the aromatic systems continues to be an area of active investigation.

One important point is that vibrational excitation must ultimately result in thermal excitation of the solvent. The crossover of excited states to the ground state may occur isoenergetically resulting in a hot ground state which is rapidly deactivated via collision and vibrational energy transfer to the solvent.

It has been convincingly demonstrated that the rate of nonradiative transitions is dependent on the energy gap between the two states. In Table IV-1 we show nonradiative decay constants for a number of aromatic molecules as a function of the energy between the two states involved in the transition.<sup>1a</sup> The fastest rates of nonradiative decay occur when the energy gap is smallest.

Within a molecule it is found that the highest energy vibrational modes contribute most significantly to the nonradiative decay rate. In Table IV-2 we list the phosphorescence lifetimes of some aromatic compounds and their perdeuterated derivatives.<sup>1b</sup> Invariably nonradiative decay is slowed down in the perdeuterio compounds. The result is rationalized quantum mechanically by noting that the mixing of two states by vibrational overlap is best for levels with small vibrational quantum numbers.<sup>1b</sup> That is, the probability of converting from an excited state in the zero vibrational level to a vibrationally excited level of the ground state is highest when the vibrational quantum number of the ground state level is small. In comparing perdeuterio with perprotio compounds we see that significantly higher vibrational quantum numbers are necessary with the perdeuterio to achieve the same energy as in the perprotio. The situation is shown schematically in Figure IV-1 comparing the C—H and C—D vibrational levels. The high  $j$  values necessary in the deuterio

Table IV-1. Rate Constants for Nonradiative Decay versus  
Magnitude of the Energy Gap,  $E(T-S_0)^a$

Compound	Energy Gap, $E(T-S_0)$ , $\text{cm}^{-1}$	Rate Constant $k$ , $\text{sec}^{-1}$
Anthracene	14,700	10
1,2 Benzanthracene	16,500	3.3
Pyrene	16,800	1.4
1,2-5,6-Dibenzanthracene	18,300	0.71
Chrysene	19,800	0.38
Napthalene	21,300	0.40
Phenanthrene	21,600	0.30

<sup>a</sup>Data from D. P. Craig and I. G. Ross, J. Chem. Soc., 1589 (1954).



Table IV-2. Phosphorescence Lifetimes for Aromatic  
Hydrocarbons and Deuterated  
Derivatives<sup>a</sup>

Compound	$\tau_p$ , sec.
Benzene	7.0
Benzene-d <sub>6</sub>	26.0
Triphenylene	16.0
Triphenylene-d <sub>12</sub>	23.0
Biphenyl	3.1
Biphenyl-d <sub>10</sub>	11.3
Phenanthrene	3.3
Phenanthrene-d <sub>10</sub>	16.4
Naphthalene	2.3
Naphthalene-d <sub>8</sub>	22.0
Pyrene	0.2
Pyrene-d <sub>10</sub>	3.2
Anthracene	0.06
Anthracene-d <sub>10</sub>	0.10

<sup>a</sup>Data from (1) M. R. Wright, R. P. Frosch, and G. W. Robinson, *J. Chem. Phys.*, 33, 934 (1960) and 38, 1187 (1963); (2) E. C. Lim, *ibid.*, 36, 3497 (1962); (3) G. W. Robinson and R. P. Frosch, *ibid.*, 37, 1962 (1962); (4) R. E. Kellogg and R. P. Schwenker, *ibid.*, 41, 2860 (1964).

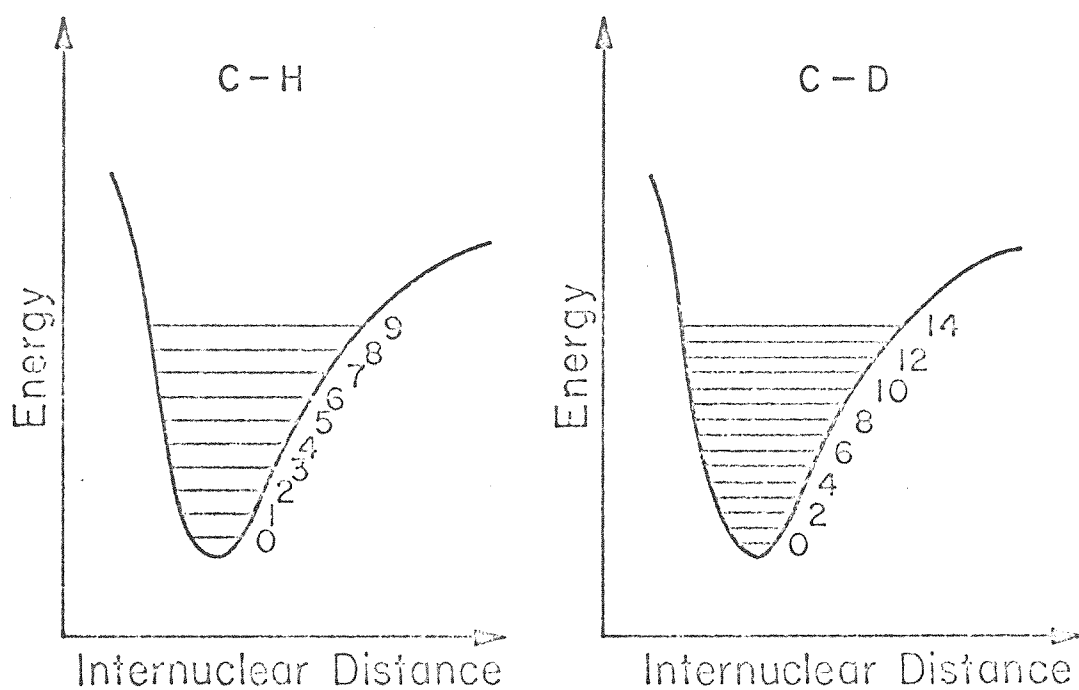


Figure IV-1. Comparison of the  $j$  value to reach a given ground state energy with C-D or C-H stretching as the highest energy vibrational mode.

compounds make nonradiative decay a less probable process than in protio species while radiative rates are unaffected, giving rise to longer lived excited states.

To measure absolute values for nonradiative decay rates one must measure both the lifetime,  $\tau$ , and the emission quantum yield,  $\phi_e$ . The lifetime is simply the inverse of the sum of all decay rates,  $k_{\text{radiative}}$ ,  $k_{\text{nonradiative}}$ ,  $k_{\text{chemistry}}$ , and is physically easily measured by monitoring directly some physical property of the excited state as it undergoes decay. The emission quantum yield expressed in equation (3-2) is much more difficult to determine and is only known to values  $\pm 10\%$  under the best of conditions. The measurement of emission quantum yields for coordination compounds is rare.

In metal containing molecules there are some differences in the possible nonradiative decay modes. First, considering d-d electronic transitions to arise from slightly perturbed metal localized levels one wonders how vibrational modes will become activated when most of the ligand modes are far removed from the metal. One wonders, too, whether specific vibrational modes can be tabbed as the dominant deactivation pathway in the molecule. Another fact is that the metal containing molecules do not always contain any high energy vibrational modes, say, comparable to C-H stretching modes. Can we, then, expect nonradiative decay rates to be slower in general? A final interesting note is that

the excited states of coordination compounds are often very well separated so that internal conversion rates between excited states may become slow enough to observe radiative decay from one excited state to another, lower lying, excited state.

Very few systems have been studied quantitatively. Specifically, few people have measured both quantum yields and emission lifetimes. It is safe to say, however, that nonradiative decay plays an important role in deactivating the excited states of coordination compounds. We can have confidence in this because few systems are highly photosensitive or luminescent.

At present there have been few attempts to correlate structure and nonradiative decay rates in a coordination compound. In Table IV-3 we show the emission lifetimes of several  $\text{W(CO)}_5(\text{X})$  compounds. We see that the lifetimes span almost two orders of magnitude ( $6.5 \times 10^{-7}$  to  $2.6 \times 10^{-5}$  sec.) depending on the nature of X. The electronic structures of the complexes are very similar with the absorption spectra being qualitatively the same. The  $^1\text{A}_1 \rightarrow ^3\text{E}$  absorption occurs at about 440 nm in each case with a similar band shape. This information allows us to estimate the relative radiative decay rate for the complexes since the emission arises from the state achieved in absorption with both transitions being radiative. Theoretically, by the Einstein Law the integrated absorption can be related to absolute values for the radiative rate constants, equation (3-7), but in practice calculations are generally poor for coordination compounds. In the  $\text{W(CO)}_5(\text{X})$

Table IV-3. Emission Lifetimes for  $W(CO)_5(X)$  Complexes<sup>a</sup>

X	$\tau$ , sec. $\times 10^6$
ammonia	0.35
cyclohexylamine	1.1
isopropylamine	0.65
<u>t</u> -butylamine	1.2
ethylamine	0.92
diethylamine	5.1
dimethylamine	2.6
piperidine	3.1
diethylmethylaniline	25.5
triethylamine	9.7
tri- <u>n</u> -butylamine	6.9
$(Me)_2N\ CH(CH_3)C_6H_5$	15.5
ethanol	11.7
isopropanol	6.6
<u>t</u> -butanol	6.3
diethylether	7.1
acetone	5.3
acetone- $d_6$	5.7
cyclohexanone	3.6
pyridine	2.5
pyridine- $d_5$	0.8
2-methylpyridine	1.7
2,4,6-trimethylpyridine	11.7
pyrazole	6.4

<sup>a</sup>In methylcyclohexane solvent at 77°K.

complexes, however, we have an excellent case since emission and absorption are so similar in all of the compounds. Relative values for  $k_r$  for several complexes are listed in Table IV-4. For four of the cases we have added relative emission quantum yields.

A generality arising from Table IV-3 is that the more highly substituted amines give  $W(CO)_5(X)$  complexes with the longest lifetime. This trend appears to be due to the fact that the large number of alkyl groups on the nitrogen slows down the rate of nonradiative decay by removing the number of N—H stretching modes. This is supported by all of our observations in the three amine complexes reported in Table IV-4. The radiative rate increases slightly  $-NR_3 > -NHR_2 > -NH_2R$ , but the lifetime increases dramatically  $-NR_3 > -NHR_2 > -NH_2R$  demanding that the rate of nonradiative decay being in the order  $-NH_2R > -NHR > -NR_3$ ; the relative quantum yields confirm our notions about the relative  $k_r$  values obtained from the absorption spectrum; the compound  $-NR_3$  has the highest quantum yield and yet it also has the largest lifetime, again demanding that the  $-NR_3$  complex have the slowest rate of nonradiative decay.

The amine complexes behave as predicted by the general theory of Robinson and Frosch explained above: the most energetic vibrational modes of a molecule will be most important in determining the rate of nonradiative decay. The N—H stretching

Table IV-4. Absorbance and Emission Data for  $W(CO)_5(X)$  Compounds

X	${}^1A_1 \rightarrow {}^3E(\epsilon), \text{ kcm}^{-1}{}^a$	Relative Absorbance	Rel. $\phi_e^b$	$\tau, \text{ sec.} \times 10^6$
cyclohexylamine	22.8 (520)	1	1	1.1
diethylamine	22.8 (727)	1.4	6	5.1
$(Me)_2NCH(CH_3)C_6H_5$	22.8 (1080)	2.1	12	15.5
triethylamine	22.8 (c)	c	18	9.7
pyridine	22.8 (630)	1.2	c	2.5
acetone	22.2 (910)	1.8	c	5.3

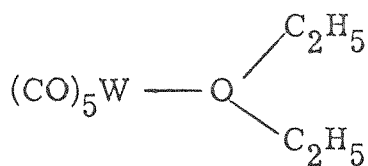
<sup>a</sup>In room temperature hydrocarbon solution.

<sup>b</sup>Relative  $\phi_e$  measured in methylcyclohexane at 77°K. by matching optical densities at 400 nm and exciting with 400 nm light.

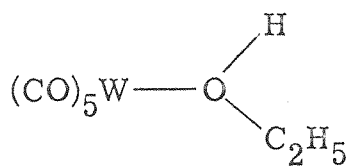
<sup>c</sup>Not determined.

modes are the most important here and are the most energetic. The fact that these specific high energy modes are utilized may be related to the fact that they are geometrically close to the chromophore. It has been shown that systematic substitution of alkyl groups for the hydrogens in acetone<sup>2</sup> significantly reduces the rate of nonradiative decay even though the number of C—H bonds is actually increased. The conclusion was that the  $\alpha$ -hydrogens of the acetone play the key role in the rate of nonradiative decay, being close to the carbonyl chromophore.

However, if we assume that the radiative decay rate is the same for 4-I and 4-II of Table IV-3 we must conclude that the O—H



4-I



4-II

stretching mode is relatively unimportant in the rate of nonradiative decay of 4-II since the lifetime of 4-II is actually longer than 4-I. This result implicates other important interactions such as the accessibility of the vibrational modes of the ligand. It is clear here, though, that changes in the ligand X are in some way affecting changes in the rates of nonradiative decay.

The only other correlation possible may be to consider disubstituted  $\text{W}(\text{CO})_4(\text{X})_2$  species and look at the effect of geometry on the rate constants for decay. In Table IV-5 we present a



Table IV-5. Comparison of Electronic Data for  $\text{W}(\text{CO})_5(\text{py})$  and  
 $\text{cis-W}(\text{CO})_4(\text{py})_2$

	$\text{S} \rightarrow \text{T}, (\epsilon) \text{ kcm}^{-1}\text{a}$	Emission Max. $\text{kcm}^{-1}\text{b}$	$\tau, \text{sec.} \times 10^6\text{b}$
$\text{W}(\text{CO})_5(\text{py})$	22.8 (630)	19.27	1.5
<u><math>\text{cis-W}(\text{CO})_4(\text{py})_2</math></u>	21.5 (c)	18.18	6.7

<sup>a</sup>Hydrocarbon solvent, room temperature.

<sup>b</sup>EPA solvent at 77°K.

<sup>c</sup>Not determined.

comparison of electronic data for  $\text{W(CO)}_5(\text{py})$  and  $\text{cis-W(CO)}_4(\text{py})_2$ . The absorptivity for the disubstituted complex is generally higher than for the monosubstituted complex and the absorption and emission maxima for the disubstituted complex are at a lower energy than for  $\text{W(CO)}_5(\text{py})$ . These two facts would both lead to the prediction of a shorter lifetime for the  $\text{cis-W(CO)}_4(\text{py})_2$  than for  $\text{W(CO)}_5(\text{py})$ , because both the radiative rate and the nonradiative rate should be faster. The  $\text{cis-W(CO)}_4(\text{py})_2$ , however, is observed to have a lifetime of  $6.7 \mu\text{sec.}$  compared to  $1.3 \mu\text{sec.}$  for the  $\text{W(CO)}_5(\text{py})$ . A more detailed and quantitative study should be undertaken to test the importance of geometry in these systems.

The  $d^3 \text{ Cr(III)}$  system is the only other system where both luminescence quantum yields and emission lifetimes have been measured. In Table IV-6 we show a series of  $\text{Cr(III)}$  complexes and the nonradiative decay rate constants for the  ${}^2\text{E} \rightarrow {}^4\text{A}_2$  transitions.<sup>3</sup> Like the  $\text{W(CO)}_5(\text{X})$  complexes the electronic transition of interest here is at about the same energy in each case as the Tanabe-Sugano diagram for  $d^3$  indicates. Both the  ${}^2\text{E}$  and the  ${}^4\text{A}_2$  states arise from the  $t_{2g}^3$  configuration and their splitting, therefore, is not dependent on the ligands involved. The 100-fold change in nonradiative decay rate, then, truly reflects the effect of ligand structure on the rate of decay. We can draw some clear structural correlations here by first examining the

Table IV-6. Nonradiative Decay Rates for Chromium(III)  
Complexes

Complex	$k_{\text{nr}}(\text{sec.}^{-1} \times 10^{-3})^{\text{a}}$
$\text{Cr}(\text{NH}_3)_6^{3+}$	18
$\text{Cr}(\text{D}_2\text{O})_6^{3+}$	7.6
$\text{t-Cr}(\text{NH}_3)_2(\text{NCS})_4^-$	3.1
$\text{t-Cr}(\text{en})_2(\text{NCS})_2^+$	7.6
$\text{Cr}(\text{NCS})_6^{3-}$	0.22
$\text{Cr}(\text{CN})_6^{3-}$	0.29
$\text{Cr}(\text{en})_3^{3+}$	9.9

<sup>a</sup>Ref. 3.

octahedral complexes:  $\text{Cr}(\text{NH}_3)_6^{3+}$ ,  $\text{Cr}(\text{CN})_6^{3-}$ ,  $\text{Cr}(\text{NCS})_6^{3-}$ , and  $\text{Cr}(\text{D}_2\text{O})_6^{3+}$ . The hexaamine complex has many N—H stretching modes which are significantly higher in energy than any of the vibrational modes for the other three complexes and a correspondingly fast rate of nonradiative decay is observed. The  $\text{Cr}(\text{D}_2\text{O})_6^{3+}$  complex had an emission quantum yield six times that of  $\text{Cr}(\text{H}_2\text{O})_6^{3+}$ , again implicating the importance of the high energy vibrational modes. The smaller number of N—H stretching modes in  $\text{Cr}(\text{en})_3^{3+}$  compared to  $\text{Cr}(\text{NH}_3)_6^{3+}$  gives a slower rate for nonradiative decay. Substitution of  $\text{NCS}^-$  for en or  $\text{NH}_3$  gives the expected slowdown in the rate of nonradiative decay. This work by Forster represents the most complete study of any transition metal system, and we see that our notions concerning structural effects on nonradiative decay are substantiated.

The dramatic increase in the rate of nonradiative decay in  $\text{Cr}(\text{NH}_3)_6^{3+}$  compared to  $\text{Cr}(\text{CN})_6^{3-}$  may account, in part, for the fact that emission from  $\text{Co}(\text{NH}_3)_6^{3+}$  has not been seen while the  $\text{Co}(\text{CN})_6^{3-}$  exhibits luminescence. The other important factor in the Co(III) case is that the energy gap between ground and excited state is much smaller in the nonluminescent  $\text{Co}(\text{NH}_3)_6^{3+}$  than in the  $\text{Co}(\text{CN})_6^{3-}$ .

Temperature effects on the nonradiative decay rate are not clearly understood but in some cases it is clear that at high temperatures (298°K.) nonradiative decay is so fast that the

emission cannot be seen from samples that emit at 77°K. In Figure IV-2 we show the effect of changing the temperature on the emission intensity of  $\text{W(CO)}_5(\text{pyridine})$ . In Figure IV-3 we plot  $\log(\text{emission intensity})$  against  $(\text{temperature})^{-1}$ . The linear relationship indicates an "activation energy" for the emission disappearance of 1.3 kcal/mole. The meaning of such an activation energy is unclear, but in this case may suggest that at higher temperatures the pyridine is partially dissociated and as such has no radiative probability to the ground state due to the large distortion.

The effect of environment may play a key part in the rates of nonradiative decay. For example, using  $\text{D}_2\text{O}$ -MeOD solvent instead of  $\text{H}_2\text{O}$ -MeOH increased the quantum yield of emission and the emission lifetimes of  $\text{Rh(NH}_3)_5(\text{X}^-)^{2+}$  complexes.<sup>4</sup> Apparently in this case a significant pathway for deactivation intimately involves the vibrational excitation of the water-methanol mixture.

The role of the solvent in nonradiative decay can be critical. In Table IV-7 the emission lifetime of  $\text{W(CO)}_5(\text{py})$  is shown for several solvents. In going from the pure solid to the nonpolar methylcyclohexane solvent essentially no effect is observed. However, both of the polar solvents yield a shorter emission lifetime. The effect here, though, is small. The small effect may merely reflect the fact that the excited state is protected from

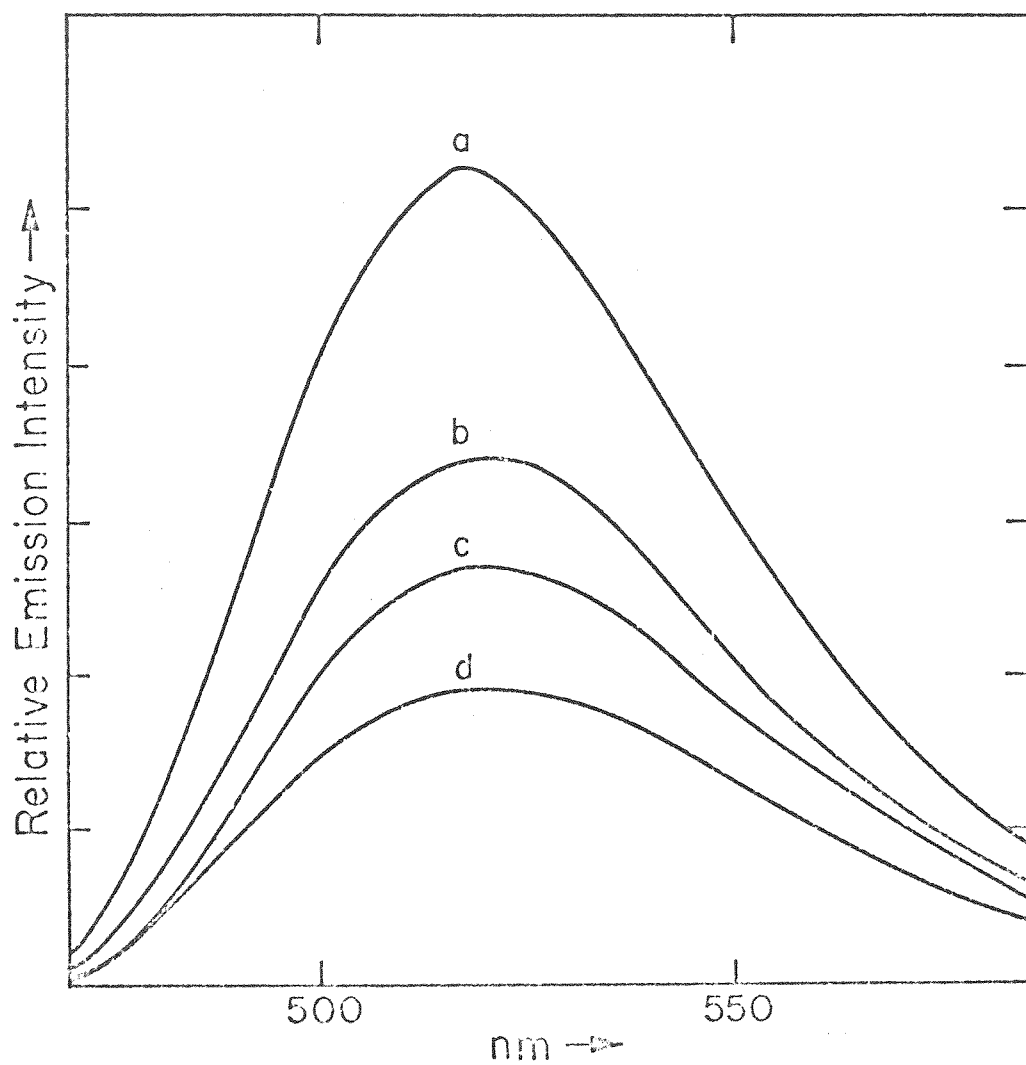


Figure IV-2. The emission of  $\text{W(CO)}_5(\text{pyridine})$  as a function of temperature: (a) 142°K., (b) 149°K., (c) 157°K., (d) 172°K.

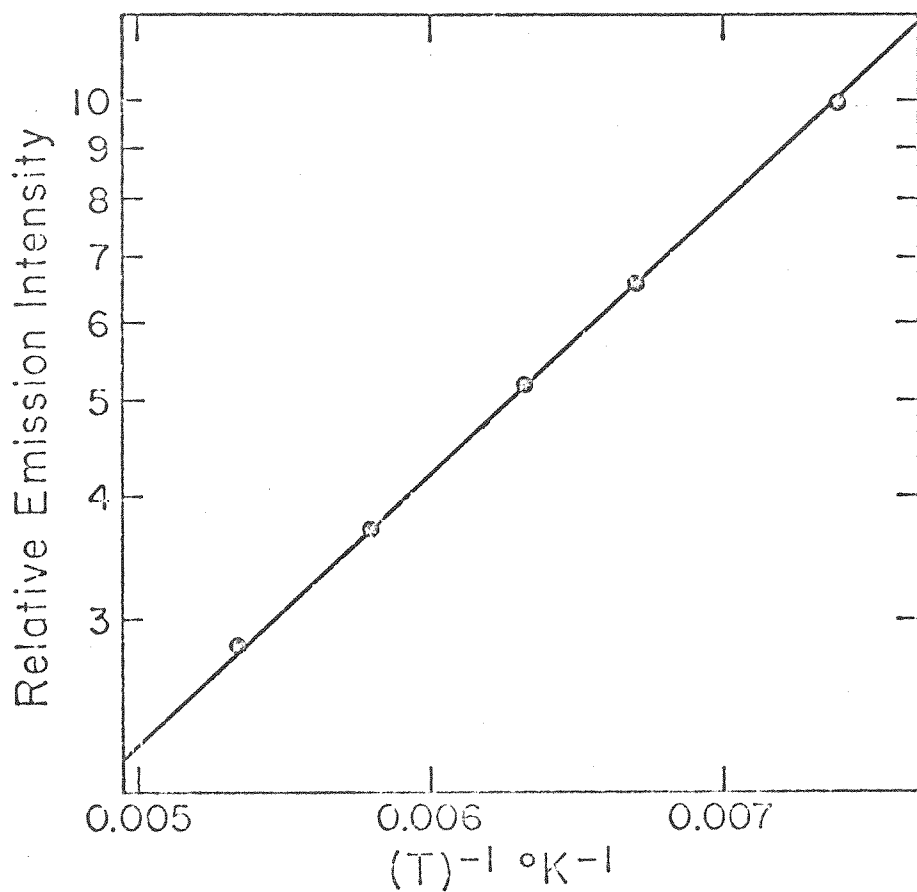


Figure IV-3. Arrhenius plot for the luminescence intensity of  $\text{W(CO)}_5(\text{pyridine})$ . The Arrhenius activation energy for the nonradiative decay is 1.3 kcal/mol.

Table IV-7. Emission Lifetime for  $\text{W}(\text{CO})_5(\text{py})$  in Several  
Solvents at 77°K.

Solvent	$\tau$ , sec. $\times 10^6$
None	2.5
Methylcyclohexane	2.5
EPA	1.5
1-pentene	1.3



primary interactions with solvent by the ligands. This implies that only the ligand vibrational modes can determine the nonradiative decay rate, with vibrational excitation of the solvent occurring via vibrational transfer from the hot ground state of  $\text{W(CO)}_5(\text{py})$ . This is in contrast to the  $\text{Rh(NH}_3)_5(\text{X}^-)^{2+}$  complexes above.

While the study of nonradiative processes in coordination compounds has not received a great deal of attention thus far, valuable information can be obtained to predict, control, and finally exploit the excited state lifetimes.

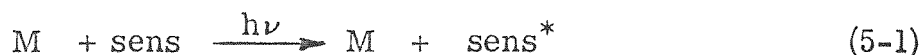
References

1. (a) J.G. Calvert and J.N. Pitts, Jr., "Photochemistry", John Wiley & Sons, Inc., New York, 1967, pp. 296-302.  
(b) N.J. Turro, "Molecular Photochemistry", W.A. Benjamin, Inc., New York, 1967, pp. 64-72; (c) M. Kasha, Disc. Faraday Soc., 9, 14 (1950); (d) M. Kasha and S.P. McGlynn, Ann. Rev. Phys. Chem., 7, 403 (1956).
2. M. O'Sullivan and A.C. Test, J. Am. Chem. Soc., 92, 5842 (1970) and ibid., 92, 258 (1970).
3. K.K. Chatterjee and L.S. Forster, Spectrochim. Acta, 20, 1603 (1964) and ibid., 21, 213 (1965).
4. T.R. Thomas and G.A. Crosby, J. Mol. Spectrosc., 38, 118 (1971).

## CHAPTER V

Energy Transfer Studies in Metal  
Containing Systems

The study of electronic energy transfer in metal containing molecules is an underdeveloped territory. Theories developed for organic molecules, however, have proven to be satisfactory in the few cases studied thus far. Photosensitized reactions, equations (5-1) and (5-2), are becoming known for inorganic



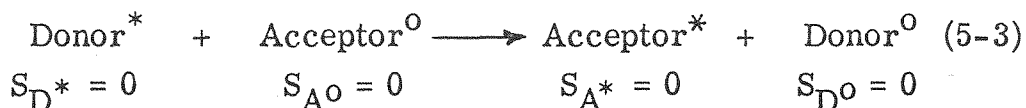
systems and should provide a fruitful area of investigation.

There exist two types of electronic energy transfer,<sup>1, 2</sup> one requiring overlap of donor and acceptor orbitals called exchange transfer and the other allowing transfer over long distances called resonance energy transfer. In solution it has been shown that the exchange transfer is much faster than the resonance transfer, and we deal exclusively with it here. The energy transfer then must occur via collision in fluid solutions. The transfer of electronic excitation is favorable when the process is spin-allowed, and the acceptor energy level is beneath that of the donor level.

Electronic energy transfer obeys a spin-selection rule: total spin angular momentum must be conserved.<sup>3</sup> The total spin angular momentum of the donor molecule is denoted  $S_D$  and that

of the acceptor is  $S_A$ . The total spin angular momentum for the system  $S_{\text{tot}}$ , has components  $S_A + S_D$ ,  $S_A + S_D - 1$ ,  $S_A + S_D - 2$ ,  $S_A + S_D - 3$ , . . . . .,  $|S_A - S_D|$ . To determine if a given interaction is spin-allowed, determine the total spin before and after the reaction and determine whether they have components which are the same before and after. If any components are the same, the process is spin-allowed. We now consider some important interactions and determine whether they are spin-allowed.

The interaction of an excited singlet state ( $S_D = 0$ ) with a ground state singlet ( $S_A = 0$ ), equation (5-3), can be shown to be

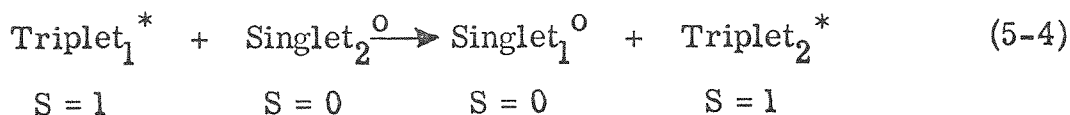


$$S_D^* + S_{A0} = 0 = S_{\text{tot before}}$$

$$S_{D0} + S_A^* = 0 = S_{\text{tot after}}$$

$\therefore$  spin allowed.

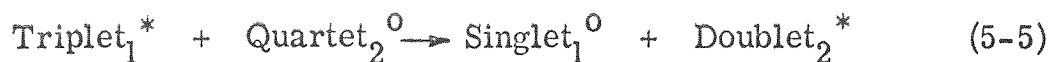
spin-allowed. Consider the interaction of an excited triplet with a ground state singlet giving a triplet plus deactivation to yield the singlet, equation (5-4). These systems are trivial because  $S_{\text{tot}}$



$$S_{\text{tot before}} = 1 = S_{\text{tot after}}$$

$\therefore$  spin allowed.

before and after are identical. Now consider a triplet excited state interacting with a quartet to yield the singlet and a doublet, equation (5-5). We see that one component of  $S_{\text{tot}}$  before is the

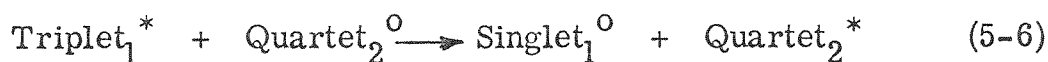


$$S_1 = 1 \quad S_2 = 3/2 \quad S_1 = 0 \quad S_2 = 1/2$$

$$S_{\text{tot}} \text{ before: } 5/2, 3/2, 1/2$$

$$S_{\text{tot}} \text{ after: } 1/2$$

same as  $S_{\text{tot}}$  after, so this process is allowed. Similarly a triplet excited state can produce a quartet  $\rightarrow$  quartet excitation in a spin-allowed fashion, equation (5-6). However, the interaction of



$$S_1 = 1 \quad S_2 = 3/2 \quad S_1 = 0 \quad S_2 = 3/2$$

$$S_{\text{tot}} = 5/2, 3/2, 1/2 \quad S_{\text{tot}} = 3/2, 1/2$$

a triplet excited state with a ground state quintet to yield two singlets, equation (5-7), is a spin-forbidden process. We have



$$S_1 = 1 \quad S_2 = 2 \quad S_1 = 0 \quad S_2 = 0$$

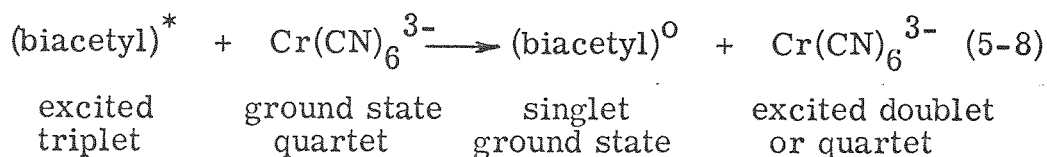
$$S_{\text{tot}} = 3, 2, 1 \quad S_{\text{tot}} = 0$$

$\therefore$  spin forbidden

detailed this spin selection rule here because of the large number of possible spin systems in metal containing molecules. A clear

understanding of the application of the rule will help to understand energy transfer phenomena in all systems.

An important consideration in the feasibility of energy transfer is the relative energy of donor and acceptor states involved in the transfer. In Figure V-1 we show the energetic considerations for  $\text{Cr}(\text{CN})_6^{3-}$  quenching of biacetyl triplets, equation (5-8).<sup>4</sup> The direct formation of either the quartet or



doublet excited state is a spin-allowed process, but the excited quartet lies well above the biacetyl triplet energetically, so we predict that the low lying doublet excited state will be produced in the  $\text{Cr}(\text{CN})_6^{3-}$ . In organic systems it has been demonstrated by triplet energy transfer experiments that when the energy of the acceptor triplet is below that of the donor, then the transfer occurs at a rate approximating diffusion controlled.<sup>1</sup> However, as the energy of the acceptor is raised above the donor the energy transfer becomes, presumably, an activated process and slows down markedly.

The deactivation of the donor excited state can occur without producing an electronic excited state in the acceptor even when the process is spin-allowed and exothermic.<sup>5</sup>

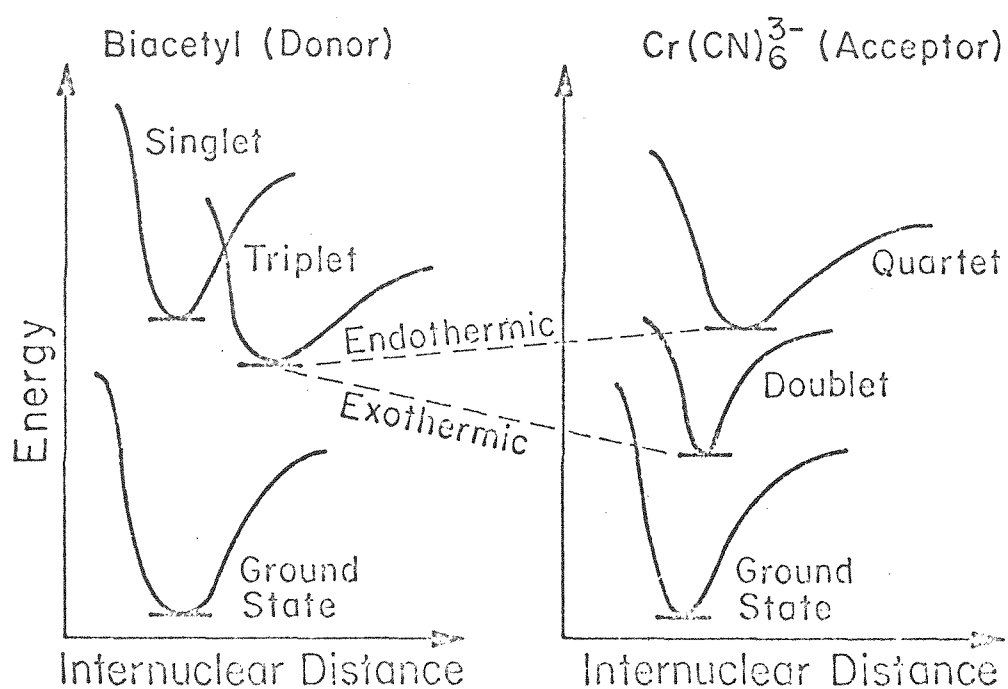


Figure V-1. Energetics for electronic energy transfer from biacetyl to  $\text{Cr}(\text{CN})_6^{3-}$  showing that quenching by the doublet state is most favorable, being an exothermic process.

Quenching of donor excited states when no acceptor level is energetically accessible is also an observed phenomenon.<sup>6</sup>

When a donor,  $D^*$ , interacts with an acceptor,  $A$ , electronic energy transfer may occur, equation (5-9) or  $A$  may merely

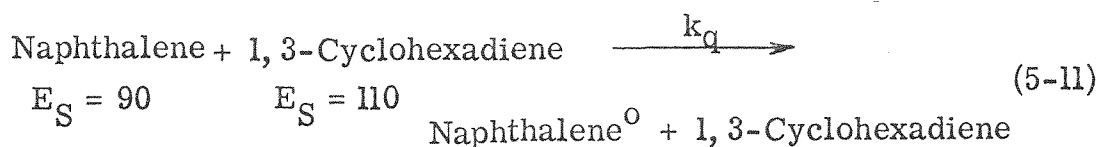


catalyze the deactivation of  $D^*$ , equation (5-10). Since an



electronic excited state is produced in equation (5-9) we can physically detect the transfer of electronic excitation by observing characteristic luminescence or chemistry of  $A^*$ . The process (5-10) results in no emission or chemical change. The relative importance of processes (5-9) and (5-10) in a given system is being actively pursued in organic systems and merits investigation in metal containing molecules.

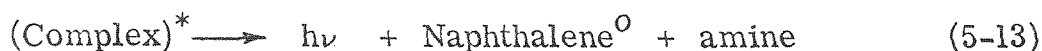
The parameters affecting the importance of process (5-9) in organic systems (spin and energy) have been unravelled. The factors dominating processes like (5-10) are just becoming clear. The early examples involved quenching of aromatic singlet excited states with 1,3-dienes with higher energy singlet excited states,<sup>7</sup> equation (5-11). The endothermic singlet-singlet energy transfer



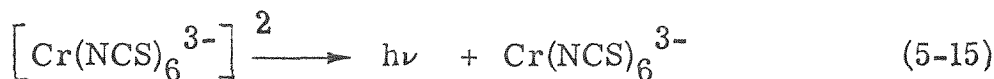
was not detectable since excited state chemistry of the diene was



not seen. While the detailed mechanism for dissipation of the energy is not fully understood, a collision complex is thought to form which can be described by a wavefunction containing excitation exchange terms,  $D^*A + DA^*$ , and charge transfer terms,  $D^+A^-$ ,  $D^-A^+$ . In a few cases, notably quenching of aromatic singlets by amines,<sup>8</sup> the excited collision complex can be detected since the excited complex luminesces to a dissociative ground state, equations (5-12) and (5-13).



Studies with metal containing systems have revealed that, indeed, both (5-9) and (5-10) can occur, but in only a few cases have definitive results been established. The most convincing work to date has been that of Forster who has shown that the benzil triplet excited state can be a donor of electronic excitation to produce Cr(III) excited states, equations (5-14) and (5-15).<sup>9</sup>



Forster showed that the emission of the Cr(III) complexes could be sensitized by the benzil triplet. While the quantitative importance of electronic energy transfer was not established, the work did show that electronic excitation of the acceptor occurs with reasonable efficiency and paved the way for new studies. Balzani

and co-workers<sup>10</sup> have now established that the photoaquation of  $\text{Cr(en)}_3^{3+}$  can be sensitized using biacetyl as a triplet donor. It was found that the sensitized quantum yield of photoaquation was 0.80 while the direct yield was 0.40. This discrepancy reveals that the direct irradiation does not produce the same state as in the sensitized experiment.

Another interesting result involving Cr(III) excited states as donors is found when  $\text{O}_2$  is used as the acceptor.<sup>11</sup> The energy transfer from a doublet excited state to produce singlet oxygen is a spin-allowed process and is also energetically favorable. The experimental findings, however, showed that the nature of the ligands surrounding the Cr(III) plays a critical role in determining the rate that  $\text{O}_2$  quenches the  $^2\text{E} \rightarrow ^4\text{A}_2$  phosphorescence of the Cr(III). In Table V-1 we show the quenching rate by  $\text{O}_2$  of some Cr(III) complexes. It should be pointed out that singlet  $\text{O}_2$  was not actually observed in this study. The correlation shows crudely that the saturated Cr(III) amine complexes are poor donors of excitation while the  $\pi$  bonding ligands yield complexes which are good donors of electronic excitation. This result may mean that the  $\pi$  bonding ligands delocalize the metal electrons more fully, allowing the  $\text{O}_2$  orbitals to overlap the donor orbitals as required in exchange energy transfer. More studies need to be done evaluating the importance of this ligand shielding effect using coordination compounds, both as donors and acceptors of electronic excitation.

Table V-1. Quenching of Cr(III) Phosphorescence by Oxygen<sup>a</sup>

Donor	Quenching Constant for O <sub>2</sub> , k <sub>q</sub> <sup>b</sup>
Cr(tn) <sub>3</sub> <sup>3+</sup> <sup>c</sup>	≤ 10 <sup>7</sup>
Cr(en) <sub>3</sub> <sup>3+</sup>	≤ 10 <sup>7</sup>
<u>t</u> -Cr(NH <sub>3</sub> ) <sub>2</sub> (NCS) <sub>4</sub> <sup>-</sup>	2 x 10 <sup>9</sup>
Cr(NCS) <sub>3</sub> <sup>3-</sup>	6 x 10 <sup>9</sup>
Cr(acac) <sub>3</sub> <sup>3-</sup>	~ 10 <sup>11</sup>
Cr(CN) <sub>6</sub> <sup>3-</sup>	2 x 10 <sup>8</sup>

<sup>a</sup>Ref. 11.

$$^b k_q = \left[ \left( \frac{1}{\tau} \right) - \left( \frac{1}{\tau_o} \right) \right] \left[ O_2 \right]^{-1}$$

where:

 $\tau_o$  = natural lifetime of donor. $\tau$  = lifetime of donor in presence of quencher.<sup>c</sup>tn is trismethylenediamine.

Other attempts to use coordination compounds as donors of electronic excitation have been fruitful. The  $\text{Ru}(\text{bipy})_3^{2+}$  cation phosphoresces in fluid solutions at room temperature and can be quenched by  $\text{PtCl}_4^{2-}$ ,<sup>12</sup> resulting in sensitized photoaquation of the  $\text{PtCl}_4^{2-}$ . In this system the aquation quantum yield was found to be 0.07 while the direct irradiation quantum yield is 0.14.<sup>13</sup> Further, biacetyl triplets have been used to sensitize the aquation of  $\text{Pt}(\text{Cl})_4^{2-}$  with a quantum yield of 0.26.<sup>14</sup> Taking these results at face value we must conclude that the states achieved by sensitization and direct irradiation are somewhat independent, with chemical reaction (aquation) competing in every case with internal conversion to the other excited states.

We have found that  $\text{W}(\text{CO})_5(\text{X})$  emission can be quenched in a number of ways. A simple alkene ( $E_T = 82$ )<sup>15</sup> will not affect  $\text{W}(\text{CO})_5(\text{X})$  emission ( $E_T = 58$ ), but 1,3-pentadiene ( $E_T = 54$ )<sup>16</sup> is an effective quencher of the metal localized luminescence. While no evidence for the transfer of electronic excitation is demonstrated, one predicts sensitized 1,3-pentadiene triplet isomerization. The 1,3-pentadiene quenches the  $\text{W}(\text{CO})_5(\text{py})$  luminescence at 77°K. in a pure pentadiene glassy solvent but does not affect the photosubstitution chemistry of the  $\text{W}(\text{CO})_5(\text{py})$  in fluid solution at room temperature. This suggests that if the state from which emission and chemical reaction occur are the same, then the lifetime from 77°K. to 298°K. changes from  $\sim 10^{-5}$  sec. to a value  $\sim 10^{-9}$  sec.!

One other transition metal has been important as an acceptor of electronic excitation: Co(III). Porter reported that the photoaquation of  $\text{Co(CN)}_6^{3-}$  could be sensitized using biacetyl as a triplet donor.<sup>17c</sup> However, Porter noted that the quenching rate was slow for this system which is surprising, because the  $\text{Co(CN)}_6^{3-}$  exhibits spin-forbidden luminescence at an energy below that of the biacetyl triplet  $\rightarrow$  singlet emission.<sup>17</sup> Thus, if we assume that the emission in the  $\text{Co(CN)}_6^{3-}$  is the T $\rightarrow$ S transition then the quenching rate should be very fast being spin-allowed, energetically favorable, and involving  $\pi$ -bonding ligands. We have now extended Porter's work to include several  $\text{Co(CN)}_5(\text{X}^-)^{2-}$  complexes to vary the electronic energy levels in the quenchers. In Table V-2 we summarize the quenching efficiency of the  $\text{Co(CN)}_5(\text{X}^-)^{2-}$  complexes using biacetyl as the donor. We have established a correlation of the energy of the first band in absorption of the quencher with the quenching rate. Since the sensitized quantum yields of  $\text{Co(CN)}_6^{3-}$ ,  $\text{Co(CN)}_5(\text{N}_3)^{3-}$ , and  $\text{Co(CN)}_5(\text{SCN})^{3-}$  are the same as the direct irradiation quantum yields for photoaquation (Table V-3), we conclude that electronic energy transfer is the dominant mode of deactivating the biacetyl triplet. Further, it is attractive to conclude that the state from which chemical reaction occurs is the same in direct absorption as in sensitization. Acetone triplets having a triplet energy of  $\sim 80$  kcal,<sup>18</sup> are quenched at a diffusion controlled rate by

Table V-2. Quenching of Biacetyl Triplets with Cyanocobaltate(III)  
Complexes

Quencher	$k_q \tau^a$	Lowest Spin-Allowed d-d Transition, $\text{kcm}^{-1}$
$\text{Co(CN)}_6^{3-}$	$2.3 \times 10^2$	32.1
$\text{Co(CN)}_5(\text{SO}_3)^{4-}$	$4.6 \times 10^3$	30.1
$\text{Co(CN)}_5(\text{CH}_3\text{CN})^{2-}$	$3.0 \times 10^4$	29.0
$\text{Co(CN)}_5(\text{py})^{2-}$	$2.3 \times 10^4$	28.3
$\text{Co(CN)}_5(\text{N}_3)^{3-}$	$1.4 \times 10^5$	26.1
$\text{Co(CN)}_5(\text{H}_2\text{O})^{2-}$	$1.4 \times 10^5$	26.3
$\text{Co(CN)}_5(\text{SCN})^{3-}$	$2.3 \times 10^5$	26.5

<sup>a</sup>Slope of Stern-Volmer plot for quenching of biacetyl phosphorescence.

Table V-3. Photoaquation Quantum Yields for Cyanocobaltate(III)  
Complexes<sup>a</sup>

Complex	$\Phi_{\text{dir}}^{\text{b}}$	$\Phi_{\text{sens}}$
$\text{Co(CN)}_6^{3-}$	0.31	0.23 <sup>c</sup> 0.25 <sup>d</sup>
$\text{Co(CN)}_5(\text{N}_3)^{3-}$	0.23	0.22 <sup>c</sup>
$\text{Co(CN)}_5(\text{SCN})^{3-}$	0.20	0.18 <sup>c</sup>

<sup>a</sup>The final product in each case is  $\text{Co(CN)}_5(\text{OH}_2)^{2-}$ .

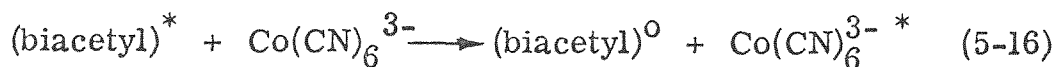
<sup>b</sup>Direct irradiation at 313 nm for  $\text{Co(CN)}_6^{3-}$  and 436 nm for the others.

<sup>c</sup>Biacetyl sensitized, 436 nm irradiation.

<sup>d</sup>Acetone sensitized, 313 nm irradiation.

$\text{Co}(\text{CN})_6^{3-}$  and give an aquation quantum yield in agreement with both the direct and biacetyl sensitized quantum yield.

The rationale for slow quenching of biacetyl triplets by  $\text{Co}(\text{CN})_6^{3-}$  must be related to the nature of the low energy emitting state in the  $\text{Co}(\text{CN})_6^{3-}$ . As pointed out earlier the  $\text{Co}(\text{CN})_6^{3-}$  could be a quintet or a highly distorted triplet. The quenching of a triplet by a  $\text{Co}(\text{CN})_6^{3-}$  to yield an excited quintet is spin-forbidden, equation (5-16). The distorted triplet is not expected



$$S_D = 1 \qquad S_A = 0 \qquad S = 0 \qquad S = 2$$

$$S_T = 1 \qquad S_T = 2$$

$\therefore$  spin forbidden.

to be an effective quencher either, since direct population of the distorted state would violate the Franck-Condon principle. Our results are most reasonably interpreted by assuming that the spectroscopic triplet state is populated in  $\text{Co}(\text{CN})_6^{3-}$ , and it undergoes decay in the same way as states achieved in direct irradiation. Unfortunately, we can offer no conclusive evidence to distinguish between the distorted triplet and the quintet excited states.

The logical extension of our results to other  $d^6$  metal cyanides was attempted (Table V-4). Both  $\text{Rh}(\text{CN})_6^{3-}$  and  $\text{Ir}(\text{CN})_6^{3-}$  quench biacetyl triplets very slowly as expected on the basis of the energy, but the correlation breaks down dramatically with



Table V-4. Quenching Activity of  $d^6$  Octahedral Cyanometalates<sup>a</sup>

Complexes <sup>b</sup>	$k_q \tau$ <sup>c</sup>
$\text{Co}(\text{CN})_6^{3-}$	$2.3 \times 10^2$
$\text{Rh}(\text{CN})_6^{3-}$	$2.0 \times 10^2$
$\text{Ir}(\text{CN})_6^{3-}$	$2.0 \times 10^2$
$\text{Ru}(\text{CN})_6^{4-}$	$2.0 \times 10^5$

<sup>a</sup>Quenching of biacetyl phosphorescence in aqueous solution.

<sup>b</sup>All complexes exhibit a singlet  $\rightarrow$  singlet transition at an energy  $32.1 \text{ kcm}^{-1}$  or greater.

<sup>c</sup>Slope of Stern-Volmer plot for quenching of the biacetyl phosphorescence by the complex.

$\text{Ru}(\text{CN})_6^{4-}$ . A process similar to (5-10), deactivation of the donor without acceptor excitation, appears to be operating here and merits investigation. The fact that  $\text{Rh}(\text{CN})_6^{3-}$  and  $\text{Ir}(\text{CN})_6^{3-}$  quench slowly discounts any large contribution of heavy metal enhanced deactivation by spin-orbital effects.

The  $\text{W}(\text{CO})_5(\text{pyridine})$  behaves as a quencher of biacetyl triplets in fluid solution,  $k_q \approx 10^8$ . The position of the phosphorescence in biacetyl and  $\text{W}(\text{CO})_5\text{py}$  is similar consistent with the observed quenching constant. The quenching by  $\text{W}(\text{CO})_6$  is extremely slow and  $\text{W}(\text{CO})_6$  has a high energy  $S \rightarrow T$  transition. The correlation is the same one invoked for  $\text{Co}(\text{CN})_5(\text{X})^{3-}$  complexes.

Ferrocene is known to quench anthracene ( $E_T = 42 \text{ kcal}$ )<sup>19</sup> triplets at a diffusion controlled rate. No evidence for electronic energy transfer was obtained and this possibility seems unlikely since ferrocene singlet  $\rightarrow$  triplet absorptions occur at higher energies than the anthracene triplet.<sup>20</sup> A comparison of the quenching activity of ruthenocene and ferrocene using biacetyl as a donor has been made. Ferrocene quenches almost two orders of magnitude faster, correlating well with the fact that the energy of the first  $S \rightarrow T$  absorption of ruthenocene is significantly higher than that for ferrocene. The data is shown in Table V-5. Ruthenocene, like  $\text{Co}(\text{CN})_6^{3-}$ , represents a case where spin-forbidden luminescence is seen at an energy lower than that of the donor<sup>21</sup> but is still not an effective quencher of biacetyl triplets. The generality of this phenomenon is established by

Table V-5. Quenching of Biacetyl with Metallocenes

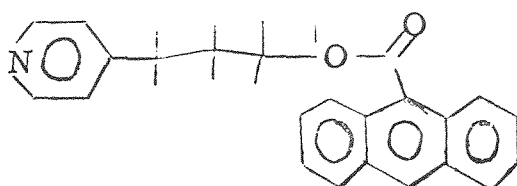
Quencher	$k_q^a$
Ferrocene	$\geq 10^9$
Ferricinium	$\geq 10^9$
Ruthenocene	$\sim 10^7$

<sup>a</sup>Determined from the slope of the Stern-Volmer plot for the biacetyl phosphorescence assuming a biacetyl triplet lifetime of 0.23 msec.

noting that both  $\text{Co}(\text{CN})_5(\text{SO}_3)^{4-}$  and  $\text{Pt}(\text{Cl})_6^{2-}$  do not quench biacetyl triplets at a diffusion controlled rate but do exhibit spin-forbidden luminescence at an energy favorable for the transfer of electronic excitation.

In contrast to the correlation established above invoking the formation of spectroscopic excited states by triplet sensitizers of Co(III) reactions is the report of the sensitized reduction of Co(III) in cobalt amine complexes.<sup>22</sup> It was shown that a number of low energy sensitizers would result in the sensitized formation of Co(II) with high efficiency even though direct irradiation at comparable energies results in little or no chemistry.<sup>23</sup> This result supports the notion that the charge transfer state responsible for the reaction is a low lying triplet but cannot be arrived at via internal conversion from d-d singlet states. The triplet donors, however, can apparently populate the charge transfer state directly.

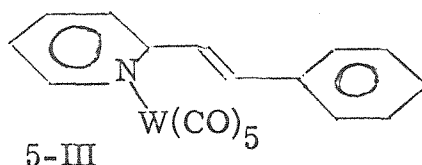
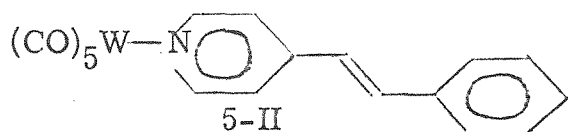
The study of energy transfer phenomena in bichromophoric systems represents a relatively unexplored area in transition metal systems but should provide fruitful results since it has been shown that intramolecular energy transfer is extremely fast.<sup>24</sup> A comparison of  $\text{W}(\text{CO})_5(\text{pyridine})$  and the system 5-I



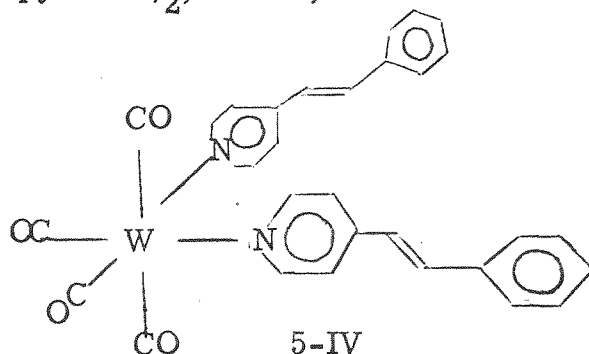
5-I

represents the first insulated bichromophoric system studied. Electronic absorption spectra in the vicinity of the  $^1A_1 \rightarrow ^3E$  transition for  $W(CO)_5(py)$  reveal that the anthracene moiety is essentially uncoupled from the  $W(CO)_5(py)$  portion of 5-I. However, at  $77^\circ K$ . no emission was detectable from the  $W(CO)_5(py)$ —, presumably due to transfer to the anthracene triplet. Whether quenching of the photodissociation of the pyridine group occurs in fluid solution was not determined.

The coordination of styryl-pyridines ( $E_T = 50$ )<sup>25</sup> to the  $W(CO)_5$ , 5-II, 5-III, results in nonluminescent complexes. Also the



cis- $W(CO)_4(4\text{-styryl-pyridine})_2$ , 5-IV, in contrast to

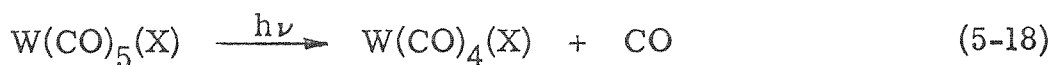


cis- $W(CO)_4(pyridine)_2$ , does not luminesce. The possibility

of energy migration from metal localized excited states to the ligand could be detected by the trans to cis isomerization of the coordinated ligand.

That the coordination of the styryl-pyridines and pyridine is similar in these examples is demonstrated by the infrared spectrum in the carbonyl stretching region (Table V-6). However, the electronic absorption spectra of the complexes 5-II, -III, and -IV reveal some coupling between the styryl-pyridine and the  $W(CO)_n$  moiety. The general effect upon coordination on the ligand transitions is to lower the extinction coefficient and to red shift the maximum. The metal localized transitions are also red shifted with some enhancement of the extinction coefficients. In Figures V-2 and V-3 we show some pertinent absorption spectra and in Table V-7 we summarize the data obtained.

The energy migration should be detected by a reduction in the normal photochemistry of the  $W(CO)_5(X)$  species which involves either loss of X or CO, equations (5-17) and (5-18). The



acceptor of the electronic excitation, the styryl-pyridine, should undergo its characteristic excited state chemistry of cis-trans isomerization.

In Table V-8 we summarize the quantum efficiencies of the photoreactions in these systems under similar conditions. The

Table V-6. Infrared Data for  $W(CO)_n(X)_{6-n}$  Complexes

Complex	CO Stretching Bands, $cm^{-1}$			
$W(CO)_5(\text{pyridine})^a$	2072(w)	1933(s)	1920(m)	
$W(CO)_5(\text{t-2-styryl-pyridine})^a$	2070(w)	1932(s)	1917(m)	
$W(CO)_5(\text{t-4-styryl-pyridine})^a$	2070(w)	1932(s)	1918(m)	
$\text{cis-}W(CO)_4(\text{pyridine})_2^b$	2008(w)	1884(m)	1866(m)	1826(m)
$\text{cis-}W(CO)_4(\text{t-4-styryl-pyridine})_2^b$	2003(w)	1884(m)	1863(m)	1825(m)

<sup>a</sup>Hydrocarbon room temperature solutions.

<sup>b</sup>Methylene chloride room temperature solutions.

Figure V-2. Room temperature absorption spectra of  $W(CO)_5(py)$  and  $W(CO)_5(t-4-stilbazole)$  in isooctane.

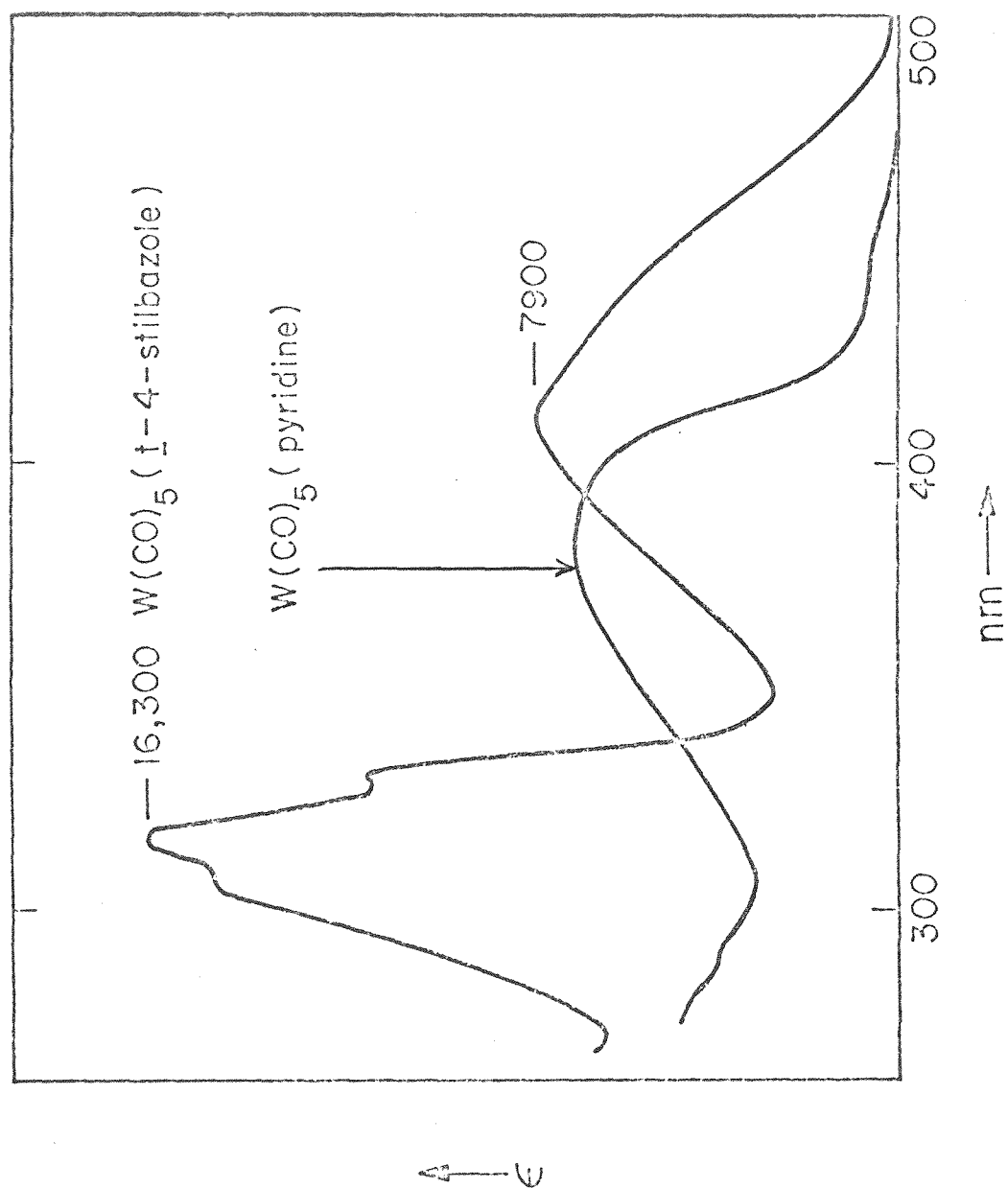




Figure V-3. Room temperature absorption spectra of cis- $\text{W}(\text{CO})_4(\text{py})_2$  and cis- $\text{W}(\text{CO})_4(4\text{-stilbazole})_2$  in benzene.

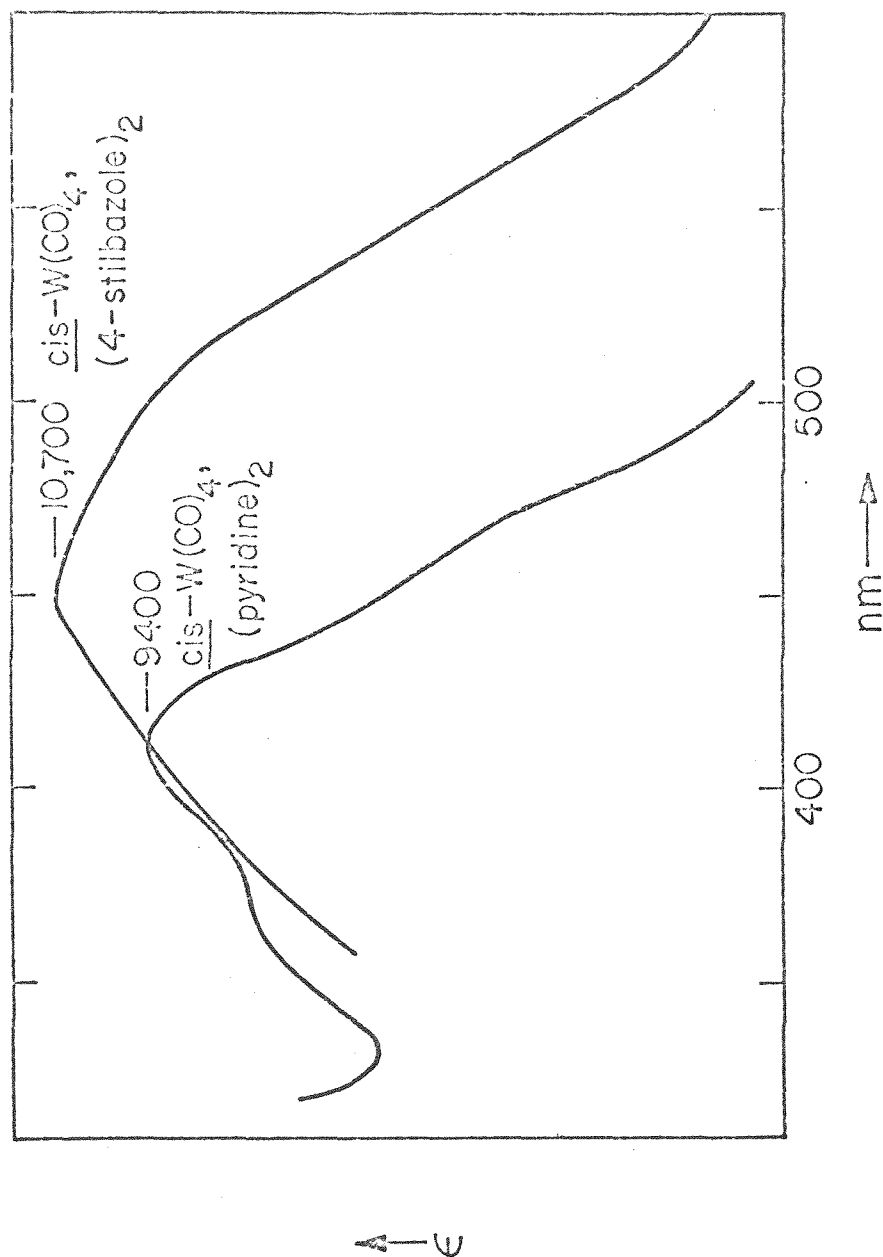


Table V-7. Electronic Absorption Data for  $W(CO)_n(X)_{6-n}$  Complexes<sup>a</sup>

Compound	$^1A_1 \rightarrow ^3E$ , nm ( $\epsilon$ )	$^1A_1 \rightarrow ^1E$ , nm ( $\epsilon$ )	Ligand Absorption, nm ( $\epsilon$ )
pyridine	—	—	252 (2090)
$W(CO)_5$ (pyridine)	440 (627)	380 (6904)	—
<u>t</u> -2-styryl-pyridine	—	—	314 (27,000)
$W(CO)_5$ ( <u>t</u> -2-styryl-pyridine)	440 (1228)	398 (4799)	314 (17,930)
<u>t</u> -4-styryl-pyridine	—	—	295 (24,400)
$W(CO)_5$ ( <u>t</u> -4-styryl-pyridine)	440 (5673)	408 (7865)	316 (16,346)

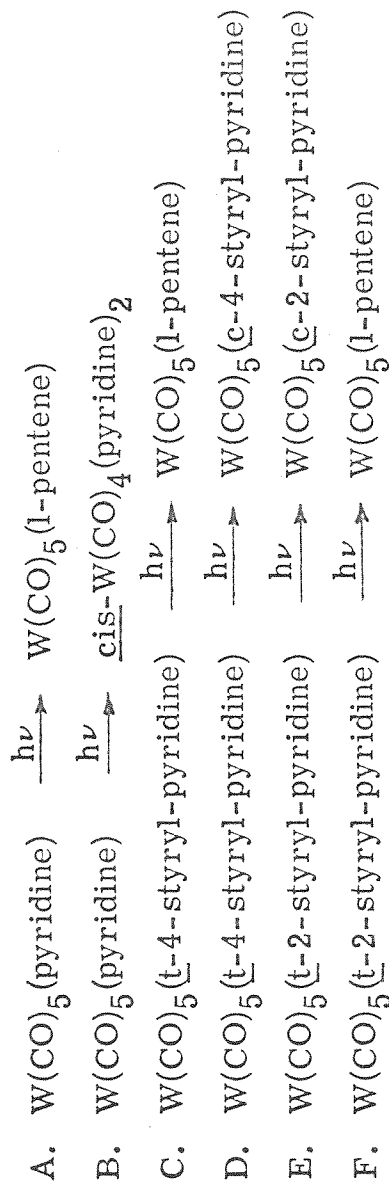
First Absorption Maximum, nm (  $\epsilon$  )

<u>cis</u> - $W(CO)_4$ (pyridine) <sub>2</sub>	413 (9400)
<u>cis</u> - $W(CO)_4$ ( <u>t</u> -4-styryl-pyridine)	448 (10,700)

<sup>a</sup>Room temperature hydrocarbon solutions.

Table V-8. Quantum Efficiencies for Photoreactions of  $W(CO)_5(X)$  Complexes

Reactions:

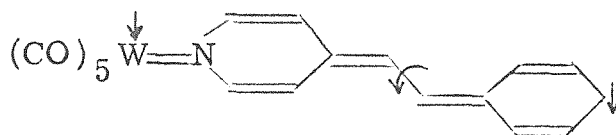


Reaction	$\phi_{436 \text{ nm}}$	$\phi_{366 \text{ nm}}$	$\phi_{313 \text{ nm}}$	$\phi_{254 \text{ nm}}$
A <sup>a</sup>	0.63	0.50	0.38	0.034
B <sup>b</sup>	0.002	0.013	0.039	0.04
C <sup>a</sup>	0.16	0.08	0.05	—
D	0.49	0.34	0.26	0.21
E	0.08 (t → c) 0.31 (c → t)	—	—	—
F <sup>a</sup>	0.16	0.07	0.13	—

<sup>a</sup>  $\phi$  measured at room temperature in the presence of 3.66 M 1-pentene, isooctane solvent.

<sup>b</sup>  $\phi$  for formation of cis- $W(CO)_4(\text{py})_2$  at room temperature in the presence of 0.25 M pyridine in isooctane.

irradiations at 436 nm indicate that the overall reaction efficiencies here are quite high. Both the 2-styrylpyridine and the 4-styrylpyridine quench quite effectively the dissociation reaction (5-17). In both cases dissociation is quenched by about two-thirds compared to the  $W(CO)_5(\text{pyridine})$ . It is interesting that the apparent greater electronic coupling in 5-II compared to 5-III does not result in a large difference in the substitution efficiencies of the complexes. An excited state may assume the geometry 5-V accounting for both the cis-trans isomerization



5-V

and the red shifts in the absorption spectrum. The state 5-V can be arrived at via a metal localized transition populating the  $d_{z^2}$  orbital. The excited electron then may pair with an electron from the pyridine ring leaving an unpaired electron in the lower  $\pi$ -d orbitals and another delocalized in the ligand system.

The wavelength effects on the chemistry in this system reveal that energy migration into state 5-V is not as facile at higher energies. The decrease in the trans  $\rightarrow$  cis isomerization follows the same trend as the dissociation of X in  $W(CO)_5(X)$ . On the other hand the process (5-18) increases in quantum

efficiency in  $\text{W}(\text{CO})_5(\text{py})$  as the exciting energy is increased. The wavelength effect implicates two different excited states, and it is attractive to assume that process (5-17) is associated exclusively with one state and (5-18) is associated exclusively with the higher energy state. The energy migration experiments suggest that the dissociative reaction from the upper state is too fast to be quenched even by the intramolecular energy migration involved here. Further, in the same way that the ligand X on the z-axis in  $\text{W}(\text{CO})_5(\text{X})$  specifically affects nonradiative decay rates, the styryl-pyridines specifically affect electronic decay associated with the excitations localized on the z-axis.

## References

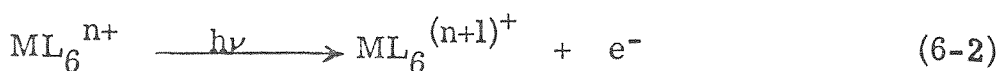
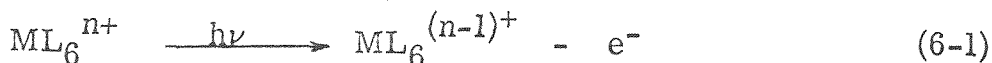
1. V. Balzani and V. Carassiti, "Photochemistry of Coordinated Compounds", Academic Press, Inc., New York, 1970, pp. 25-26.
2. (a) N.J. Turro, "Molecular Photochemistry", W.A. Benjamin, Inc., New York, 1967, pp. 92-136; (b) J.G. Calvert and J.N. Pitts, Jr., "Photochemistry", John Wiley & Sons, Inc., New York, 1967, pp. 321-355.
3. The Wigner spin-conservation rule is discussed in 2b and in: F. Wilkinson, *Adv. in Photochem.*, 3, 241 (1964). I wish to thank Jack Thibeault for assistance in the application of this rule to metal containing molecules presented here.
4. Energetics are estimated from values for spectroscopic energies for the  $\text{Cr}(\text{CN})_6^{3-}$   $^4\text{T}_2$  and  $^2\text{E}$  excited states reported in: P.D. Fleischauer and P. Fleischauer, Chem. Rev., 70, 199 (1970). We have found the biacetyl phosphorescence maximum at  $\sim 19.0 \text{ kcm}^{-1}$ .
5. Reference 1 p. 29.
6. (a) A.J. Fry, R.S.H. Liu, and G.S. Hammond, J. Am. Chem. Soc., 88, 4761 (1966); (b) G.S. Hammond and R.P. Foss, J. Phys. Chem., 68, 3739 (1964); (c) J.A. Bell and H. Linschitz, J. Am. Chem. Soc., 85, 528 (1963).
7. L.M. Stephenson, D.G. Whitten, G.F. Vesley, and G.S. Hammond, ibid., 88, 3665 (1966).
8. S.P. Van, Ph.D. Thesis, California Institute of Technology, 1969.
9. D.J. Binet, E.L. Goldberg, and L.S. Forster, J. Phys. Chem., 72, 3017 (1968).
10. V. Balzani, R. Ballardini, M.T. Gondolfi, and L. Moggi, J. Am. Chem. Soc., 93, 339 (1971).
11. A. Pfeil, ibid., 93, 5395 (1971).
12. J.N. Demas and A.W. Adamson, ibid., 93, 1800 (1971).

13. V. Balzani and V. Carassiti, J. Phys. Chem., 72, 383 (1968).
14. V.S. Sastri and C.H. Langford, J. Am. Chem. Soc., 91, 7533 (1969).
15. D.F. Evans, J. Chem. Soc., 1735 (1960).
16. G.S. Hammond, et.al., J. Am. Chem. Soc., 86, 3197 (1964).
17. (a) M. Mingardi and G.B. Porter, J. Chem. Phys., 44, 4354 (1966); (b) G.A. Crosby, J. Chim. Phys., 64, 160 (1967); (c) G. B. Porter, J. Am. Chem. Soc., 91, 3980(1969).
18. R.A. Borkman and D.R. Kearns, J. Chem. Phys., 44, 945 (1966) and J. Am. Chem. Soc., 88, 3467 (1966).
19. D. P. Craig and I.G. Ross, J. Chem. Soc., 1589 (1954).
20. Y.S. Sohn, D.N. Hendrickson, and H.B. Gray, J. Am. Chem. Soc., 93, 3603 (1971).
21. See Figure III-18 , p.121.
22. (a) A. Vogler and A.W. Adamson, J. Am. Chem. Soc., 90, 5943 (1968); (b) Reference 1 p. 229.
23. Reference 1 pp. 231-234.
24. Reference 2a pp. 123-129.
25. D.G. Whitten and M. T. McCall, J. Am. Chem. Soc., 91, 5097 (1969).

## CHAPTER VI

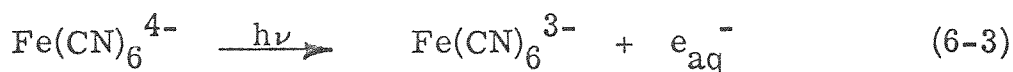
Photoredox Reactions in Metal  
Containing Molecules

Redox reactions (6-1, 6-2) are logically associated with decay



from charge transfer excited states. The large reorganization of electron density, especially to configurations which look like final oxidation or reduction products, can readily give the chemistry in (6-1) or (6-2). Besides reduction or oxidation of the central metal one can classify the reactions that give complexes which are stable and retain the original coordinated ligands and those that produce very unstable molecules which undergo rapid thermal decomposition.

Usually, it is not clear where the electrons involved end up. Most studies have centered on the fate of the metal complex and the oxidation state of the central metal. In a remarkably large number of simple complexes the actual photoproduction of the hydrated electron has been proposed. One fairly convincing case is shown in equation (6-3). Evidence for the production

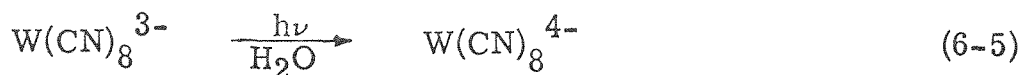
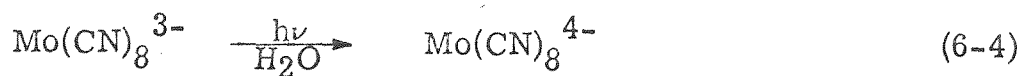


of  $e_{\text{aq}}^-$  is obtained by the addition of  $\text{N}_2\text{O}$  which scavenges the



$e_{aq}^-$  yielding  $N_2$ . The quantum yield is high, measurements ranging from 0.35 to 1.35 at 254 nm.<sup>1</sup> The absorption is thought to be a metal to solvent or a metal to  $CN^-$  charge transfer transition which results in an excited state which looks like the oxidation product  $Fe(CN)_6^{3-}$ . The actual electron transfer step is not understood. The isoelectronic  $Ru(CN)_6^{4-}$  also produces the hydrated electron upon photoexcitation at 254 nm with a quantum yield of 0.36.<sup>2</sup> These are good examples of complexes of six-coordination undergoing redox without decomposition since  $ML_6$  is stable in the two oxidation states involved. The  $Co(CN)_6^{3-}$  anion, isoelectronic with the  $Ru(CN)_6^{4-}$  and  $Fe(CN)_6^{4-}$ , is thought to produce the hydrated electron upon 254 nm excitation, but the fate of the Co(IV) species is not known.<sup>3</sup>

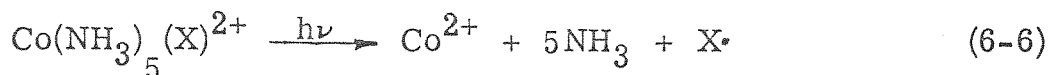
The best examples of photoreduction with retention of original geometry seem to be reactions (6-4) and (6-5).<sup>4</sup> The mechanism



of this reaction is still in doubt, but workers have ruled out a true intramolecular reduction which would result in the formation of cyanogen. A chain mechanism perhaps involving nine-coordinate intermediates may be involved. Nine coordination may be possible in the excited state of this  $d^1$  system since by exciting

this one electron the lowest d orbital is vacant. Thus far, however, all mechanisms proposed have been criticized.

Co(III) Systems. The cobalt(III) amines represent the most well studied examples of photoreduction resulting in decomposition of the complex. Irradiation of the ligand  $\rightarrow$  metal charge transfer band of  $\text{Co}(\text{NH}_3)_5(\text{X}^-)^{2+}$  results in the formation of  $\text{Co}(\text{II})$  with high efficiency, (6-6).<sup>4</sup> We can understand this



reaction in the following way: the  $\text{Co}(\text{III})$  system is a  $d^6$  low spin system requiring the population of either  $d_{z^2}$  or  $d_{x^2-y^2}$  in the  $\text{L} \rightarrow \text{M}$  CT transition. The excited state looks like  $\text{Co}(\text{II})$  with seven d electrons, however, six-coordinate  $\text{Co}(\text{II})$  with strong field ligands like  $\text{NH}_3$  are unstable and release of the ligands occurs. Examination of the data<sup>5</sup> in Table VI-1 reveals that the reaction is occurring from a state essentially inaccessible from ligand field excited states. On the other hand low energy triplet sensitizers have been used to sensitize cobalt(III) amine photoreduction<sup>6</sup> implicating the importance of low lying triplet charge transfer excited states. A possible ordering scheme for relaxed excited states is shown in Figure VI-1 where the CT triplet is the lowest excited state in the system. The inter-conversion of excited states does not occur since there is such a strong wavelength effect, and from Figure VI-1 we conclude

Table VI-1. Wavelength Effects on Photoreduction of Cobalt(III)  
Ammine Complexes<sup>a</sup>

Complex	Irrdn. $\lambda$ , nm	Type of Transition	$\phi^b$
$\text{Co}(\text{NH}_3)_6^{3+}$	254	$\text{L} \rightarrow \text{M CT}$	0.16
	365	d-d	0
	472	d-d	0
$\text{Co}(\text{NH}_3)_5\text{Cl}^{2+}$	254	$\text{Cl} \rightarrow \text{Co CT}$	0.25
	313	$\text{Cl} \rightarrow \text{Co CT}$	0.16
	370	d-d	0
	550	d-d	0
$\text{Co}(\text{NH}_3)_5(\text{NCS})^{2+}$	370	CT, d-d	0.03
	550	d-d	0

<sup>a</sup>Reference 5.

<sup>b</sup>Quantum yield for  $\text{Co(II)}$  formation.

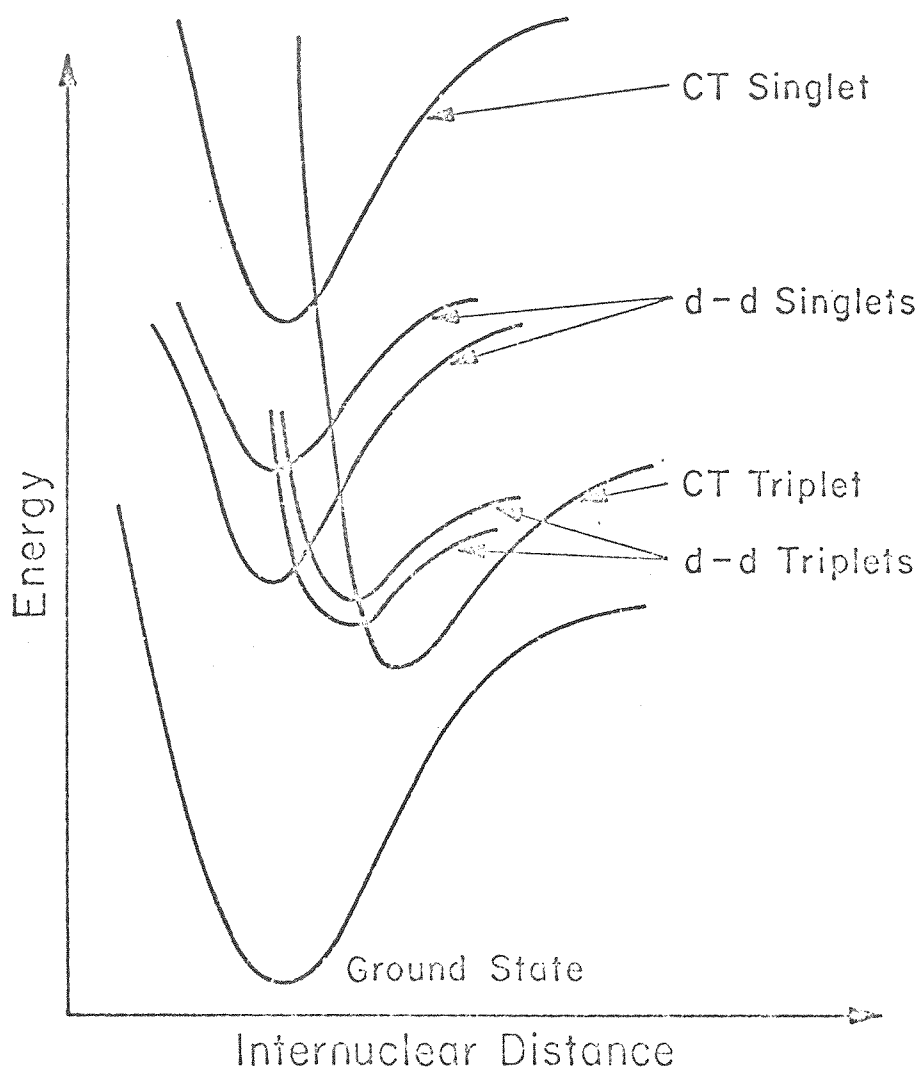
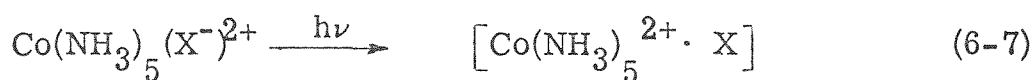


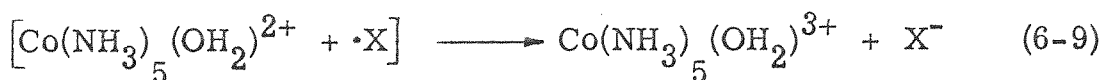
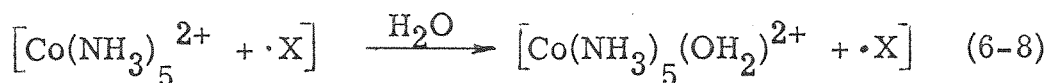
Figure VI-1. Possible state diagram for  $\text{Co}(\text{NH}_3)_5(\text{X}^-)^{2+}$  complexes.

that irradiation into d-d bands must not result in formation of the low lying CT state. Whether the triplet CT state is the sole reactive excited state awaits the comparison of triplet sensitized and direct photoreduction quantum yields.

The formation of the Co(II) species by photolysis of Co(III) amine complexes is logically viewed<sup>7</sup> as the result of homolytic cleavage of the Co-X bond, (6-7). The caged radicals can



either recombine or diffuse apart. The effect of viscosity has not been reported and merits investigation. The homolytic cleavage mechanism also accounts for the observation of substitution from CT states via the sequence (6-8) through (6-9).



Direct formation of the caged radical pair implicates a CT state which is not a bound state, possibly accounting for the noninterconverting excited states.

In contrast to the Co(III) amine complexes cyanocobaltate(III) complexes do not undergo efficient photoreduction. Further, the cyanide complexes have rich photosubstitution chemistry upon ligand field excitation while the amine complexes have

comparatively unreactive ligand field excited states. The differences in redox photochemistry may be related to the differences in stability of possible "d<sup>7</sup>" type excited states formed in  $L \rightarrow M$  CT transitions. Apparently, with the amines, decomposition of the complex occurs before other pathways for decay occur, but cyanide complexes dissipate energy via ligand field states resulting in substitution. The ligands play a critical role in determining the nature of the excited state reaction.

The amines interact in a  $\sigma$  fashion only, while  $CN^-$  can be a  $\sigma$ -donor,  $\pi$ -acceptor, or a  $\pi$ -donor. While no trends are obvious, Co(III) amine complexes substituted with halides give respectable substitution yields relative to the photoreduction, Table VI-2. The "d<sup>7</sup>" CT excited state is a lower energy intermediate with the weak field ligands, and other modes of decay compete with complete degradation of the complex.

Neither  $Co(CN)_6^{3-}$  nor  $Co(CN)_5(X)^{n-}$  complexes give Co(II) as a primary photoproduct. However, both trans- $Co(CN)_4(SO_3)(OH_2)^{3-}$  and  $Co(CN)_4(OH_2)_2^-$  give sizable yields of Co(II). In Figure VI-2 we show the production of Co(II) from the photodecomposition of trans- $Co(CN)_4(SO_3)(OH_2)^{3-}$ . The figure reveals two facts: (1) Co(II) is a primary photoproduct since its increase is linear in time and (2) Co(II) is also a photoproduct of  $Co(CN)_4(OH_2)_2^-$  since the Co(II) production does not drop off while the rate of loss of the sulfite complex is

Table VI-2. Reactivity of Substituted Co(III) Ammine Complexes<sup>a</sup>

Complex	Irrdn. $\lambda$ , nm	Type of Transition	$\phi_{\text{Co(II)}}$	$\phi_{\text{subst.}}$
$\text{Co(en)}_3^{3+}$	254	L $\rightarrow$ M CT	0.13	0.0
	365	d-d	0.00	10 <sup>-4</sup>
	400	d-d	0.00	0.00
<u>cis</u> -Co(en) <sub>2</sub> Cl <sub>2</sub> <sup>+</sup>	254	Cl $\rightarrow$ Co	0.05	—
	313	Cl $\rightarrow$ Co	0.02	0.01
	340-375	CT, d-d	0.0003	—
<u>trans</u> -Co(en) <sub>2</sub> Cl <sub>2</sub> <sup>+</sup>	254	Cl $\rightarrow$ Co	0.06	0.01
	313	Cl $\rightarrow$ Co	0.04	0.01
<u>cis</u> -Co(en) <sub>2</sub> Br <sub>2</sub> <sup>+</sup>	370	Br $\rightarrow$ Co	0.005	0.095
	550	d-d	0.0003	0.004
<u>trans</u> -Co(en) <sub>2</sub> Br <sub>2</sub> <sup>+</sup>	370	Br $\rightarrow$ Co	0.007	0.063
	550	d-d	0.000	0.0006

<sup>a</sup>Reference 5.

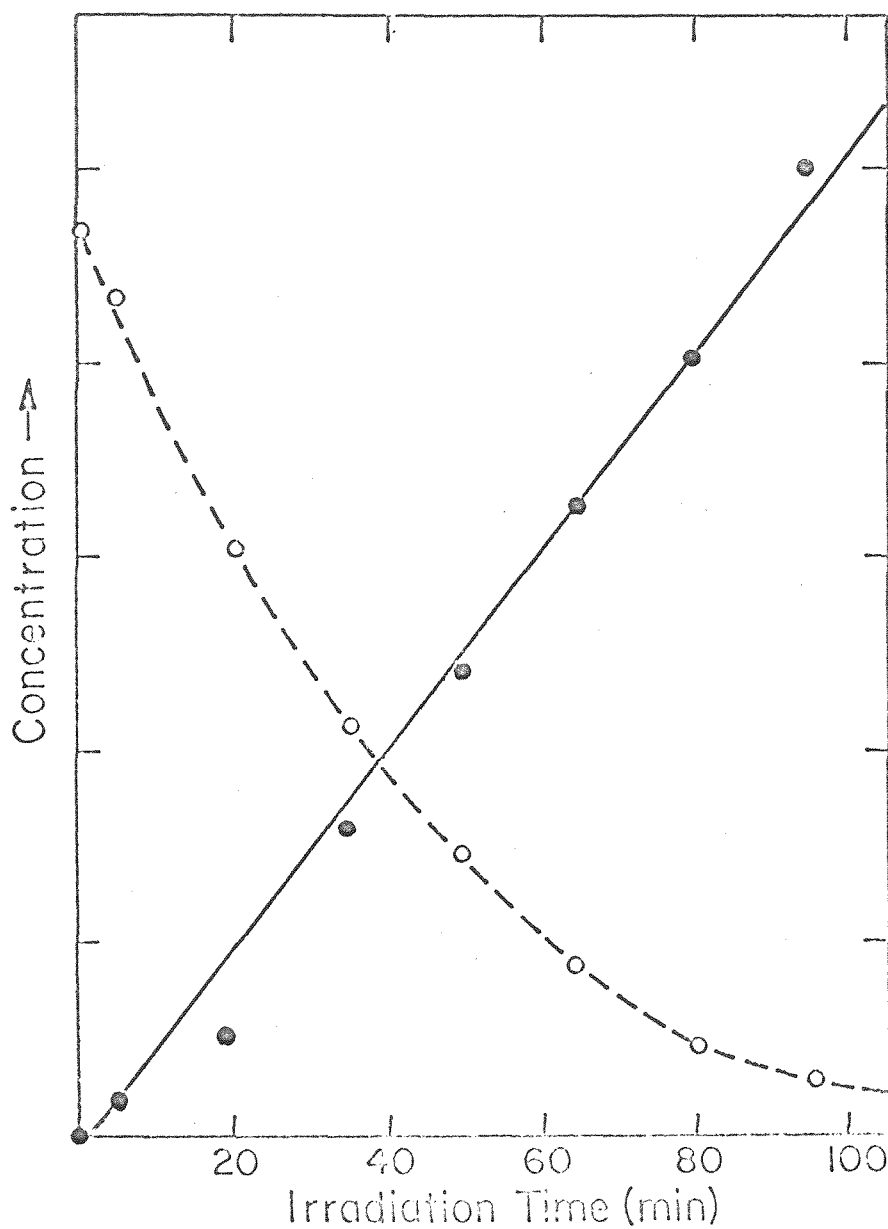


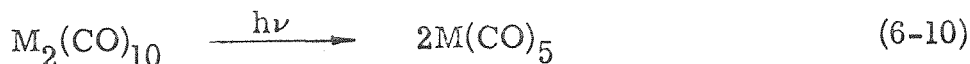
Figure VI-2. Decrease in  $\text{trans-Co(CN)}_4(\text{SO}_3)(\text{OH}_2)_3^{3-}$  (o) and the increase in  $\text{Co(II)}^4$  (●) as a function of 254nm irradiation time. Concentration scales for the two plots are not the same.



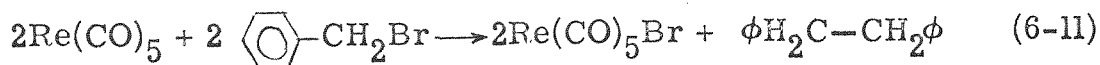
diminished considerably due to competitive absorption of light by the diaquo product. The quantum yield at 254 nm for Co(II) production is  $\sim 0.01$  compared to a disappearance yield of 0.15 for the monosulfito complex.

Apparently four cyanides cannot stabilize the CT state while the five cyanides provide sufficient stability to allow photo-substitution processes to dominate. It is well known that  $\text{Co(CN)}_5^{3-}$  is relatively stable, and further, it is known that species like  $\text{Co(NH}_3)_5^{2+}$  are very labile. At this point enough data is available to conclude that the ligand plays a key role in relative reaction paths, but not enough data exists to predict and control these systems.

$\text{M}_2(\text{CO})_{10}$  Systems. The photochemistry of  $\text{M}_2(\text{CO})_{10}$  ( $\text{M} = \text{Mn, Tc, Re}$ ) represents a case where caged radicals can again be formed, but here the metal complex is oxidized. The dimeric  $\text{M}-\text{M}$  bonded systems exhibit a  $\sigma \rightarrow \sigma^*$  transition associated with the  $\text{M}-\text{M}$  bond. The one-electron excitation should result in homolytic cleavage to form two  $d^7 \text{M(CO)}_5$  species, (6-10). The  $\text{M(CO)}_5$  moiety is isoelectronic with the



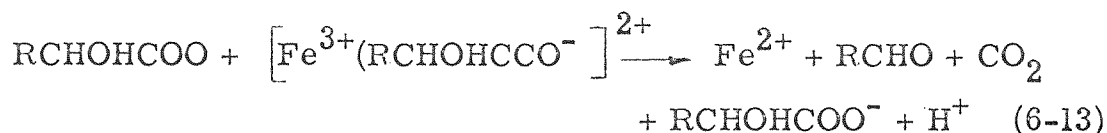
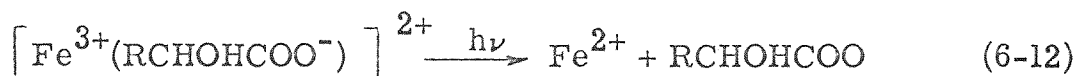
radical-like  $\text{Co(CN)}_5^{3-}$ , and it is not surprising that reaction (6-11)



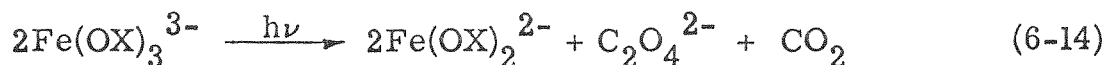
occurs.

The rhenium is formally oxidized to the +1 oxidation state achieving the stable  $d^6$  configuration. Quantum efficiencies, medium effects, and other reaction pathways are being investigated. Initial results indicate that the  $M(CO)_5$  species are extremely good reducing agents.

Fe(III) Systems. A number of Fe(III) complexes undergo photo-reduction to form Fe(II).<sup>8</sup> Particularly interesting are cases where the reduction of the iron is accompanied by oxidation of an organic substrate as in (6-12) and (6-13).<sup>9</sup> The formation of



the strong ion pair or complex between the  $Fe^{3+}$  and the organic anion produces a  $L \rightarrow M$  CT transition or an ion pair CT transition. Ion pair CT transitions can be responsible for Co(III) reduction, and these excited states seem to be responsible for a number of Fe(III) photoreductions as well.<sup>10</sup> Reduction of Fe(III) in true molecular complexes is also known, with the best example being the standard chemical actinometry system  $Fe(OX)_3^{3-}$  ( $OX = C_2O_4^{2-}$ ). The  $Fe(OX)_3^{3-}$  reduces according to (6-14).<sup>11</sup>



While work in this area has revealed a broad scope of photogenerated chemistry, little conclusive mechanistic work exists due to difficulties in determining what absorbs the light and the nature of secondary thermal processes. Of particular interest would be the sequence (6-15), (6-16). This is



representative of the concept of photocatalysis discussed in Chapter VIII. The process (6-15), (6-16) is conceivable since it is known that photolysis of  $[\text{Fe}^{3+} \cdot \text{OH}^-]$  can result in the oxidation of an organic substrate,<sup>12</sup> and importantly,  $\text{Fe}^{2+}$  is oxidized in basic media by  $\text{O}_2$ .<sup>13</sup>

We have attempted to gain understanding of  $\text{Fe(III)} \rightarrow \text{Fe(II)}$  photoreduction by an investigation of the photoredox chemistry of ferricinium.<sup>14</sup> Irradiation at 313 nm of  $\text{Fe(cp)}_2^+$  in 0.01 M  $\text{HClO}_4$  aqueous solutions yielded essentially no disappearance of the starting material with the quantum yield being  $\sim 10^{-3}$ . However, addition of 2,3-butanedione (biacetyl) to the solution yields facile photoinduced disappearance of the  $\text{Fe(cp)}_2^+$  resulting in the formation of ferrocene.

While the detailed mechanism is not understood in the biacetyl- $\text{Fe(cp)}_2^+$  system some key results have been obtained. Ferricinium quenches biacetyl triplets at a rate close to diffusion controlled, but the disappearance of the  $\text{Fe(cp)}_2^+$  is not a

biacetyl triplet sensitized reaction, since irradiation at 366 nm in a solution where biacetyl absorbed all of the light resulted in no reaction. The reaction quantum yield is dependent on the biacetyl concentration, Table VI-3. As seen in Table VI-4 the system is complicated by the fact that the rate of photoreduction is inhibited by added  $\text{Fe}(\text{cp})_2^+$ . The reaction quantum yield at  $1 \times 10^{-3} \text{ M}$   $\text{Fe}(\text{cp})_2^+$  and  $6 \times 10^{-2} \text{ M}$  biacetyl is  $\sim 0.1$ . The effect of oxygen is small and somewhat nonreproducible indicative of large experimental error. The photoreduction of  $\text{Fe}(\text{cp})_2^+$  is also accelerated by irradiation in the presence of other organic substrates such as ethanol, methanol, ethylene glycol, and acetone. Relative rates in 30% by volume aqueous solutions of these substrates are shown in Table VI-5. Unfortunately, possible oxidation products from the organic substrates have not been identified in any case.

At this point it is premature to speculate on a detailed mechanism, but the reactions can be viewed as similar to other  $\text{Fe}(\text{III})$  photocatalyzed oxidations of organic molecules. The distinguishing feature here is that the oxidized and reduced metal complex has the same stoichiometry. This feature is necessary in the development of the photocatalytic redox systems.

Table VI-3. Biacetyl Concentration Effect on  $\text{Fe}(\text{cp})_2^+$   
Photoreduction<sup>a</sup>

Biacetyl, <u>M</u>	Irrdn. Time, min.	Rel. $\phi$
0.00	64	0
0.01 <sub>1</sub>	64	0.2 <sub>3</sub>
0.11	64	0.4 <sub>2</sub>
0.57	64	1.00
0.00	390	0
0.01 <sub>1</sub>	390	0.1 <sub>3</sub>
0.11	390	0.66
0.57	390	1.00

<sup>a</sup>Irradiation in 313 nm merry-go-round, 0.01 M  $\text{HClO}_4$  solvent,  
 $5.6 \times 10^{-3}$  M  $\text{Fe}(\text{cp})_2\text{BF}_4$ .

Table VI-4. Ferricinium Concentration Effect on its Biacetyl  
Catalyzed Photoreduction<sup>a</sup>

$\text{Fe}(\text{cp})_2\text{BF}_4$ , <u>M</u>	Rel. $\phi$
$2.73 \times 10^{-3}$	0.21
$1.98 \times 10^{-3}$	0.48
$0.82 \times 10^{-3}$	1.00

<sup>a</sup>Irradiation in 313 nm merry-go-round in 0.001 M  $\text{HClO}_4$  with 0.029 M biacetyl.

Table VI-5. Relative Rates of Photoreduction of  $\text{Fe}(\text{cp})_2^+$  in  
Different Solvents<sup>a</sup>

Solvent	Rel. $\phi$
7:3 $\text{H}_2\text{O}$ /acetone	1.00
7:3 $\text{H}_2\text{O}$ /EtOH	0.55
7:3 $\text{H}_2\text{O}$ /ethylene glycol	0.28
7:3 $\text{H}_2\text{O}$ /MeOH	0.17
$\text{H}_2\text{O}$	0

<sup>a</sup>313 nm irradiation in a merry-go-round.

## References

1. (a) M. Shiron and G. Stein, Nature, 204, 778 (1964); (b) G. Stein, Adv. in Chem., 50, 238 (1965); (c) P. L. Airey and F. S. Dainton, Proc. Roy. Soc. (London), A291, 340 (1966); (d) S. Ohno and G. Tsuchihashi, Bull. Chem. Soc. Japan, 38, 1052 (1965); (e) S. Ohno, ibid., 40, 1770 (1967); (f) M. Shiron and G. Stein, J. Chem. Phys., 55, 3372 (1971).
2. V. Balzani and V. Carassiti, "Photochemistry of Coordination Compounds", Academic Press, Inc., New York, 1970, p. 308.
3. S. Ohno, Bull. Chem. Soc. Japan, 40, 1779 (1967).
4. (a) E. L. Goodenow and C. S. Garner, J. Am. Chem. Soc., 77, 5268 (1955); (b) ibid., 77, 5272 (1955); (c) V. Carassiti and V. Balzani, Ann. Chim. Rome, 51, 518 (1961); (d) V. Balzani and V. Carassiti, ibid., 51, 533 (1961), ibid., 52, 432 (1962).
5. (a) L. Moggi, N. Sabbatini, and V. Balzani, Gazz. Chim. Ital., 97, 980 (1967); (b) J. F. Endicott and M. Z. Hoffman, J. Am. Chem. Soc., 87, 3348 (1965); (c) M. F. Manfrin, G. Varani, L. Moggi, and V. Balzani, Mol. Photochem., 1, 387 (1969); (d) A. W. Adamson and A. H. Sporer, J. Am. Chem. Soc., 80, 3865 (1958); (e) A. W. Adamson and A. H. Sporer, J. Inorg. Nucl. Chem., 8, 209 (1958); (f) A. W. Adamson, Discuss. Faraday Soc., 29, 163 (1960); (g) A. W. Adamson, W. L. Waltz, E. Zinato, D. W. Watts, P. D. Fleischauer, and R. D. Lindholm, Chem. Rev., 68, 541 (1968); (h) Reference 2 pp. 197-217 and references cited therein.
6. (a) A. Vogler and A. W. Adamson, J. Am. Chem. Soc., 90, 5943 (1968); (b) D. Valentine, Jr., Adv. in Photochem., 6, 123 (1968); (c) Reference 2 p. 229.
7. Reference 2 pp. 211-214.
8. (a) J. Legros, Compt. Rend., 265, 225 (1967); (b) J. H. Baxendale and N. K. Bridge, J. Phys. Chem., 59, 783 (1955); (c) F. S. Dainton and R. G. Jones, Trans. Faraday Soc., 63, 1512 (1967); (d) G. J. Brealey, M. G. Evans, and N. Uri, Nature, 166, 959 (1950); (e) G. J. Brealey and N. Uri, J. Chem. Phys., 20, 257 (1952).



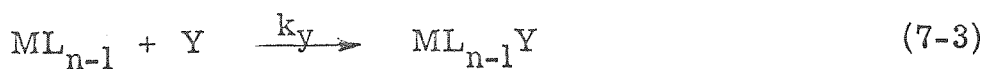
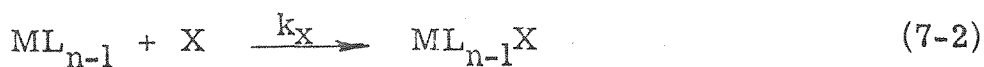
9. (a) T.S. Glikman, V.A. Kalibabchuk, and V.P. Sosnovskaya, J. Gen. Chem. U.S.S.R., 35, 1533 (1965); (b) G.V. Bakore and S.D. Bhardwaj, Proc. Natl. Inst. Sci. India, 29A, 90 (1963).
10. (a) N. Uri, Chem. Rev., 50, 375 (1952); (b) F.S. Dainton, J. Chem. Soc. (Special Publ.), 1, 18 (1954).
11. C.G. Hatchard and C.A. Parker, Proc. Roy. Soc. (London), A235, 518 (1956).
12. J.H. Baxendale and J. Magee, Trans. Faraday Soc., 51, 205 (1955).
13. A.B. Lamb and L.W. Elder, J. Am. Chem. Soc., 53, 137 (1931).
14. The gamma radiolysis of  $\text{Fe}(\text{cp})_2^+$  has been reported and gives ferrocene as a product: R. Blackburn and A. Kabi, Chem. Comm., 862 (1966).

## CHAPTER VII

Photosubstitution Processes in  
Coordination Compounds

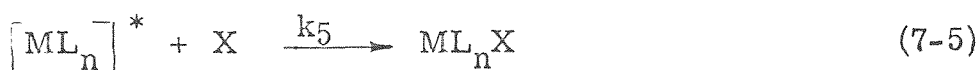
The electronically excited state of a coordination compound can have substitution pathways which are different from the ground state. Generally, we associate weakly bound ligands with those that are most substitution labile. The problem in understanding the substitution chemistry of excited state complexes is determining which ligands are most labile in the excited state. In short, we need to know the electronic and geometrical structure involved and the types of metal-ligand bonding.

Mechanisms of Photosubstitution. As in thermal substitution processes two types of photosubstitution are distinguished. A dissociative mechanism involves the formation of a coordinatively unsaturated intermediate which can discriminate entering ligands. A dissociative scheme for substitution is outlined in equations (7-1) through (7-3). The nature of the excited state involved is



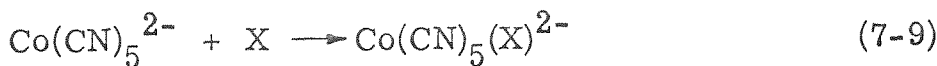
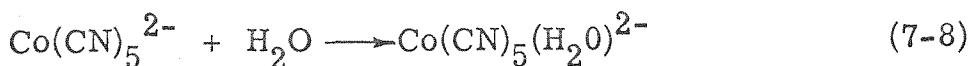
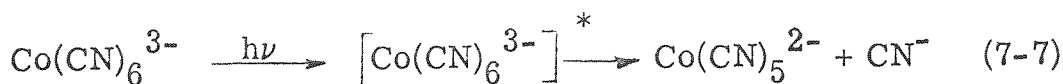
unimportant at this time. The associative mechanism for

substitution involves the formation of an intermediate complex containing both the leaving ligand and the entering ligand. This mechanism is outlined in equations (7-4) through (7-6). Very



little work has been done to show which of these mechanisms obtains.

We have investigated the photoaquation of  $\text{Co}(\text{CN})_6^{3-}$  in this regard. First reports of the photosubstitution of  $\text{Co}(\text{CN})_6^{3-}$  in water involved the dissociative loss of  $\text{CN}^-$  to form the  $\text{Co}(\text{CN})_5^{2-}$  intermediate which could then be scavenged by either water or an added nucleophile.<sup>1</sup> By this dissociative mechanism, (7-7) through (7-9), one predicts the formation of  $\text{Co}(\text{CN})_5(\text{X})^{2-}$



as a primary photoproduct. The  $\text{Co}(\text{CN})_6^{3-}$  system offers a unique way to determine the validity of the dissociative pathway: the  $\text{Co}(\text{CN})_6^{3-} \longrightarrow \text{Co}(\text{CN})_5(\text{H}_2\text{O})^{2-}$  reaction exhibits an isosbestic point in the uv spectrum at 330 nm (Figure VII-1).

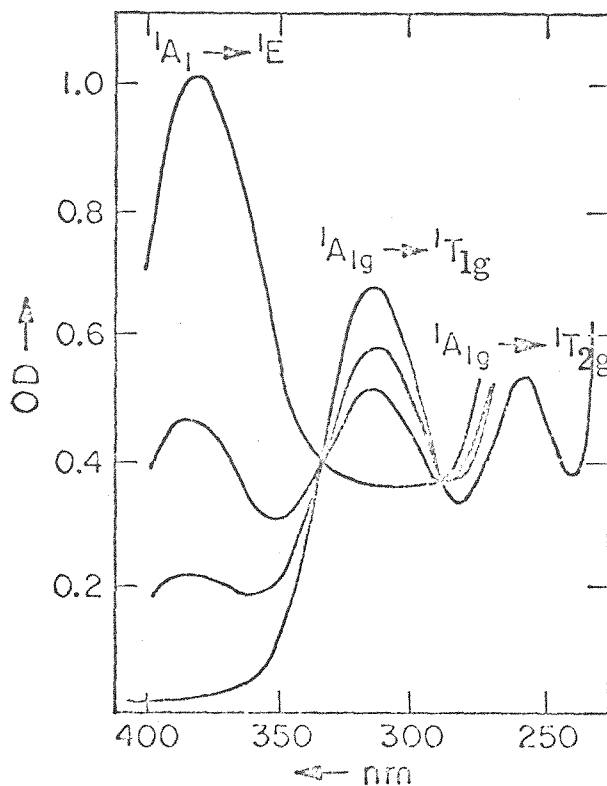
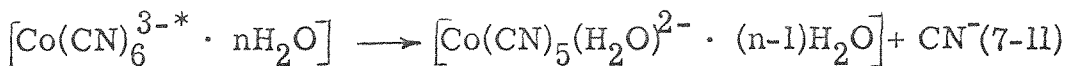
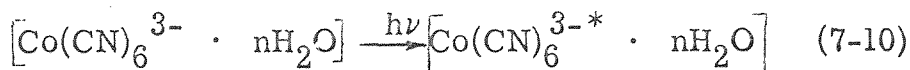


Figure VII-1. Spectral changes in the conversion of  $\text{Co(CN)}_6^{3-}$  to  $\text{Co(CN)}_5(\text{OH}_2)^{2-}$ . The lowest energy band is due to the aquo complex while the two higher energy bands are due to the  $\text{Co(CN)}_6^{3-}$ .

If the  $\text{Co(CN)}_5(\text{X})^{3-}$  products are formed directly the isosbestic point will not be maintained. By simultaneously monitoring the absorbance at 330nm and irradiating an aqueous sample of  $\text{Co(CN)}_6^{3-}$  in the presence of high concentrations of either  $\text{I}^-$  or  $\text{N}_3^-$ , one should easily detect the direct formation of the  $\text{Co(CN)}_5(\text{I})^{3-}$  or  $\text{Co(CN)}_5(\text{N}_3)^{3-}$ . Either of these products absorbs much more intensely than either the  $\text{Co(CN)}_6^{3-}$  or the  $\text{Co(CN)}_5(\text{H}_2\text{O})^{2-}$  at 330nm. However, when this experiment was performed the absorbance at 330nm did not change until a significant amount of the  $\text{Co(CN)}_5(\text{H}_2\text{O})^{2-}$  was formed, Figures VII-2 and VII-3. That is, there is no direct formation of  $\text{Co(CN)}_5(\text{X})^{3-}$  products. The most reasonable interpretation of these results is that an associative type mechanism obtains, involving interchange of an inner sphere  $\text{CN}^-$  and outer sphere  $\text{H}_2\text{O}$  as outlined in equations (7-10) and (7-11). At least it is



clear that a discrete five-coordinate intermediate similar to that formed in the thermal exchange reactions<sup>2,3</sup> of  $\text{Co(CN)}_5\text{X}^{3-}$ , (7-12) and (7-13), is not formed in the direct irradiation of

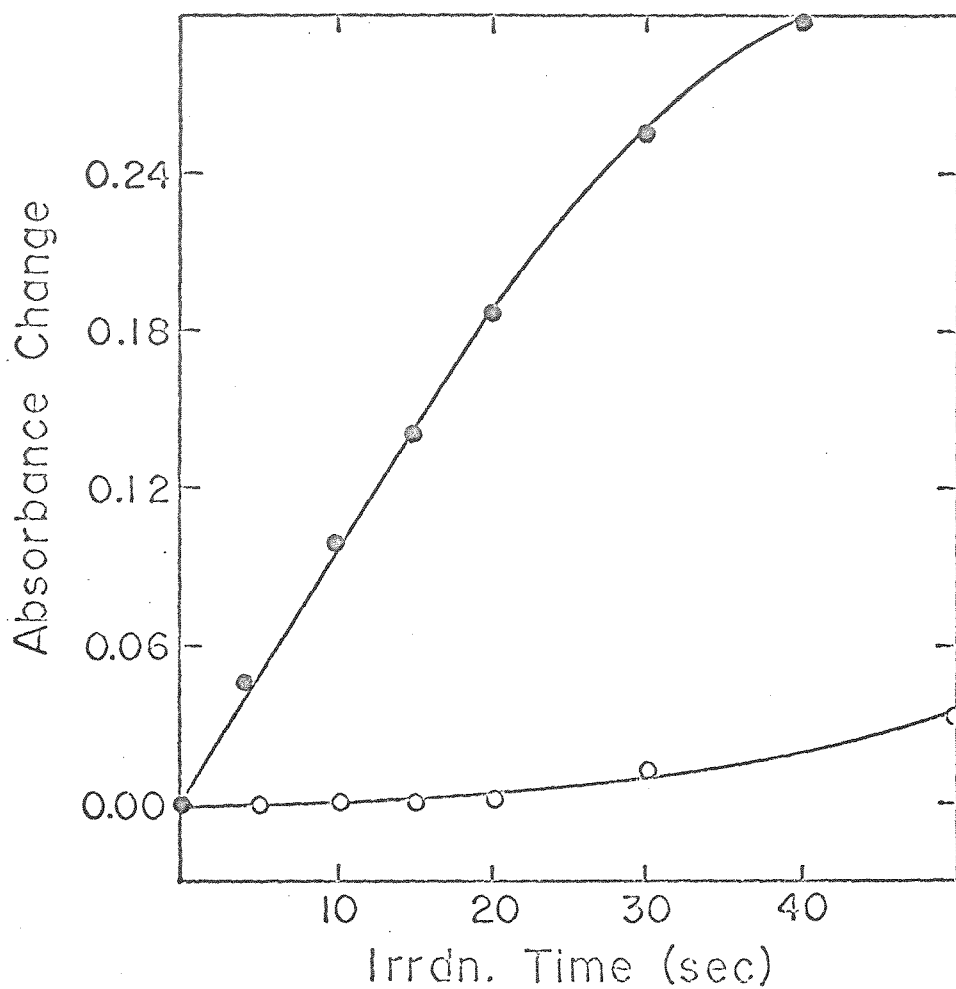


Figure VII-2. Absorbance change at 380nm (●) and 330nm (○) during irradiation of  $\text{Co(CN)}_6^{3-}$  ( $1.76 \times 10^{-4} \text{ M}$ ) in the presence of  $0.37 \text{ M NaI}$  at  $15^\circ\text{C}$ .

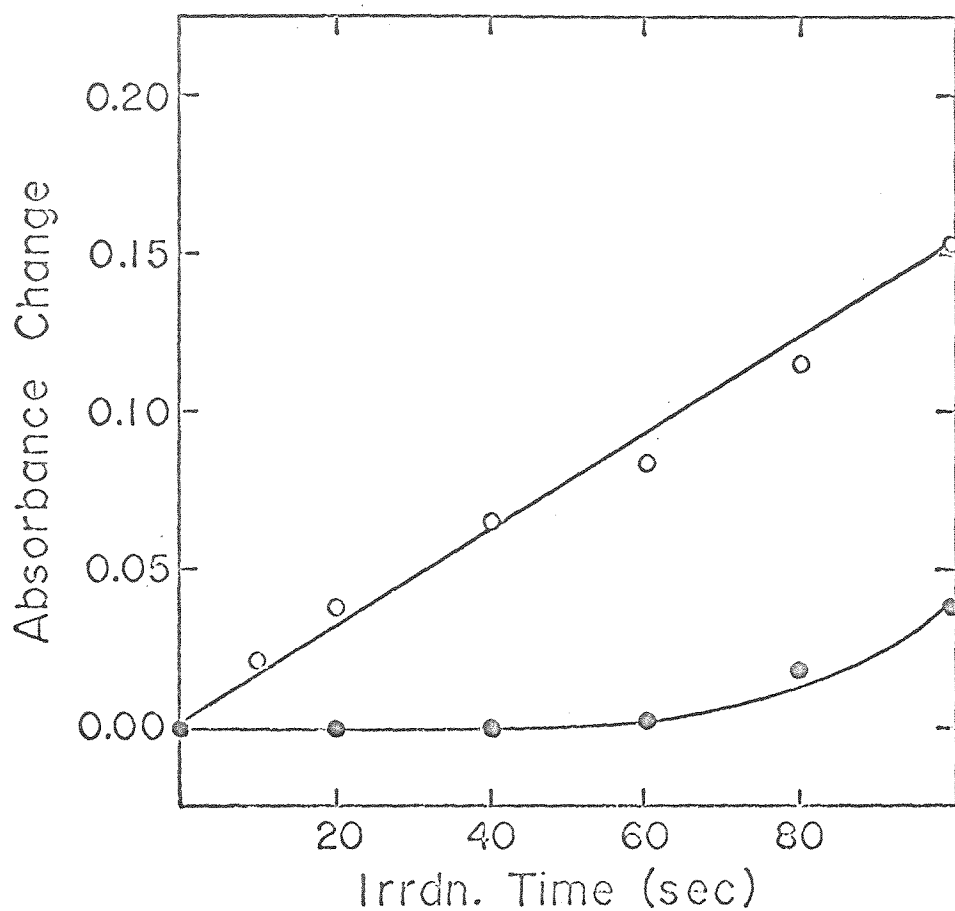
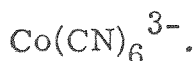
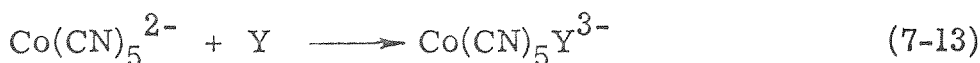
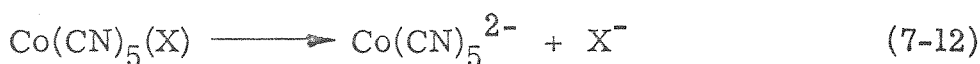
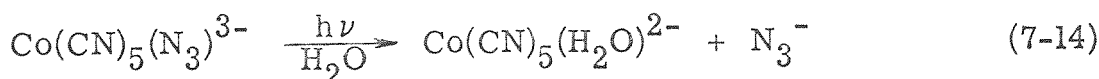


Figure VII-3. Comparison of change in absorbance at 330nm during irradiation of  $\text{Co}(\text{CN})_6^{3-}$  (●) and  $\text{Co}(\text{CN})_5(\text{H}_2\text{O})_2^{2-}$  (o) in the presence of 0.56 M  $\text{NaN}_3$  at 70°C.

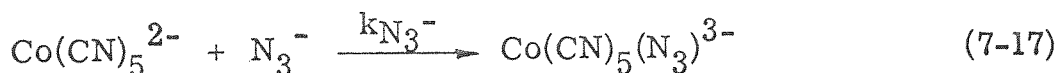
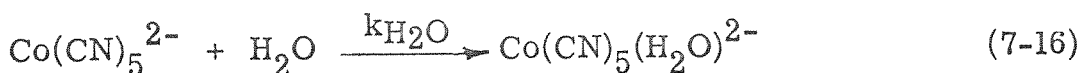
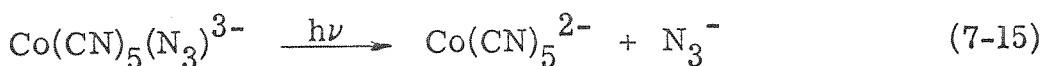


In contrast, that the photoaquation of  $\text{Co(CN)}_5(\text{X})^{3-}$  proceeds via a dissociative type mechanism seems to be conclusive.

First, the direct irradiation of  $\text{Co(CN)}_5(\text{H}_2\text{O})^{2-}$  results in  $\text{Co(CN)}_5(\text{X})^{3-}$  in the presence of X. Further, the reverse reaction  $\text{Co(CN)}_5(\text{X})^{3-} \longrightarrow \text{Co(CN)}_5(\text{H}_2\text{O})^{2-}$  can be quenched when X is added. One example has been investigated in detail, equation (7-14). The initial rate of the aquation as a function of



added  $\text{N}_3^-$  concentration is shown in Figure VII-4. The results are consistent with the dissociative mechanism outlined in (7-15) through (7-17), and we do predict the linear relationship



between the inverse of the aquation quantum yield and  $[\text{N}_3^-]$ , equation (7-18). From the slope to intercept ratio and assuming

$$(\text{Rate})^{-1} = \text{const.} \left[ 1 + \frac{k_{\text{N}_3^-} [\text{N}_3^-]}{k_{\text{H}_2\text{O}} [\text{H}_2\text{O}]} \right] \quad (7-18)$$



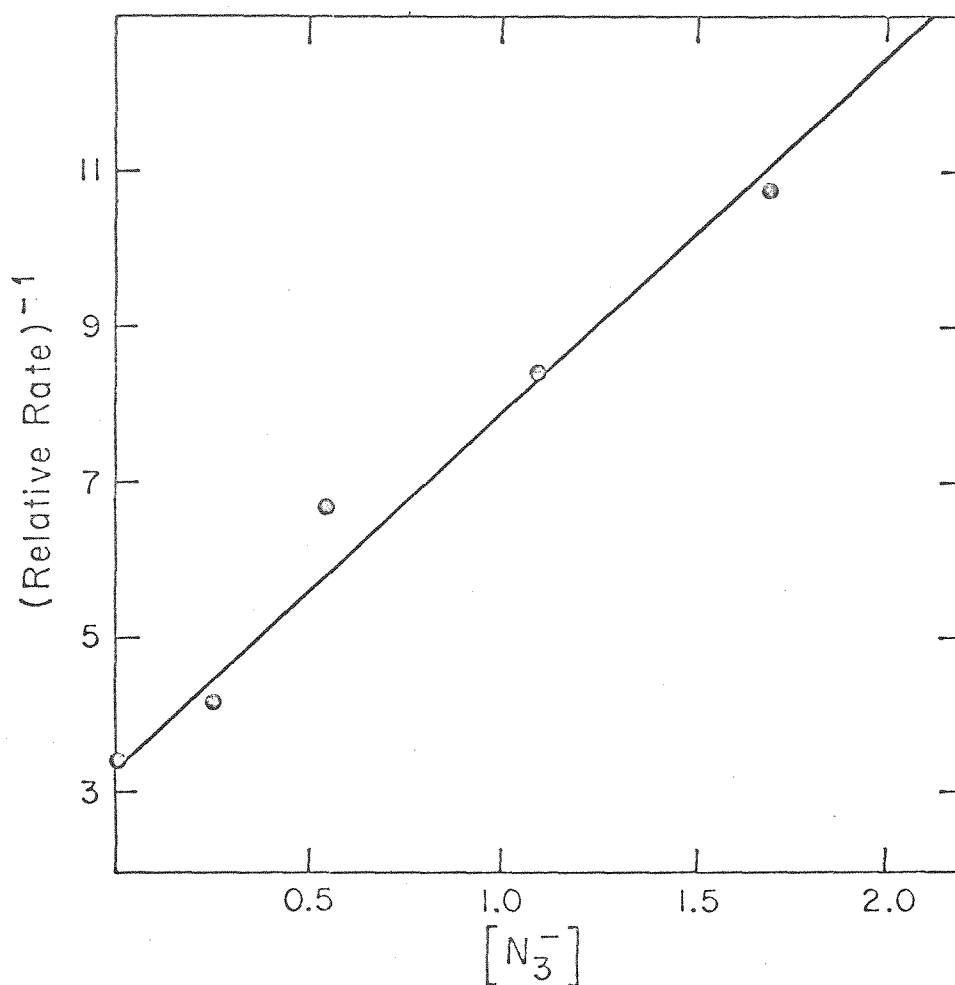
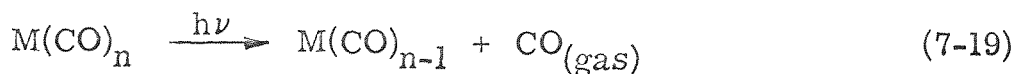


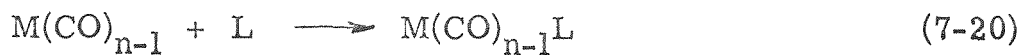
Figure VII-4. Suppression of the initial rate of photoaquation of  $\text{Co(CN)}_5(\text{N}_3)^{3-}$  by added  $\text{NaN}_3$  at  $40^\circ\text{C}$ . in aqueous solution.

$\text{H}_2\text{O} = 55 \text{ M}$ , we obtain here that  $\frac{k_{\text{N}_3^-}}{k_{\text{H}_2\text{O}}} = 76$  at  $40^\circ \text{ C}$ . In the thermal anation reaction one obtains a  $\frac{k_{\text{N}_3^-}}{k_{\text{H}_2\text{O}}} = 30$  at  $40^\circ \text{ C}$ .<sup>3</sup> This difference in attack ratio implicates a different intermediate in the two cases reflecting the different reactivities. While the details remain to be understood in this system we see that a photodissociation reaction is consistent with the  $\text{C}_{4v}$   $\text{Co}(\text{CN})_5(\text{X})^{3-}$  complexes while a different mechanism exists for the photosubstitution of the  $\text{O}_h$   $\text{Co}(\text{CN})_6^{3-}$ .

Some of the difficulties involved in determining whether a photosubstitution reaction is dissociative are relieved when the reaction can be performed in an inert solvent. There is universal agreement that the photosubstitution reactions of metal carbonyls involve dissociative loss of CO, equation (7-19).<sup>4</sup> The structure and reactivity of the coordinatively

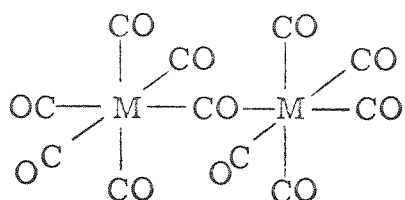


unsaturated metal carbonyl has been a topic of fundamental and synthetic interest for over ten years.<sup>5</sup> The question of whether or not a true dissociative mechanism obtains is seemingly answered by noting that the quantum yield for substitution is independent of the entering ligand, L, (7-20). However, very



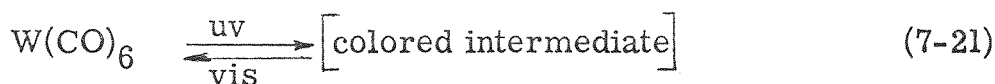
little attempt has been made to see if the  $\text{M}(\text{CO})_{n-1}$  is at all selective when different ligands are available.

The  $O_h$   $M(CO)_6$  ( $M = Cr, Mo, W$ ) complexes have received considerable attention and large numbers of  $M(CO)_5(L)$  complexes can be prepared photochemically. Upon irradiation of  $M(CO)_6$  in noncoordinating solvents an intermediate can be observed spectroscopically (uv-vis and ir) which is thought to be  $M(CO)_5$ .<sup>5</sup> However, this point is now controversial in that evidence for species like 7-I is now in the literature.<sup>6</sup> Further, it has been



7-I

observed that at 77° K. in glassy solvents the reaction (7-21) can



77° K.  
glassy solvent

proceed in the forward direction with high energy uv irradiation and reversed with visible 436 nm light. The most reasonable explanation here is that the colored intermediate is either 7-II or 7-III. Slow diffusion in glassy solvents at 77° K. can

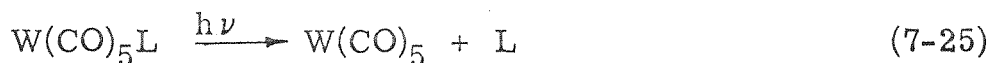
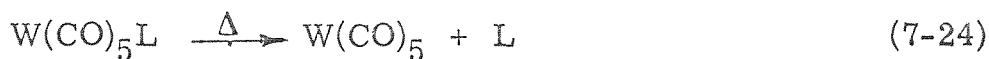


7-II

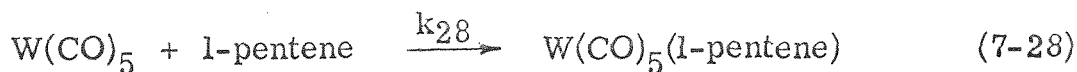
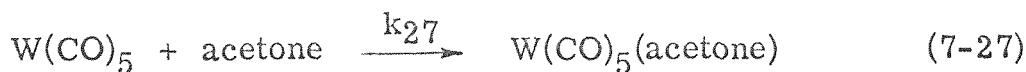
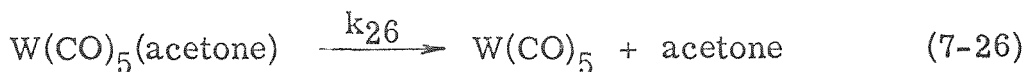
7-III

occur, so if  $M(CO)_5 + CO$  were formed with  $M(CO)_5$  being the

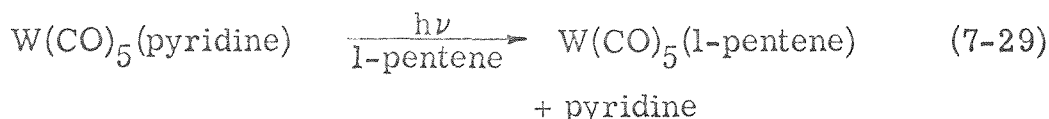
colored intermediate, the reverse photochemically induced reaction would be unlikely. We have found that  $W(CO)_5(X)$  ( $X = \pi$ -electron donor) compounds give release of  $X$  so the linkage isomerization of 7-II should occur upon excitation by 436 nm light, regenerating  $W(CO)_6$ . One important question regarding this system is whether the postulated intermediates for the thermal and photochemical cases are chemically distinguishable:



Unfortunately no systematic study is available to compare the reactivity of  $W(CO)_5$  in these examples. We have established that when  $L$  is weakly bound in  $W(CO)_5L$ , dissociation of  $L$  appears to be rate limiting in thermal substitution reactions.<sup>7</sup> Further, for the equations below, (7-26) through (7-28), we determined the



value  $\frac{k_{27}}{k_{28}}$  (attack ratio) to be of the same order as the attack ratio of acetone and 1-pentene for the photochemically generated  $W(CO)_5$  from  $W(CO)_6$ . The photoreaction (7-29) also appears



to involve the generation of a scavengeable  $W(CO)_5$ . In Figure VII-5 we show the effect of added pyridine on reaction (7-29). A quantitative evaluation of the reactivity of  $W(CO)_5$  in these systems merits investigation.

The only other six-coordinate systems of importance are the Cr(III) complexes. While a plethora of information is available<sup>8</sup> for these complexes there seems to have been only one experiment directed toward the question of whether an associative or dissociative type mechanism obtains.<sup>9</sup> In Table VII-1 results are presented which indicate that the  $O_h$   $Cr(NCS)_6^{3-}$  complex undergoes photoaquation with a quantum yield independent of the concentration of the added  $CH_3CN$ . On the other hand, the  $D_{4h}$  system trans- $Cr(NH_3)_2(NCS)_4^-$  has a photoaquation quantum yield which is dependent on the  $CH_3CN$  concentration. These results are reminiscent of the Co(III) cyanide complexes where the  $O_h$  and  $C_{4v}$  complexes react via different pathways. Further, like the Co(III) systems, the  $Cr(NCS)_6^{3-}$  exhibits differences in thermal and photochemical reactivity with the  $Cr(NCS)_6^{3-}$  being sensitive to  $CH_3CN$

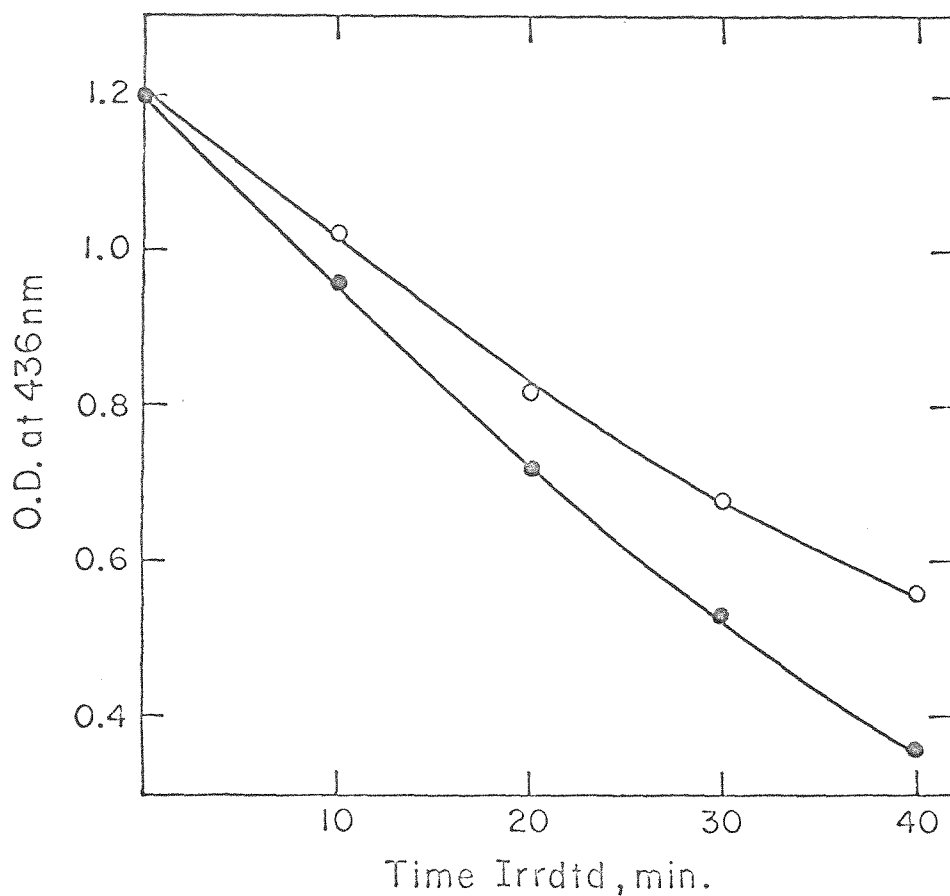


Figure VII-5. Disappearance of  $\text{W(CO)}_5(\text{pyridine})$  upon 436nm photolysis in the presence of 3.66M 1-pentene (•) and in the presence of 3.66M 1-pentene plus added 0.025M pyridine (o).

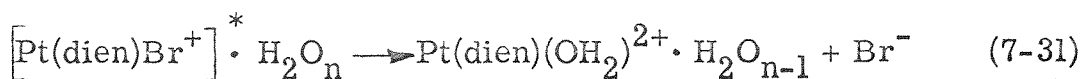
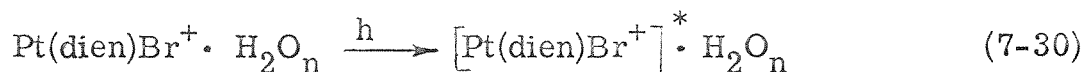
Table VII-1. Quantum Yields for Photoaquation of Thiocyanatochromium(III) Complexes<sup>a</sup>

Mole Fraction of CH <sub>3</sub> CN	$\text{t-Cr(NH}_3)_2\text{(NCS)}_4^-$ $\phi$ at 520 nm	$\text{Cr(NCS)}_3^-$ $\phi$ at 565 nm
0.00	0.286	0.332
0.04	0.267	—
0.10	0.234	—
0.20	0.218	0.366
0.30	0.192	—
0.50	0.178	0.356
0.80	0.182	0.338
1.00	0.164	0.370

<sup>a</sup>From reference 9.

concentration in the thermal aquation<sup>10</sup> but not in the photochemical aquation. These results, however, do not really distinguish between an associative or dissociative type mechanism since it has not been shown whether products other than  $\text{Cr}(\text{NCS})_5(\text{H}_2\text{O})^{2-}$  are formed as primary photoproducts.

The only four-coordinate system which has been investigated in detail is the Pt(II) system.<sup>11</sup> Thermal substitutions of Pt(II) are thought to proceed exclusively by associative type mechanisms.<sup>12</sup> The photosubstitution of  $\text{Br}^-$  in  $[\text{Pt}(\text{diethylenetriamine})\text{Br}]^+$  is best viewed as always resulting in formation of an aquo complex which undergoes rapid anation in the presence of a nucleophile X.<sup>13</sup> The photo-interchange mechanism for the Pt(II) system is shown in (7-30), (7-31).



Medium Effects on Photosubstitution Reactions. While no one has directed attention solely to medium effects, some information is available. Included here would be the effect of temperature, solvent, viscosity, ionic strength, and pH.

(a) Ionic Strength. In Table VII-2 we show the effect of added  $\text{NaClO}_4$  on the photoaquation of some cyanocobaltate(III)



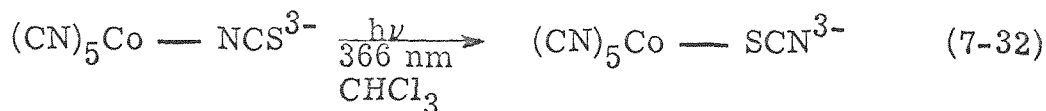
Table VII-2. Ionic Strength Effect on Photosubstitution of  
Cyanocobaltate(III) Complexes

Reactant	NaClO <sub>4</sub> , <u>M</u>	Rel. $\phi_{\text{aquation}}$
$\text{Co(CN)}_6^{3-}$ <sup>a</sup>	0.0	1.00
	1.0	0.95
	2.0	0.95
$\text{t-Co(CN)}_4(\text{SO}_3)_2^{5-}$	0.0	1.0
	1.4	1.0
$\text{Co(CN)}_5(\text{N}_3)^{3-}$	0.0	1.0
	1.1	1.0

<sup>a</sup>Reference 2.

complexes. We see that even at very high ionic strengths no effect on the quantum yield is seen. Whether this is a generality awaits experimentation with other systems.

(b) Solvent Effects. Insight into many photosubstitution reactions is complicated by the necessity of working in aqueous media which is typically a coordinating medium. It is possible to prepare inorganic complex anions as the salt of a large organic cation such as the tetrabutylammonium cation, TBA. The resulting complex may be soluble in polar or aromatic organic solvents which are noncoordinating media. The linkage photoisomerization of  $(\text{TBA})_3\text{Co}(\text{CN})_5(\text{NCS})$ , (7-32), occurs readily in  $\text{CHCl}_3$ . This

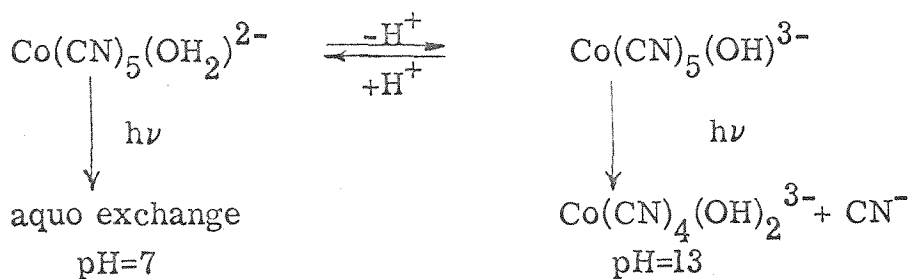


experiment rules out the necessity for the formation of an intermediate aquo complex for changes to occur in the coordination sphere. Direct substitution of  $\text{X}^-$  in  $\text{Co}(\text{CN})_5(\text{X})^{3-}$  can be studied in these noncoordinating media. Besides new mechanistic information derived from such studies, the discovery of new excited state chemistry is inevitable.

(c) Temperature and Viscosity Effects. The effects of viscosity and temperature have not been adequately explored, but few excited state reactions exhibit a strong temperature dependence.

In Table VII-3 we show relative photoaquation rates at several temperatures for  $\text{Co(CN)}_6^{3-}$  and in Table VII-4 relative rates are shown for solvents of different viscosity. The viscosity effect here is consistent with the photointerchange mechanism. The temperature effect probably merely reflects the viscosity changes of the water. Temperature effects may be important when two reactive excited states are possible. Such a case may be the temperature effects on substitution reactions of  $\text{Rh(NH}_3)_5(\text{X}^-)^{2+}$  where the relative yield of X and  $\text{NH}_3$  substitution is temperature dependent.<sup>14</sup>

(d) pH Effects. The effect of hydrogen ion concentration on photo-substitution seems to be prevalent when the ground state is susceptible to protonation. A good example of this type of pH effect is presented in the scheme below:



7-IV

While the hydroxy complex yields a ligand field absorption

Table VII-3. Temperature Effect on Photoaquation of  $\text{Co}(\text{CN})_6^{3-}$

Temperature, °C.	Rel. $\phi_{\text{aquation}}$
1.1	0.405
6.2	0.705
14.3	0.955
28.4	1.535
28.5	1.65
50.9	1.28
70.4	1.18
88.8	1.29

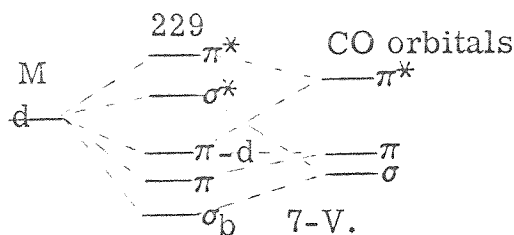
Table VII-4. Viscosity Effect on Photoaquation of  $\text{Co}(\text{CN})_6^{3-}$

Solvent	Rel. $\phi_{\text{aquation}}$
100% $\text{H}_2\text{O}$	1.00
20% MeOH	0.9 <sub>1</sub>
20% Glycerol	0.5 <sub>7</sub>

spectrum similar to the aquo complex, the reactions from these states are significantly different. This system is complicated further when it is noted that at pH = 2 the aquo complex does give significant amounts of a diaquo complex upon 254 nm photolysis. This implicates possible protonation of coordinated cyanides and merits further investigation.

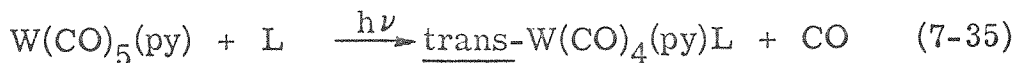
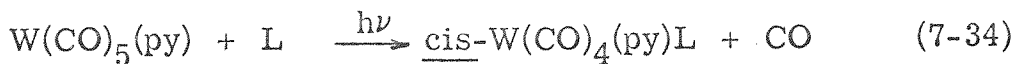
Excited State Reactivity. Of more interest to photochemists has been the attempt to predict the excited state reactivity by identifying the state from which reaction occurs. Here we will discuss a set of considerations (affectionately tabbed the Wrighton-Gray rules) which allow us to correlate structure and reactivity of ligand field excited states. We restrict ourselves to cases where the excited state chemistry is significantly different from the ground state reactions.

To illustrate the considerations involved we will consider several problems of interest. First, why are  $M(CO)_6$  ( $M = W, Mo, Cr$ ) so sensitive to irradiation in ligand field bands? Consider the binding interactions before and after excitation with light. We are dealing with an  $O_h$ ,  $d^6$  system, and the  $t_{2g}$  and  $e_g$  orbitals are split a significant amount by the strong field CO ligands. In fact, the  $t_{2g}$  orbitals interact strongly with the  $\pi^*$  orbitals of CO delocalizing electron density into them forming a  $\pi$ -back bond. The CO's also interact strongly as  $\sigma$ -donors, and the  $e_g$  orbitals are  $\sigma^*$  molecular orbitals as in 7-V. The ligand is then bound in two

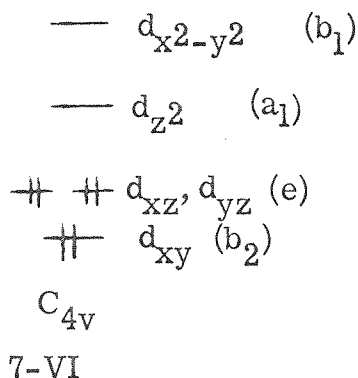


ways: (1)  $\sigma$ -bonded and (2)  $\pi$ -back bonded. The ligand field excited states have the configuration  $t_{2g}^5 e_g^1$ , ie., one electron is taken from a bonding orbital ( $\pi$ -d) and placed in an anti-bonding orbital ( $\sigma^*$ ). The loss in binding is enough to result in labilization of the CO ligands, and thus photosubstitution is facile. Note that we have not considered the multiplicity of the excited state but only the effect of depopulating a bonding orbital and populating an anti-bonding orbital. The point may be made that it is possible for the excited  $t_{2g}^5 e_g^1$  configuration to internally convert to the ground state  $t_{2g}^6$  configuration by population of high vibrational states from which loss of CO occurs. It is for this reason that we must direct our thoughts toward systems whose chemistry is different from the ground state. The  $M(CO)_6$  systems, however, are consistent with the Wrighton-Gray rules.

Now consider some cases where the excited state chemistry is markedly different from the ground state chemistry. Three possible reactions can occur in  $W(CO)_5(\text{pyridine})$ , equations (7-33) through (7-35). We investigated the photochemistry of



W(CO)<sub>5</sub>(pyridine) and found that (1) only reactions (7-33) and (7-34) occur, and (2) there is a wavelength effect on the quantum yields for (7-33) and (7-34) which implicates two reactive excited states. In Table VII-5 we summarize the wavelength effect: at low excitation energies only reaction (7-33) occurs, but as the energy is increased reaction (7-34) becomes important, apparently at the expense of reaction (7-33) whose quantum efficiency drops. In Figure VII-6 the isosbestic point in the ir spectrum during 436 nm irradiation insures a clean reaction. While the thermal exchange of pyridine can occur readily at elevated temperatures, CO exchange is much slower, and the lability of CO and pyridine in the ground state is vastly different. Now consider the organization of the d orbitals in C<sub>4v</sub> symmetry. The six d electrons occupy the lower three orbitals, 7-VI. We



have already associated the low energy excitation in this system with the  $b_2^2 e^4 \longrightarrow b_2^2 e^3 a_1^1$  transition. The effect on the binding is clear: we populate the sigma anti-bonding level which



Table VII-5. Wavelength Effect on  $W(CO)_5$ (pyridine)

Irrdn. Wavelength, nm	<u>Photochemistry</u>	
	$\phi_{(7-33)}^a$	$\phi_{(7-34)}^b$
436	0.63	0.00 <sub>2</sub>
366	0.50	0.01 <sub>3</sub>
313	0.38	0.03 <sub>9</sub>
254	0.34	0.04

<sup>a</sup>Formation yield of  $W(CO)_5$ (1-pentene) in 3.66 M 1-pentene, isooctane solvent at room temperature.

<sup>b</sup>Formation yield of cis- $W(CO)_4$ (py)<sub>2</sub> in 0.25 M pyridine, isooctane solvent at room temperature.

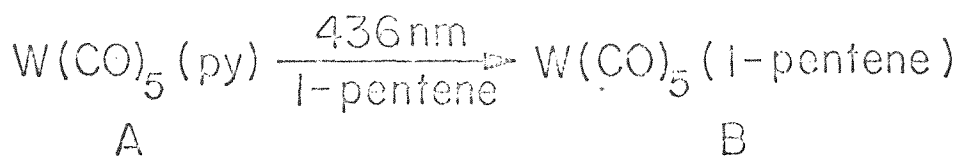
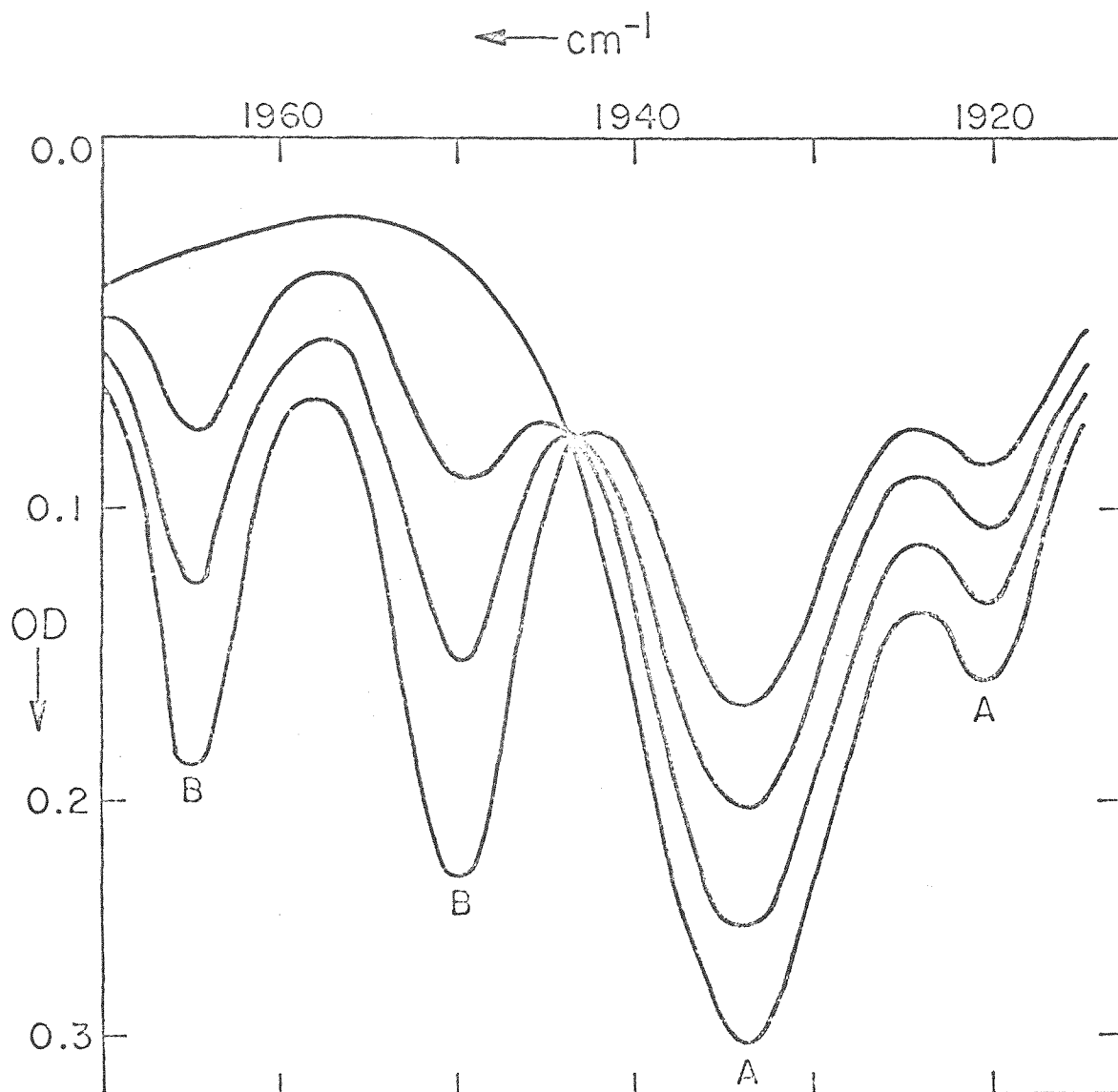
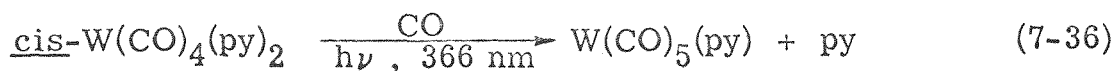


Figure VII-6. Infrared spectral changes in the conversion of A to B. Solvent is isooctane and reaction is carried out at room temperature with irradiation at 436nm.

mainly affects the ligands which are on the z-axis of the molecule. The doughnut-shaped cloud of electron density of  $d_{z^2}$  contributes to anti-bonding character for equatorial ligands, too, but to a lesser extent. The effect of depopulating  $d_{xz}$ ,  $d_{yz}$  is again to reduce  $\pi$ -back bonding for the CO ligands. The observed chemistry, only loss of pyridine, while not surprising, is not predictable. In any substitution reaction the most weakly bound ligands are lost; we can only predict which bonds will be weakened, but a quantitative measure is unavailable. We can only suggest that the z-axis is labilized, not which ligand is weakened the most. It is instructive to point out, though, that the CO's are still being held by  $\sim 5/6$  of the  $\pi$ -back bond. At higher energies of irradiation we observed loss of CO to give stereospecifically cis- $W(CO)_4(py)(L)$  while the quantum efficiency for loss of pyridine decreases. Higher energy transitions in  $W(CO)_5(py)$  are logically associated with the population of the  $d_{x^2-y^2} (\sigma^*)$  orbital. The sigma anti-bonding character of the  $b_2^1 e^4 b_1^1$  excited state is associated with the ligands in the xy plane; i.e., the four equatorial CO's. Loss of CO from the equatorial plane will give rise to the cis- $W(CO)_4(L)(py)$  products (assuming the intermediate five-coordinate complex to be rigid). Thus, with this qualitative understanding of bonding, electronic structure, and spectra, we have rationalized both the strong wavelength effect and the geometry of the product.

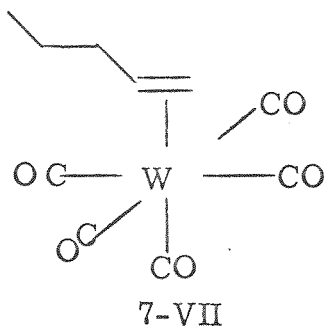
To test the possibility that the five-coordinate intermediate in the  $\text{W}(\text{CO})_5(\text{X})$  photolysis is nonrigid and only fortuitously gives all cis- $\text{W}(\text{CO})_4(\text{py})(\text{L})$ , consider the photosubstitution chemistry of  $\text{W}(\text{CO})_5(\text{PPh}_3)$ . The cis- $\text{W}(\text{CO})_4(\text{PPh}_3)_2$  and trans- $\text{W}(\text{CO})_4(\text{PPh}_3)_2$  compounds thermally interconvert and give a mixture containing cis and trans complexes.<sup>15</sup> This is taken as evidence that both isomers are possible products and they interconvert slowly enough to prove whether there is stereochemical significance to an all cis- $\text{W}(\text{CO})_4(\text{PPh}_3)_2$  photoproduct. The irradiation of  $\text{W}(\text{CO})_5(\text{PPh}_3)$  in the presence of  $\text{PPh}_3$  yields only the cis-disubstituted compound. The  $\text{W}(\text{CO})_5(\text{AsPh}_3)$  complex gives only the cis- $\text{W}(\text{CO})_4(\text{AsPh}_3)_2$ . Both Mo and Cr carbonyl complexes behave qualitatively in the same manner as the tungsten complexes. Thus, the qualitative predictive powers of the Wrighton-Gray rules is extensive in these systems.

We can also qualitatively rationalize the lack of further loss of CO when we have a cis- $\text{W}(\text{CO})_4(\text{L}_2)$  ( $\text{L} = \pi$ -electron donor). These complexes exhibit lowest ligand field transitions associated only with the  $\text{L} - \text{M} - \text{CO}$  axis which is analogous to the situation with z-axis labilization in  $\text{W}(\text{CO})_5(\text{pyridine})$ . In the cis- $\text{W}(\text{CO})_4(\text{L}_2)$  complexes we expect exchange of L before loss of CO as in  $\text{W}(\text{CO})_5(\text{X})$ . The prediction is borne out since reaction (7-36) occurs with good yield. A more quantitative

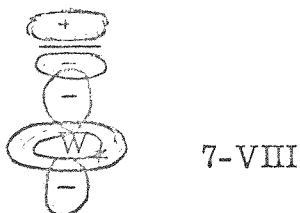


study is needed before further conclusions can be drawn here.

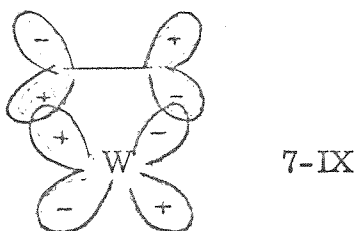
Finally in regard to the W, Mo, and Cr carbonyls, consider the substitution reactions of  $\text{W(CO)}_5(1\text{-pentene})$  (7-VII). The



alkene interacts with the metal orbitals in a fashion very similar to CO. First, the alkene interacts in a sigma fashion by overlapping the  $\pi$ -bonding orbital of the ligand with orbitals of sigma symmetry on the metal, 7-VIII. Secondly, like CO,

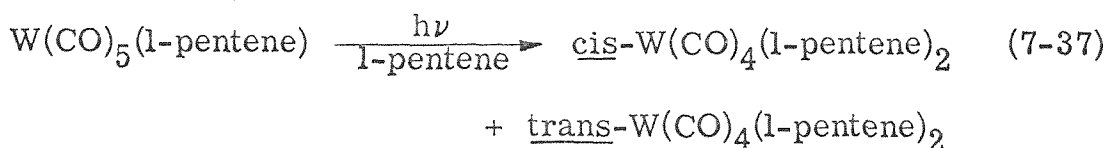


alkenes are good  $\pi$ -acceptor ligands delocalizing electrons from  $d_{xy}$ ,  $d_{xz}$ , or  $d_{yz}$  into the alkene  $\pi^*$  orbital giving the  $\pi$ -back bond, 7-IX. This mode of interacting ( $\sigma$ -donor,



$\pi$ -acceptor) is like CO, and alkenes are placed near CO in the

spectrochemical series. The uv spectrum of  $\text{W}(\text{CO})_5(\text{l-pentene})$  supports our predictions: it is very similar to  $\text{W}(\text{CO})_6$ ; spectral changes occurring in the conversion of  $\text{W}(\text{CO})_6$  to  $\text{W}(\text{CO})_5(\text{ethylene})$  are shown in Figure VII-7. While we have substituted one CO for L to give formally a  $\text{C}_{4v}$  structure the bonding of alkenes is so similar to CO that we are effectively dealing with an octahedral arrangement of six ligands. The splitting then of the d orbitals for the alkene complex is only slightly changed from  $\text{W}(\text{CO})_6$ , and with a similar electronic structure we predict similar excited state behavior. Indeed, this is what is found. Both CO and alkene can be substituted in  $\text{W}(\text{CO})_5(\text{alkene})$ , and there appears to be no strong isomeric specificity in the reaction, (7-37), with no strong wavelength



effects. In Figures VII-8 and VII-9 we show the disappearance of  $\text{W}(\text{CO})_5(\text{l-pentene})$  as a function of 313 nm and 366 nm irradiation.

The six-coordinate  $d^6$  system can be used to illustrate another important factor:  $\pi$ -donor ability. The  $\text{Co}(\text{CN})_5(\text{X})^{3-}$  ( $\text{X} = \text{SO}_3^{2-}$ ,  $\text{N}_3^-$ ,  $\text{NO}_2^-$ ,  $\text{NCS}^-$ ,  $\text{OH}_2$ ) complexes all undergo loss of X as their sole photosubstitution path. We have compared the photochemistry of  $\text{Co}(\text{CN})_5(\text{OH}_2)^{2-}$  and

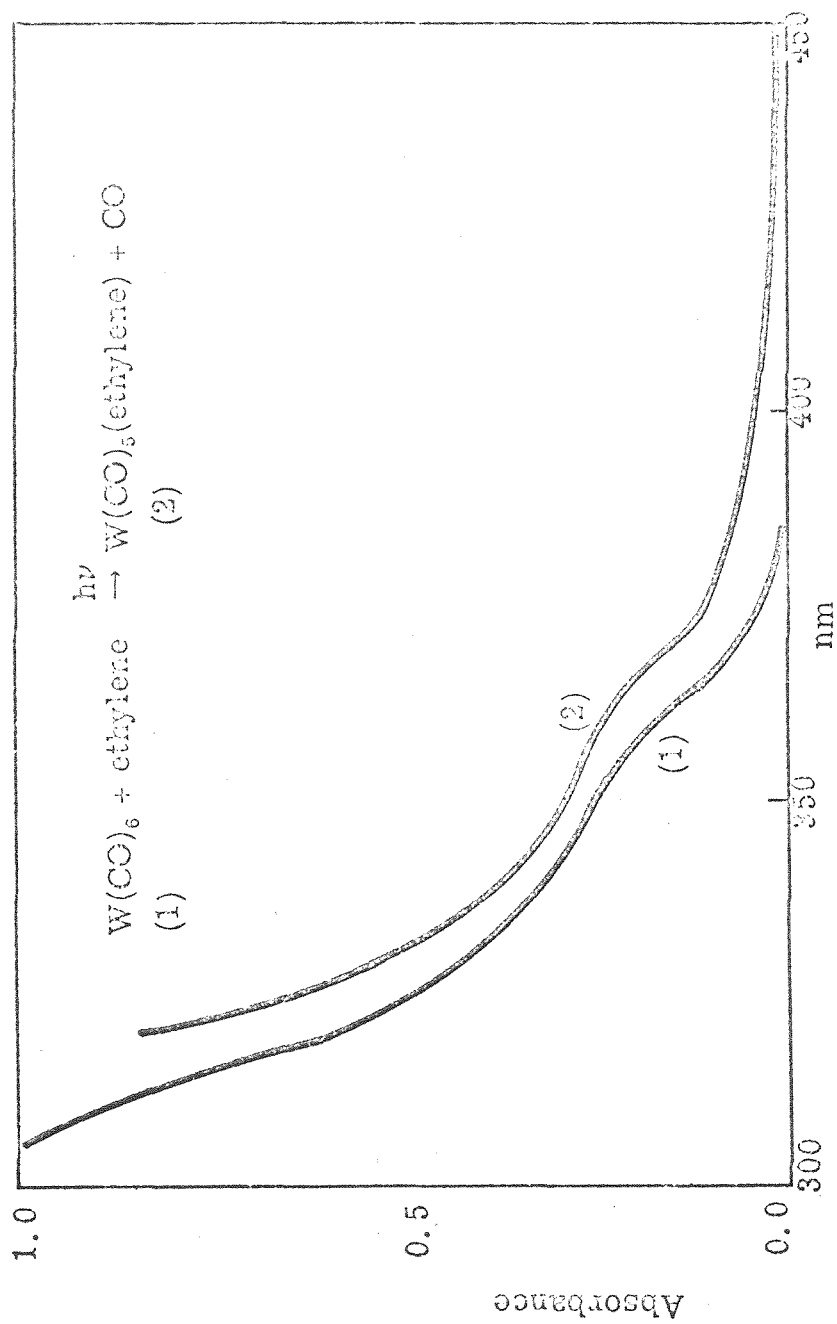


Figure VII-7. Spectral changes in the conversion of  $\text{W(CO)}_6$  to  $\text{W(CO)}_5(\text{ethylene})$ .

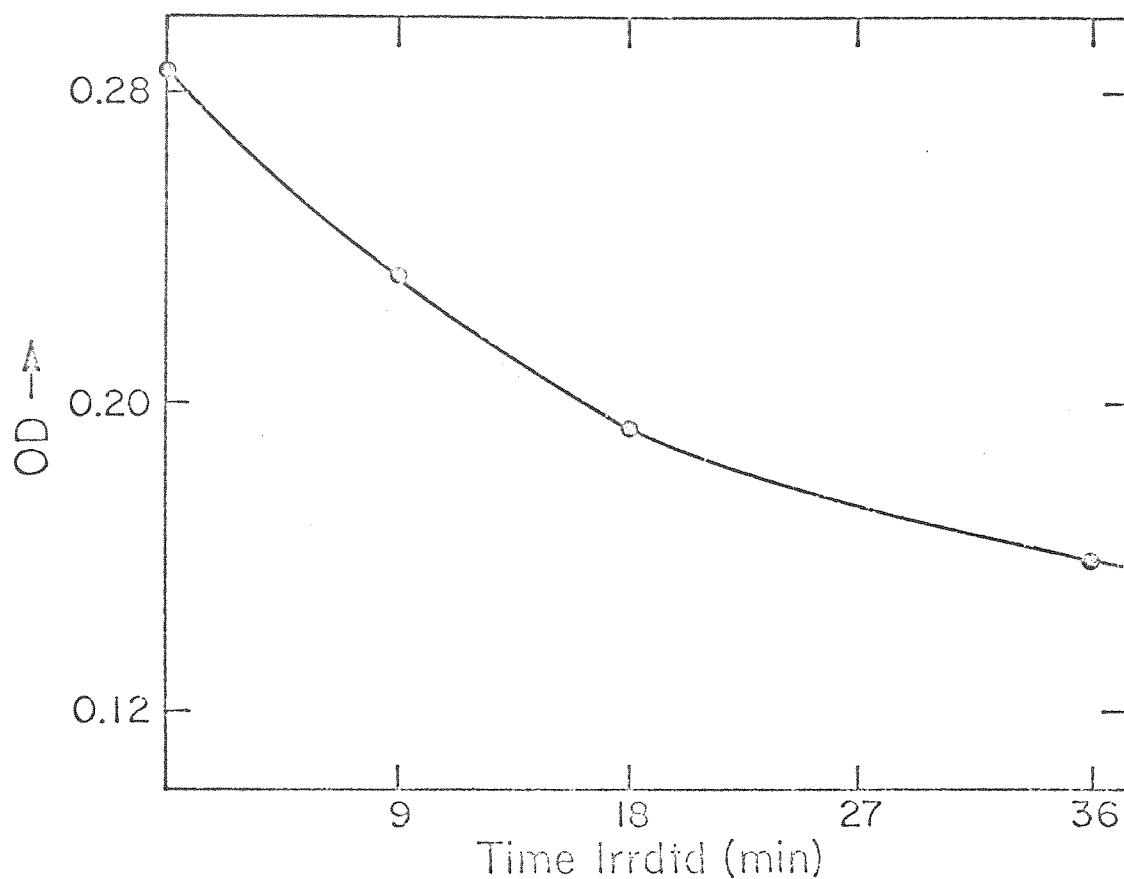


Figure VII-8. Disappearance of  $W(CO)_5(1\text{-pentene})$  upon photolysis at 313nm ( $2.40 \times 10^{-7}$  ein/min) in the presence of 3.66M 1-pentene. The initial quantum yield for disappearance is 0.44.



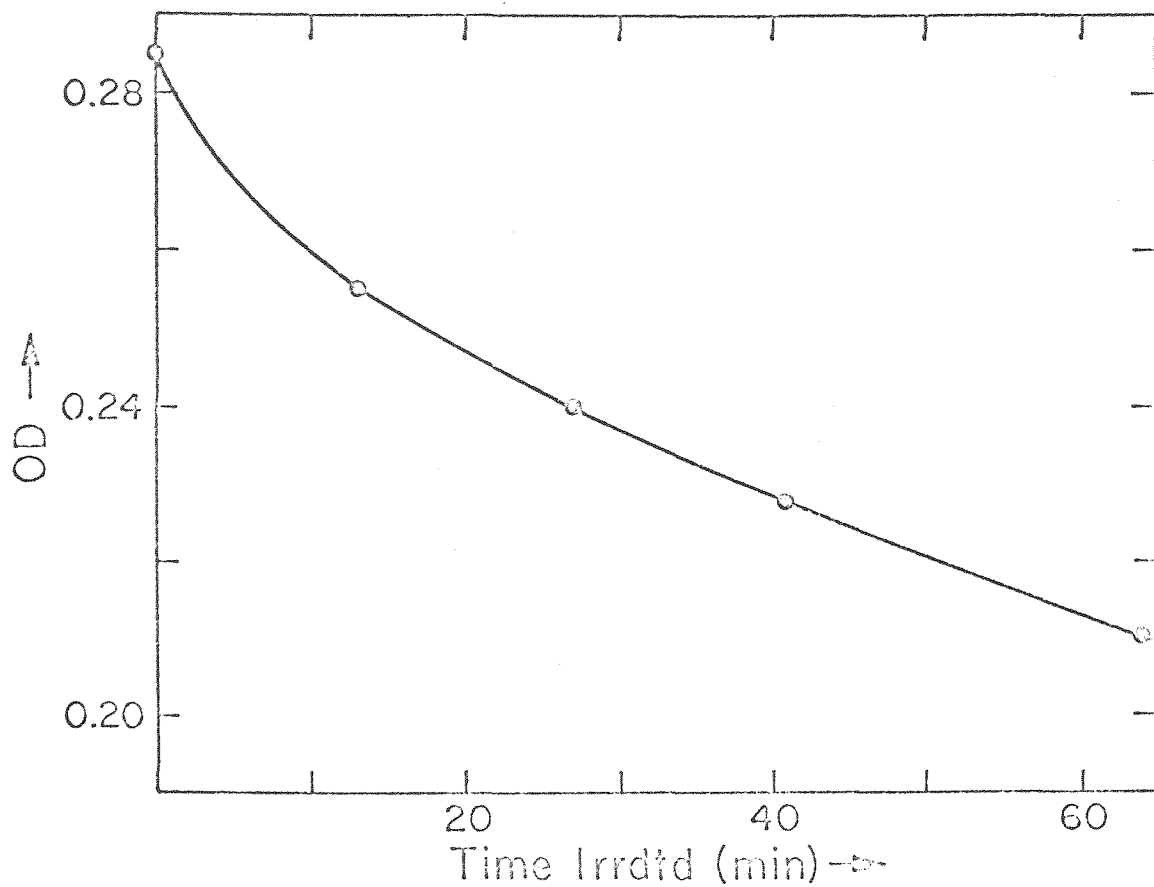


Figure VII-9. Disappearance of  $W(CO)_5(1\text{-pentene})$  upon photolysis at 366nm ( $1.38 \times 10^{-7} \text{ ein/min}$ ) in the presence of 3.66M 1-pentene. The initial quantum yield for disappearance is 0.30.

$\text{Co}(\text{CN})_5(\text{OH})^{3-}$  (cf. p225 ). These complexes have almost identical uv spectral characteristics for the first transition. The complexes are  $\text{C}_{4v}$  and exhibit a band associated with the population of the  $d_z^2$  orbital. With  $\text{Co}(\text{CN})_5(\text{OH}_2)^{2-}$  this  $b_2^2 e^4 \rightarrow b_2^2 e^3 a_1^1$  transition results in exchange of  $\text{H}_2\text{O}$ . No other photoproducts are observed. The  $\text{Co}(\text{CN})_5(\text{OH})^{3-}$ , however, behaves very differently. With excess  $\text{CN}^-$  present, formation of the  $\text{Co}(\text{CN})_6^{3-}$  does not occur, thus ruling out a facile dissociative process involving loss of  $\text{OH}^-$ . But  $\text{Co}(\text{CN})_5(\text{OH})^{3-}$  does react giving rise to  $\text{Co}(\text{CN})_4(\text{OH})_2^{3-}$  with a probable trans configuration. The quantum yield (0.05) and the product obtained are the same at either 313 nm or 366 nm irradiation, Figures VII-10 and VII-11. This reaction can be understood in the following way:  $\text{OH}^-$  unlike  $\text{H}_2\text{O}$  has the capability of being a  $\pi$ -donor. However, in the ground state the  $\pi$ -d orbitals are filled, and only in the excited state can  $\text{OH}^-$  realize its potential of being a  $\pi$ -donor since there is a "hole" in the  $\pi$ -d orbitals. The  $\sigma$ -anti-bonding effect in  $\text{Co}(\text{CN})_5(\text{OH})^{3-}$  affects  $\text{OH}^-$  less than  $\text{H}_2\text{O}$  since the  $\text{OH}^-$  can become a  $\pi$ -donor in the excited state. However, the trans  $\text{CN}^-$  is still labilized since some back bonding capability is removed in the excited state and  $\sigma$ -anti-bonding character is strong along the z-axis. We correlate the large change in

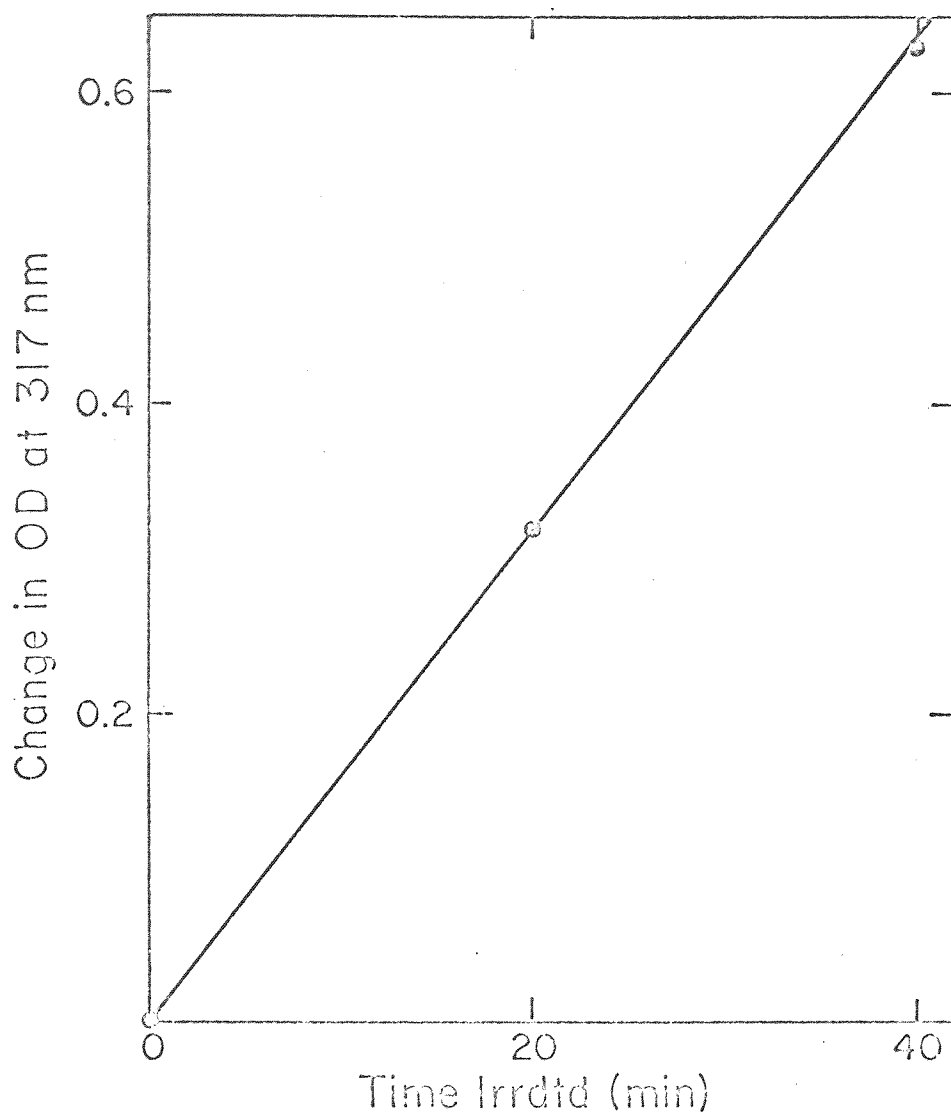


Figure VII-10. Production of  $\text{Co}(\text{CN})_4(\text{OH})_2^{3-}$  from the 313nm photolysis ( $2.40 \times 10^{-7}$  ein/min) of  $\text{Co}(\text{CN})_5(\text{OH})^{3-}$  in 0.1M NaOH. Analysis is by measuring the optical density at 317nm of irradiated solutions after adding excess  $\text{Na}_2\text{SO}_3$  to form the  $\text{trans-Co}(\text{CN})_4(\text{SO}_3)_2^{5-2}$ . The quantum yield for the reaction is ~0.05.

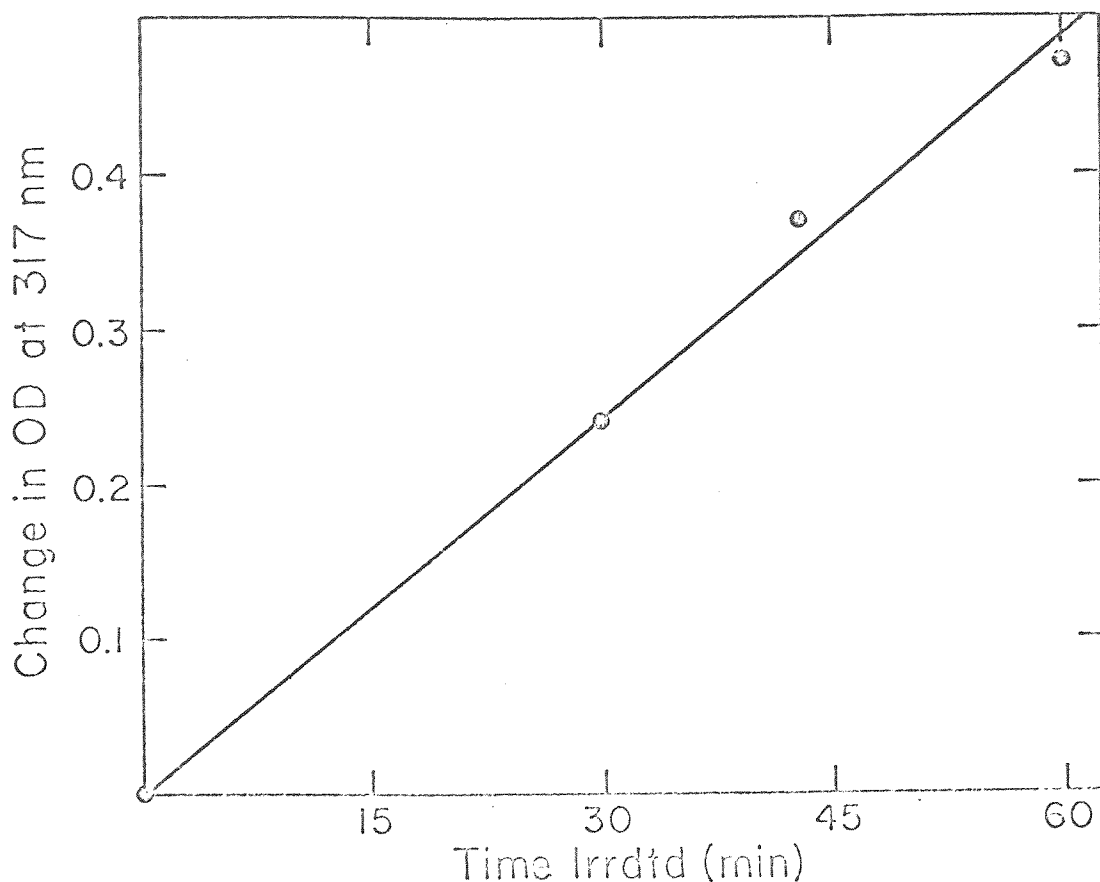
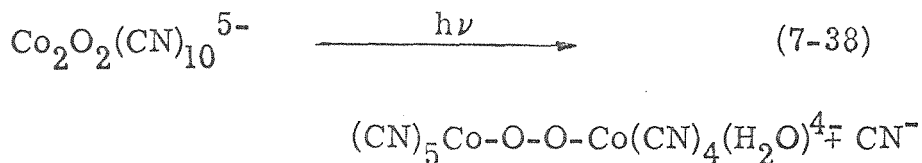


Figure VII-11. Production of  $\text{Co(CN)}_4(\text{OH})_2^{3-}$  from the 366nm photolysis ( $1.38 \times 10^{-7} \text{ ein/min}$ ) of  $\text{Co(CN)}_5(\text{OH})^{3-}$  in 0.1M NaOH. Analysis is by measuring the optical density at 317nm of irradiated solutions after adding excess  $\text{Na}_2\text{SO}_3$  to form the  $\text{trans-Co(CN)}_4(\text{SO}_3)_2^{5-}$ . The quantum yield for the reaction is  $\sim 0.05$ .

photochemical reactivity of the  $\text{Co}(\text{CN})_5(\text{OH}_2)^{2-}$  and the  $\text{Co}(\text{CN})_5(\text{OH})^{3-}$  with the change in bonding characteristics of the  $\text{OH}^-$  and  $\text{H}_2\text{O}$ .

In this regard it is interesting to note that  $(\text{CN})_5\text{Co} - \text{O} - \text{O} - \text{Co}(\text{CN})_5^{5-}$  gives upon irradiation a significant amount of trans- $\text{Co}(\text{CN})_4(\text{OH}_2)_2^-$  as a final product. This implicates reaction (7-38) as a primary photoprocess which



is then followed by thermal or photochemical degradation. The notion here is that the  $\mu$ -superoxide linkage can serve as a reasonable  $\pi$ -donor ligand in the excited state.

Another interesting Co(III) system is trans- $\text{Co}(\text{CN})_4(\text{SO}_3)(\text{H}_2\text{O})^{3-}$ . Thermally, the sulfito group exerts a large trans effect causing rapid exchange of the  $\text{H}_2\text{O}$  molecule.<sup>16</sup> Photochemically, however, loss of  $\text{SO}_3^{2-}$  occurs with a substantial quantum yield. In Table VII-6 we summarize photosubstitution quantum yields for the trans- $\text{Co}(\text{CN})_4(\text{SO}_3)(\text{X})^{n-}$  complexes. The  $\text{D}_{4h}$  symmetry of these complexes gives a d orbital splitting similar to the  $\text{C}_{4v}$  complexes, but generally it

Table VII-6. Disappearance Quantum Yields<sup>a</sup> for  $K_nCo(CN)_4(SO_3)(X)$  Complexes

Compound	pH	$\phi_{254 \text{ nm}}$	$\phi_{313 \text{ nm}}$	$\phi_{366 \text{ nm}}$	$\phi_{436 \text{ nm}}$
$K_4Co(CN)_5(SO_3)$	7	0.25	b	--	--
$K_5Co(CN)_4(SO_3)_2^c$	13	b	0.36	0.57	0.57
$K_3Co(CN)_4(SO_3)(OH)_2^d$	2	0.15	0.11	0.14	b
$K_4Co(CN)_4(SO_3)(OH)^d$	13	0.13	0.09	0.19	b

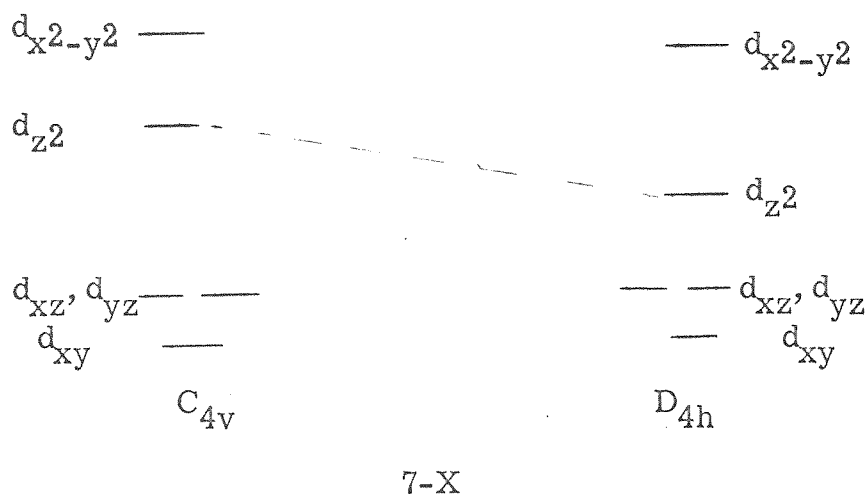
<sup>a</sup>Quantum yields are  $\pm 10\%$ .

<sup>b</sup>Not determined.

<sup>c</sup>Major product is trans- $Co(CN)_4(SO_3)(OH)^{4-}$ .

<sup>d</sup>Major product is  $Co(CN)_4(OH_2)^-$ , pH = 2 or  $Co(CN)_4(OH)_2^{3-}$ , pH = 13.

is found that trans-ML<sub>4</sub>X<sub>2</sub> has a lower energy first transition than ML<sub>5</sub>X. This is shown schematically in 7-X. The electronic



spectra of the sulfito complexes are dominated by an intense charge-transfer transition, Figures VII-12 and VII-13.

The CT band is associated with a sulfito  $\rightarrow$  Co electron transfer consistent with the direct formation of Co(II) upon 254 nm photolysis (pp.196-9). The low energy ligand field band,  $d_{xz}, d_{yz} \rightarrow d_z^2$ , is observable in each case, but higher energy d-d transitions are obscured by the CT transition.

The photochemistry for all of the complexes is similar: ligands on the z-axis are labilized. The dominant photoreactions

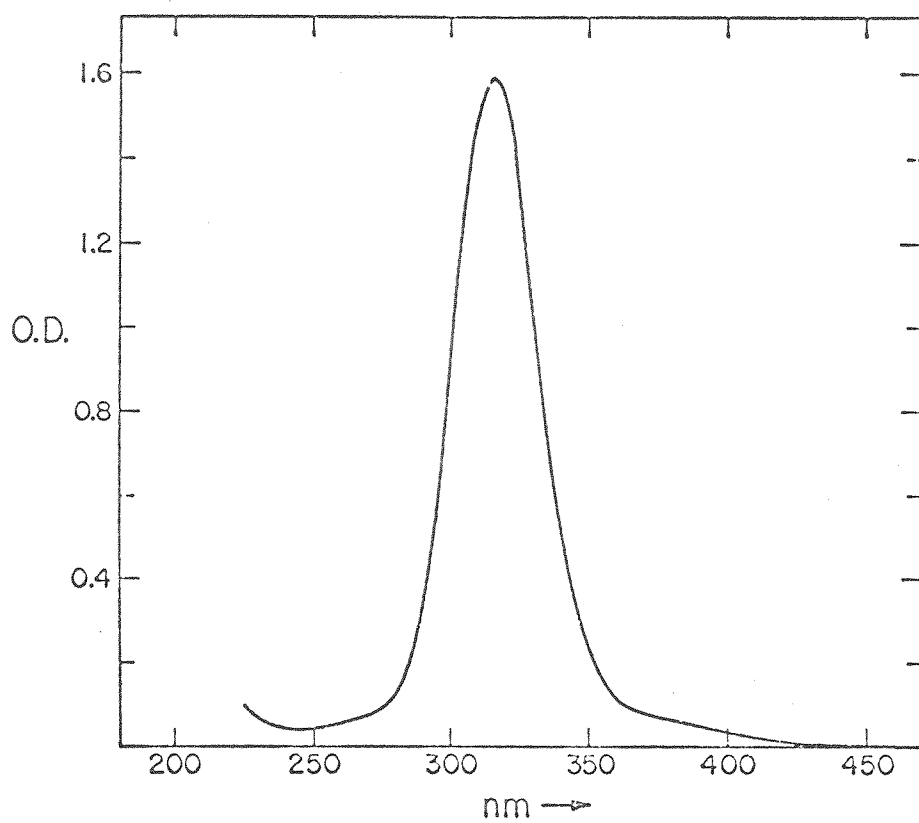


Figure VII-12. Absorption spectrum of  $\text{trans-Co(CN)}_4(\text{SO}_3)_2^{5-}$  in 0.1 M NaOH aqueous solution. Bands are at 317nm ( $\epsilon = 31,900$ ) and 380nm ( $\epsilon = 1350$ ).



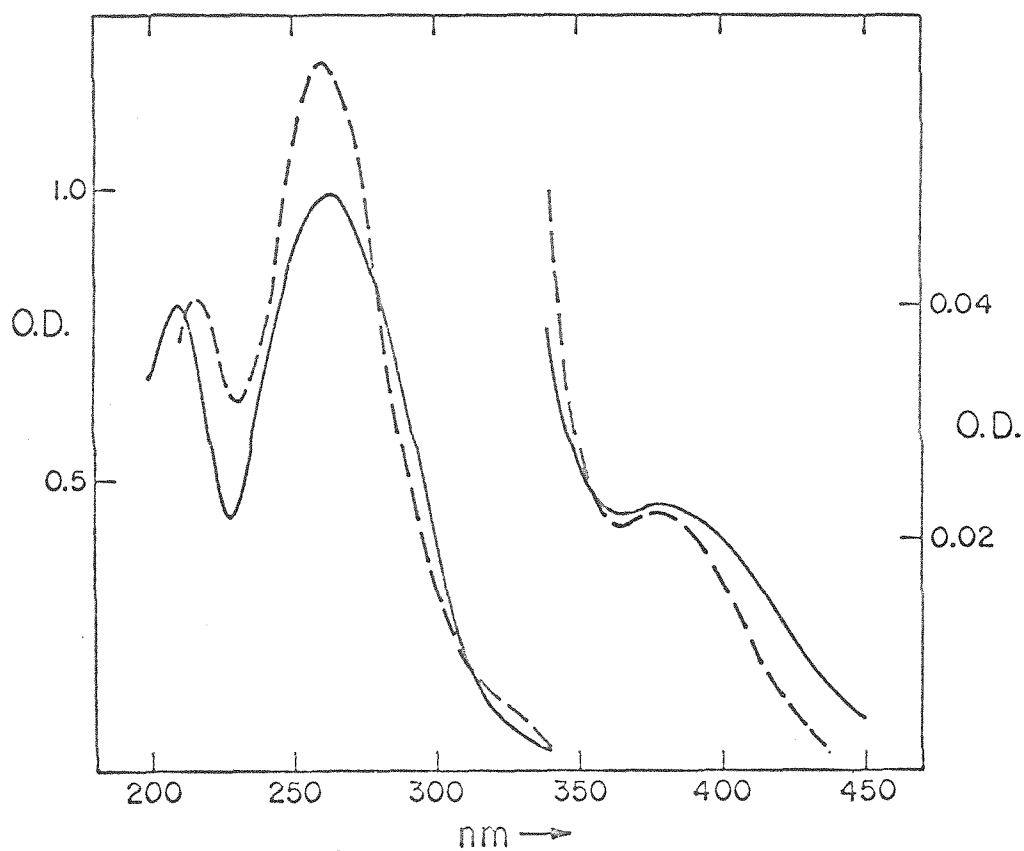
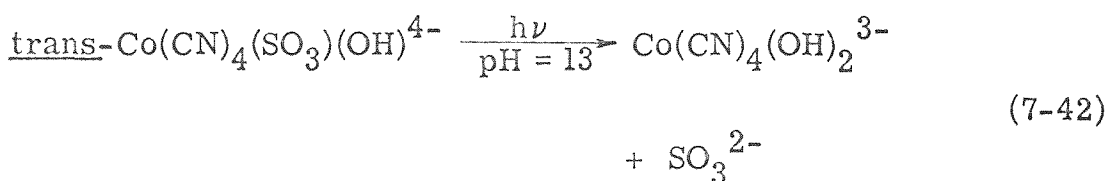
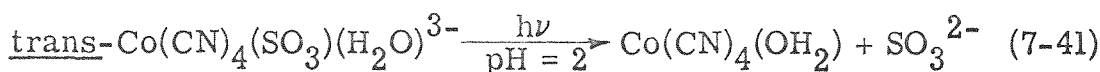
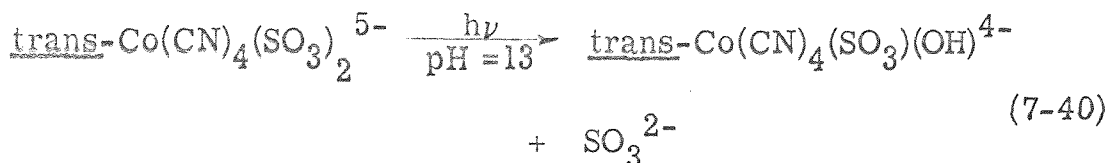
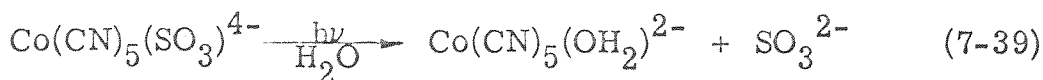


Figure VII-13. Absorption spectra of trans -  $\text{Co}(\text{CN})_4(\text{SO}_3)(\text{OH}_2)_3^-$  (—) and trans -  $\text{Co}(\text{CN})_4(\text{SO}_3)(\text{OH})_4^{4-}$  (---). For the aquo complex the bands are at 263nm ( $\epsilon = 10,300$ ) and 380nm ( $\epsilon = 240$ ), and for the hydroxy the bands are at 260nm ( $\epsilon = 12,500$ ) and 374nm ( $\epsilon = 240$ ).

are (7-39) through (7-42). The spectrum of the  $\text{Co(CN)}_4(\text{OH})_2^{3-}$



is shown in Figure VII-14. The first ligand field band is at  $\sim 380$  nm which is very close to the  ${}^1\text{A}_1 \longrightarrow {}^1\text{E}$  of  $\text{Co(CN)}_5(\text{OH})^{3-}$ .

A trans dihydroxy complex should give a lower energy band,

7-X ; on the other hand trans- $\text{Co(CN)}_4(\text{SO}_3)_2^{5-}$  can be completely regenerated upon addition of  $\text{SO}_3^{2-}$  to solutions of the diaquo or neutralized dihydroxy complex. The geometry is probably trans, but further spectral data are necessary (ir and Raman). The reactions (7-39) through (7-42) are probably dissociative since substitution can be quenched by added  $\text{SO}_3^{2-}$ , Table VII-7. Besides the fact that the diaquo complexes are readily formed photochemically and not thermally, the disulfito complex undergoes facile photosubstitution at  $\text{pH} = 13$  while the thermal rate is extremely slow at  $\text{pH} = 13$  compared to acidic media.<sup>16</sup>

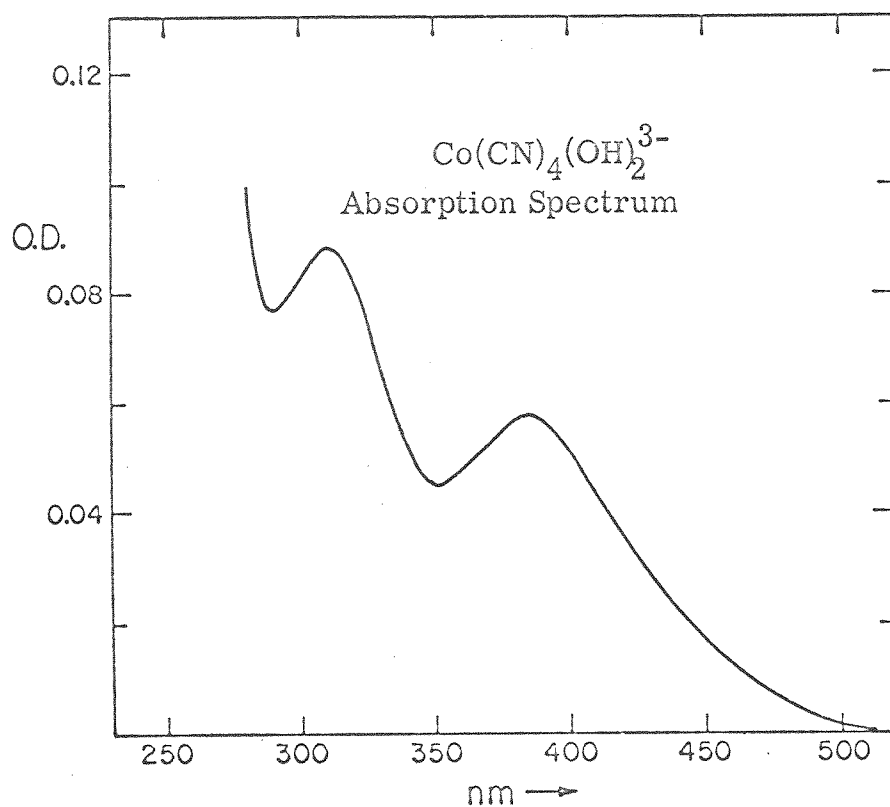
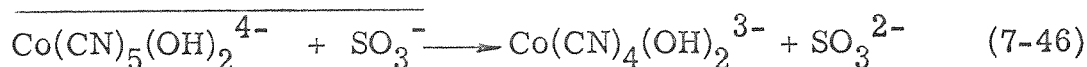
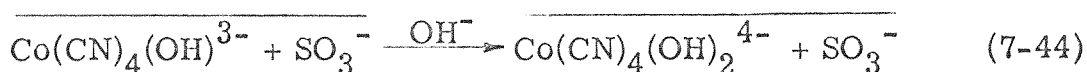
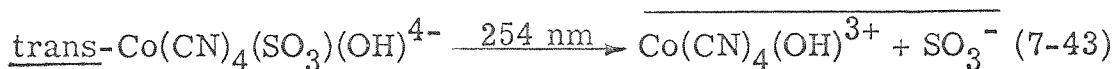


Figure VII-14. Spectrum of photolysis product of trans- $\text{Co(CN)}_4(\text{SO}_3)(\text{OH})^{4-}$  in 0.1M NaOH. Bands are at 308nm ( $\epsilon=403$ ) and 380nm ( $\epsilon=262$ ).

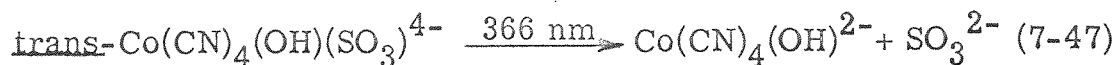
Table VII-7. Quenching of Photosubstitution of  
trans-Co(CN)<sub>4</sub>(SO<sub>3</sub>)<sub>2</sub><sup>5-</sup> with SO<sub>3</sub><sup>2-</sup>

Additive	Concentration, <u>M</u>	Rel. $\phi_{\text{aquation}}$
None	—	1.00
SO <sub>3</sub> <sup>2-</sup>	0.2	0.61
SO <sub>3</sub> <sup>2-</sup>	0.4	0.36
SO <sub>3</sub> <sup>2-</sup>	1.0	0.25
NaClO <sub>4</sub>	1.4	1.0

The lack of a large wavelength effect on the photoreactions suggests that most excited states decay to the lowest excited state from which reaction occurs. However, it is interesting to speculate on the origin of the effects that are seen: relatively high yields at longer wavelengths, dipping at 313 nm, and increasing again at 254 nm. A reasonable explanation is that two excited states are reactive and a third state, populated by 313 nm irradiation, is unreactive. The high energy state populated at 254 nm is the charge-transfer state and could lead to both substitution and production of Co(II) by a mechanism similar to that for  $\text{Co}(\text{NH}_3)_5(\text{X})^{2+}$  (p.195 ), (7-43) through (7-46). Ligand



field excitation at low energies, 366 nm and 436 nm, yields simple dissociation of the  $\text{SO}_3^{2-}$  forming a five-coordinate intermediate, (7-47) and (7-48). Apparently higher lying ligand field states



can decay directly to the ground state before undergoing reaction or decaying to a reactive state. The Wrighton-Gray rules applied to the ligand field reaction again rationalize the results. The z-axis is labilized by population of the  $d_{z^2}$  orbital. The sulfite is labilized significantly because some  $\pi$ -back bonding is lost and a  $\sigma^*$  orbital is populated. The exchange rate of the  $H_2O$  was not measured but would be of interest. Here the Wrighton-Gray rules predict that trans- $Co(CN)_4(SO_3)(OH)^{4-}$  will give only loss of sulfite with no exchange of  $OH^-$  because the  $OH^-$  again can be a  $\pi$ -donor in the excited state.

It is difficult to rationalize the lack of photosubstitution chemistry in the ammine complexes of  $Co(III)$ . Since ligand field excitation does not result in substitution in these complexes, the Wrighton-Gray rules do not apply. Since N — H vibrational modes are known (p. 153 ) to play a key role in the deactivation of ligand field excited states of  $Cr(III)$  complexes, it is reasonable that nonradiative decay could occur faster than substitution in  $Co(NH_3)_n(X)_{6-n}$ . To test this hypothesis one could look at substitution yields of the  $Co(ND_3)_n(X)_{6-n}$  and the  $Co(NR_3)_n(X)_{6-n}$  derivatives as well as the  $Co(NH_3)_6$ ,  $Co(NH_3)_5(X)$ , . . . .  $Co(NH_3)_n(X)_{6-n}$  series to study the effect of systematic changes in the number of N — H vibrational modes.

In contrast to the Co(III) ammine complexes, though, the  $\text{Rh}(\text{NH}_3)_5(\text{X})^{2+}$  ( $\text{X} = \text{Cl}^-$ ,  $\text{Br}^-$ ,  $\text{I}^-$ ) complexes are sensitive to ligand field excitation.<sup>17</sup> Again only ligands on the z-axis are labilized consistent with a lowest excited state being population of the  $d_{z^2}$  orbital. However, the three complexes have different relative yields of X versus trans  $\text{NH}_3$  aquation, Table VII-8. Further, the overall quantum yield is larger as the halide is changed from  $\text{Cl}^-$  to  $\text{Br}^-$  to  $\text{I}^-$ . The latter effect can be due to the fact that the  $d_{z^2}$  orbital is a more "pure state" with the weaker field halides since the splitting of the lowest T state of  $\text{O}_h$  symmetry is largest. This prevents mixing of  $d_{x^2-y^2}$  and  $d_{z^2}$  excitation and reduces significantly vibrational decay via N — H stretching modes of the four equatorial  $\text{NH}_3$  groups. The second effect of different ratios of  $\text{NH}_3$  to X release may be related to the fact that  $\text{I}^-$  is a significantly better  $\pi$ -donor than  $\text{Cl}^-$  and is thus bound relatively firmly in the excited state compared to the trans  $\text{NH}_3$ , while with the chloro complex the  $\text{NH}_3$  is more firmly bound than the halide.

The trans- $\text{M}(\text{en})_2(\text{X}_2)^+$  ( $\text{M} = \text{Ir(III)}, \text{Rh(III)}$ ), ( $\text{X} = \text{Cl}^-$ ,  $\text{Br}^-$ ,  $\text{I}^-$ ) complexes illustrate the importance of knowing whether significant  $d_{z^2}$ - $d_{x^2-y^2}$  mixing occurs in the excited state. All of these complexes give as their only product trans- $\text{M}(\text{en})_2(\text{X})(\text{OH}_2)^{2+}$ .<sup>18</sup> That the lowest lying state labilizes the z-axis only is consistent with the Wrighton-Gray rules. However,

Table VII-8. Quantum Yields for  $\text{Rh}(\text{NH}_3)_5(\text{X})^{2+}$  Complexes<sup>a</sup>

Complex	irradtd.	$\phi_{\text{aquation}}$	$\phi_{\text{trans NH}_3 \text{ aquation}}$
$\text{Rh}(\text{NH}_3)_5(\text{Cl})^{2+}$	350	0.16	$10^{-3}$
$\text{Rh}(\text{NH}_3)_5(\text{Br})^{2+}$	360	0.019	0.18
$\text{Rh}(\text{NH}_3)_5(\text{I})^{2+}$	385	0.01	0.82

<sup>a</sup>Reference 17, aqueous media 25° C.

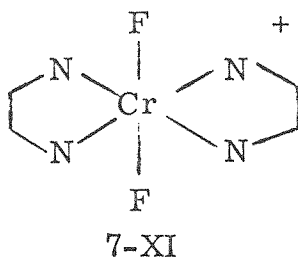


the halide that is lost is a  $\pi$ -donor in the excited state while the amines are only  $\sigma$ -donors and could be labilized upon equatorial excitation. Apparently  $d_{z^2}$  is always achieved and is very axially directed with the equatorial ring of electron density having a relatively small effect. Finally, that the monoaquo complex apparently only gives aquo photoexchange is predicted since the halides can be  $\pi$ -donors in the excited state. This may mean that  $\text{NH}_3$  is more firmly bound in the excited state than is the  $\text{H}_2\text{O}$  since  $\text{Cl}^-$  is not lost readily from trans- $\text{M(en)}_2(\text{Cl})(\text{OH}_2)^{2+}$  while it is lost exclusively from  $\text{Rh}(\text{NH}_3)_5(\text{Cl})^{2+}$ .

The Cr(III) complexes represent a major class of compounds whose photosubstitution chemistry has been investigated.<sup>19</sup> There has been some controversy concerning the states responsible for substitution chemistry. The lowest excited states for the strong field cases are the  $^2\text{E}$  and  $^2\text{T}$  arising from the pairing of electrons of the  $t_{2g}^3$  configuration. With the arguments developed above it seems unlikely that these states could be important in Cr(III) photochemistry because the transition apparently does not involve large changes in bonding. We can qualitatively gain this information by noting that the  $^2\text{E}$ ,  $^2\text{T}$  states are insensitive to ligand field (types of bonding) in the Cr(III) complexes. However, there is the possibility that the  $^2\text{E}$ ,  $^2\text{T}$  states give rise to the "hot ground state" from

which chemistry occurs. The  ${}^4T_2$  state is very sensitive to the binding, and the configuration of  $t_{2g}^2 e_g^1$  jolts the ground state binding interactions significantly. It has been shown by energy transfer experiments that the  ${}^4T_2$  is the most likely reactive state.<sup>20</sup>

Applying the Wrighton-Gray rules to the Cr(III) complexes we again find a satisfying rationalization of the chemistry observed. Consider trans-Cr(en) $_2$ F $_2^+$ , 7-XI. The ligand

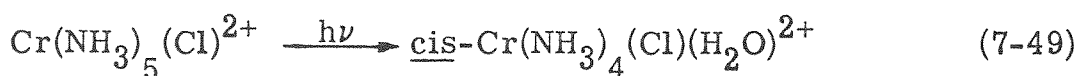


field spectrum reveals that the  $d_{x^2-y^2}$  and  $d_{z^2}$  orbitals are not split significantly,<sup>21</sup> so localized excitation cannot obtain.

Excitation results in  $\sigma$ -anti-bonding characters for all of the ligands. None of the ligands here are  $\pi$ -acceptor ligands so none lose binding by depopulation of the  $\pi$ -d orbitals. However, the  $F^-$  ligands are weak  $\pi$ -donors, and this is an important factor here because the  $\pi$ -d orbitals are only partially filled, and in the excited configuration  $t_{2g}^2 e_g^1$  the situation is even more favorable for  $\pi$ -donor interaction. The observation that the photosubstitution of

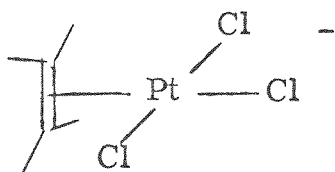
one end of ethylenediamine occurs<sup>22</sup> is not surprising. The  $\sigma^*$  character affects the  $\sigma$ -donor ligands of N but not the  $F^-$  ligands because these are held on by the  $\pi$ -donor binding interaction.

The photosubstitution of  $Cr(NH_3)_5Cl^{2+}$  is known to proceed as in equation (7-49).<sup>23</sup> The release of  $NH_3$  is predictable in



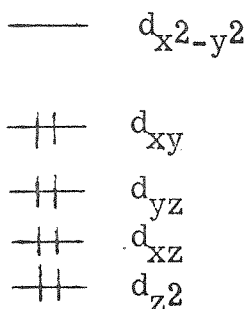
analogy with the trans- $Cr(en)_2F_2^+$ . The  $Cl^-$  is held on in the  $Cr(III)$  because of its  $\pi$ -donor ability while the  $NH_3$  as only a  $\sigma$ -donor is labilized by  $\sigma^*$  character in the excited state. The cis  $NH_3$  being labilized is reasonable since the ligand field excitation is a mixture of  $d_{z^2}$  and  $d_{x^2-y^2}$  which both have significant directed  $\sigma^*$  character for the equatorial ligands. The  $Cr(NH_3)_5(Br)^{2+}$ <sup>24</sup> behaves in a fashion very similar to the  $Cr(NH_3)_5(Cl)^{2+}$ ; i.e., release preferentially of a cis- $NH_3$ .

Until now we have only considered six-coordinate situations. The same considerations of bonding, electronic structure, and spectra can be applied to all  $d^n$  configurations and geometries. Consider Zeise's anion  $Pt(Cl)_3(C_2H_2)^-$ , a  $d^8$  square planar complex as shown in 7-XII. By crystal



7-XII

structure the ethylene is perpendicular to the plane of the  $\text{Pt}-(\text{Cl})_3$ . The predicted ordering of the d levels is shown in 7-XIII. Thermally the ethylene exerts a large trans effect



7-XIII

labilizing the trans chloride giving rapidly the trans aquo species in solution.<sup>25</sup> Photochemically a large deviation is observed in the reactivity.<sup>26</sup> The first transition,  $d_{xy} \rightarrow d_{x^2-y^2}$  should be sigma-anti-bonding for all four ligands, however, ethylene does not exchange with  $\text{H}_2\text{O}$ . The sigma-anti-bonding character of the excited state does affect the chlorides though and gives rise to cis aquo derivatives which do not form thermally. As the energy of the incident irradiation is increased one begins to observe the substitution of ethylene.

Substitution of ethylene does not occur thermally, but in the excited state the ethylene is labilized since the  $\pi$ -back bond is weakened considerably. As with the CO in the metal carbonyls, the ethylene-metal bond is weakened in two ways: (1) population of the  $d_{x^2-y^2}$  orbital creates sigma anti-bonding character and (2) removal of an electron from the  $\pi$ -d orbitals weakens the  $\pi$ -back bonding. Again, with a qualitative description of the bonding and the electronic structure, the strong wavelength effect and stereospecificity of the photoreaction has been rationalized.

The four-coordinate  $d^8$  complexes are expected to have excited states which are distorted from a square planar geometry toward a tetrahedral geometry.<sup>27</sup> Such large geometrical changes may account for intramolecular cis-trans isomerization of Pt(II) complexes upon direct irradiation.<sup>28</sup> The effect of such a geometrical change on the substitution chemistry has not been evaluated but may sterically prevent an associative mechanism like that found in thermal substitution. The  $\text{Pt}(\text{dien})\text{Br}^+$  reacts via an associative mechanism, however, and the fact that both  $\text{PtCl}_4^{2-}$ <sup>29</sup> and  $\text{Pt}(\text{Cl})_3(\text{C}_2\text{H}_4)^-$ <sup>26</sup> emit suggests that the excited state may only be slightly distorted.

In the examples discussed above we have shown that a consideration of bonding, electronic structure, and spectra have provided a satisfying rationalization of the observed photo-substitution pathways. In some cases prediction of the course of

the reactions has been successful. The Wrighton-Gray rules provide the guidelines necessary to systematically elucidate structure-reactivity relationships in coordination compounds.

Reactivity and Excited State Multiplicity. Unlike organic systems, transition metal complexes have shown few differences in their triplet sensitized and direct irradiation photochemistry (Chapter V). In the treatment above the excited state multiplicity was ignored entirely. Since spin-orbital coupling effects in metals are large, it is assumed that population of excited states with multiplicities different from the ground state will be facile. It is reasonable, though, that direct and sensitized reactions will differ when a ligand can undergo a chemical change in a localized excited state. Until more data concerning the reactivity of different multiplicities is available no generalizations can be drawn.

## References

1. A.W. Adamson, A. Chiang, and E. Zinato, J. Am. Chem. Soc., 91, 5467 (1969).
2. A. Haim, R.J. Grassi, and W.K. Wilmarth, Advances in Chemistry Series, No. 49, American Chemical Society, Washington, D.C., 1965, p. 31.
3. A. Haim and W.K. Wilmarth, Inorg. Chem., 1, 573 (1962) and ibid., 1, 583 (1962).
4. E. Koerner von Gustorf and F. — W. Grevels, Fort. Chem. Forsch, 13, 366 (1969) and references cited therein.
5. (a) G.R. Dobson, M.F.A. El-Sayed, I.W. Stolz, and R.K. Sheline, Inorg. Chem., 1, 526 (1962); (b) I.W. Stolz, G.R. Dobson, and R.K. Sheline, J. Am. Chem. Soc., 84, 3589 (1962) and ibid., 1013 (1963); (c) A.J. Rest and J.J. Turner, Chem. Comm., 1026 (1969); (d) K. Noack and M. Ruch, J. Organometal. Chem., 18, 26 (1969); (e) D.J. Darensbourg, M.Y. Darensbourg, and R.J. Denenberg, J. Am. Chem. Soc., 93, 2807 (1971); (f) M.A. Grahm, A.J. Rest, and J.J. Turner, J. Organometal. Chem., 24, C54 (1970).
6. M.A. Grahm, M. Poliakoff, and J.J. Turner, J. Chem. Soc., A2939 (1971).
7. M. Wrighton, G.S. Hammond, and H.B. Gray, J. Am. Chem. Soc., 93, 6048 (1971).
8. V. Balzani and V. Carassiti, "Photochemistry of Coordination Compounds", Academic Press, Inc., New York, 1970, pp. 81-112.
9. V.S. Sastri, R.W. Henwood, S. Behrendt, and C.H. Langford, J. Am. Chem. Soc., 94, 753 (1972).
10. S. Behrendt, C.H. Langford, and L.S. Frankel, ibid., 91, 2236 (1969).
11. Reference 8 pp. 245-256.

12. (a) F. Basolo and R.G. Pearson, "Mechanisms of Inorganic Reactions", John Wiley & Sons, New York, 1967; (b) C.H. Langford and H.B. Gray, "Ligand Substitution Processes", W.A. Benjamin, Inc., New York, 1966.
13. (a) C. Bartocci, F. Scandola, O. Traverso, and V. Balzani, Annual Meeting Chimica Inorganica (Padova), 23; (b) C. Bartocci, F. Scandola, and V. Balzani, J. Am. Chem. Soc., 91, 6948 (1969).
14. T.L. Kelly and J.F. Endicott, ibid., 94, 278 (1972).
15. R. Poilblanc and M. Bigorgne, Bull. Soc. Chim. France, 1301 (1962).
16. (a) H.H. Chen, M.—S. Tsao, R.W. Gaver, P.H. Tewari, and W.K. Wilmarth, Inorg. Chem., 5, 1913 (1966); (b) P.H. Tewari, R.W. Gaver, and W.K. Wilmarth, ibid., 6, 611 (1967).
17. cf. ref. 14 and (a) T.L. Kelly and J.F. Endicott, J. Am. Chem. Soc., 92, 5733 (1970); (b) L. Moggi, Gazz. Chim. Ital., 97, 1089 (1967); (c) T.L. Kelly and J.F. Endicott, J. Am. Chem. Soc., 94, 1797 (1972).
18. R.A. Bauer and F. Basolo, ibid., 90, 2437 (1968) and Inorg. Chem., 8, 2231 (1969).
19. (a) R.A. Plane and J.P. Hunt, J. Am. Chem. Soc., 79, 3343 (1957); (b) M.R. Edelson and R.A. Plane, J. Phys. Chem., 63, 327 (1959) and Inorg. Chem., 3, 231 (1964); (c) E.E. Wegner and A.W. Adamson, J. Am. Chem. Soc., 88, 394 (1966); (d) H.F. Wastegian and H.L. Schläfer, Z. Physik Chem. Frankfurt, 57, 282 (1966) and ibid., 62, 127 (1968); (e) R.D. Lindholm, E. Zinato, and A.W. Adamson, J. Phys. Chem., 71, 3713 (1967); (f) E. Zinato, R.D. Lindholm, A.W. Adamson, J. Am. Chem. Soc., 91, 1076 (1969); (g) A. Chiang and A.W. Adamson, J. Phys. Chem., 72, 3827 (1968); (h) A.W. Adamson, Adv. Chem., 49, 237 (1965).
20. G.B. Porter, S.N. Chen, H.L. Schläfer, and H. Gansmann, Theor. Chim. Acta, 20, 81 (1971).



21. (a) L. Dubicki and R. L. Martin, Aust. J. Chem., 22, 839 (1969); (b) L. Dubicki, M. A. Hitchman, and P. Day, Inorg. Chem., 9, 188 (1970); (c) D. A. Rowley, ibid., 10, 397 (1971).
22. S. C. Pyke and R. G. Linck, J. Am. Chem. Soc., 93, 5281 (1971).
23. M. F. Manfrin, L. Moggi, and V. Balzani, Inorg. Chem., 10, 209 (1971).
24. P. Riccieri and H. L. Schläfer, ibid., 9, 727 (1970).
25. I. Leden and J. Chatt, J. Chem. Soc., 2936 (1955).
26. P. Natarjan and A. W. Adamson, J. Am. Chem. Soc., 93, 5599 (1971).
27. (a) D. S. Martin, Jr., M. A. Tucker, and A. J. Kassman, Inorg. Chem., 4, 1682 (1965) and ibid., 5, 1298 (1966); (b) C. J. Ballhausen, N. Bjerrum, R. Dingle, K. Eriks, and C. R. Hare, ibid., 4, 514 (1965).
28. V. Balzani and V. Carassiti, J. Phys. Chem., 72, 383 (1968).
29. P. D. Fleischauer and P. Fleischauer, Chem. Rev., 70, 199 (1970).

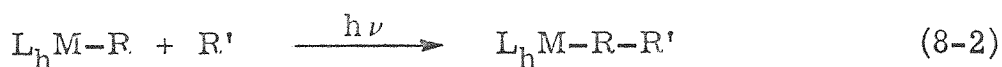
## CHAPTER VIII

Photoreactions of Coordinated Ligands

The photoinduced transformation of ligands is a major class of photoreactions of metal containing molecules. The types of reactions that occur can be classified as those that involve a simple intramolecular rearrangement, equation (8-1), and those



that involve addition of another molecule to the ligand, equation (8-2). The ligand undergoing transformation has typically



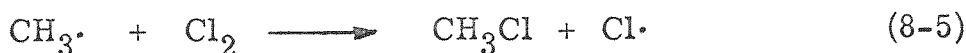
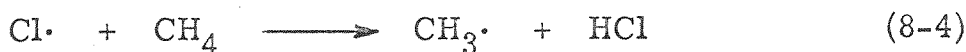
been an olefin, and most work has been done with iron(0) carbonyl complexes. A large number of reactions like (8-1) or (8-2) have been observed, but few have been subjected to careful mechanistic inquiry.

The techniques involved here offer several advantages over normal synthetic paths and these include: (1) molecules coordinated to metals often assume a favorable, stable conformation, (2) since light is used there exists the possibility of producing nonthermodynamic products, (3) transition metals are known to produce unusual transformations thermally, and similar effects may be expected in excited state chemistry, (4) the metal localized and new charge transfer electronic

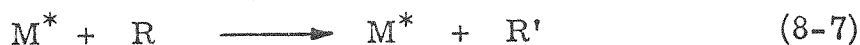
transitions provide for light absorption at low energies, (5) separation of the product can be facilitated since it is coordinated to the metal, and (6) thermally unstable products can be realized since high temperatures are not typically used.

The Concept of Photocatalysis. In some cases the transformation of a molecule does not occur as a primary photoprocess.

Sensitized reactions are one example, but here at least the reaction is an excited state decay process. In contrast, the reaction of chlorine radicals with methane is a secondary reaction involving a photogenerated, thermally reactive species. The sequence (8-3) through (8-5) is a photocatalytic process in that a

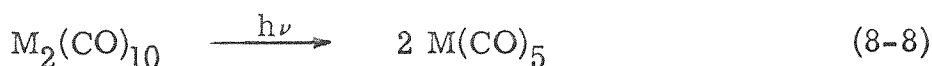


single photon initiates a chain reaction which proceeds until the radicals couple resulting in termination. In general, we define a photocatalytic process as one where a reactive intermediate is produced photochemically and proceeds to react in a catalytic fashion as shown in (8-6) and (8-7). To date, few



photocatalytic processes exist with the best examples being photogeneration of radicals. Transition metal systems might provide the best photocatalytic systems since a number of good thermal catalysts contain transition metals. The problem, then, is to generate the catalyst photochemically starting with a thermally inert complex.

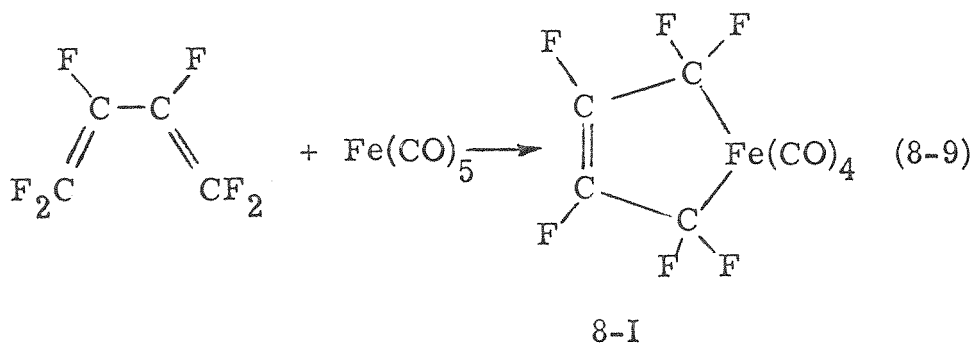
One example of a photocatalyst involving transition metals is now being explored. The  $d^7$  five-coordinate  $\text{Co}(\text{CN})_5^{3-}$  is a catalyst for the hydrogenation of olefins.<sup>1</sup> The  $\text{M}_2(\text{CO})_{10}$  ( $\text{M} = \text{Re}, \text{Tc}, \text{Mn}$ ) systems are very similar but the  $d^7$   $\text{M}(\text{CO})_5$  moieties are stabilized by the formation of the M-M bond. The formation of the M-M bond arises from overlap of the singly occupied  $d_{z^2}$  orbitals as discussed in Chapter II. The  $\sigma \rightarrow \sigma^*$  transition is a prominent feature of the absorption spectra of  $\text{M}_2(\text{CO})_{10}$ .<sup>2</sup> The irradiation into the  $\sigma \rightarrow \sigma^*$  transition reduces the M-M bond order to zero producing two  $\text{M}(\text{CO})_5$  moieties, equation (8-8). We have thus photogenerated a  $d^7$  five-coordinate



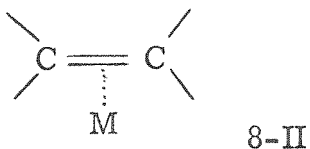
system capable of being a hydrogenation catalyst. The catalytic activity of  $\text{M}(\text{CO})_5$  is now under investigation. The use of  $\text{Mn}_2(\text{CO})_{10}$  as a photoinitiator of polymerization has already been reported.<sup>3</sup>

The photocatalytic processes provide the most economical use of light, and may prove useful in large scale photosynthetic applications.

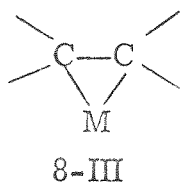
Reactions of Molecules Coordinated to Fe(0). A number of olefin complexes of iron carbonyls have been investigated.<sup>4</sup> The iron carbonyls involved are not only the mononuclear  $\text{Fe}(\text{CO})_5$  derivatives, but complexes containing two, three, or four iron atoms have been important. The bonding of olefins and CO in these systems is understood in terms developed in Chapter I. The effective atomic number rule dictates that the iron is to be surrounded by eighteen electrons. The five CO's for  $\text{Fe}(\text{CO})_5$  provide ten electrons giving a  $d^8$  configuration for the central metal. Coordination compounds of  $d^8$  metals are susceptible to oxidative addition as in (8-9).<sup>5</sup> The Fe in 8-I is formally a



$d^6$  configuration and is six-coordinate. In bonding olefins to metals there are two extremes, 8-II featuring only slight

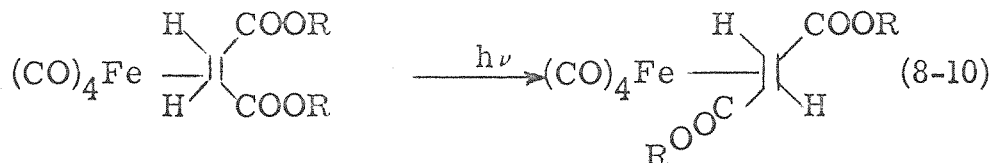


perturbation of the double bond of the olefin, and 8-III featuring

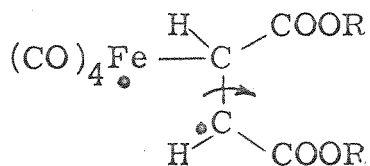


complete oxidative addition resulting in the formation of the metallo-cyclopropane structure. The  $d^8$  Fe(0) tends to form complexes like 8-III to achieve the stable  $d^6$  configuration.

One of the dominant reactions of iron carbonyl olefin complexes is cis-trans isomerization; an example is shown in (8-10).<sup>6</sup> Since sigma bound olefin complexes of iron are known,



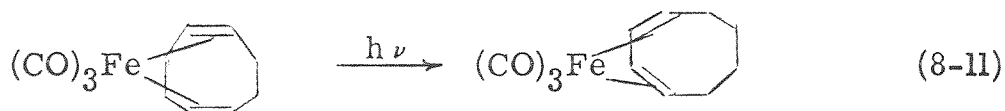
it is attractive to invoke the intermediacy of the diradical 8-IV



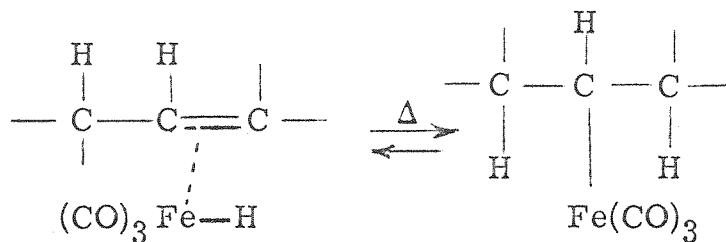
as a pathway for the cis-trans isomerization of the olefin; the transient 8-IV may be a precursor to generation of a species

such as 8-III. The formation of an electronically excited olefin can usually be ruled out on the basis of energetics.

A second characteristic photoreaction involving iron carbonyl olefin complexes is hydrogen migration; an example is shown in (8-11).<sup>7</sup> Existing thoughts concerning thermal double bond

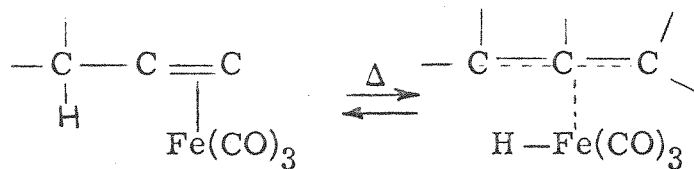


shifts of this sort (1-octene  $\rightarrow$  2-octene, etc.) all include iron carbonyl hydrides as an important species in the isomerization with the iron either binding to the olefin in a  $\sigma$ -fashion, 8-V,



8-V

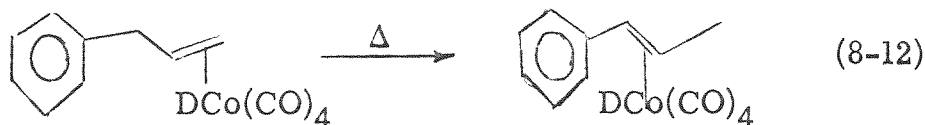
or by having a  $\pi$ -allyl metal system 8-VI. Light is thought



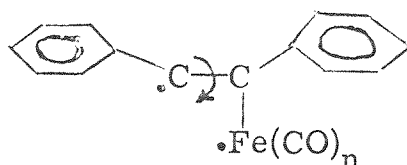
8-VI

to produce the thermally active Fe-H species in either case.<sup>8</sup>

However, there are cases where an intermediate  $\pi$ -allyl-hydride apparently is unimportant, equation (8-12).<sup>9</sup> In the

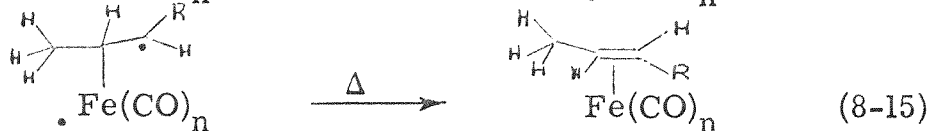
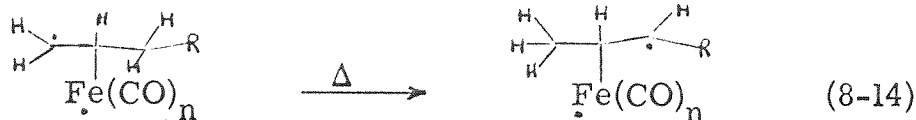
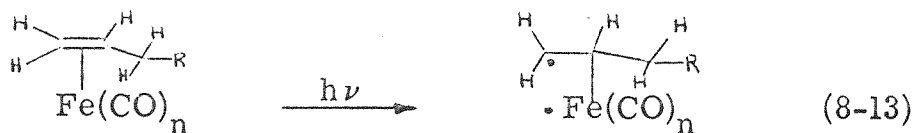


cobalt carbonyl deuteride photocatalyzed isomerization of allylbenzene no deuterium was incorporated into the  $\beta$ -methylstyrene product. Further,  $\text{Fe}(\text{CO})_5$  has been shown to catalyze the cis to trans isomerization of stilbene<sup>10</sup> which has no allylic hydrogens, implicating an intermediate similar to 8-VII. This intermediate



8-VII

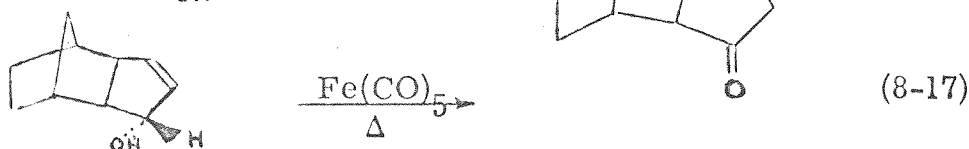
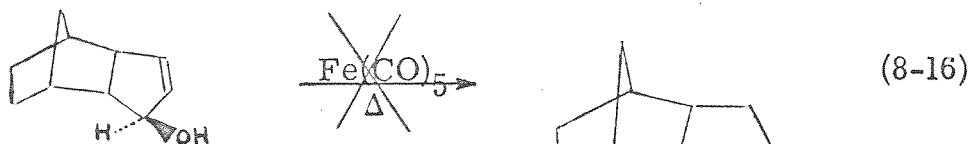
is that suggested above, 8-IV, to account for the photochemical isomerization of coordinated olefins. In the double bond migration reactions the sequence (8-13) through (8-15) is a reasonable



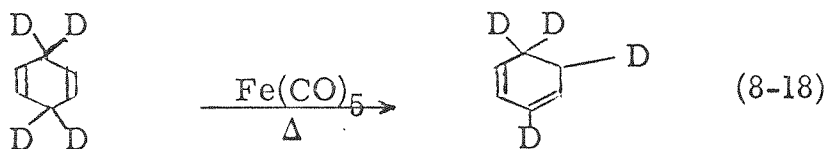
description of events occurring in reactions such as (8-11). The diradical intermediates account for both cis-trans isomerization and hydrogen migration. Also, the radicals are expected to decay to give the thermodynamic products obtained with iron carbonyl olefin complexes. The key experiment of attempting to incorporate deuterium into the olefin with  $\text{Fe}(\text{CO})_4\text{D}^-$  as a test of the



Fe-H intermediate has not been reported. Strong evidence has been presented for iron -hydrogen interaction by measuring the rates of reactions of (8-16) and (8-17).<sup>11</sup> Reaction (8-16) does not

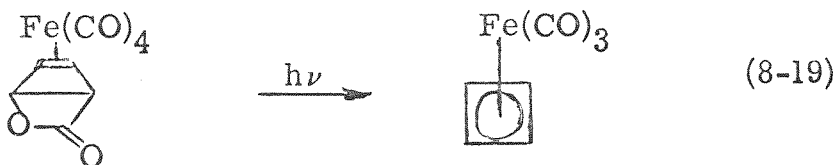


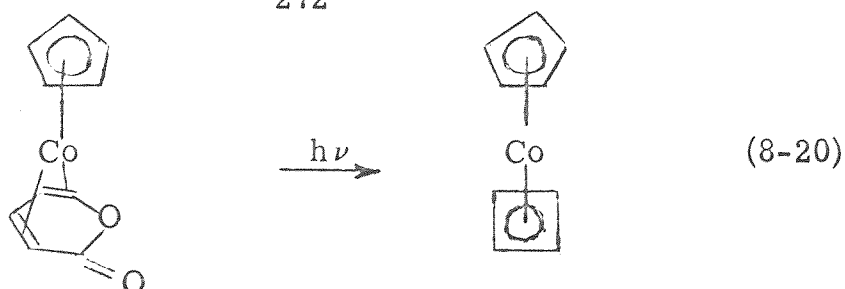
proceed at a measurable rate while (8-17) proceeds readily. The implication is that the hydrogen has to be on the same side as the iron suggesting the formation of the metal-hydride intermediate. The reaction (8-18)<sup>12</sup> establishes that these reactions are intra-



molecular, consistent with either the diradical or  $\pi$ -allyl metal-hydride mechanism. It is safe to say, at least, that the  $\pi$ -allyl-metal-hydride mechanism cannot be the exclusive one for both cis-trans isomerization and hydrogen migration since the isomerization of stilbene is catalyzed by  $\text{Fe}(\text{CO})_5$ .

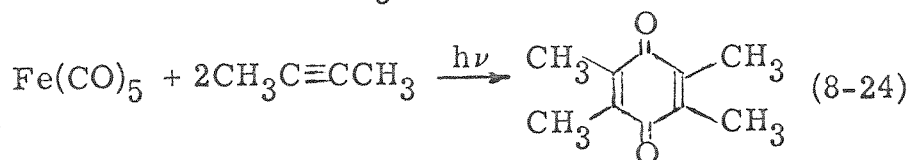
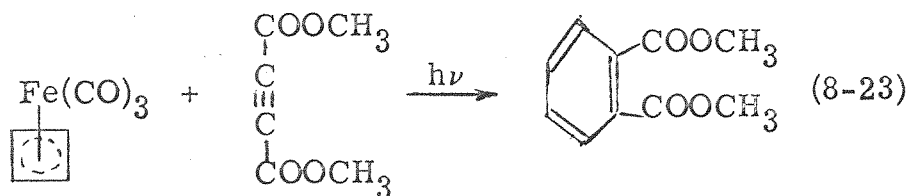
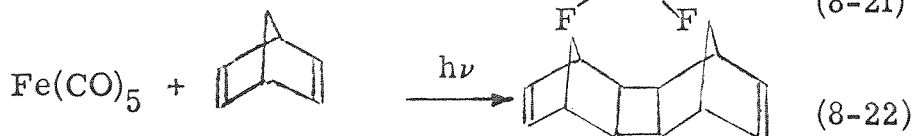
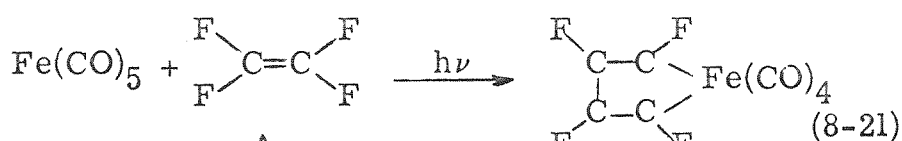
The reactions (8-19)<sup>13</sup> and (8-20)<sup>14</sup> provide interesting examples of intramolecular photoreactions of coordinated ligands. The





trapping of the cyclobutadiene photoproduct by coordination to the metal represents a relatively unexplored technique.

Other interesting photoreactions of iron carbonyl olefin complexes include intermolecular oligomerization of the olefin. Mechanistic detail is even less well resolved than in the intramolecular isomerization reactions. Some representative photoreactions are shown in (8-21) through (8-24).<sup>15-18</sup> These unique

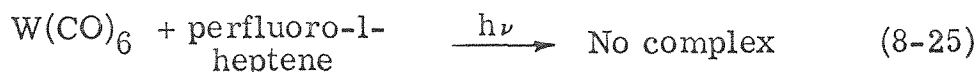


reactions afford products of unusual structure and provide a significant challenge for mechanistic photochemists. It is clear that the metal somehow facilitates reactions which are formally

forbidden by the principles of orbital symmetry. However, how these principles apply here will remain a mystery until one gains insight into the nature of the excited states responsible for these reactions. This non-trivial area of photochemistry merits investigation to enable us to productively exploit the special reactions associated with transition metals.

Reactions of Molecules Coordinated to Cr(0), Mo(0), and W(0).

The carbonyl complexes of Cr(0), Mo(0), and W(0) are all six-coordinate and have a  $d^6$  configuration. Being  $d^6$ , the olefin complexes have a structure more similar to 8-II without significant perturbation of the olefin. Indeed, attempts to coordinate perfluoro-1-heptene, (8-25), failed under conditions

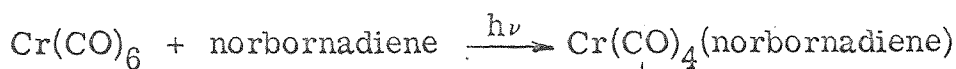


where 1-pentene forms a stable complex. The spectroscopy of  $W(CO)_5(\text{alkene})$  was discussed in Chapter VII. The d orbitals in the olefin complex are not perturbed greatly from the  $W(CO)_6$  since the alkene is similar to CO in its binding interactions. The tungsten complexes exhibit intense spin-forbidden transitions which are diminished or non-existent in the corresponding Cr or Mo complexes.

The number of reactions with these complexes seems to be fewer than with the Fe(0) systems, and the reactions are less complex. This statement may merely reflect the fact that much

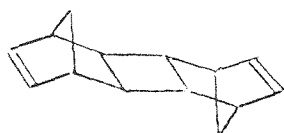
less work has been attempted with these metals. Thus far, cycloaddition reactions, cis-trans isomerization, hydrogen shifts, and hydrogenation reactions have been promoted by the photolysis of these  $d^6$  metal carbonyl olefin complexes. Since the metal carbonyl complexes have very efficient photosubstitution reactions we have undertaken exploration of the possibility of using this energy to promote reactions of a coordinated ligand.

An initial effort with these metals was the report of  $\text{Cr}(\text{CO})_6$  photoassisted dimerization of norbornadiene, (8-26).<sup>19</sup> The



(8-26)

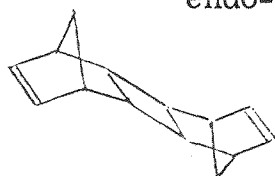
↓  $h\nu$   
Dimers (8-VIII)



exo-trans-exo  
(a)



endo-trans-exo  
(b)



endo-trans-endo  
(c)

Yield: (a):(b):(c)=1.8:1.0:1.4

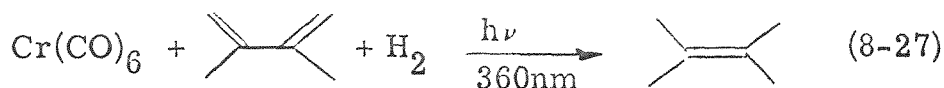
8-VIII

intermediate norbornadienetetracarbonylchromium(0) was isolated and invoked as the immediate precursor to the dimers. This system seems to be the only one to yield all three dimers, 8-VIII. Quantum efficiencies were not measured, but the overall yield of

40% based on the  $\text{Cr}(\text{CO})_6$  suggests that the reaction is not catalytic. The  $\text{Mn}(\text{CO})_6$  and  $\text{W}(\text{CO})_6$  photoassisted dimerization of norbornadiene has not been reported.

The irradiation of  $\text{W}(\text{CO})_6$  in neat isoprene leads to dimeric products. The acetophenone sensitized dimerization of isoprene<sup>20</sup> under identical conditions yielded some products which were the same as those obtained with the  $\text{W}(\text{CO})_6$  reaction, but the ratio of products was significantly different. This data rules out the possibility that a free triplet excited isoprene molecule is produced by the irradiation of the  $\text{W}(\text{CO})_n(\text{isoprene})_{6-n}$  complexes. An interesting possibility in this case is that a cis- $\text{W}(\text{CO})_4(\text{isoprene})_2$  is photolysed resulting in dimerization of the two coordinated diene units. The corresponding trans disubstituted complex would not be expected to give intramolecular dimerization due to geometrical restrictions.

Another example of an intermolecular reaction is (8-27).<sup>21</sup>



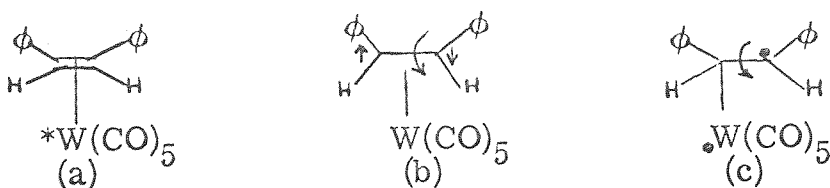
Interestingly, no 2,3-dimethyl-1-butene was formed in the reaction. The conversion of 1,3-cyclohexadiene to cyclohexene occurs by the same procedure.<sup>21</sup> No mechanistic detail regarding this system has been reported.

The  $\text{M}(\text{CO})_6$  photoassisted cis-trans isomerization of stilbene provides the first evidence that nonthermodynamic products can be obtained from photolysis of metal-olefin complexes. In Figure

VIII-1 we show the %trans-stilbene as a function of irradiation time of the tungsten carbonyl complex. The final photostationary state of the stilbenes is seen to be independent of the starting isomer ratio. The stationary state established with the  $W(CO)_6$  is far different from the thermodynamic ratio for the stilbenes.<sup>22</sup> In the  $Fe(0)$  systems it has not been demonstrated whether non-thermodynamic products can be obtained.

The effect of metal on the photoassisted isomerization of stilbene is summarized in Table VIII-1. The drop in the ability to affect the isomerization with the lighter metal complexes is correlated with the ability of the metal to bind the olefin and in the extent of singlet to triplet character of the electronic transitions in the  $M(CO)_n(stilbene)_{6-n}$  complexes.<sup>23</sup>

The character of an excited state of a complex must reflect some of the features of the metal and some of the features of the ligand by the principles of MO theory developed in Chapter I. In the stilbene metal carbonyl complexes the excited state must feature free rotation about the double bond to account for cis-trans photoisomerization. It is attractive to assume that contributions to the excited state arise from the three idealized species in 8-IX. Species (a) and (b) are metal-localized and ligand-



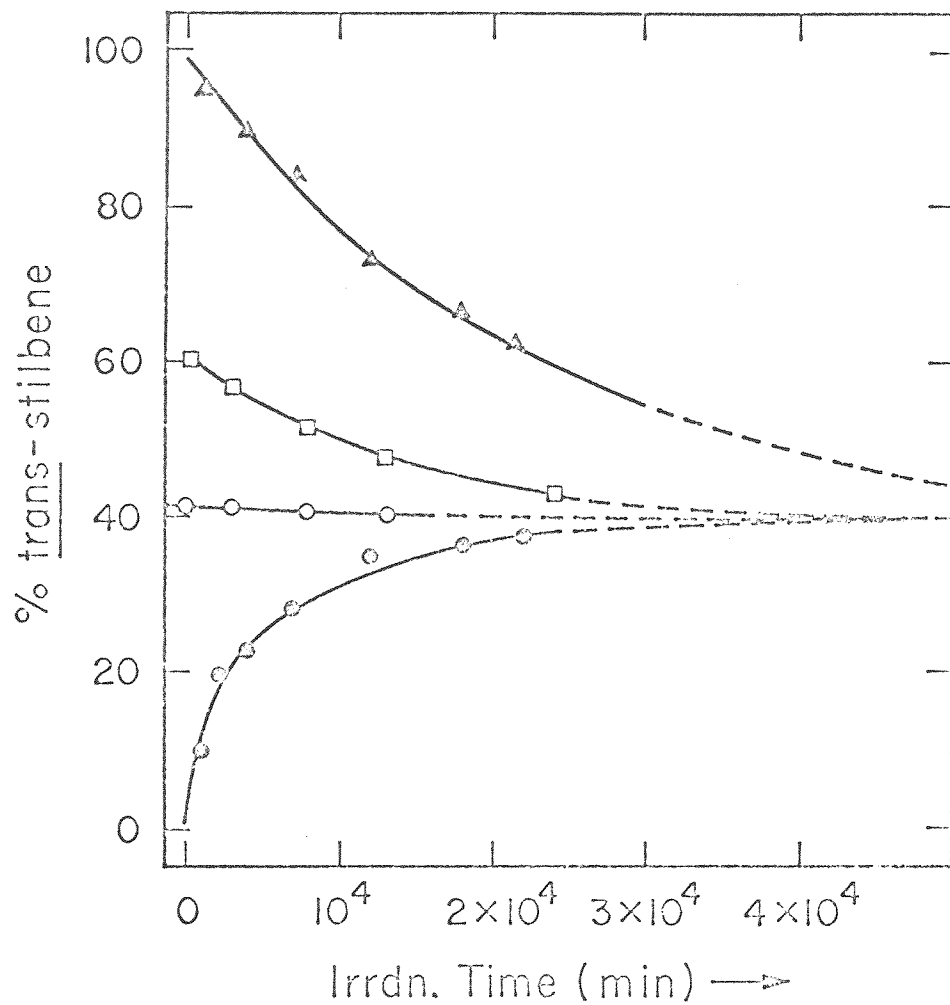


Figure VIII-1. Percent trans-stilbene as a function of 366nm irradiation time using  $W(CO)_6$  as the photocatalyst.

Table VIII-1. Observed Initial Relative Rates of Isomerization  
of Stilbenes<sup>a</sup>

Metal Carbonyl	$\phi_{c \rightarrow t}$	$\phi_{t \rightarrow c}$
W(CO) <sub>6</sub>	1.000 <sup>b</sup>	0.18
Mo(CO) <sub>6</sub>	0.04 <sub>9</sub>	0.07 <sub>3</sub>
Cr(CO) <sub>6</sub>		0.00 <sub>0</sub>

<sup>a</sup>366 nm irradiation,  $5.83 \times 10^{-10}$  ein/sec beginning with pure M(CO)<sub>6</sub> and excess stilbene.

<sup>b</sup>Corresponds to observed quantum efficiency of 0.1<sub>1</sub>.



localized excited states respectively while (c) may be an excited state or an intermediate resulting from nonradiative decay from the metal-localized excited state. Difficulty in distinguishing the species involved arises in not knowing the thermodynamic ratio of the complexes  $W(CO)_5(\text{cis-stilbene})$  and  $W(CO)_5(\text{trans-stilbene})$ . Unfortunately the relative binding strengths of the cis and trans isomers of the olefin are not known. If the cis-stilbene is much more firmly bound than trans-stilbene this binding stability may swamp the stability gained from having the trans double bond. It is unclear, then, whether absorption of light by the complex results in the primary selective formation of nonthermodynamic products. The absorption of light by the complex may merely lead to a nonthermodynamic ratio of the two isomers by optical pumping with isomerization of the olefin occurring in the ground state diradical.

Results presented in Figure VIII-2 show that optical pumping is unimportant as a means of producing an overall nonthermodynamic mixture of the stilbenes. It is shown that the disappearance of the  $W(CO)_5(\text{trans-stilbene})$  is not accelerated over the thermal rate of disappearance by photolysis while significant amounts of trans to cis isomerization have occurred. The spectral change which occurs due to the formation of the stilbene complex is shown in Figure VIII-3; irradiation at  $\lambda > 380\text{nm}$  should only produce photoexchange of olefin, isomerization, and regeneration of  $W(CO)_6$ , but no new formation of  $W(CO)_5(\text{stilbene})$ . In the

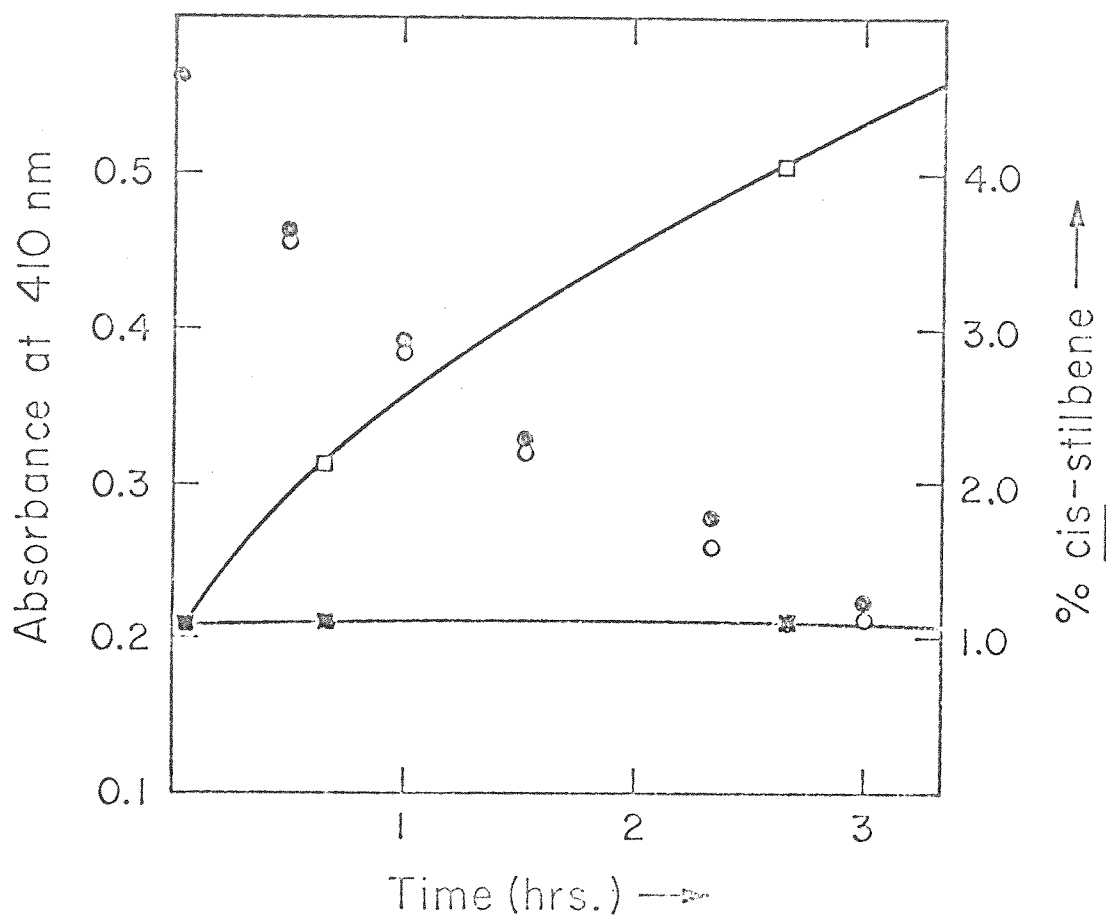


Figure VIII-2. Thermal bleaching of  $W(CO)_5(t\text{-stilbene})$  in irradiated ( $\lambda \geq 380\text{nm}$ ) samples (●) and in non-irradiated samples (○) and concurrent trans to cis photocatalyzed isomerization of stilbene in irradiated (□) and nonirradiated (■) samples.

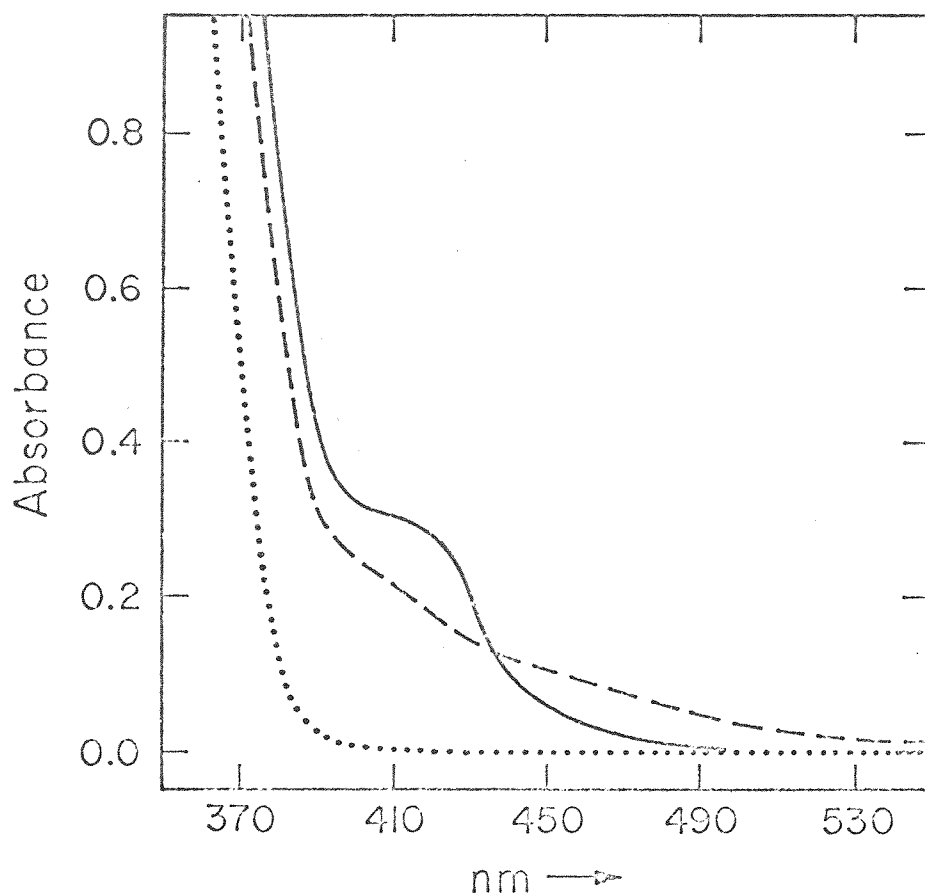
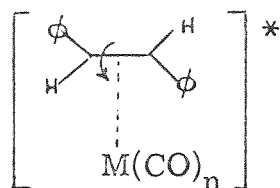


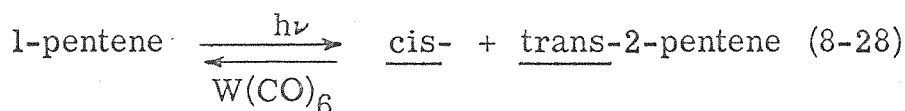
Figure VIII-3. Spectral changes in the uv-vis region due to photochemical formation of  $\text{W(CO)}_5(\text{c-stilbene})$  (-----) and  $\text{W(CO)}_5(\text{t-stilbene})$  (—) from 366nm irradiation of  $\text{W(CO)}_6$  (·····).

sealed, degassed systems the disappearance of the complex is thought to be regeneration of the  $W(CO)_6$  and is accompanied by exchange of the olefin with the free olefin in the medium. In conclusion, the intermediate for photoisomerization has excited state character and is probably best represented simply as 8-X.



8-X

In contrast to the  $M(CO)_6$  photoassisted isomerization of the stilbenes the reaction (8-28) leads to thermodynamic products.



The double bond migration is thought to occur via photolysis of  $W(CO)_n(1\text{-pentene})_{6-n}$  complexes. Figure VIII-4 shows the percent disappearance of the 1-pentene as a function of the irradiation time. The short induction period during which the olefin complex concentration is building up is revealed, and it is seen that a small amount of 1-pentene remains at the stationary state. The 3% 1-pentene, 80% trans-2-pentene, 17% cis-2-pentene mixture found at the stationary state is very close to the thermodynamic mixture for these olefins. The same stationary state is approached starting with any of the three linear pentenes, and the intercon-

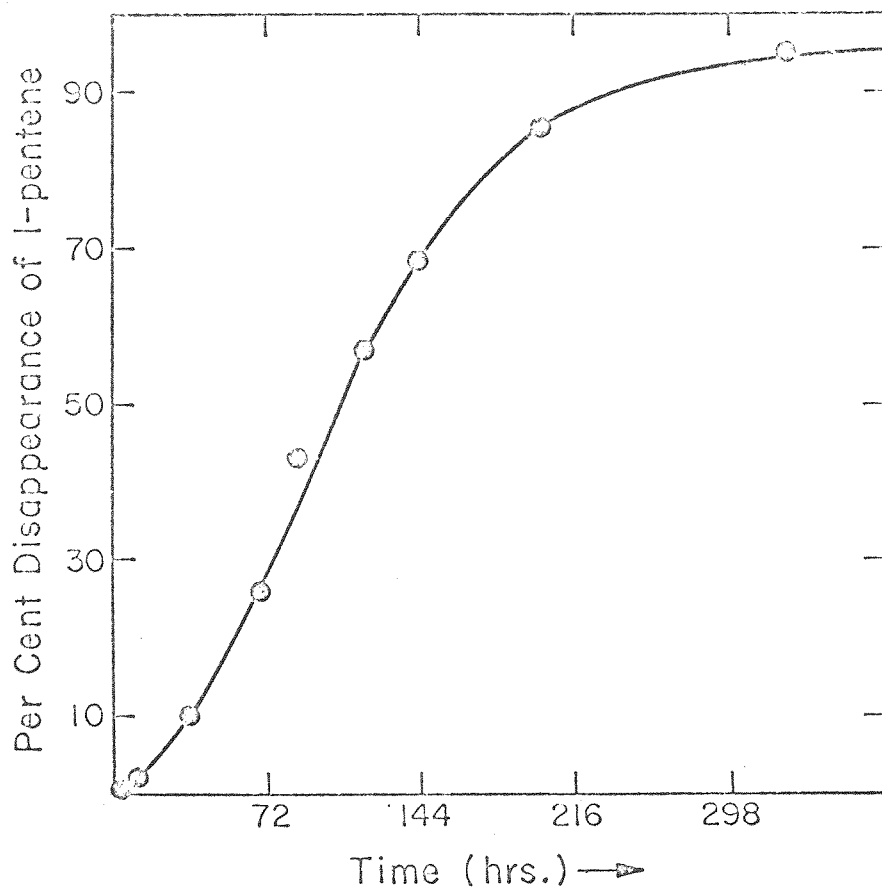


Figure VIII-4.  $W(CO)_6$  photocatalyzed disappearance of 1-pentene as a function of 313nm irradiation time. Products are the isomeric 2-pentenenes.

version of the 2-pentene isomers is a primary photoprocess. The cis to trans and trans to cis  $W(CO)_6$  photoassisted isomerization of 2-pentene is shown as a function of time in Figures VIII-5 and VIII-6. The induction period is again revealed in each case. That the olefin complexes formed do absorb light is proven by noting that the disappearance of the  $W(CO)_6$  is not linear in time, Figure VIII-7. However, the relative importance of mono- and multiply substituted carbonyl complexes is not known. It is reasonable to assume that any or all of the possible olefin complexes could result in reaction of the coordinated olefin.

We have shown, Table VIII-2, that a photocatalyst is produced in the reaction. For example, 1388min. of "thermolysis" yields 1.60% isomerization with 1.19 going to trans - and 0.41 going to cis-2-pentene, a trans/cis ratio of 2.90, compared to the initial 6.44 ratio for the primary 1350min. irradiation. More of the photocatalyst seems to be generated, or it is more effective after the longer 4233min. irradiation since 7.03% isomerization occurred. The trans/cis ratio of 1.30 differs from the earlier thermal value and from the photochemical value. The data is consistent with both a thermal and a photochemical pathway for isomerization and with the intermediacy of complexes of different stoichiometry.

In Table VIII-3 the metal effect on the photoassisted 1-pentene to 2-pentene conversion is summarized. The effect is reminiscent

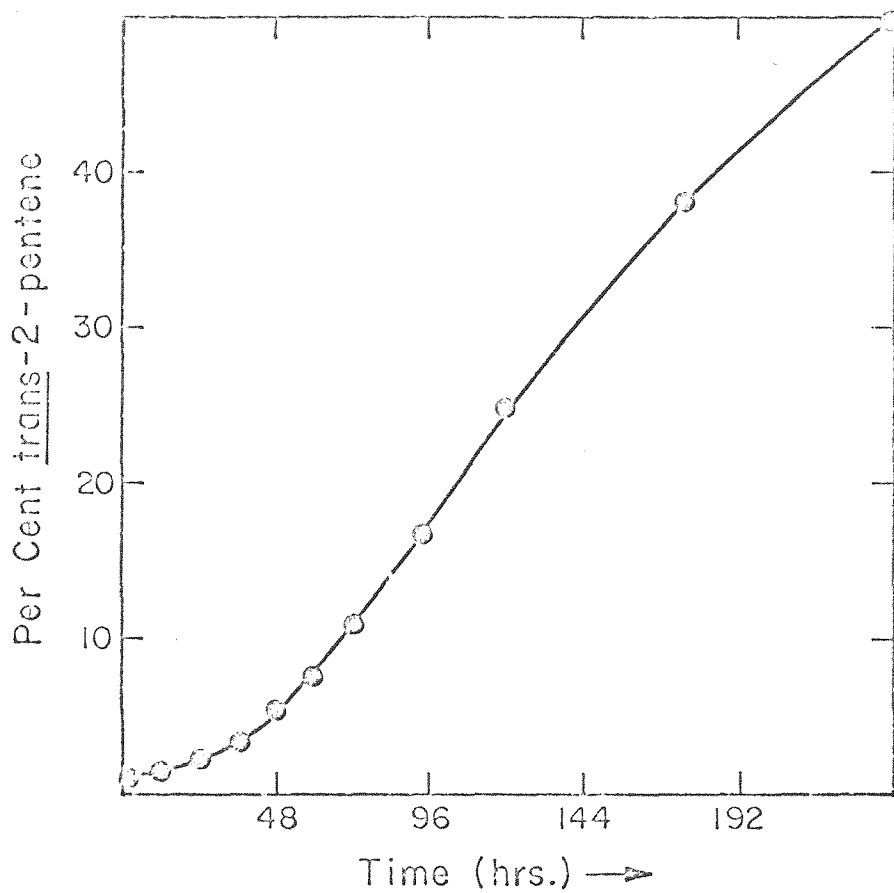


Figure VIII-5.  $W(CO)_6$  photocatalyzed cis to trans -2-pentene isomerization as a function of irradiation time.

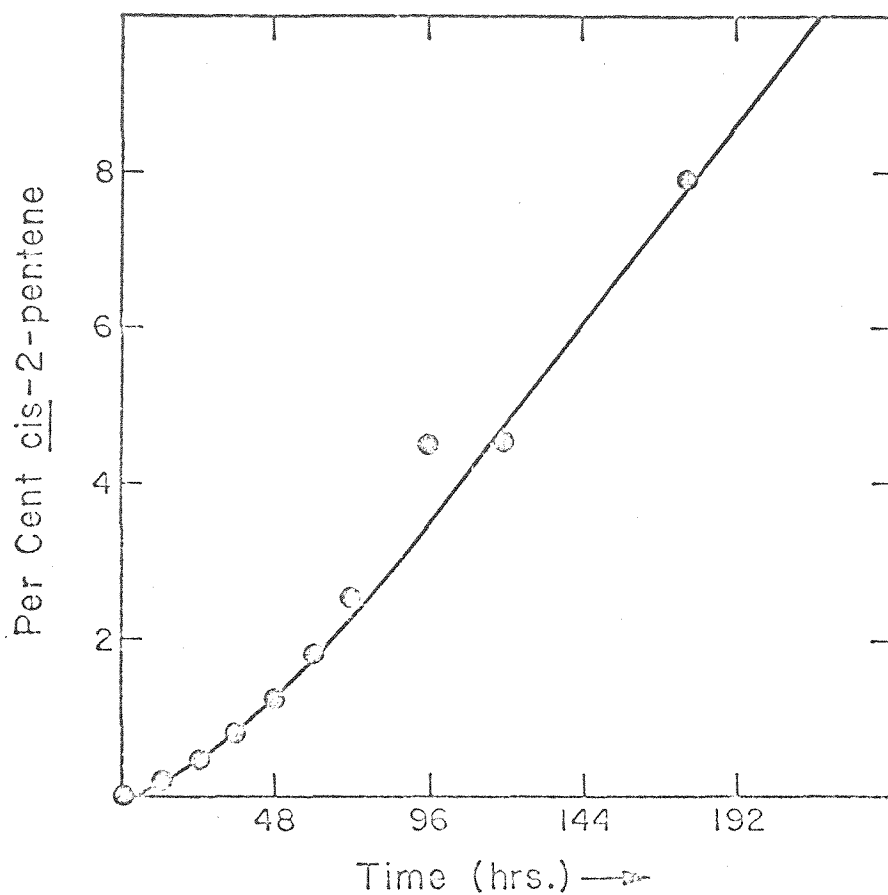


Figure VIII-6.  $W(CO)_6$  photocatalyzed trans to cis-2-pentene isomerization as a function of irradiation time.



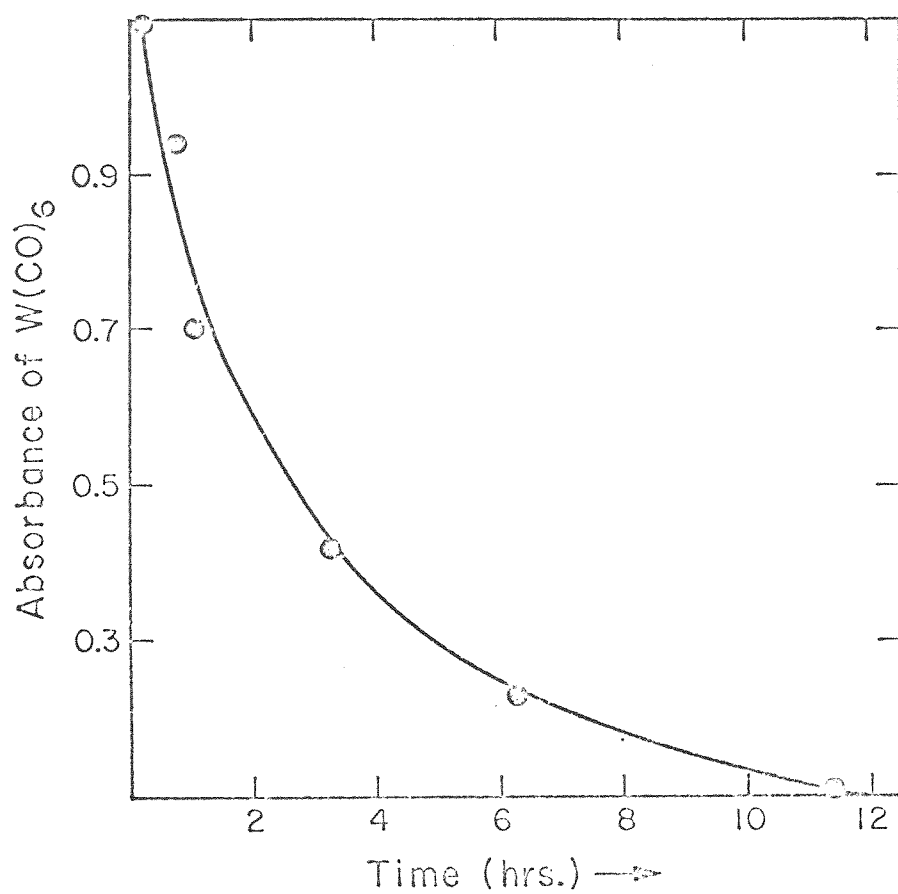


Figure VIII-7. Non-linear disappearance of  $\text{W(CO)}_6$  when irradiated in the presence of olefins.

Table VIII-2.  $W(CO)_6$  1-Pentene Photoassisted Conversion to 2-Pentene

Time Irrdtd., min.	Time Thermolysed, <sup>a</sup> min.	% 1-pentene	% <u>cis</u> -2-pentene	% <u>trans</u>	(t/ε)
1350	0	96.27	3.22	0.50	6.44
1356	1388	94.67	4.42	0.91	4.90
2744	0	83.74	14.11	2.14	6.64
4226	0	68.85	27.37	3.78	7.31
4233	3503	61.82	31.35	6.83	4.59
7054	0	43.55	48.95	7.60	6.44
					288

<sup>a</sup>Thermolysis is under same conditions as photolysis (30°C.) except the sample is shielded from the light.

Table VIII-3. Metal Effect on  $\text{M}(\text{CO})_6$  Photoassisted 1-Pentene to 2-Pentene Conversion

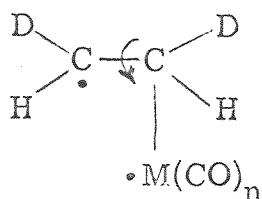
Metal Carbonyl	Time Irrdtd., <sup>a</sup> min.	% conversion	% <u>trans</u>	% <u>cis</u>	<u>t/c</u>
$\text{Cr}(\text{CO})_6$	4042	0.0	—	—	—
	8600	0.0	—	—	—
$\text{Mo}(\text{CO})_6$	4042	24.19	12.82	11.37	1.13
	8600	37.02	19.87	17.15	1.16
$\text{W}(\text{CO})_6$	4042	33.79	29.53	4.26	6.97
	8600	68.64	59.87	8.75	6.84

<sup>a</sup>Irradiation of 0.05 M 1-pentene, 0.002 M  $\text{M}(\text{CO})_6$  degassed isooctane solutions at room temperature in a 366 nm merry-go-round.

of the metal effect for the stilbene isomerization, Table VIII-1. Presumably, the fact that the Cr(0) does not bind the alkene accounts for its total inactivity as a photocatalyst. The Cr(0) and the Fe(0) carbonyl complexes are both first row transition metal systems yet there is a vast difference in their ability to bind olefins. This difference arises because Fe(0) has a  $d^8$  configuration and has a tendency to bind the olefin by strong back-bonding or undergoing complete oxidative addition. The Cr(0) on the other hand has the stable  $d^6$  configuration and is not susceptible to oxidative addition to reduce the charge of the central metal. The Mo(0) and W(0) have the larger 4d and 5d orbitals allowing greater delocalization of the d electrons to form pi bonds with the alkenes. The  $d^8$  Ni(II), Pd(II), and Pt(II) also illustrate the heavy metal effect with the Pt(II) binding alkenes much more firmly than the lighter Ni(II). The difference in binding strength between the  $d^8$  Fe(0) and Ni(II) arises because the Ni(II) has less tendency to give up electron density since it is positively charged.

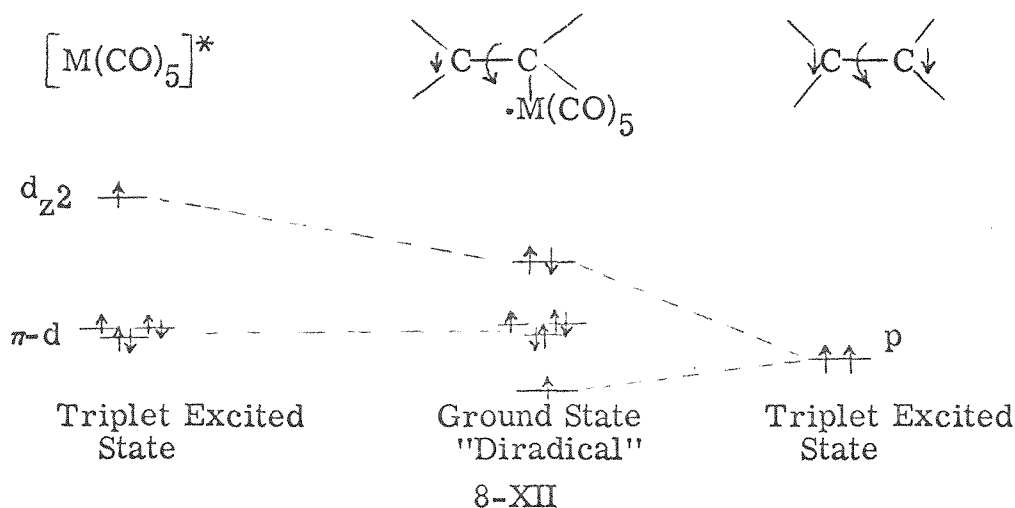
Some mechanistic information has been obtained by considering the  $W(CO)_6$  photoassisted isomerization of trans-ethylene- $d_2$ . Slow isomerization to the cis isomer was observed upon 313nm irradiation of the metal carbonyl. Like the stilbene, ethylene- $d_2$  has no allylic hydrogens, and the observation of metal assisted isomerization precludes the notion that the  $\pi$ -allyl-metal hydride is the exclusive intermediate in the alkene isomerizations. This

provides unequivocal evidence for the importance of intermediates featuring metal-carbon sigma bonds as in 8-XI. Since reactions

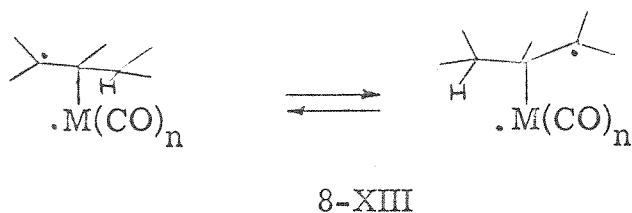


8-XI

of the simple alkenes tend to give thermodynamic products it is attractive to conclude that the isomerization intermediate has no excited state character and is a true photocatalyst. The intermediate can be achieved by nonradiative decay of a spectroscopic excited triplet state involving  $\pi$ - $d \rightarrow d_{z^2}$  excitation. Removing one of the six  $\pi$ - $d$  electrons leaves an unpaired electron in the lower  $d$  orbitals. The excited  $d_{z^2}$  electron may pair with one of the electrons of the C-C double bond leaving one unpaired electron localized on one of the carbons. A molecular orbital formulation of the metal-carbon sigma bond is shown in 8-XII. To be sure,



8-XI is a high energy intermediate, but it does account for all of the observations: free C-C bond rotation, formation of thermodynamic products, and it can be achieved photochemically. While no proof exists, it is attractive to assume that intermediates like 8-XIII are important in the hydrogen shift reactions. The



driving force for the hydrogen shift reaction would then be the formation of the most stable carbon radical.

The hydrogen shifts observed in these systems are forbidden in the free alkene by orbital symmetry rules.<sup>24</sup> The observation of stereospecificity in the metal assisted reactions would be strong evidence for the usefulness of applying the rules to the metal catalyzed reactions. In Table VIII-4 we show the results of the  $W(CO)_6$  photoassisted isomerization of cis and trans-3-hexene. The data provide unequivocal evidence that the intermediate responsible for the 3-hexene to 2-hexene conversion is not the same with cis- and trans-3-hexene. Some isomeric integrity is retained during the hydrogen shift as evidenced by the different trans/cis ratio of 2-hexenes produced from the two isomeric 3-hexenes. While stereospecificity is not complete the result provides the first evidence that the reactions may be concerted. The suprafacial  $[1, 3]$  sigmatropic rearrangement

Table VIII-4. W(CO)<sub>6</sub> Photoassisted Isomerization of Linear Hexenes<sup>a</sup>

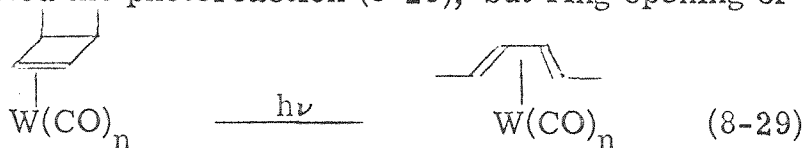
Starting Isomer	Time Irrdtd., min.	1-hexene	<u>t</u> -2-hexene	<u>t</u> -3	<u>c</u> -2	<u>c</u> -3
1-hexene	600	—	1.49	0.00	b	0.00
	1352	—	3.88	0.00	b	0.00
	1900	—	7.31	0.00	b	0.00
<u>cis</u> -3-hexene	3824	0.00	1.46	1.32	0.96	—
	6152	0.00	4.39	3.29	2.88	—
<u>trans</u> -3-hexene	3824	0.00	11.66	—	1.74	0.80
	6152	0.00	31.13	—	4.16	1.28

<sup>a</sup>We report % conversion.<sup>b</sup>Too small to measure.

observed here has been rationalized by including metal orbitals in the application of the orbital symmetry rules.<sup>25</sup>

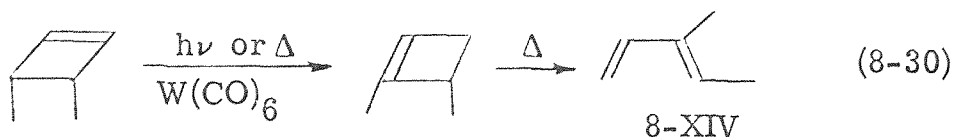
The data in Table VIII-4 reveals other interesting facts: (1) the trans-3-hexene reacts faster than the cis isomer, the reverse of the reactivity of cis- and trans-2-pentene; (2) no two bond shifts occur, i. e., 1-hexene does not go directly to 3-hexene; and (3) cis-trans isomerization of the alkene does not require a hydrogen shift. The fact that no two bond hydrogen shifts occur suggests that reaction (8-11) may be a two photon process.

We attempted the photoreaction (8-29), but ring opening of



the coordinated cis-dimethylcyclobutene was not detectable.

However, thermolysis of the complex after extended photolysis revealed that a hydrogen shift had occurred photochemically or thermally since 3-methyl-1,3-pentadiene 8-XIV was formed.



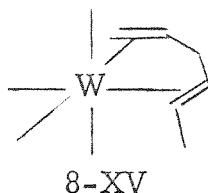
The  $\text{W(CO)}_6$  photoassisted reactions of the 1,4-hexadienes have been investigated, and results are summarized in Table VIII-5. No interconversion of cis- and trans-1,4-hexadiene was detectable. Besides the 2,4-hexadienes one other very minor product was observed and is believed to be trans-1,3-hexadiene. The isomeric 1,3-pentadienes are formed in a trans/cis ratio



Table VIII-5.  $W(CO)_6$  Photoassisted Isomerization of 1, 4-Hexadienes

Starting Isomer	Time Irrdtd., min.	% Products		
		<u>tt</u>	<u>ct</u>	<u>cc</u>
<u>cis</u> -1, 4-hexadiene	900	0.77	6.38	1.23
	1343	1.25	8.74	2.18
	2500	2.43	14.07	3.20
<u>trans</u> -1, 4-hexadiene	900	4.60	2.29	0.09
	1343	5.98	2.93	0.08
	2500	9.93	4.81	0.10

of 6:1 as the only products of the  $W(CO)_6$  photoassisted isomerization of 1,4-pentadiene. Crudely, cis-1,4-hexadiene yields cis,trans-2,4-hexadiene selectively, and trans-1,4-hexadiene yields trans,trans-2,4-hexadiene. This observation leads to the conclusion that the nonconjugated double bonds do not interact significantly in these reactions. However, from cis-1,4-hexadiene we note the direct formation of trans,trans-2,4-hexadiene; i.e., a hydrogen shift and isomerization of the other double bond. If the 1,4-diene can chelate (8-XV) one may be able



to rationalize this result.

The interaction of the double bonds in conjugated dienes is demonstrated by the data in Table VIII-6 for the  $W(CO)_6$  photoassisted isomerization of the 2,4-hexadienes. The direct formation of the trans,trans isomer from the cis,cis is taken as evidence for the interaction of the two double bonds. As with the 3-hexenes the 2,4-hexadienes do not isomerize via a common intermediate since the quantum yield for trans,trans to cis,trans is not the same as the yield for cis,cis to cis,trans. The effect of metal on the relative isomerization yields is shown in Table VIII-7 and is qualitatively the same as that for the stilbenes and 1-pentene.

Table VIII-6. Quantum Yields for  $W(CO)_6$  Photoassisted Isomerization of 2,4-Hexadienes

Time Irrdtd., <sup>a</sup> min.	$\phi_{\underline{tt} \rightarrow \underline{ct}}$	$\phi_{\underline{tt} \rightarrow \underline{cc}}$	$\phi_{\underline{cc} \rightarrow \underline{ct}}$	$\phi_{\underline{cc} \rightarrow \underline{tt}}$	$\phi_{\underline{ct} \rightarrow \underline{tt}}$	$\phi_{\underline{ct} \rightarrow \underline{cc}}$
175	0.038	b	0.053	0.019	0.046	0.005
460	0.026	b	0.085	0.019	0.065	0.010

<sup>a</sup>313 nm irradiation.

<sup>b</sup>  $\phi_{\underline{tt} \rightarrow \underline{cc}}$  0.002.

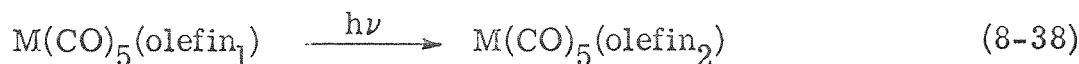
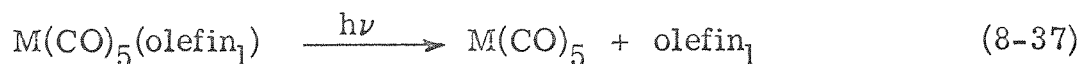
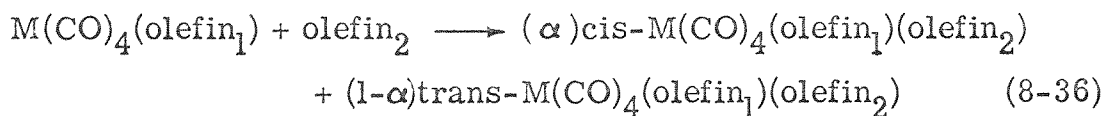
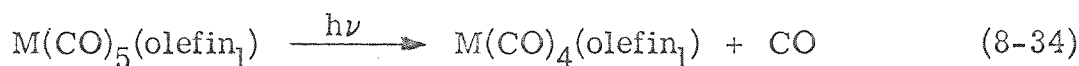
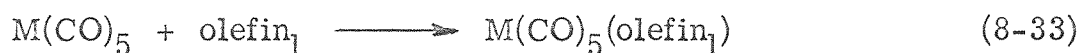
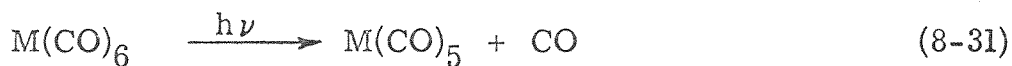
Table VIII-7. Effect of Metal on  $M(CO)_6$  Photoassisted  
Isomerization of 1,3-Pentadiene<sup>a</sup>

Metal Carbonyl	Time Irrdtd., min.	% <u>cis</u> → <u>trans</u>
$W(CO)_6$	360	7.52
	820	18.69
$Mo(CO)_6$	360	0.47
	820	0.81
$Cr(CO)_6$	360	0.00
	820	0.00

<sup>a</sup>313 nm irradiation in a merry-go-round.

Another experiment with the conjugated diene complexes allows us to rule out a process which involves production of a free 1,3-diene in its excited triplet state. Irradiation of  $\text{W(CO)}_6$  in the presence of 0.2 M isoprene failed to produce any of the dimers produced by triplet sensitization under the same conditions.

An overall mechanism for the  $\text{M(CO)}_6$  photoassisted reactions is outlined in (8-31) through (8-38). We have focused on the



transformation (8-38) in our discussion, but irradiation of multiply substituted complexes can result in transformation of the olefin. Detailed elucidation of all steps involves both thermal and photochemical substitution processes. We have characterized

the reactivity pattern for Cr, Mo, and W and determined the types of transformation possible in the coordinated olefin.

References

1. J. Halpern, in "Homogeneous Catalysis", Adv. in Chem. Series, 70, American Chemical Society, 1968, pp. 1-24.
2. R.A. Levenson, Ph.D. Thesis, Columbia University, 1970.
3. C.H. Bamford, P.A. Crowe, J. Hobbs, and R.P. Wayne, Proc. Roy. Soc. (London), A292, 153 (1966).
4. A good review is available: E. Koerner v. Gustorf and F. — W. Grevels, Fort. der Chem. Forsch., 13, 366 (1969).
5. R.L. Hunt, D.M. Roundhill, and G. Wilkinson, J. Chem. Soc., A982, (1967).
6. G.O. Schenck, E. Koerner v. Gustorf, and M. — J. Jun, Tet. Lett., 1059 (1962).
7. J.C. Hogan, Ph.D. Thesis, Boston College, 1969. Other examples of hydrogen shifts induced by irradiation of  $\text{Fe}(\text{CO})_5$ : (a) F. Assinger, B. Fell, U.K. Schrage, Chem. Ber., 98, 381 (1965); (b) ibid., 98, 372 (1965); (c) F. Assinger, B. Fell, and G. Collin, ibid., 96, 716 (1963); (d) M.D. Carr, V.V. Kane, and M.C. Whiting, Proc. Chem. Soc. (London), 408 (1964).
8. This may represent true photocatalysis, but quantum yields have not been measured.
9. L. Foos and M. Orchin, J. Am. Chem. Soc., 87, 5502 (1965).
10. T.A. Manuel, J. Org. Chem., 27, 3941 (1962). This reference also describes cis-trans isomerization of 1,2-dichloroethylene and isomerization of 1,2-dibromoethylene is thought to occur: F. — W. Grevels, Diploma Thesis, Technical University Aachen, 1968.
11. F.G. Cowherd and J.L. von Rosenberg, J. Am. Chem. Soc., 91, 2157 (1969).
12. H. Alper, P.C. LePort, and S. Wolfe, ibid., 91, 7553 (1969).

13. M. Rosenblum and C. Gatsonis, ibid., 89, 5074 (1967).
14. M. Rosenblum and B. North, ibid., 90, 1060 (1968).
15. R. Fields, M.M. Germain, R.N. Haszeldine, and P.W. Wiggins, Chem. Comm., 243 (1967).
16. R. Pettit, J. Am. Chem. Soc., 81, 1266 (1959).
17. W.J.R. Tyerman, M. Kato, P. Kebarle, S. Masamune, O.P. Strausz, and H.E. Gunning, Chem. Comm., 497 (1967).
18. H.W. Sternberg, P. Markby, and I. Wender, J. Am. Chem. Soc., 80, 1009 (1958).
19. W. Jennings and B. Hill, ibid., 92, 3199 (1970).
20. (a) G.S. Hammond, N.J. Turro, and A. Fischer, ibid., 83, 4674 (1961); (b) N.J. Turro and G.S. Hammond, ibid., 84, 2841 (1962); (c) G.S. Hammond, N.J. Turro, and R.S.H. Liu, J. Org. Chem., 28, 3297 (1963); (d) R.S.H. Liu, J. Am. Chem. Soc., 85, 477 (1963); ibid., 87, 3406 (1965).
21. J. Nasielski, P. Kirsch, and L. Wilputte-Steinert, J. Organometal. Chem., 27, C13 (1971).
22. R.B. Williams, J. Am. Chem. Soc., 64, 1395 (1942).
23. (a) N.A. Beach and H.B. Gray, ibid., 90, 5713 (1968); (b) M. Wrighton, G.S. Hammond, and H.B. Gray, ibid., 93, 4336 (1971); (c) D. Ottesen, M. Wrighton, H.B. Gray, and G.S. Hammond, unpublished results.
24. R.B. Woodward and R. Hoffmann, "The Conservation of Orbital Symmetry", Academic Press, Inc., 1970.
25. (a) F.D. Mango, Adv. in Catalysis, 291 (1969); (b) R. Pettit, H. Sugahara, J. Wristers, and W. Merk, Disc. Faraday Soc., 71 (1969).



## APPENDIX

Experimental Methods

Luminescence Experiments. Routine emission spectra were measured using an Aminco-Bowman or a Hitachi MPF-3 spectrometer. Low temperatures were achieved using liquid nitrogen cryostats commercially available. Either methylcyclohexane, EPA, or 1-pentene are appropriate glassy solvents at 77°K. Where the temperature was varied a stream of liquid nitrogen cooled helium was passed by the sample and the temperature measured with a thermocouple in contact with the sample. All emission spectra are uncorrected.

In certain cases luminescence spectra were obtained using a Cary 14 or Cary 17 absorption spectrometer. When these instruments were used the visible source was removed and the sample mounted in its place. The sample was then externally excited using an appropriately filtered mercury lamp. Luminescence was detected by using the single beam mode of the instruments.

A final aid in determining luminescence spectra is the use of the Cary 81 Raman spectrometer equipped with a He-Ne laser exciting source. The sample to be studied was simply mounted in the instrument as if its Raman spectrum were to be studied. Emission from electronically excited states is distinguished from Raman bands by being significantly

broader. The 632.8 nm output of the laser was typically about 50 mw.

Luminescence lifetimes were determined using a TRW Systems Lifetime Apparatus. The excitation source was a  $N_2$  lamp of flash time approximately 16 nsec and pulsed at 5 kc. A photomultiplier tube was used to detect the luminescence and its output displayed on a Tektronix Type 556 Oscilloscope. Plots of log (luminescence intensity) against time were linear. The luminescence lifetime was taken to be the time required for the emission intensity to decay to  $1/e$  of its original intensity. Appropriate filtering of the excitation source prevented interference of the scattered light. Low temperature measurements could be made by using a liquid nitrogen Dewar available as a sample holder for the Aminco-Bowman emission spectrometer.

Relative emission quantum yields were determined using samples of matched optical density at the exciting wavelength. The relative excitation source output of the Aminco-Bowman spectrometer was established by measuring anthracene relative luminescence yields at several wavelengths between 300 nm and 400 nm. The spectral distribution of  $W(CO)_5(X)$  luminescence was so similar that differences due to photomultiplier response were neglected in determining their relative luminescence yields.

Photochemical Reactions. Quantum yields were measured using merry-go-rounds previously described.<sup>1</sup> Light intensities at the 254, 313, 366, and 436 nm lines of the mercury lamps used were determined by a number of different chemical actinometers: (a) ferrioxalate,<sup>2</sup> (b) benzophenone-pierylene,<sup>3</sup> (c) benzil-stilbene,<sup>4</sup> or (d) trans → cis stilbene isomerization.<sup>5</sup>

A Hewlett-Packard Model 700 Gas Chromatograph was used to measure metal carbonyl photoassisted isomerization reactions of alkenes, stilbenes, and dienes. A 25 ft., 25%  $\beta,\beta'$ -ODPN column was used for separations of all isomers of the linear pentenes, 1,4-dienes, and 1,3-dienes employed in this study. A 6 ft.  $\text{AgNO}_3$ /glycerol column was used to separate isomers of the linear hexenes. A 6 ft. UCW-98 column was used for analysis of stilbenes and stilbazoles. A Disc integrator was used to determine peak areas when separation was good and cutting and weighing was used when baseline drift was a problem.

A typical procedure for  $\text{M}(\text{CO})_6$  photoassisted reactions of olefins is outlined. Catalytic amounts of  $\text{M}(\text{CO})_6$  ( $\text{M} = \text{Cr}, \text{Mo}, \text{W}$ ) ( $10^{-4}$  to  $10^{-3}$  M) were dissolved in an aliphatic hydrocarbon solvent. Excess olefin was added ( $10^{-2}$  to  $10^{-1}$  M) and the solutions were degassed by at least three freeze-pump-thaw cycles. Pyrex 13 x 100 mm test tubes were used as reaction

vessels and after degassing were hermetically sealed. Irradiation was performed using the merry-go-rounds. The presence of  $W(CO)_n(olefin)_{6-n}$  complexes could be determined by infrared spectra recorded on a Perkin-Elmer 225 spectrometer. The disappearance of  $M(CO)_6$  could be followed quantitatively by optical density measurements of the CO stretching peak in the ir. Gas chromatographic analysis of the olefins was done without removal of the metal carbonyl or its olefin complexes. Controls proved that the results were not distorted by this procedure.

In contrast to  $W(CO)_n(olefin)_{6-n}$  complexes which proved to be too unstable to isolate,  $W(CO)_5(pyridine)$ ,  $W(CO)_5(t\text{-}2\text{-styrylpyridine})$ ,  $W(CO)_5(t\text{-}4\text{-styrylpyridine})$ , cis- $W(CO)_4(pyridine)_2$ , and cis- $W(CO)_4(4\text{-styrylpyridine})_2$  could be isolated as pure solids, purified by column chromatography on neutral alumina, and characterized by their ir and uv-vis spectra.<sup>6</sup> These complexes were isolated from irradiated solutions of  $W(CO)_6$  and the ligand. Photoexchange of the ligands was measured both by ir and uv-vis spectral changes. The solutions were not degassed. Isomerization quantum yields for the coordinated styrylpyridines were measured by irradiating solutions of the complex, monitoring conversion by gas chromatography. Gas chromatograph results were unaffected by coordination of the styrylpyridine

to the metal presumably due to the fact that decomposition to the free olefin occurred in the  $\sim 200^\circ\text{C}$ . injection port.

Photochemical preparations of solutions of  $\text{M}(\text{CO})_5(\underline{n}\text{-electron donor})$  were achieved by irradiating solutions of  $\text{M}(\text{CO})_6$  in the presence of the  $\underline{n}$ -electron donor. For the most part, the  $\text{M}(\text{CO})_5(\text{X})$  complexes thus prepared were not isolated but were characterized by ir and uv-vis<sup>6</sup> spectra in solution.

The disappearance quantum yields for  $\text{W}(\text{CO})_5(1\text{-pentene})$  were measured by preparing pure solutions of  $\text{W}(\text{CO})_5(1\text{-pentene})$  by photolysis of  $\text{W}(\text{CO})_5(\text{pyridine})$  at 436 nm in the presence of 1-pentene. Quantitative analysis was obtained from ir absorbance data.

The experiments to determine the mechanism of  $\text{Co}(\text{CN})_5(\text{X})^{3-}$  photoaquation were carried out by simultaneously irradiating and monitoring the absorbance (at a given wavelength) of an aqueous solution of the potassium salt of the complex. The same source (75 W Hg) was the analyzing and irradiating beam. The flash photolysis<sup>7</sup> technique was also used to cause the photoaquation reaction. The photoaquation reaction could be studied at room temperature without complicating secondary dark reactions since the absorbance changes could be measured immediately after the flash of  $50\mu\text{sec}$ . The reactions of  $\text{Co}(\text{CN})_5(\text{X})^{3-}$  species were studied in aerated solutions except in energy transfer experiments.

The formation of  $\text{Co(CN)}_4(\text{OH})_2^{3-}$  from  $\text{Co(CN)}_5(\text{OH})^{3-}$  was determined by neutralizing the basic solutions with  $\text{HClO}_4$  and adding excess  $\text{Na}_2\text{SO}_3$  to form trans- $\text{Co(CN)}_4(\text{SO}_3)_2^{5-}$  and the optical density measured at its CT absorption maximum at 317 nm. The formation of  $\text{Co(II)}$  was determined spectrophotometrically by adding  $\text{NH}_4\text{SCN}$ -acetone to acidic  $\text{Co(II)}$  containing aqueous solutions and measuring the  $\text{Co(SCN)}_4^{2-}$  absorbance at 623 nm.

The disappearance quantum yields for  $\text{Co(CN)}_4(\text{SO}_3)(\text{X})^{n-}$  complexes were determined by measuring the change in absorbance at the CT absorption maximum. Solid samples of the  $\text{K}_5\text{Co(CN)}_4(\text{SO}_3)_2$  were prepared by V. Miskowski following a published procedure.<sup>8</sup> The  $\text{Co(CN)}_4(\text{SO}_3)(\text{OH}_2)^{3-}$  was produced by dissolving the disulfito complex in acidic solution. The hydroxy complex was prepared by making the solution basic with  $\text{NaOH}$ . Other  $\text{K}_n\text{Co(CN)}_5(\text{X})$  complexes were prepared as pure solids by either V. Miskowski or D. F. Gutterman.

The disappearance of  $\text{Fe(cp)}_2^+$  was monitored by measuring the decrease of its 617 nm absorption maximum. The  $\text{Fe(cp)}_2\text{BF}_4$  was prepared by Y. Sohn.

Electronic Energy Transfer and Quenching Studies. Most experiments were done using biacetyl as a triplet donor since it phosphoresces at room temperature in well degassed

fluid solutions.<sup>9</sup> The quenching of the biacetyl triplets by various metal complexes in aqueous solution is followed by monitoring the decrease in phosphorescence intensity as a function of quencher concentration. Linear Stern-Volmer plots were obtained in all cases studied. In the biacetyl sensitized aquation of  $\text{Co}(\text{CN})_5(\text{X})^{3-}$  irradiation was at 436 nm, and corrections were made for competing absorption and direct irradiation of the metal complex. All studies were carried out in the absence of  $\text{O}_2$ .

The quenching rate of acetone triplets by  $\text{Co}(\text{CN})_6^{3-}$  was determined by the following technique. Acetone was used to sensitize biacetyl phosphorescence. Addition of  $\text{Co}(\text{CN})_6^{3-}$  in a concentration equal to that of biacetyl resulted in 50% diminished sensitized biacetyl phosphorescence. The  $\text{Co}(\text{CN})_6^{3-}$  does not measurably quench the biacetyl triplets directly at the concentration employed here, so it is inferred that the acetone triplets are intercepted directly by the  $\text{Co}(\text{CN})_6^{3-}$ . Since biacetyl quenches acetone at a diffusion controlled rate the  $\text{Co}(\text{CN})_6^{3-}$  also quenches at a diffusion controlled rate because both quench the same number of acetone triplets at equal concentrations.

References

1. F.G. Moses, R.S.H. Liu, and B.M. Monroe, Mol. Photochem., 1, 245 (1969).
2. (a) C.A. Parker, Proc. Roy. Soc. (London), 220A, 104 (1953) and (b) C.G. Hatchard and C.A. Parker, ibid., 235A, 518 (1956).
3. A.A. Lamola and G.S. Hammond, J. Chem. Phys., 43, 2129 (1965).
4. H.A. Hammond, D.E. DeMeyer, and J.L.R. Williams, J. Am. Chem. Soc., 91, 5180 (1969).
5. S. Malkin and E. Fischer, J. Phys. Chem., 68, 1153 (1964).
6. "Organic Synthesis via Metal Carbonyls", Vol. I, I. Wender and P. Pino, Ed., Wiley, 1968 and references cited therein.
7. W.G. Herkstroeter and G.S. Hammond, J. Am. Chem. Soc., 88, 4769 (1966).
8. H.H. Chen, M.-S. Tsao, R.W. Gaver, P.H. Tewari, and W.K. Wilmarth, Inorg. Chem., 5, 1913 (1966).
9. H.L.J. Backstrom and K. Sandros, Acta Chem. Scand., 12, 823 (1958) and 14, 48 (1960).